



LEHIGH  
UNIVERSITY

Library &  
Technology  
Services

The Preserve: Lehigh Library Digital Collections

# Bacterial Cell Surfaces: Exploiting Metabolic Pathways for Fundamental Understanding of Antibiotic Resistance and Growth

## Citation

Pidgeon, Sean, and Marcos Pires. *Bacterial Cell Surfaces: Exploiting Metabolic Pathways for Fundamental Understanding of Antibiotic Resistance and Growth*. 2019, <https://preserve.lehigh.edu/lehigh-scholarship/graduate-publications-theses-dissertations/theses-dissertations/bacterial-cell-0>.

Find more at <https://preserve.lehigh.edu/>

*This document is brought to you for free and open access by Lehigh Preserve. It has been accepted for inclusion by an authorized administrator of Lehigh Preserve. For more information, please contact [preserve@lehigh.edu](mailto:preserve@lehigh.edu).*

Bacterial Cell Surfaces: Exploiting Metabolic Pathways for Fundamental Understanding  
of Antibiotic Resistance and Growth

by

Sean E. Pidgeon

A Dissertation

Presented to the Graduate and Research Committee

of Lehigh University

in Candidacy for the Degree of

Doctor of Philosophy

in

Chemistry

Lehigh University

January 2019

Approved and recommended for acceptance as a dissertation in partial fulfillment of the requirements for the degree of Doctor of Philosophy.

Sean E. Pidgeon

Bacterial Cell Surfaces: Exploiting Metabolic Pathways for Fundamental Understanding of Antibiotic Resistance and Growth

---

Defense Date

---

Dissertation Director  
Marcos M. Pires, PhD

---

Approved Date

Committee Members

---

Damien Thévenin, PhD

---

Dmitri Vezenov, PhD

---

Angela Brown, PhD

**© 2019 Copyright  
Sean E. Pidgeon**



## Table of Contents

<b>List of Figures</b> .....	<b>ix</b>
<b>Abstract</b> .....	<b>1</b>
<b>Chapter 1: Fundamentals of Antibiotic Resistance</b> .....	<b>4</b>
1.1 Antibiotic Resistance .....	4
1.2 Antibiotic Targets .....	6
1.3 Bacterial Cell Wall.....	6
1.4 Peptidoglycan Biosynthesis .....	9
1.5 Resistance to Cell Wall Antibiotics .....	11
1.5.1 $\beta$ -lactam Resistance .....	11
1.5.2 Glycopeptide Resistance.....	14
1.6 Conclusions.....	17
1.7 References.....	19
<b>Chapter 2: Metabolic Labeling of Bacterial Cell Surfaces</b> .....	<b>21</b>
2.1 Introduction.....	21
2.2 Metabolic Probes for Peptidoglycan Synthesis.....	22
2.3 Metabolic Probes for Carbohydrate Synthesis.....	26
2.4 Additional Bacterial Cell Surface Probes .....	27
2.5 Conclusions and Future Outlook .....	28
2.6 References.....	30
<b>Chapter 3: Metabolic Profiling of Bacteria by Unnatural C-terminated</b> <b>D-Amino Acids</b> .....	<b>33</b>
3.1 Abstract.....	33

3.2 Introduction.....	33
3.3 Results and Discussion .....	36
3.3.1 Incorporation of Non-native C-terminated D-Amino Acids .....	36
3.3.2 Confirmation of D-Amino Acid Incorporation .....	38
3.3.3 Growth Phase effect of D-Amino Acid Incorporation .....	43
3.3.4 Amidation Effects on Crosslinking.....	44
3.3.5 Kinetics of D-Amino Acid Incorporation .....	45
3.3.6 Bacteria Profiling with D-Amino Acids.....	48
3.4 Conclusion .....	49
3.5 Materials and Methods.....	50
3.6 References.....	56
<b>Chapter 4: Metabolic Remodeling of Bacterial Surfaces via Tetrazine Ligations ....</b>	<b>57</b>
4.1 Abstract.....	57
4.2 Introduction.....	57
4.3 Results and Discussion .....	60
4.3.1 Alkene D-Amino Acid Incorporation.....	60
4.3.2 Competition and Kinetics of Alkene D-Amino Acids.....	63
4.3.3 Amidation of Alkene D-Amino Acid.....	65
4.3.4 Live Cell Tetrazine Ligations and Stereospecificity.....	66
4.3.5 Trans-cyclooctene-Tetrazine Live Cell Ligation.....	68
4.4 Conclusion .....	70
4.5 Materials and Methods.....	70
4.6 References.....	75

<b>Chapter 5: Cell Wall Remodeling of <i>Staphylococcus aureus</i> in Live Hosts</b> .....	<b>77</b>
5.1 Abstract.....	77
5.2 Introduction.....	77
5.3 Results and Discussion .....	80
5.3.1 Tetrazine D-Amino Acid Incorporation.....	80
5.3.2 Kinetics of Tetrazine D-Amino Acids.....	84
5.3.3 <i>In vivo</i> D-Amino Acid Labeling.....	85
5.4 Conclusion .....	90
5.5 Materials and Methods.....	90
5.6 References.....	94
<b>Chapter 6: Vancomycin-dependent Response in Live Drug-Resistant Bacteria via Metabolic Labeling</b> .....	<b>96</b>
6.1 Abstract.....	96
6.2 Introduction.....	96
6.3 Results and Discussion .....	100
6.3.1 Alkyne Dipeptide Incorporation .....	100
6.3.2 Dipeptide Incorporation with Diverse Bacteria .....	104
6.3.3 VanX Dipeptide Hydrolysis.....	105
6.3.4 Kinetics of Cell Wall Remodelling.....	112
6.3.5 Vancomycin Variants and Pathway Activation .....	114
6.4 Conclusions.....	115
6.5 Materials and Methods.....	116
6.6 References.....	125

<b>Chapter 7: Cell Wall Piracy by a Synthetic Analog Reveals Metabolic Adaptation in Vancomycin Resistant Enterococci</b> .....	<b>127</b>
7.1 Abstract .....	127
7.2 Introduction.....	127
7.3 Results and Discussion .....	131
7.3.1 D-Laclick Incorporation .....	131
7.3.2 <i>In vitro</i> Ligation of D-Laclick .....	134
7.3.3 Analysis of D-Laclick in <i>E. Faecium</i> .....	139
7.3.4 Kinetics of Cell Wall Remodeling.....	141
7.3.5 Vancomycin Variants and Pathway Activation .....	143
7.4 Conclusions.....	145
7.5 Materials and Methods.....	145
7.6 References.....	154
<b>Chapter 8: L,D-transpeptidase Specific Probe Reveals Spatial Organization of Peptidoglycan Crosslinking</b> .....	<b>156</b>
8.1 Abstract .....	156
8.2 Introduction.....	157
8.3 Results and Discussion .....	162
8.3.1 Incorporation of Tetra- and Penta-peptide Probes .....	162
8.3.2 Structural Variations of Stem Peptide.....	165
8.3.3 Antibiotic Effects of Crosslinking .....	168
8.3.4 Kinetics of Stem Peptide Probe Incorporation.....	170
8.3.5 Localization of Crosslinking Modes .....	172

8.3.6 <i>In vivo</i> Labeling with Stem Peptide Probes .....	174
8.3.6 Mycobacteria Labeling with Stem Peptide Probes .....	175
8.4 Conclusions.....	181
8.5 Materials and Methods.....	182
8.6 References.....	187
<b>Appendix</b>	
A.3 Synthesis and Characterization of Compounds in Chapter 3.....	192
A.4 Synthesis and Characterization of Compounds in Chapter 4.....	202
A.5 Synthesis and Characterization of Compounds in Chapter 5.....	208
A.6 Synthesis and Characterization of Compounds in Chapter 6.....	211
A.7 Synthesis and Characterization of Compounds in Chapter 7.....	224
A.8 Synthesis and Characterization of Compounds in Chapter 8.....	232
<b>Curriculum Vitae .....</b>	<b>275</b>

## List of Figures

### Chapter 1

1.1 Timeline of Antibiotic Discovery .....	5
1.2 Cell wall of Bacteria .....	7
1.3 Chemical Structure of Peptidoglycan .....	8
1.4 Schematic of Peptidoglycan Crosslinking .....	9
1.5 Peptidoglycan Biosynthesis .....	10
1.6 Chemical Structures of Common $\beta$ -lactams .....	12
1.7 Vancomycin Peptidoglycan Binding .....	15
1.8 Genes for Glycopeptide Resistance .....	16

### Chapter 2

2.1 Metabolic Labeling of Bacterial Cell Surfaces .....	22
2.2 D-Amino Acid Incorporation into Peptidoglycan .....	23

### Chapter 3

3.1 PBP Processing and Promiscuity .....	35
3.2 <i>Bacillus subtilis</i> D-Amino Acid Incorporation .....	37
3.3 Stereospecificity of Incorporation.....	39
3.4 Sodium Dithionite Quenching of NBD Labelled Bacteria .....	40
3.5 Fluorescence Microscopy of DK-TAMRA Amide Bacteria .....	40
3.6 Peptidoglycan Characterization of DK-Amide Labelled Bacteria.....	41
3.7 D-Cysteine Labelling of Bacteria.....	42
3.8 Growth Phase Effects of D-Amino Acid Incorporation .....	43

3.9 Porosity of Amidated Peptidoglycan .....	45
3.10 Kinetics of Incorporation of DK-Amide and DK-Acid .....	46
3.11 Force-Indentation Curve of D-Ala-OH and D-Ala-NH <sub>2</sub> Labelled Bacteria .....	47
3.12 Profiling of Various Bacteria Using D-Amino Acids .....	48

## **Chapter 4**

4.1 D-Amino Acid Swapping and Decoration with Alkene Handles .....	58
4.2 Alkene-Tetrazine Reaction and Alkene Containing D-Amino Acid Derivatives .....	61
4.3 Norbornene-Tetrazine Reaction .....	62
4.4 Labelling of <i>S. aureus</i> with Alkene D-Amino Acids .....	63
4.5 Competition of D-Amino Acids .....	64
4.6 Reaction Analysis of Alkene D-Amino Acids .....	64
4.7 Live Cell Kinetics of Tetrazine Ligation .....	66
4.8 Peptidoglycan Isolation of D-Dap-NB-NH <sub>2</sub> Labelled <i>S. aureus</i> .....	67
4.9 Stereospecificity of Alkene Containing Amino Acids .....	68
4.10 Tetrazine-Transcyclooctene Reaction .....	69

## **Chapter 5**

5.1 D-Amino Acid Catch and Release .....	78
5.2 D-Amino Acid Swapping and Tetrazine-TCO Ligation .....	79
5.3 <i>S. aureus</i> Labelling with D-Tetrazine Amino Acid .....	82
5.4 D-Tet Competition with D-Ala .....	84
5.5 D-Tet-TCO Ligation Kinetics .....	85
5.6 D-Lys-FITC Labelling of <i>S. aureus in vivo</i> .....	86
5.7 <i>Ex vivo</i> and <i>in vivo</i> Peptidoglycan Labeling Scheme .....	87

5.8 <i>Ex vivo</i> and <i>in vivo</i> Peptidoglycan Labeling .....	88
5.9 <i>In vivo</i> Labeling with Tetrazine L-Amino Acids .....	89
<b>Chapter 6</b>	
6.1 Intracellular Peptidoglycan Biosynthesis and Vancomycin Lipid II Binding .....	97
6.2 VanX Mechanism and <i>E. faecium</i> Dipeptide Labeling .....	99
6.3 Dipeptide Labeling with <i>B. subtilis</i> .....	101
6.4 Structure of VanX with D-Pra-D-Ala in Active Site .....	102
6.5 Peptidoglycan Precursor Isolation .....	103
6.6 D-Pra-D-Ala Labeling with Various Bacteria .....	104
6.7 Visualization of VanX Activity .....	105
6.8 D-Pra Labeling of <i>E. faecium</i> .....	106
6.9 Fluorescence Microscopy of <i>E. faecium</i> Labelled with D-Pra-D-Ala.....	106
6.10 Lysozyme Digestion of Labeled <i>E. faecium</i> .....	107
6.11 Vancomycin Concentration Curve of D-Pra-D-Ala Labeled <i>E. faecium</i> .....	108
6.12 D-Pra-D-Ala Concentration Curve with <i>E. faecium</i> .....	108
6.13 VanX Activity in Vancomycin Sensitive <i>E. faecium</i> .....	109
6.14 Stereospecificity of Dipeptide Incorporation.....	109
6.15 VanX Activity towards Cysteine Containing Dipeptides .....	110
6.16 VanX Substrate Specificity.....	111
6.17 VanX Activity in <i>E. faecalis</i> .....	112
6.18 Cell Wall Remodeling and VanX Kinetics .....	114
6.19 Vancomycin Derivatives and VanX Activation .....	115



## Chapter 7

7.1 Vancomycin Lipid II Binding and Ligase Activity .....	129
7.2 Cell Surface Labeling of <i>E. faecalis</i> with D-Laclick .....	132
7.3 Flow Cytometry Analysis of D-Laclick Labeled <i>E. faecalis</i> .....	133
7.4 Fluorescence Microscopy of <i>E. faecalis</i> Labelled with D-Laclick .....	133
7.5 Lysozyme Digestion of <i>E. faecalis</i> Labeled with D-Laclick.....	134
7.6 SDS-PAGE of VanB Ligase .....	135
7.7 <i>In vitro</i> VanB Ligase Assay .....	136
7.8 LC-MS of VanB Ligase <i>In vitro</i> Assay .....	137
7.9 MurF Selectivity of Didepsipeptide.....	138
7.10 Vancomycin Sensitive <i>E. faecalis</i> Comparison .....	139
7.11 D-Laclick Labeling with <i>E. faecium</i> (VanA) .....	140
7.12 Visualization of D-Laclick Labeling.....	141
7.13 VanB Induction and Persistence .....	142
7.14 Vancomycin Derivatives and VanB Activation.....	144

## Chapter 8

8.1 Peptidoglycan Crosslinking Modes .....	158
8.2 L,D- vs D,D- Transpeptidase Crosslinking.....	160
8.3 Incorporation of TetraFl and PentaFl Stem Mimics .....	163
8.4 Additional <i>E. faecium</i> Strains .....	164
8.5 Structural Variations of Stem Peptides .....	166
8.6 Labeling of Structural Variations with <i>E. faecium</i> D344s.....	167

8.7 Kinetics and Antibiotic Effects of Labeling .....	169
8.8 Labeling of <i>E. faecium</i> with Asparagine Side Chain .....	170
8.9 Additional Antibiotics and Their Effects .....	171
8.10 DADA Structure .....	172
8.11 Confocal Microscopy of <i>E. faecium</i> with Stem Peptide Mimics.....	173
8.12 Mycobacterium Smegmatis Analysis with Stem Peptide Mimics .....	176
8.13 Microscopy of <i>M. smegmatis</i> Treated with Pentapeptide Variants .....	178
8.14 <i>Mycobacterium tuberculosis</i> Microscopy.....	179
8.15 <i>Mycobacterium tuberculosis</i> Microscopy treated with meropenem.....	180
8.16 Flow Cytometry Analysis of <i>M. tuberculosis</i> .....	180
8.17 Confocal microscopy image of <i>M. tuberculosis</i> with iso-Glx Variants.....	181

## **Abstract**

The worldwide problem of antibiotic resistance has become one of the most serious health threats of this century and will undoubtedly become top clinical priority. In the U.S. alone, antibiotic-resistant bacteria cause at least 2 million infections and 23,000 deaths a year resulting in a \$55-70 billion per year economic impact. The rise in the number of resistant bacteria is mainly attributed to the improper and overuse of antibiotics, and the ability of these bacteria to evolve elaborate genetic systems to counteract pharmaceuticals. As the number of efficacious antibiotics continues to rapidly dwindle without replenishment, the possibility of entering a post-antibiotic era can become a reality. To combat this ever-growing threat, the Centers of Disease Control and Prevention (CDC) stress four core actions; (1) preventing infections from occurring and spreading, (2) tracking resistant bacteria, (3) improving the use of antibiotics, and (4) promoting the development of new antibiotics and new diagnostic tests for resistant bacteria. With those actions in mind, our goal is to rededicate efforts towards understanding fundamental bacterial physiology and pathology, with a special focus on mechanisms of cell wall growth and drug resistance. A clearer understanding of the molecular events underpinning antibiotic resistance phenotypes can be instrumental in guiding the design of next generation diagnostics, antibiotics, and therapeutics.

The bacterial cell envelope is a vital extracellular component of prokaryotic cells, providing structural support and osmotic stability. Some of the most potent antibiotics in use today are molecules that inhibit the assembly of the bacterial cell wall. Despite the tremendous clinical importance of bacterial cell wall targeted antibiotics, it is surprising that several key aspects of cell wall biosynthesis and processing remain poorly

characterized. A deeper understanding of the catalysis of cell wall associated enzymes will undoubtedly bestow researchers with the complemented ability to identify new antibiotic targets and antibiotics. Chapter 2 will discuss the technologies that have been developed to date to understand cell wall coordination. These molecular probes are designed for the understanding of enzymatic mechanisms and dynamics of biosynthesis pathways.

The work discussed in Chapter 3 describes the initial efforts to combat antibiotic resistance, with the specific goal of developing a novel bacterial diagnostic assay. Diverse fluorescent D-amino acids were synthesized and incubated with different bacterial species. These D-amino acids containing C-terminus variations were shown to be incorporated into bacterial peptidoglycan with subtle differences within and between bacterial species. We show that the enzymes responsible for incorporation (transpeptidases) have remarkable flexibility in accepting unnatural D-amino acid derivatives. The incorporation profile has the potential to form the basis of a novel bacterial detection method.

We next exploited the incorporation of unnatural D-amino acids for decoration of bacterial cell surfaces with tetrazine ligation handles, as discussed in Chapter 4. Such an approach can provide an alternative method of installing molecules of interest to the exterior of the cell. Peptidoglycan labeling of live bacteria through this ligation approach paves the way for future *in vivo* studies due to its non-toxic effects and proven biocompatibility, as mentioned in Chapter 5. In this section, we present the first evidence that bacteria remodel their PG with exogenous D-amino acids in a live host animal. These results suggest that extracellular D-amino acids may provide pathogens with a mode of late-stage *in vivo* cell-surface remodeling.

The work discussed in Chapter 6 and 7, as opposed to previous methods, starts to explore and exploit the intracellular pathway of peptidoglycan biosynthesis. We developed a novel strategy aimed at hijacking peptidoglycan biosynthetic machinery to install specific reporter handles that track changes in cell wall composition. Described is a panel of synthetic cell wall precursor analogs that mimic substrates for vancomycin resistant-linked enzymes. Reporter handles were included at strategic points within these molecules to generate resistance-specific output signals. Monitoring cell wall alterations during drug evasion with temporal resolution revealed insight into adaptation dynamics and kinetics. In Chapter 8, we demonstrated that cell wall analogs can be unparalleled chemical probes in revealing key features of the cell wall crosslinking in live bacteria. We assessed the proficiency of two vital enzymes (D,D- and L,D-transpeptidases) with the goal of unraveling the interplay between these two modes of crosslinking. We showed how subtle structural modifications to the primary sequence of peptidoglycan can control crosslinking efficiency. Such probes may guide drug regimen and establish new drug targets.

# Chapter 1

## Fundamentals of Antibiotic Resistance

### 1.1 Antibiotic Resistance

The worldwide problem of antibiotic resistance has become one of the most serious health threats of the 21st century and will undoubtedly become a top clinical priority. An estimated 23,000 people each year in the United States alone are killed from complications of drug-resistant bacteria.<sup>1</sup> Once was a time when a plethora of antibiotics were available at our disposal to combat almost any class of bacterial infection. Since golden age of drug discovery (1940-1970), the selective pressure forced upon bacteria has now created potential life-threatening infections. For many decades, the number of new FDA approved antibiotics easily outpaced the emergence of resistant bacterial strains. Infections that could have previously been life-threatening were quickly cleared with a simple treatment of antibiotics. Unfortunately, the current landscape is vastly different. Drug resistant bacterial infections are now commonplace. Hospitals are becoming primary sites for the dissemination of resistant strains.<sup>2</sup> The rampant, and sometimes unnecessary, use of antibiotics has directly contributed to the rapid rise in drug resistance. As a result, a large fraction of clinically important antibiotics have had their potency dramatically reduced. Not only are bacteria becoming drug-resistant, but severe infections and strains have emerged that are resistant to every antibiotic available.<sup>3</sup> The World Health Organization recently warned that “we are heading for a post-antibiotic era, in which common infections and minor injuries can once again kill”.<sup>4</sup>

Most of the drugs in the clinical pipeline are based off and are simply modifications of existing antibiotics. Our supply of efficacious drugs has rapidly dwindled, therefore leaving

few treatment options when a multi-drug resistant bacterial infection arises. Although the development of new antibiotics was abundant after their initial discovery, more recently it has proven to be increasingly difficult to identify new antibiotic agents, with no new discoveries within the past 30 years (Figure 1.1). Nearly every antibiotic used in the clinic today is based off a discovery decade's ago.

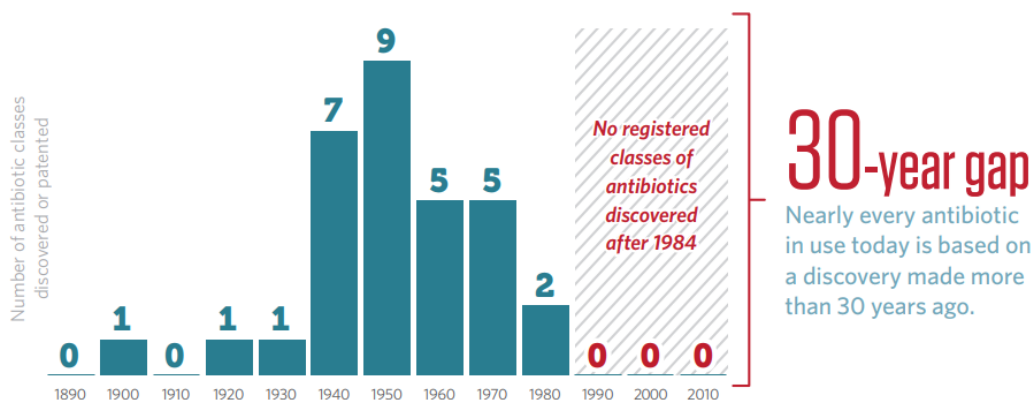


**Figure 1.1 Timeline of Antibiotic Discovery.** Chart highlighting the number of antibiotic classes discovered by decade.<sup>5</sup>

New sources of sensitizing and treating bacteria are therefore needed to solve the challenge of resistance. To combat this ever-growing threat, the Centers of Disease Control and Prevention (CDC) stress four core actions; (1) preventing infections from occurring and spreading, (2) tracking resistant bacteria, (3) improving the use of antibiotics, and (4) promoting the development of new antibiotics and new diagnostic tests for resistant bacteria.<sup>1</sup> With these alarming threats and stressed actions in mind, our lab set out to combat resistance by gaining a clearer understanding of the molecular events underpinning antibiotic resistance phenotypes. Access to such mechanisms will allow for development of new antibiotic targets and diagnostic tests.

## **1.2. Antibiotic Targets**

Antibiotics can be classified into five major categories by mechanism of action: (1) interference with membrane integrity (2) inhibition of nucleic acid synthesis (3) inhibition of protein synthesis (4) inhibition of essential small molecules and (5) inhibition of cell wall synthesis.<sup>6</sup> Antibiotics such as cationic polymyxins act to disrupt cellular membranes and onset cell lysis. These drugs are an older class that fell out of favor due to toxicity and are often referred to as the “last resort” antibiotics for threatening multidrug resistant gram-negative infections. Fluoroquinolones are an example of drugs that act to inhibit bacterial DNA synthesis. They are the one of the most commonly used antibiotics due to their broad-spectrum, however resistance develops quickly. Aminoglycosides are examples of protein synthesis inhibitors, functionalized with hydrophilic sugars containing protonated polycations. They function to specifically inhibit ribosomes to prevent translation of mRNA. Small molecule inhibitors include the antibiotic trimethoprim, an inhibitor of dihydrofolate reductases, preventing synthesis of vital tetrahydrofolate.<sup>6</sup> The focus of this thesis will be on the bacterial cell wall processing and resistance to antibiotics that act to inhibit its synthesis and overall integrity.

## **1.3 Bacterial Cell Wall**

Nearly all bacteria are protected by a cell wall that resides to the exterior of the cytoplasmic membrane. This multilayered organelle contributes morphological structure and maintains osmotic stability from environmental factors. Surfaces are comprised of heterogenous mixtures of lipids, proteins, and glycans. Of the primary targets for induction of bacteria death, the cell envelope remains one of the more prolific means of inhibiting vital biochemical processes.<sup>7</sup> Its fundamental importance has been highlighted by the many



antimicrobial agents developed to inhibit cell wall synthesis and/or disrupt the cells structural foundation. Some of the most potent antibiotics in use today are molecules that inhibit the assembly of the bacterial cell wall. More specifically, most block peptidoglycan (PG) biosynthesis, an essential constituent of the cell wall. Gram-negative bacteria contain an outer membrane that encloses a thin layer of PG (5-7 nm). Gram-positive bacteria in comparison lack an outer membrane but compensate their integrity with a thick PG layer (20-80 nm) on the outer layer. A third, less prominent class are mycobacterium which are structurally characterized by long-chain mycolic acids, arabinogalactan, and a thin layer of PG (Figure 1.2).<sup>8</sup>

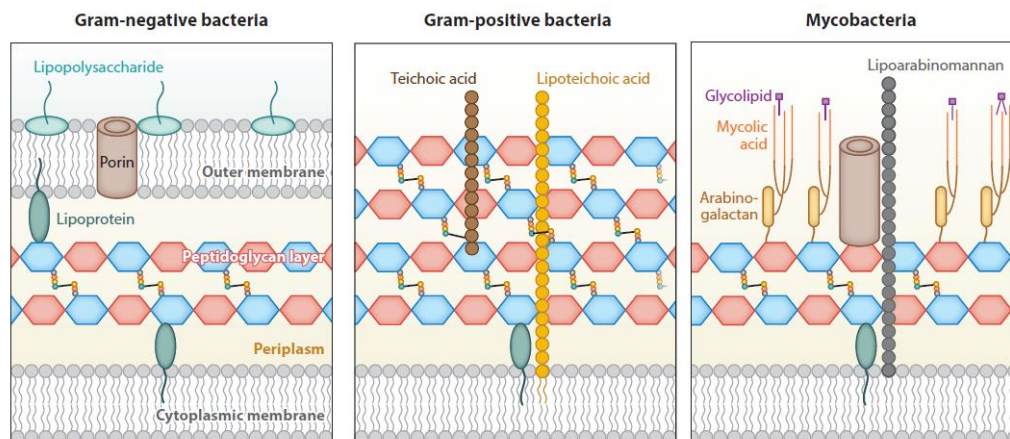


**Figure 1.2 Cell Wall of Bacteria.** Schematic representation of Gram-negative (left), Gram-positive (middle), and mycobacteria (right) bacteria. Gram-negative bacteria consist of peptidoglycan between a cytoplasmic and outer membrane. Gram-positive bacteria are comprised of a thick peptidoglycan layer. Mycobacteria have a thick layer of mycolic acids, followed by a thin layer of peptidoglycan.

Peptidoglycan is a polymer matrix composed of the repetitive glycan units N-acetylglucosamine (GlcNAc) and N-acetylmuramic acid (MurNAc).<sup>8</sup> Extension of these sugar strands is accomplished through transglycosylases, with further crosslinking by D,D-transpeptidases (Ddt) or sometimes referred to as penicillin binding proteins (PBPs) linking adjacent oligopeptides. Of note, the oligopeptide unit contains several D-amino acids, a

distinctive characteristic of bacteria. The transpeptidase domains of PBPs are responsible for this cross-linking to provide the peptidoglycan with increased integrity and to endow strength to the cell. PBPs create an acyl intermediate from its natural substrate pentapeptide. A nearby amine nucleophile displaces the intermediate to form a covalent bond between two peptide chains. Many antimicrobial agents reduce the mechanical strength of peptidoglycan by interfering with this process, such as  $\beta$ -lactams and glycopeptides.<sup>9</sup>  $\beta$ -lactams inhibit cell wall maturation by acting as a suicide substrate, forming a covalent bond with PBPs thus inhibiting crosslinking from occurring. Glycopeptide antibiotics inhibit crosslinking by binding D-Ala-D-Ala at the end of the stem peptide, sterically preventing PBPs from interacting with its pentapeptide substrate.<sup>10</sup> Nevertheless, the two mechanisms of cell wall targeting ( $\beta$ -lactam, glycopeptides) act to block crosslinking, preventing the cell from gaining proper rigidity and strength.<sup>6</sup>

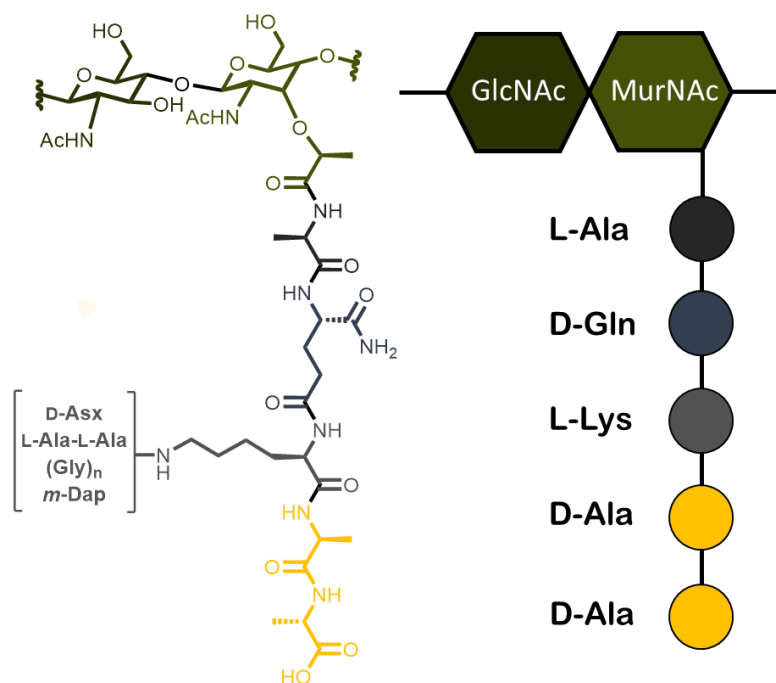


**Figure 1.3 Chemical structure of peptidoglycan and cartoon representation.** The glycan strands consist of alternating GlcNAc and MurNAc residues. Linked to each MurNAc residue is a peptide, sequence varying among bacterial species.

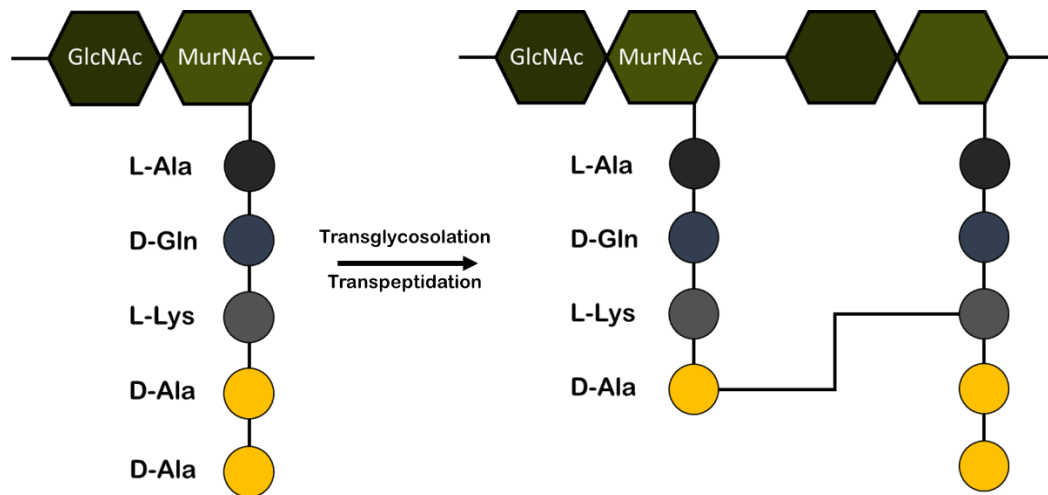


**Figure 1.4 Schematic of Peptidoglycan Crosslinking.** Cartoon representation of the enzymatic processes of transglycosolation (glycosidic bond formation) and transpeptidation by PBPs (stem peptide cross-linking). Above is a 4-3 crosslink generated by PBPs, linking the fourth position D-alanine to the third L-lysine of a nearby stem peptide.  $\beta$ -lactam antibiotics act to inhibit the process of transpeptidation to prevent cell wall crosslinking.

#### **1.4 Peptidoglycan Biosynthesis**

The PG biosynthetic pathway is a critical process in the cell and is exploited as a target for the design of many efficacious antibiotics. Biosynthesis is a complex process that involves approximately 20 enzyme reactions (Figure 1.5). Reactions to generate the building blocks of peptidoglycan occur both in the cytoplasm and on the inner and outer sides of the cytoplasmic membrane. Every enzyme involved in the biosynthetic pathway is essential for the bacteria to survive, making them excellent antibiotic targets. However, the ever-developing resistance to  $\beta$ -lactam antibiotics and vancomycin has led to increased efforts to characterize the metabolic activity of other less-studied enzymes of this peptidoglycan pathway. Although there are many steps in the biosynthetic pathway, the overall process can be simplified into three main stages: (1) synthesis of Park's nucleotide

in the cytoplasm (2) synthesis of critical lipid I and lipid II and (3) translocation of lipid II across the membrane for PG polymerization and crosslinking.<sup>11</sup>

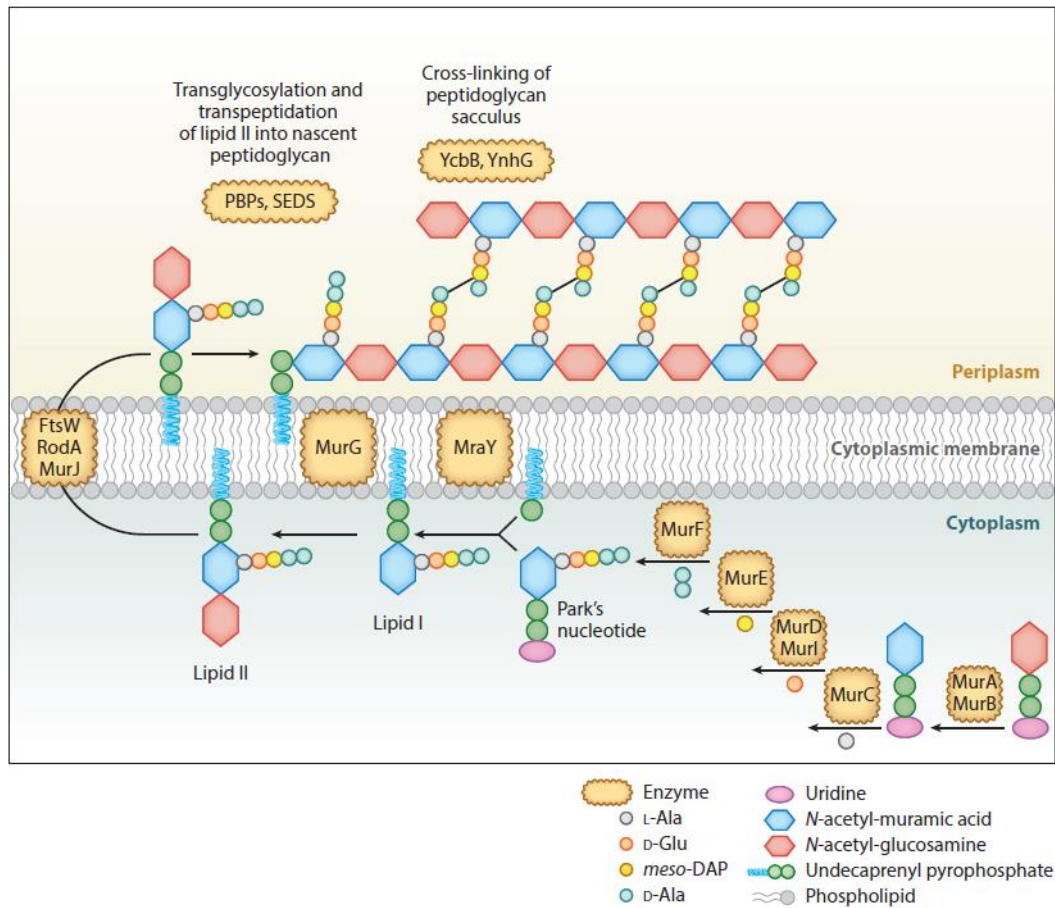


**Figure 1.5 Peptidoglycan Biosynthesis.** The biosynthesis pathway starts with the formation of Park's nucleotide in cytoplasm, followed by linking to a lipid to produce lipid II. Finally, lipid II is translocated across the cytoplasmic membrane and then inserted into the existing PG through transglycosylation and transpeptidation reactions.<sup>12</sup>

Peptidoglycan biosynthesis initiates in the cytoplasm with the conversion, of fructose-6-phosphate to UDP-MurNAc by the Glm enzymes. The Mur proteins then catalyze the sequential addition of the stem peptide amino acids to generate Park's nucleotide, a soluble nucleotide precursor.<sup>13,14</sup> Covalent linkage of Park's nucleotide to the inner cell wall is accomplished by MraY, resulting in a undecaprenol bound PG precursor, termed Lipid I.<sup>15</sup> The ensuing PG processing reactions are all membrane bound enzyme

catalysis. MurG adds GlcNAc to the Lipid I intermediate to generate Lipid II, a disaccharide PG precursor. Lipid II is then transferred to the outer side of the cell membrane by a lipase protein.<sup>16</sup> The identity of this flippase is still under debate, with studies supporting the claim of MurJ, FtsW or RodA as proteins responsible for translocating Lipid II from the inner cell membrane to the outer cell membrane.<sup>17-21</sup> Following translocation of Lipid II across the plasma membrane, the PG precursor is polymerized into the cell wall finalizing the ultimate PG structure. This polymerization step, as stated previously, is accomplished by the PBPs.<sup>22</sup> The PBPs are membrane bound proteins that are structurally related, but mechanistically diverse, catalyzing the transglycosylation and transpeptidation reactions. As mentioned previously, these enzymes are the targets of  $\beta$ -lactam antibiotics (penicillins, cephalosporins, monobactams, and carbapenems) (Figure 1.6). The mechanism by which PBPs are inhibited is through mimicry of the D-Ala-D-Ala residue of the stem peptide, forming irreversible covalent bonds with the enzymes, rendering them inactive.<sup>23</sup> The glycopeptide antibiotics, including vancomycin, inhibit PBPs through binding of the D-Ala-D-Ala motif of lipid II blocking the ensuing transglycosylation and transpeptidation reactions. Therefore, glycopeptides generally act as steric inhibitors of PG maturation to reduce cellular mechanical strength.<sup>24</sup> Resistance to  $\beta$ -lactam antibiotics and glycopeptides are a result of bacteria chemically modifying their PG to withstand and reduce affinity of antibiotic towards the PG structure.

## **1.5 Resistance to Antibiotics that Target PG Crosslinking**

### **1.5.1 $\beta$ -lactam Resistance**

The stem peptide structure of PG varies as a function of the stage of the bacterium, shape, the growth medium, the presence of resistance determinants relating to the cell wall,

and the presence of antibiotics. The selective pressure of antibiotics has caused bacteria to evolve mutations in enzymes associated with PG processing, deconstructing normal synthesis of the stem peptide to evade cell wall acting drugs. As stated earlier,  $\beta$ -lactam antibiotics impose their activity by forming an irreversible covalent bond with PBPs. Blocking of transpeptidation and transglycosylation leads to weakening of the PG causing cell lysis. Since there are more than one essential PBP in bacteria, resistance involves complex mechanisms. The use of  $\beta$ -lactam antibiotics has resulted in four major categories of resistance mechanism: (1) reduced membrane permeability or action of efflux pumps (2) expression of PBPs with reduced affinity to  $\beta$ -lactams (3) degradation of  $\beta$ -lactams by  $\beta$ -lactamases and (4) bypassing PBP crosslinking with L,D-transpeptidases.<sup>10</sup>

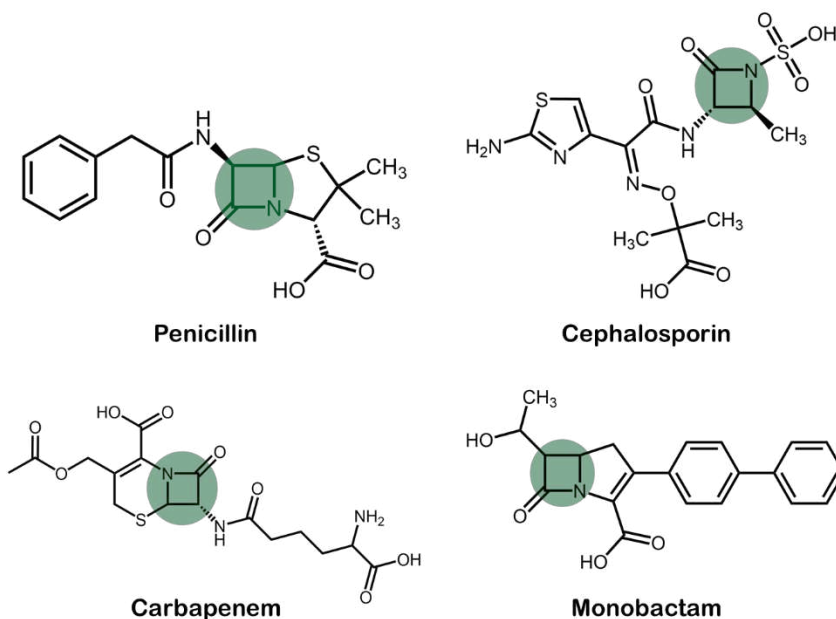


**Figure 1.6 Chemical structures of four clinically important  $\beta$ -lactam antibiotics.** The  $\beta$ -lactam ring is highlighted in green.

An inherent feature of some bacteria to resist antibiotics is through prohibiting antibiotic access to its molecular target in sufficient concentration. Both Gram-positive and Gram-negative bacteria possess peptidoglycan, yet the outer lipid membrane of Gram-

negative bacteria restricts some antibiotics from accessing its target. Some bacteria have also overexpressed membrane proteins that act as efflux pumps. Efflux pumps export toxic material outside of the cells and can exhibit this activity towards  $\beta$ -lactam antibiotics, preventing them from inhibiting their PBP targets.<sup>25</sup>

PBPs involved in  $\beta$ -lactam resistance present mutations in the protein sequence concentrated around the active site region. For example, a subtle modification in the active site region of PBP2a from *Staphylococcus aureus* (*S. aureus*) generates low affinity towards  $\beta$ -lactam antibiotics. This enzyme becomes primarily expressed when the major PBPs of *S. aureus* become inhibited by  $\beta$ -lactams. These low  $\beta$ -lactam affinity PBPs, however, in some cases can only initiate transpeptidation if the stem peptide is branched (i.e. (Gly)<sub>n</sub>) (Figure 1.3).<sup>26</sup> In *S. aureus*, the genes *femA* and *femB* are essential for the incorporation of glycine on the stem peptide cross bridges. Knockout studies of these proteins show PBP2a is essentially unable to perform crosslinking on substrates lacking glycines, therefore represent a practical antibiotic target.<sup>27</sup>

The third mechanism of  $\beta$ -lactam resistance involves chemical degradation of the antibiotic.  $\beta$ -lactamases act to hydrolyze the  $\beta$ -lactam ring (Figure 1.6), thus inactivating the antibiotics before getting to their intended PBP targets. Release of the ring strain renders the antibiotic non-reactive towards PBPs and is mainly found in Gram-negative pathogens. These enzymes can ultimately be found associated to the cell membrane, secreted into the extracellular space, or secreted in the periplasmic space (for Gram-negative bacteria). Although  $\beta$ -lactams are susceptible to  $\beta$ -lactamases, cocktail therapeutics have been applied to counteract their function.  $\beta$ -lactamase inhibitors such as

Tebipenem are used in combination of  $\beta$ -lactams to extend their lifetime and PBP inhibition.<sup>28</sup>

The final major class of  $\beta$ -lactam resistance was only recently discovered and involves the complete bypass of PBP crosslinking. Bacteria of this resistance are shown to have highly active D,D-carboxypeptidases, enzymes that generate stem tetrapeptides from the natural stem pentapeptides by hydrolyzing the terminal D-alanine (Figure 1.3). This essentially renders PBPs ineffective, as tetrapeptides are not substrates for these enzymes. Bacteria then funnel their crosslinking towards L,D-transpeptidases (Ldts), with tetrapeptides as their substrates. Ldts, unlike PBPs that catalyze a 4-3 peptide bond, generate 3-3 crosslinks. Due to this crosslinking mechanism,  $\beta$ -lactam antibiotic are ineffective due to differences in stem peptide substrates. These enzymes were first identified in *Enterococcus*, *Mycobacterium*, and *Clostridium* spp.<sup>29,30</sup> Ldts will be the major focus and will be discussed in greater detail in Chapter 8 of this thesis.

### **1.5.2 Glycopeptide Resistance**

The glycopeptides vancomycin, teicoplanin, and telavancin are currently employed in hospital settings as “last resort” antibiotics for Gram-positive pathogens. As mentioned previously, these antibiotics act to bind to the terminal D-Ala-D-Ala of peptidoglycan lipid II precursors through hydrogen bonds, impeding the transpeptidation and transglycosylation reactions (Figure 1.7).<sup>31</sup> Resistance mechanisms associated with these antibiotics are primarily linked to the generation of alternate peptidoglycan precursors. To decrease antibiotic affinity to peptidoglycan, bacteria synthesize intracellularly the dipeptides D-Ala-D-Lac or in some bacteria D-Ala-D-Ser. These peptidoglycan building blocks get incorporated into the grown stem peptide by the enzyme MurF (Figure 1.5).



Lipid II precursors displaying one of these altered C-termini results in poor affinity of glycopeptides to the stem peptide, *via* loss of a hydrogen bond (-D-Ala-D-Lac) or steric effects (-D-Ala-D-Ser). Reduced glycopeptide affinity results in PBP crosslinking and viable bacteria.

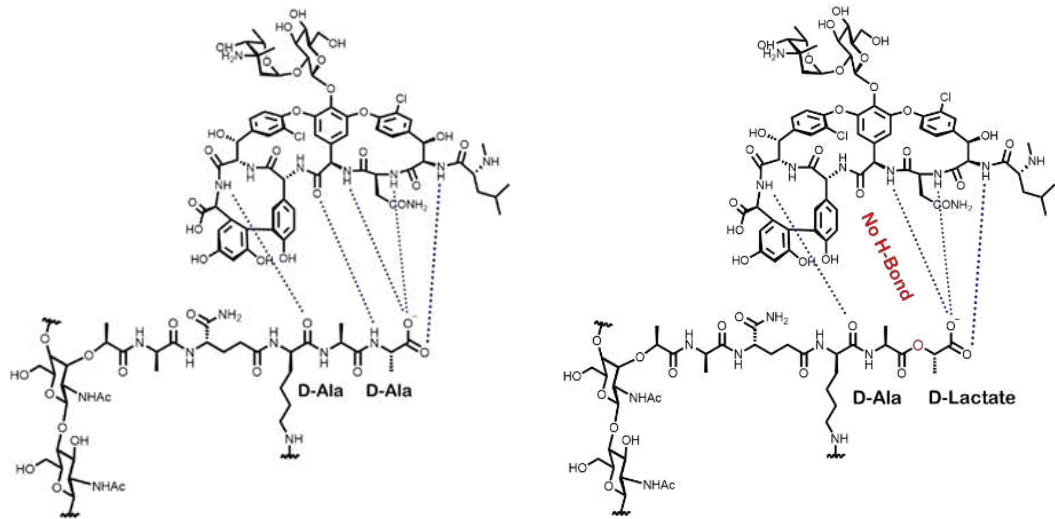


**Figure 1.7 Vancomycin Peptidoglycan Binding.** Vancomycin binding to D-Ala-D-Ala of PG stem peptide through five hydrogen bonds. By binding to D-Ala-D-Ala, transpeptidation is inhibited and cell death occurs. Replacing terminal D-Ala with D-Lac causes 1000-fold reduced affinity of vancomycin towards PG and crosslinking still occurs.

There are six primary genes responsible for the development of glycopeptide resistance (*vanR*, *vanS*, *vanH*, *vanA*, *vanX*, *vanY*) (Figure 1.8). *VanR* and *vanS* are proteins part of a two-component regulatory system that control the transcription and expression of the remaining *vanHAXY* genes. Membrane bound *vanS* senses a glycopeptide antibiotic resulting in a structural change becoming a kinase, phosphorylating the cytoplasmic protein *vanR*, a transcription factor in the expression of the *vanHAXY* genes. *VanH* is a dehydrogenase, which reduces pyruvate to D-lactic acid (D-Lac), and the *vanA* ligase, catalyzes the formation of an ester bond between D-Ala and D-Lac. The resulting depsipeptide D-Ala-D-Lac replaces the native D-Ala-D-Ala dipeptide in peptidoglycan

synthesis via the MurF ligation step. However, the production of peptidoglycan precursors terminating in D-Lac is still insufficient to lead to high-level of glycopeptide resistance. Bacteria must also deplete their intracellular pool of D-Ala-D-Ala dipeptide to prevent competing ligations. Two enzymes are involved in D-Ala-D-Ala peptidoglycan precursor depletion, *vanX* and *vanY*, which hydrolyze the D-Ala-D-Ala dipeptide and hydrolyze the stem peptide to reduce pentapeptide precursor pools, respectively. All these genes combined turnover D-Ala-D-Ala containing peptidoglycan precursors to D-Ala-D-Lac precursors, effectively causing glycopeptide resistance.<sup>32</sup>

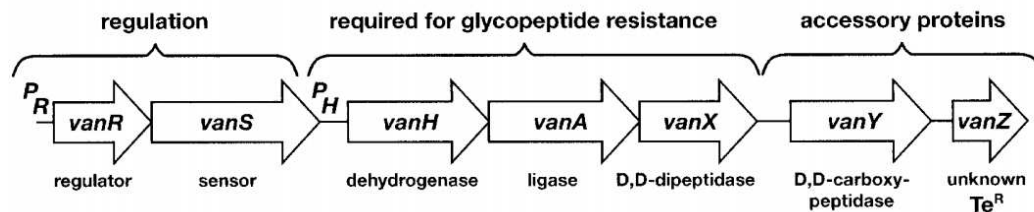


**Figure 1.8 Genes for glycopeptide resistance.** The two-component regulatory system *vanS-vanR* respond to vancomycin to activate downstream genes. *VanH* produces D-Lac from pyruvate, *vanA* ligates D-Ala and D-Lac to produce D-Ala-D-Lac dipeptide. *VanX* acts cleaves the glycopeptide building block D-Ala-D-Ala, and *vanY* is a D,D-carboxypeptidase that cleaves D-Ala terminal peptide to reduce the pentapeptide precursor pool.<sup>31</sup>

There are six types of glycopeptide resistance that have been characterized mainly in the bacterial class of *Enterococci*. Five of the classes (VanA, B, D, E, and G) are associated with acquired resistance from other bacteria by gene transfer of an unknown origin. VanC is intrinsic glycopeptide resistance to the bacteria *Enterococcus gallinarum* and *Enterococcus flavescens*. These classes of resistance are distinguished by the location of the resistance genes (plasmid vs chromosome) and by the mode of gene regulation and expression (inducible vs constitutive) (Table 1.1).

Strain characteristic	Acquired resistance level, type					Intrinsic resistance, low level, type VanC1/C2/C3
	High, VanA	Variable, VanB	Moderate, VanD	Low		
				VanG	VanE	
MIC, mg/L						
Vancomycin	64–100	4–1000	64–128	16	8–32	2–32
Teicoplanin	16–512	0.5–1	4–64	0.5	0.5	0.5–1
Conjugation	Positive	Positive	Negative	Positive	Negative	Negative
Mobile element	Tn1546	Tn1547 or Tn1549	...	...	...	...
Expression	Inducible	Inducible	Constitutive	Inducible	Inducible	Constitutive Inducible
Location	Plasmid chromosome	Plasmid chromosome	Chromosome	Chromosome	Chromosome	Chromosome
Modified target	D-Ala-D-Lac	D-Ala-D-Lac	D-Ala-D-Lac	D-Ala-D-Ser	D-Ala-D-Ser	D-Ala-D-Ser

NOTE. D-Ala-D-Lac, D-alanine-D-lactate; D-Ala-D-Ser, D-alanine-D-serine.

**Table 1.1** Level and type of resistance in *Enterococci*.<sup>31</sup>

For the purposes of this thesis, only VanA and VanB type of glycopeptide resistance will be discussed. VanA is the most common type of glycopeptide resistance to date. Bacteria with this set of genes are highly resistant to vancomycin (MIC 64-1000 µg/mL) and also the glycopeptide teicoplanin (MIC 16-512 µg/mL). VanB type bacteria have a similar mechanism of becoming resistant, however, are shown to have moderate resistance to vancomycin (4-64 µg/mL). A major distinction between VanA and VanB is the sensitivity to teicoplanin, where VanB *Enterococci* do not trigger the expression of the genes in the presence of teicoplanin. There is approximately 67%-76% sequence identity of the proteins between VanA and VanB, which may also contribute to their overall activity and contribution to glycopeptide resistance.<sup>31</sup>

## **1.6 Conclusions**

Although much has been learned in the peptidoglycan biosynthetic pathway and crosslinking, there remains a large gap in our fundamental understanding of the metabolic processes at play pertaining to bacterial cell wall synthesis. Research is now being directed to understand the fundamentals of bacterial cell wall processing. Technologies are now being developed to probe and image the biosynthesis and dynamics of the cell wall to answer long-standing questions in the microbiology field. Efforts are being rededicated towards understanding basic bacterial physiology and pathology, with a special focus on

specific mechanisms related to drug resistance. Chapter 2 of this thesis will solely focus on some of the efforts directed at elucidating the cell wall biosynthetic pathway.

## **1.7 References**

- (1) Solomon, S. L.; Oliver, K. B. *Am Fam Physician* **2014**, *89*, 938.
- (2) Fischbach, M. A.; Walsh, C. T. *Science* **2009**, *325*, 1089.
- (3) McGann, P.; Snesrud, E.; Maybank, R.; Corey, B.; Ong, A. C.; Clifford, R.; Hinkle, M.; Whitman, T.; Lesho, E.; Schaecher, K. E. *Antimicrob Agents Chemother* **2016**.
- (4) Morehead, M. S.; Scarbrough, C. *Prim Care* **2018**, *45*, 467.
- (5) Pewtrusts 2018.
- (6) Kohanski, M. A.; Dwyer, D. J.; Collins, J. J. *Nat Rev Microbiol* **2010**, *8*, 423.
- (7) Silhavy, T. J.; Kahne, D.; Walker, S. *Cold Spring Harb Perspect Biol* **2010**, *2*, a000414.
- (8) Vollmer, W.; Blanot, D.; de Pedro, M. A. *FEMS Microbiol Rev* **2008**, *32*, 149.
- (9) Macheboeuf, P.; Contreras-Martel, C.; Job, V.; Dideberg, O.; Dessen, A. *FEMS Microbiol Rev* **2006**, *30*, 673.
- (10) Nikolaidis, I.; Favini-Stabile, S.; Dessen, A. *Protein Sci* **2014**, *23*, 243.
- (11) Lovering, A. L.; Safadi, S. S.; Strynadka, N. C. *Annu Rev Biochem* **2012**, *81*, 451.
- (12) Radkov, A. D.; Hsu, Y. P.; Booher, G.; VanNieuwenhze, M. S. *Annu Rev Biochem* **2018**, *87*, 991.
- (13) Barreteau, H.; Kovac, A.; Boniface, A.; Sova, M.; Gobec, S.; Blanot, D. *FEMS Microbiol Rev* **2008**, *32*, 168.
- (14) Bugg, T. D.; Braddick, D.; Dowson, C. G.; Roper, D. I. *Trends Biotechnol* **2011**, *29*, 167.
- (15) Chung, B. C.; Zhao, J.; Gillespie, R. A.; Kwon, D. Y.; Guan, Z.; Hong, J.; Zhou, P.; Lee, S. Y. *Science* **2013**, *341*, 1012.
- (16) Mann, P. A.; Muller, A.; Xiao, L.; Pereira, P. M.; Yang, C.; Ho Lee, S.; Wang, H.; Trzeciak, J.; Schneeweis, J.; Dos Santos, M. M.; Murgolo, N.; She, X.; Gill, C.; Balibar, C. J.; Labroli, M.; Su, J.; Flattery, A.; Sherborne, B.; Maier, R.; Tan, C. M.; Black, T.; Onder, K.; Kargman, S.; Monsma, F. J., Jr.; Pinho, M. G.; Schneider, T.; Roemer, T. *ACS Chem Biol* **2013**, *8*, 2442.
- (17) Butler, E. K.; Davis, R. M.; Bari, V.; Nicholson, P. A.; Ruiz, N. *J Bacteriol* **2013**, *195*, 4639.
- (18) Ruiz, N. *Proc Natl Acad Sci U S A* **2008**, *105*, 15553.
- (19) Ruiz, N. *Lipid Insights* **2015**, *8*, 21.
- (20) Fraipont, C.; Alexeeva, S.; Wolf, B.; van der Ploeg, R.; Schloesser, M.; den Blaauwen, T.; Nguyen-Disteche, M. *Microbiology* **2011**, *157*, 251.
- (21) Mohammadi, T.; van Dam, V.; Sijbrandi, R.; Vernet, T.; Zapun, A.; Bouhss, A.; Diepeveen-de Bruin, M.; Nguyen-Disteche, M.; de Kruijff, B.; Breukink, E. *Embo J* **2011**, *30*, 1425.
- (22) Pratt, R. F.; McLeish, M. J. *Biochemistry* **2010**, *49*, 9688.
- (23) Josephine, H. R.; Charlier, P.; Davies, C.; Nicholas, R. A.; Pratt, R. F. *Biochemistry* **2006**, *45*, 15873.
- (24) Reynolds, P. E. *Eur J Clin Microbiol Infect Dis* **1989**, *8*, 943.
- (25) Webber, M. A.; Piddock, L. J. *J Antimicrob Chemother* **2003**, *51*, 9.
- (26) Lim, D.; Strynadka, N. C. *Nat Struct Biol* **2002**, *9*, 870.

- (27) Kobayashi, N.; Wu, H.; Kojima, K.; Taniguchi, K.; Urasawa, S.; Uehara, N.; Omizu, Y.; Kishi, Y.; Yagihashi, A.; Kurokawa, I. *Epidemiol Infect* **1994**, *113*, 259.
- (28) Paterson, D. L.; Ko, W. C.; Von Gottberg, A.; Mohapatra, S.; Casellas, J. M.; Goossens, H.; Mulazimoglu, L.; Trenholme, G.; Klugman, K. P.; Bonomo, R. A.; Rice, L. B.; Wagener, M. M.; McCormack, J. G.; Yu, V. L. *Clin Infect Dis* **2004**, *39*, 31.
- (29) Lavollay, M.; Arthur, M.; Fourgeaud, M.; Dubost, L.; Marie, A.; Veziris, N.; Blanot, D.; Gutmann, L.; Mainardi, J. L. *J Bacteriol* **2008**, *190*, 4360.
- (30) Mainardi, J. L.; Hugonnet, J. E.; Rusconi, F.; Fourgeaud, M.; Dubost, L.; Mouri, A. N.; Delfosse, V.; Mayer, C.; Gutmann, L.; Rice, L. B.; Arthur, M. *J Biol Chem* **2007**, *282*, 30414.
- (31) Courvalin, P. *Clin Infect Dis* **2006**, *42 Suppl 1*, S25.
- (32) Hughes, D. *Nat Rev Genet* **2003**, *4*, 432.

## Chapter 2

### Metabolic Labeling of Bacterial Cell Surfaces

#### 2.1 Abstract

As mentioned previously in Chapter 1, the cell wall is a key structural component of the cell envelope of bacteria. This highly complex structure and its construction provides the cell with the needed integrity to survive hostile environmental conditions. In this chapter, focus will be on the techniques and applications area of bacterial cell surface remodeling. The repertoire of tools at our disposal has allowed researchers to modulate the cell surface with non-native molecules to gain access to key dynamics and mechanisms of cell wall biosynthesis. Chemical probes have been designed to monitor and track a subset of macromolecules including peptidoglycan, proteins, glycans, and lipids. Metabolic labeling of the bacterial cell envelope is an evolving technology that will lead to better understanding of cell wall growth and dynamics, improve diagnostics, and may potentially lead to new medical therapeutics. This Chapter will serve as a published review and will be based only on the most recent applications of metabolic labeling, rather than a comprehensive outlook.

#### 2.2 Introduction

Metabolic labeling is a technique in which a non-biologically synthesized molecule is utilized as a substrate by endogenous machinery of the living organism. The probe synthesized is incorporated into a macromolecule of interest by enzymes, essentially “tricking” the organism being studied in accepting this unnatural substrate. Many studies previously took advantage of this metabolism with radioactive molecules or isotopes. Such an approach has its advantages, however, is not ideal as in most circumstances as it is

costly, requires specialized equipment, and such probes simply may not be feasibly developed to study specific metabolic pathways. Many metabolic studies today have departed from these approaches and are now utilizing metabolic probes containing fluorophores or reactive handles to perform specific chemistries (i.e. biotin pull-down) (Figure 2.1).

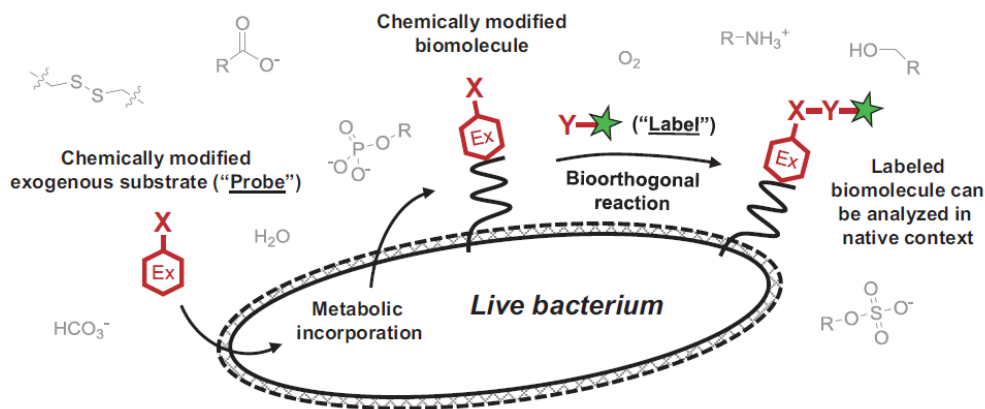


**Figure 2.1 Metabolic Labeling of Bacterial Cell Surfaces.** A synthesized probe (red hexagon) modified with a reporter group X (i.e. fluorophore, bioorthogonal handle) is incorporated through the metabolic pathway of bacteria and gets displayed on the cell surface. If X contains a bioorthogonal handle, a secondary step can be done to covalently attach a molecule of interest Y (i.e. fluorophore).<sup>1</sup>

Metabolic probes functionalized with fluorescent trackers has flooded the bacteria research field with new discoveries. Long-standing questions in microbiology related to enzymatic activity have been answered ever since their discovered use. This review will focus on a subset of bacterial cell surface targets, surveying the most recent studies of the extracellular macromolecules of peptidoglycan, carbohydrates, surface proteins, and lipids.

### **2.3 Metabolic Probes for Peptidoglycan Synthesis**

The majority of metabolic probes in this review involve incorporation of non-native molecules into peptidoglycan of the cell wall. Peptidoglycan synthesis involves both a



cytoplasmic and an extracellular phase (Figure 1.4). The ability of noncanonical D-amino acids to incorporate into the peptidoglycan by transpeptidases was critical to the early studies on peptidoglycan machinery and synthesis (Figure 2.2).<sup>2-12</sup> These past efforts sparked a rededicated effort to understand physiological processes associated with peptidoglycan synthesis. Key events with respect to peptidoglycan biosynthesis are now well understood, and significant progress has been made in enzyme substrate mimicry to understand more complex mechanisms.<sup>12</sup>

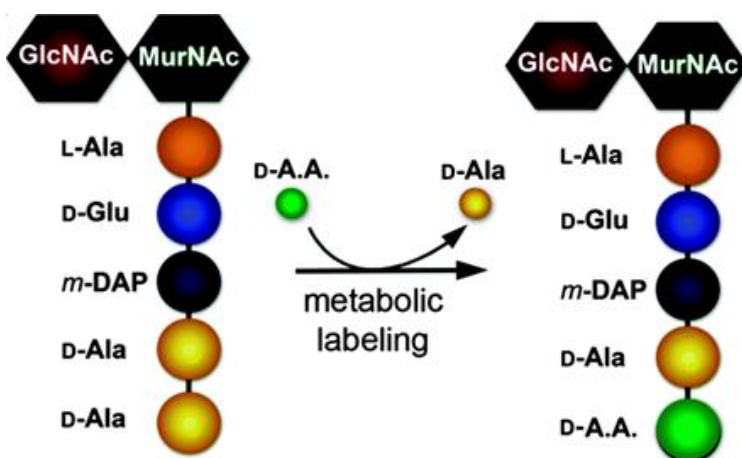


**Figure 2.2 D-Amino Acid Incorporation into Peptidoglycan.** Schematic representation of unnatural D-amino acid incorporation into the peptidoglycan stem peptide.

Fluorescent D-amino acids since then have been developed to tailor to photochemical needs and the biological system being studied. For example, it was shown that D-amino acids can be modified for enhanced solubility and be applied for high spatiotemporal STORM imaging to obtain virtual time-lapse images of peptidoglycan synthesis.<sup>13</sup> In another study, fluorescent D-amino acids were utilized to study peptidoglycan maturation and dynamics in *Mycobacterium tuberculosis* (*M. tuberculosis*). It was found that the transpeptidases associated with this pathogen are localized in compartments, showing variations in peptidoglycan synthesis at polar ends of the cell.<sup>14</sup> Modified peptidoglycan precursors have also been shown to hijack intracellular synthetic pathways to probe the

presence of peptidoglycan and the activity of enzymes associated with modifying precursors to become resistant to cell wall antibiotics.<sup>15-19</sup> In addition, to test the effectiveness of cell wall antibiotics simple assays were developed with coherent use of D-amino acids as probes of cell wall growth and morphology.<sup>20-22</sup>

Significant advances in these labeling techniques have allowed exploration of peptidoglycan and its implication in host-microbe interactions. Hudak and coworkers elegantly displayed a powerful approach in which D-amino acids can be utilized to visualize endogenous bacteria and their localization within a mammalian host.<sup>23</sup> Pinpointing infectious bacteria or microbiota location has implications in fundamental understanding of intestinal diseases and inflammatory responses. Our lab has recently applied peptidoglycan remodeling to study *Staphylococcus aureus* (*S. aureus*) bacterial colonization within *Caenorhabditis elegans*.<sup>24</sup> We showed that bacterial cell surfaces remodeled with tetrazine based D-amino acids can be manipulated for the fast trans-cyclooctene ligation of fluorophores to study *in vivo* cell wall reconstruction. Other similar bioorthogonal chemistries have been developed to remodel bacterial surfaces using azabicyclononene dienophiles.<sup>25</sup> The method of fluorescent D-amino acids labelling has also been developed to compare peptidoglycan and teichoic acid synthetic processes in a one-pot metabolic approach, showing real time differences in growth patterns.<sup>26</sup>

More recently, fluorescently tagged D-amino acids are now being utilized to track new sites of peptidoglycan synthesis and its co-localization with other cell wall components important for cell coordination.<sup>27</sup> For example, the correlation between peptidoglycan synthesis and activity of the bacterial protein FtsZ, a central component of cell division responsible for coordinating an assembly of cell wall proteins, was analyzed by the use of

a fluorescent D-amino acid analog.<sup>28-31</sup> Fluorescent probes were also applied toward the investigation of another crucial cell division protein, MreB.<sup>32,33</sup> These experiments showed through the use of these probes the consequential result of MreB inhibition and its role in proper bacterial shape for division.

Other enzymatic approaches of cell wall remodeling besides D-amino acid incorporation are also being investigated. Recent studies have hijacked the function of sortase A, a surface-bound transpeptidase enzyme that covalently attaches bacterial proteins onto the PG scaffold of most notably *S. aureus*. In anchoring proteins, sortase A recognizes the short, LPXTG peptide motif

(where X is any amino acid) and catalyzes the acyl-transfer onto lipid II of *S. aureus*.<sup>34-36</sup>

Speigel and co-workers showed that a fluorescein-tagged sortase peptide was metabolically incorporated into the bacterial cell surface.<sup>37</sup> Installment of a fluorescein molecules on the cell surface further led to bacterial opsonization by anti-fluorescein antibodies for as a potential immunomodulation strategy. Sabulski and co-workers improved sortase incorporation efficiency by combining the antibiotic cell wall targeting with the sortase sequence to covalently remodel the cell surface at lower dosages.<sup>38</sup> They showed that this combination led to high antibody recruitment at low micromolar concentrations, and also showed this metabolic process can be used to modify bacterial surfaces in live hosts. Another peptide substrate containing a VLK motif was discovered to be incorporated into the cell wall of *S. aureus*, shown to be independent of sortase activity providing yet another technique of remodeling bacterial cell surfaces.<sup>39</sup>

The carbohydrate backbone of bacterial peptidoglycan can also be metabolically labelled, adapting from the pioneering work of Bertozzi and Kiessling.<sup>40</sup> Efforts by Grimes

and colleagues selectively labelled *N*-acetyl-muramic acid residues with bioorthogonal derivatives to track mechanisms of cell wall recycling and immune system responses.<sup>41,42</sup> Bacterial cell consumption and visualization of glycan units of peptidoglycan upon macrophage engulfment can be useful to identify specific fragments that are broken down during infection. Similarly, another carbohydrate backbone derivative was synthesized to monitor peptidoglycan remodeling and cytoplasmic transport in the gram-negative pathogen *Pseudomonas aeruginosa*.<sup>43</sup>

### **2.3 Metabolic Probes for Carbohydrate Synthesis**

Bacterial surfaces contain a great diversity of glycans, including polysaccharides, glycoproteins, teichoic acids, and glycolipids. More recently, research has been dedicated towards the study of Mycobacterial pathogenesis and cell wall synthesis of carbohydrates. In order to develop more efficacious therapeutic treatments of pathogenic *M. tuberculosis*, the understanding of the mycobacteria cell envelope in both extracellular and intracellular bacteria is necessary. This class of bacteria have a peptidoglycan layer surrounded by glycolipids, arabinogalactan, and mycolic acids attached to trehalose disaccharides.<sup>44</sup> Fluorescent unnatural trehalose molecules have initially been developed to be incorporated through *M. tuberculosis* metabolic pathways for diagnostics.<sup>45-47</sup> Bertozzi and colleagues have applied trehalose metabolic labelling for visualization of antibiotic perturbations on mycobacterial cell envelope.<sup>48-50</sup> Other probes have been designed to be readily applied for high-throughput screening for inhibitors essential mycobacterial processes.<sup>51</sup>

Additional methods have been devised to label cell surface-associated glycans. More specifically, the outer membrane lipopolysaccharide (LPS) of pathogenic Gram-negative bacteria that contributes to virulence.<sup>23,52</sup> A chemical approach was shown to

enable selective imaging of Gram-negative and Gram-positive microbiota through the use of 3-deoxy-D-manno-octulosonic acid (KDO), a molecule selective for metabolic labelling of the outer surface LPS in Gram-negative bacteria.<sup>53</sup> Other components of the LPS core have been metabolically labeled as well. For instance, pseudaminic acid residues were remodeled with azido click chemistry handles for potential screening of agents inhibiting this biosynthetic pathway.<sup>54</sup> Chemical glycoengineering has also been extended beyond lipoglycans to glycoproteins. Azide-containing analogs of naturally abundant monosaccharide N-acetylglucosamine (GlcNAc) as well as rare bacterial monosaccharides FucNAc, bacillosamine, and DATDH that are exclusive to pathogenic strains such as *Helicobacter pylori* were synthesized and metabolic preferences explored.<sup>55</sup>

#### **2.4 Additional Bacterial Cell Surface Probes**

Bacterial cell surfaces are decorated with a plethora of proteins which can serve as effective targets for modulation of the bacterial envelope. The use of recombinant technology to incorporate cell surface modulations has provided a valuable platform for studying proteins within the cell wall. Labelling of bacterial proteins has been extensively investigated and applied in a wide range of techniques by use of orthogonal tRNA/aminoacyl-tRNA synthetase pairs that transfer a defined unnatural amino acid to a growing polypeptide chain.<sup>56</sup> More recently, an approach was utilized that metabolically labeled newly expressed bacterial surface proteins. Pezacki and co-workers employed bioorthogonal non-canonical amino acid tagging (BONCAT) to fluorescently detect surface proteins.<sup>57,58</sup> Endogenous methionine residues were replaced with homopropargylglycine to metabolically label surface proteins for subsequent click

chemistry with fluorophores. This method allowed for rapid screening and identification of living pathogenic bacteria.

Metabolic labeling of lipoproteins has also been an area of investigation in cell surface remodeling. These bacterial proteins are essential for membrane maintenance, transport, and signal transduction.<sup>59</sup> In one study, metabolically altered lipoproteins were biotinylated via copper catalyzed click chemistry, which provided a handle for selective pull down of metabolically labeled targets. Ensuing selective pulldown, proteomic analysis identified the lipoprotein targets and led to the discovery of lipoprotein modifications.<sup>59</sup> Other studies described an alkyne-modified trehalose monomycolate chemical reporter that can metabolically tag *O*-mycoloylated proteins in *Corynebacterium glutamicum*, a subgroup of mycobacteria.<sup>60,61</sup>

## **2.5 Conclusions and Future Outlook**

Metabolic labeling of the bacterial cell surface has yielded unique insights into growth, division, and enzyme dynamics. Only a small fraction of metabolic probes have been described in this review to provide powerful information of biosynthesis of peptidoglycan, carbohydrates, proteins, and lipids of the cell envelope. The incorporation of non-genetically encoded molecules using cell wall analogues has greatly advanced the field of microbiology within the past decade. Remodeling the cell surface has provided new directions of research that were previously unattainable. Our understanding of cell wall biosynthesis and dynamics is still in its infancy. Extraordinary breakthroughs remain with the use of cell surface probes, that hopefully may lead to solved long-standing mysteries and new therapeutics interventions. From herein, the focus of the remaining

chapter will concern the use of metabolic probes for the study of fundamental peptidoglycan processes.

## 2.6 References

- (1) Siegrist, M. S.; Swarts, B. M.; Fox, D. M.; Lim, S. A.; Bertozzi, C. R. *FEMS Microbiol Rev* **2015**, *39*, 184.
- (2) de Pedro, M. A.; Quintela, J. C.; Holtje, J. V.; Schwarz, H. *J Bacteriol* **1997**, *179*, 2823.
- (3) Cava, F.; de Pedro, M. A.; Lam, H.; Davis, B. M.; Waldor, M. K. *Embo J* **2011**, *30*, 3442.
- (4) Lupoli, T. J.; Tsukamoto, H.; Doud, E. H.; Wang, T. S.; Walker, S.; Kahne, D. *J Am Chem Soc* **2011**, *133*, 10748.
- (5) Kuru, E.; Hughes, H. V.; Brown, P. J.; Hall, E.; Tekkam, S.; Cava, F.; de Pedro, M. A.; Brun, Y. V.; VanNieuwenhze, M. S. *Angew Chem Int Ed Engl* **2012**, *51*, 12519.
- (6) Fura, J. M.; Kearns, D.; Pires, M. M. *J Biol Chem* **2015**, *290*, 30540.
- (7) Fura, J. M.; Sabulski, M. J.; Pires, M. M. *ACS Chem Biol* **2014**, *9*, 1480.
- (8) Pidgeon, S. E.; Fura, J. M.; Leon, W.; Birabaharan, M.; Vezenov, D.; Pires, M. M. *Angew Chem Int Ed Engl* **2015**, *54*, 6158.
- (9) Lebar, M. D.; May, J. M.; Meeske, A. J.; Leiman, S. A.; Lupoli, T. J.; Tsukamoto, H.; Losick, R.; Rudner, D. Z.; Walker, S.; Kahne, D. *J Am Chem Soc* **2014**, *136*, 10874.
- (10) Lam, H.; Oh, D. C.; Cava, F.; Takacs, C. N.; Clardy, J.; de Pedro, M. A.; Waldor, M. K. *Science* **2009**, *325*, 1552.
- (11) Siegrist, M. S.; Whiteside, S.; Jewett, J. C.; Aditham, A.; Cava, F.; Bertozzi, C. R. *ACS Chem Biol* **2013**, *8*, 500.
- (12) Gautam, S.; Kim, T.; Shoda, T.; Sen, S.; Deep, D.; Luthra, R.; Ferreira, M. T.; Pinho, M. G.; Spiegel, D. A. *Angew Chem Int Ed Engl* **2015**, *54*, 10492.
- (13) Hsu, Y. P.; Rittichier, J.; Kuru, E.; Yablonowski, J.; Pasciak, E.; Tekkam, S.; Hall, E.; Murphy, B.; Lee, T. K.; Garner, E. C.; Huang, K. C.; Brun, Y. V.; VanNieuwenhze, M. S. *Chem Sci* **2017**, *8*, 6313.
- (14) Botella, H.; Yang, G.; Ouerfelli, O.; Ehrt, S.; Nathan, C. F.; Vaubourgeix, J. *MBio* **2017**, *8*.
- (15) Liechti, G. W.; Kuru, E.; Hall, E.; Kalinda, A.; Brun, Y. V.; VanNieuwenhze, M.; Maurelli, A. T. *Nature* **2014**, *506*, 507.
- (16) Pidgeon, S. E.; Pires, M. M. *ACS Chem Biol* **2017**, *12*, 1913.
- (17) Pidgeon, S. E.; Pires, M. M. *Angew Chem Int Ed Engl* **2017**, *56*, 8839.
- (18) Garcia-Heredia, A.; Pohane, A. A.; Melzer, E. S.; Carr, C. R.; Fiolek, T. J.; Rundell, S. R.; Chuin Lim, H.; Wagner, J. C.; Morita, Y. S.; Swarts, B. M.; Siegrist, M. S. *Elife* **2018**, *7*.
- (19) Zhang, J. Y.; Lin, G. M.; Xing, W. Y.; Zhang, C. C. *Front Microbiol* **2018**, *9*, 791.
- (20) Sugimoto, A.; Maeda, A.; Itto, K.; Arimoto, H. *Sci Rep* **2017**, *7*, 1129.
- (21) Morales Angeles, D.; Liu, Y.; Hartman, A. M.; Borisova, M.; de Sousa Borges, A.; de Kok, N.; Beilharz, K.; Veening, J. W.; Mayer, C.; Hirsch, A. K.; Scheffers, D. J. *Mol Microbiol* **2017**, *104*, 319.



- (22) Dajkovic, A.; Tesson, B.; Chauhan, S.; Courtin, P.; Keary, R.; Flores, P.; Marliere, C.; Filipe, S. R.; Chapot-Chartier, M. P.; Carballido-Lopez, R. *Mol Microbiol* **2017**, *104*, 972.
- (23) Hudak, J. E.; Alvarez, D.; Skelly, A.; von Andrian, U. H.; Kasper, D. L. *Nat Microbiol* **2017**, *2*, 17099.
- (24) Pidgeon, S. E.; Pires, M. M. *Bioconjug Chem* **2017**, *28*, 2310.
- (25) Siegl, S. J.; Vazquez, A.; Dzijak, R.; Dracinsky, M.; Galeta, J.; Rampmaier, R.; Klepetarova, B.; Vrabel, M. *Chemistry* **2018**, *24*, 2426.
- (26) Bonnet, J.; Wong, Y. S.; Vernet, T.; Di Guilmi, A. M.; Zapun, A.; Durmort, C. *ACS Chem Biol* **2018**, *13*, 2010.
- (27) Monteiro, J. M.; Fernandes, P. B.; Vaz, F.; Pereira, A. R.; Tavares, A. C.; Ferreira, M. T.; Pereira, P. M.; Veiga, H.; Kuru, E.; VanNieuwenhze, M. S.; Brun, Y. V.; Filipe, S. R.; Pinho, M. G. *Nat Commun* **2015**, *6*, 8055.
- (28) Yang, X.; Lyu, Z.; Miguel, A.; McQuillen, R.; Huang, K. C.; Xiao, J. *Science* **2017**, *355*, 744.
- (29) Bisson-Filho, A. W.; Hsu, Y. P.; Squyres, G. R.; Kuru, E.; Wu, F.; Jukes, C.; Sun, Y.; Dekker, C.; Holden, S.; VanNieuwenhze, M. S.; Brun, Y. V.; Garner, E. C. *Science* **2017**, *355*, 739.
- (30) Yao, Q.; Jewett, A. I.; Chang, Y. W.; Oikonomou, C. M.; Beeby, M.; Iancu, C. V.; Briegel, A.; Ghosal, D.; Jensen, G. J. *Embo J* **2017**, *36*, 1577.
- (31) Pereira, A. R.; Hsin, J.; Krol, E.; Tavares, A. C.; Flores, P.; Hoiczky, E.; Ng, N.; Dajkovic, A.; Brun, Y. V.; VanNieuwenhze, M. S.; Roemer, T.; Carballido-Lopez, R.; Scheffers, D. J.; Huang, K. C.; Pinho, M. G. *MBio* **2016**, *7*.
- (32) Liechti, G.; Kuru, E.; Packiam, M.; Hsu, Y. P.; Tekkam, S.; Hall, E.; Rittichier, J. T.; VanNieuwenhze, M.; Brun, Y. V.; Maurelli, A. T. *PLoS Pathog* **2016**, *12*, e1005590.
- (33) Schirner, K.; Eun, Y. J.; Dion, M.; Luo, Y.; Helmann, J. D.; Garner, E. C.; Walker, S. *Nat Chem Biol* **2015**, *11*, 38.
- (34) Marraffini, L. A.; Dedent, A. C.; Schneewind, O. *Microbiol Mol Biol Rev* **2006**, *70*, 192.
- (35) Kruger, R. G.; Otvos, B.; Frankel, B. A.; Bentley, M.; Dostal, P.; McCafferty, D. G. *Biochemistry* **2004**, *43*, 1541.
- (36) Nelson, J. W.; Chamessian, A. G.; McEnaney, P. J.; Murelli, R. P.; Kazmierczak, B. I.; Spiegel, D. A. *ACS Chem Biol* **2010**, *5*, 1147.
- (37) Gautam, S.; Kim, T.; Lester, E.; Deep, D.; Spiegel, D. A. *ACS Chem Biol* **2016**, *11*, 25.
- (38) Sabulski, M. J.; Pidgeon, S. E.; Pires, M. M. *Chem Sci* **2017**, *8*, 6804.
- (39) Hansenova Manaskova, S.; Bikker, F. J.; Nazmi, K.; van Zuidam, R.; Slotman, J. A.; van Cappellen, W. A.; Houtsmuller, A. B.; Veerman, E. C.; Kaman, W. E. *Bioconjug Chem* **2016**, *27*, 2418.
- (40) Bertozzi, C. R.; Kiessling, L. L. *Science* **2001**, *291*, 2357.
- (41) Liang, H.; DeMeester, K. E.; Hou, C. W.; Parent, M. A.; Caplan, J. L.; Grimes, C. L. *Nat Commun* **2017**, *8*, 15015.
- (42) DeMeester, K. E.; Liang, H.; Jensen, M. R.; Jones, Z. S.; D'Ambrosio, E. A.; Scinto, S. L.; Zhou, J.; Grimes, C. L. *J Am Chem Soc* **2018**, *140*, 9458.

- (43) Perley-Robertson, G. E.; Yadav, A. K.; Winogrodzki, J. L.; Stubbs, K. A.; Mark, B. L.; Vocadlo, D. J. *ACS Chem Biol* **2016**, *11*, 2626.
- (44) Thanna, S.; Sucheck, S. J. *Medchemcomm* **2016**, *7*, 69.
- (45) Backus, K. M.; Boshoff, H. I.; Barry, C. S.; Boutureira, O.; Patel, M. K.; D'Hooge, F.; Lee, S. S.; Via, L. E.; Tahlan, K.; Barry, C. E., 3rd; Davis, B. G. *Nat Chem Biol* **2011**, *7*, 228.
- (46) Swarts, B. M.; Holsclaw, C. M.; Jewett, J. C.; Alber, M.; Fox, D. M.; Siegrist, M. S.; Leary, J. A.; Kalscheuer, R.; Bertozzi, C. R. *J Am Chem Soc* **2012**, *134*, 16123.
- (47) Foley, H. N.; Stewart, J. A.; Kavunja, H. W.; Rundell, S. R.; Swarts, B. M. *Angew Chem Int Ed Engl* **2016**, *55*, 2053.
- (48) Rodriguez-Rivera, F. P.; Zhou, X.; Theriot, J. A.; Bertozzi, C. R. *Angew Chem Int Ed Engl* **2018**, *57*, 5267.
- (49) Rodriguez-Rivera, F. P.; Zhou, X.; Theriot, J. A.; Bertozzi, C. R. *J Am Chem Soc* **2017**, *139*, 3488.
- (50) Kamariza, M.; Shieh, P.; Ealand, C. S.; Peters, J. S.; Chu, B.; Rodriguez-Rivera, F. P.; Babu Sait, M. R.; Treuren, W. V.; Martinson, N.; Kalscheuer, R.; Kana, B. D.; Bertozzi, C. R. *Sci Transl Med* **2018**, *10*.
- (51) Hodges, H. L.; Brown, R. A.; Crooks, J. A.; Weibel, D. B.; Kiessling, L. L. *Proc Natl Acad Sci U S A* **2018**, *115*, 5271.
- (52) Dumont, A.; Malleron, A.; Awwad, M.; Dukan, S.; Vauzeilles, B. *Angew Chem Int Ed Engl* **2012**, *51*, 3143.
- (53) Wang, W.; Zhu, Y.; Chen, X. *Biochemistry* **2017**, *56*, 3889.
- (54) Andolina, G.; Wei, R.; Liu, H.; Zhang, Q.; Yang, X.; Cao, H.; Chen, S.; Yan, A.; Li, X. D.; Li, X. *ACS Chem Biol* **2018**.
- (55) Clark, E. L.; Emmadi, M.; Krupp, K. L.; Podilapu, A. R.; Helble, J. D.; Kulkarni, S. S.; Dube, D. H. *ACS Chem Biol* **2016**, *11*, 3365.
- (56) Wang, L.; Brock, A.; Herberich, B.; Schultz, P. G. *Science* **2001**, *292*, 498.
- (57) Mahdavi, A.; Szychowski, J.; Ngo, J. T.; Sweredoski, M. J.; Graham, R. L.; Hess, S.; Schneewind, O.; Mazmanian, S. K.; Tirrell, D. A. *Proc Natl Acad Sci U S A* **2014**, *111*, 433.
- (58) Sherratt, A. R.; Rouleau, Y.; Luebbert, C.; Strmiskova, M.; Veres, T.; Bidawid, S.; Corneau, N.; Pezacki, J. P. *Cell Chem Biol* **2017**, *24*, 1048.
- (59) Rangan, K. J.; Yang, Y. Y.; Charron, G.; Hang, H. C. *J Am Chem Soc* **2010**, *132*, 10628.
- (60) Kavunja, H. W.; Piligian, B. F.; Fiolek, T. J.; Foley, H. N.; Nathan, T. O.; Swarts, B. M. *Chem Commun (Camb)* **2016**, *52*, 13795.
- (61) Issa, H.; Huc-Claustre, E.; Reddad, T.; Bonade Bottino, N.; Tropis, M.; Houssin, C.; Daffe, M.; Bayan, N.; Dautin, N. *PLoS One* **2017**, *12*, e0171955.

## Chapter 3

### Metabolic Profiling of Bacteria by Unnatural C-terminated D-Amino Acids

#### **3.1 Abstract**

Bacterial peptidoglycan is a mesh-like network comprised of sugars and oligopeptides. Transpeptidases cross-link peptidoglycan oligopeptides to provide vital cell wall rigidity and structural support. It was recently discovered that the same transpeptidases catalyze the metabolic incorporation of exogenous D-amino acids onto bacterial cell surfaces with vast promiscuity for the side-chain identity. It is now shown that this enzymatic promiscuity is not exclusive to side chains, but that C-terminus variations can also be accommodated across a diverse range of bacteria. Atomic force microscopy analysis revealed that the incorporation of C-terminus amidated D-amino acids onto bacterial surfaces substantially reduced the cell wall stiffness. We exploited the promiscuity of bacterial transpeptidases to develop a novel assay for profiling different bacterial species.

#### **3.2 Introduction**

Tremendous strides have been made in the treatment and prevention of bacterial infections. However, two major hurdles in diagnostics continue to impede further progress: identification of the type of bacteria and the level of drug resistance. These two time-sensitive components often dictate the course of treatment. Methods that improve our ability to address these needs may have significant clinical utility. We envisioned a peptidoglycan metabolic labeling strategy that could form the basis of a precise and facile diagnostic test to determine these two components in a single step. Many enzymatic transformations are necessary to properly assemble the peptidoglycan precursors. The

lipid-anchored peptidoglycan precursors are then flipped to the outside of the cytoplasmic membrane where they are incorporated onto the growing peptidoglycan matrix. These covalent modifications are crucial for tuning the physical and mechanical properties of the peptidoglycan. The amount and nature of these modifications are inherently linked to the type of bacteria and may also be related to phenotypic differences within these species. Chemical modifications of the peptidoglycan can mainly be attributed to the enzymatic processes by penicillin binding proteins (PBPs). The transpeptidase domains of PBPs are responsible for the cross-linking of neighboring stem peptides, a function that endows the peptidoglycan with increased rigidity and strength.<sup>1</sup> The cross-linking of the peptidoglycan is vital to bacteria. Interference with this process via  $\beta$ -lactam and glycopeptide treatment is lethal to many bacteria.<sup>2</sup> Recently, an alternate reaction of transpeptidase was discovered whereby terminal D-alanines were “swapped” with D-amino acids from the surrounding medium (Figure 3.1a).<sup>3</sup> We and others have recently demonstrated that bacterial cell surfaces can be labeled with unnatural D-amino acids with expansive promiscuity in the identity of the side chain.<sup>3-11</sup> This led us to explore the possibility that non-native C-terminal variants are competent transpeptidase substrates (Figure 3.1b). Furthermore, we hypothesized that species- and strain-specific variations in the physical composition of the peptidoglycan (for example, thickness, charge, and cross-linking level) and peptidoglycan processing (for example, transpeptidase and carboxypeptidase domains of PBPs) could be probed and profiled with these C-terminal variants. Herein, we show that non-native C-terminated D-amino acids are incorporated onto bacterial cell surfaces. Most importantly, these variants may provide a facile and sensitive platform to differentiate between bacterial species and phenotypes within individual species.

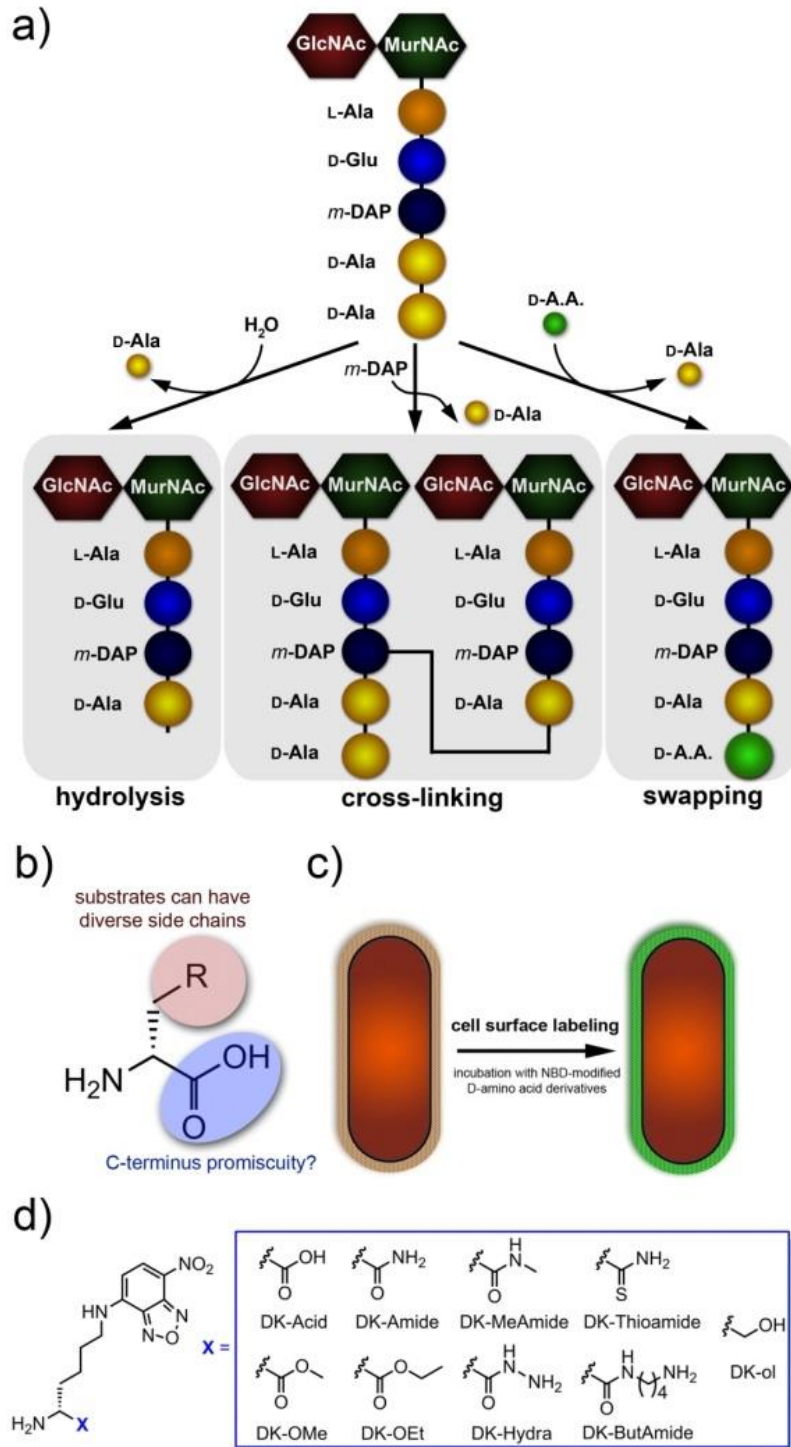


**Figure 3.1** a) Schematic representation of the peptidoglycan processing by PBP transpeptidase. b) Basic unit of D-amino acid and derivatives that have been shown to be tolerated. c) Schematic representation of the assay to assess D-amino acid incorporation. d) Chemical structures of D-amino acid derivatives synthesized and evaluated.

### **3.3 Results and Discussion**

#### **3.3.1 Incorporation of Non-native C-terminated D-Amino Acids**

Initially, we synthesized a panel of fluorescently labeled D-amino acid derivatives to probe the promiscuity of the C-terminus by PBP transpeptidases (Figure 3.1d). The fluorescent nitrobenzoxadiazole (NBD) was chosen for its small size and we had previously shown that the native D-lysine (DK) carboxylic acid version (DK-Acid) is readily incorporated onto the surface of bacteria.<sup>11</sup> This panel of variants was designed to allow the interrogation of the heteroatom specificity at the C-terminus, a requirement of a carbonyl group, and the ability to accommodate bulky functional groups.

We first evaluated the relative incorporation levels of the various D-amino acid derivatives using the Gram-positive bacterium *Bacillus subtilis* (*B. subtilis*)  $\Delta$ dacA, which lacks the carboxypeptidase gene (*dacA*).<sup>12</sup> The *dacA* PBP carboxypeptidase enzyme catalyzes the hydrolysis of the fifth position D-alanine, thus effectively reducing the overall level of incorporation by exogenously supplemented D-amino acids. *B. subtilis* cells were incubated in the presence of the C-terminus variants from our panel of compounds and incorporation levels were quantified based on the NBD fluorescence using flow cytometry. As we had previously observed, the carboxylic acid variant (DK-Acid) is readily incorporated onto the bacterial surface (Figure 3.2a).

Next, we probed the requirement of a negatively charged terminus by evaluating the neutral D-amino carboxamide derivative (DK-Amide). Remarkably, the incubation with DK-Amide led to a nearly two-fold increase in incorporation levels compared to DK-Acid.<sup>10</sup> It is interesting to note that vegetative *B. subtilis* cells naturally possess a high level of amidated *meso*-diaminopimelic acid (*m*-DAP), which becomes the acyl acceptor upon

cross-linking (Figure 3.1A).<sup>13,14</sup> Therefore, the final cross-linked product will also have a carboxamide group at the same location as the amide of a peptidoglycan swapped with D-amino carboxamide. The similarly charged and sized carbothioamide variant (DK-Thioamide) highlights the importance of an oxygen atom at the carbonyl position for *B. subtilis* PBP transpeptidase. This requirement for the presence of a carbonyl group was further probed by the incubation of cells with a variant lacking carbonyl (DK-ol). The loss of fluorescence signal suggests that the carbonyl group is essential for substrate recognition by PBP transpeptidase. A slight increase in steric bulk in the

amidated terminus (DK-MeAmide) proved to be deleterious for surface labeling of *B. subtilis*, with a near complete loss of incorporation. The intolerance of the methyl group in DK-MeAmide suggests that the lack of charge and steric bulkiness combine to endow the compound with incompatible attributes as a substrate for transpeptidase-mediated

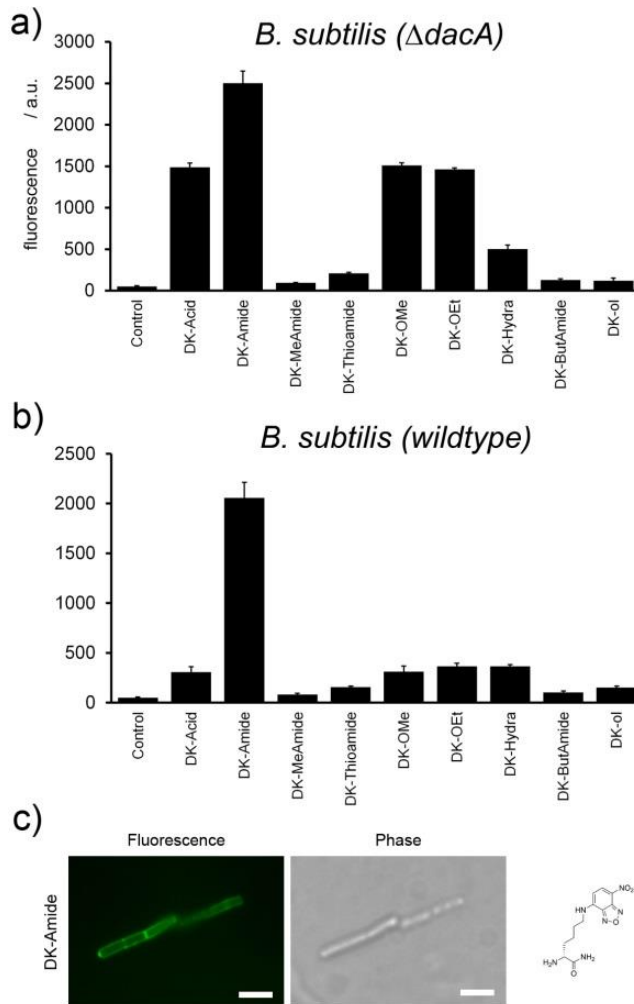


**Figure 3.2. Incorporation of D-amino acid derivatives.** Flow cytometry analysis of *B. subtilis*  $\Delta dacA$  (a) and wildtype *B. subtilis* (b) incubated overnight in the presence of 100  $\mu\text{M}$  of stated compounds. Data are represented as mean + SD (n=3). c) Fluorescence and differential interference contrast (DIC) microscopy imaging of *B. subtilis* wildtype cells labeled overnight with 200  $\mu\text{M}$  DK-Amide. Scale bar represents 3  $\mu\text{m}$ .

swapping. The basic amide scaffold was investigated further by the extension of four methylene units with a terminal amino group (DK-ButAmide). This perturbation led to a complete loss of incorporation, which is presumably due to the size and charge reversal of the terminal modification.

The introduction of an additional amino group (DK-Hydra), generating a modification similar in size to methyl-amide, mostly restored the ability of the molecule to be incorporated onto bacterial surfaces (Figure 3.2). The site-specific surface display of hydrazide moieties provided by DK-Hydra should be compatible with bio-orthogonal chemistries involving complementary aldehyde/ketone groups, thus opening up the possibility of the installation of a second and distinct molecule on the surface.<sup>15-18</sup> The esterification of the D-amino acid to the neutral C-terminus DK-OMe is also well tolerated as indicated by the level of surface labeling. The homologation of the methyl ester (DK-OEt) yielded a slightly bulkier variant that labeled bacteria to a comparable level to DK-OMe. As expected, the presence of *dacA* causes a reduction in incorporation levels for several of the D-amino acid variants (Figure 3.2B).

### **3.3.2 Confirmation of D-Amino Acid Incorporation**

In order to confirm that the observed fluorescence signal was a result of the replacement of surface bound D-alanine with exogenously supplied D-amino acid variants, we performed a series of secondary assays. First, the stereospecificity of the labeling process was evaluated by monitoring the surface labeling with enantiomeric counterparts LK-Acid, LK-Amide, LK-OMe (Figure 3.3). Minimal fluorescence levels were observed for the L-amino acid derivatives, thus highlighting the importance of the stereochemistry in the transpeptidase mediated swapping.



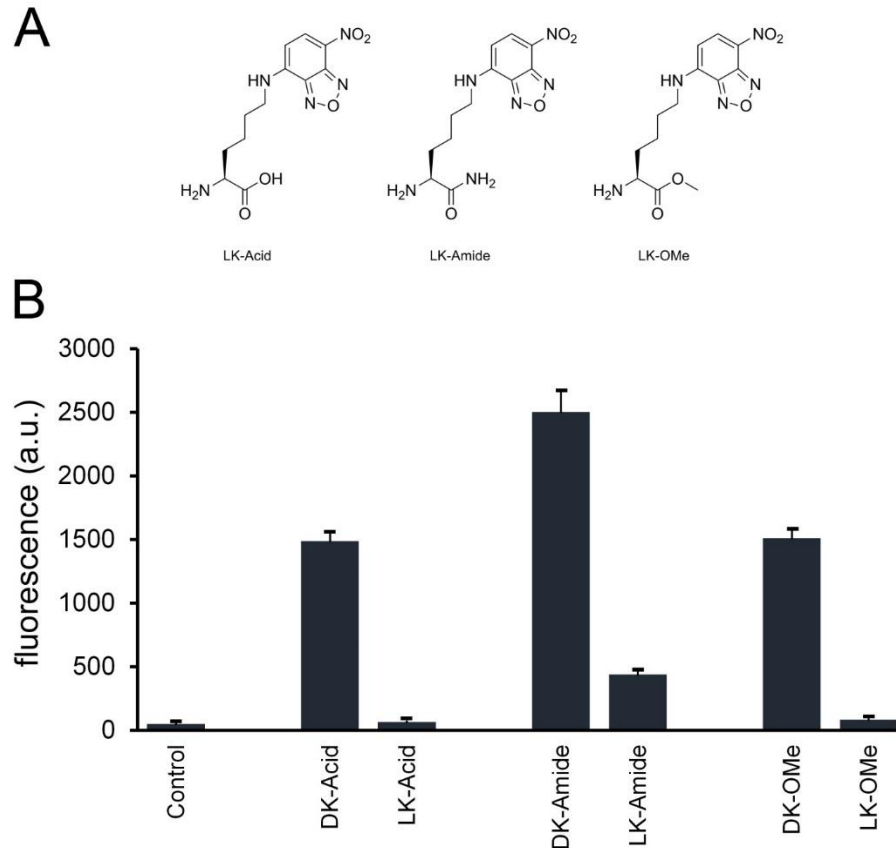


**Figure 3.3. Stereospecificity of incorporation.** (A) Chemical structures of LK-Acid, LK-Amide, and LK-OMe. (B) Flow cytometry analysis of *B. subtilis*  $\Delta$ dacA incubated overnight in the presence of 100  $\mu$ M of DK-Acid, LK-Acid, DK-Amide, LK-Amide, DK-OMe, and LK-OMe. Data are represented as mean + SD (n=3).

To further demonstrate that these D-amino acid variants were indeed incorporated on the bacterial surface we treated labeled cells with dithionite, which readily reduces the NBD nitro group to a non-fluorescent aryl amine derivative. Dithionite was chosen as the reducing agent because of its poor lipid bilayer permeation, limiting the quenching to NBD moieties present on the extracellular space of gram-positive bacteria (Figure 3.4). *B. subtilis* cells were labeled with D-amino acid variants and subsequently treated with dithionite. This reducing agent treatment led to a complete loss of fluorescence signal. The results suggest that these D-amino acid variants reside in the extracellular space of bacteria – consistent with their incorporation within the peptidoglycan.

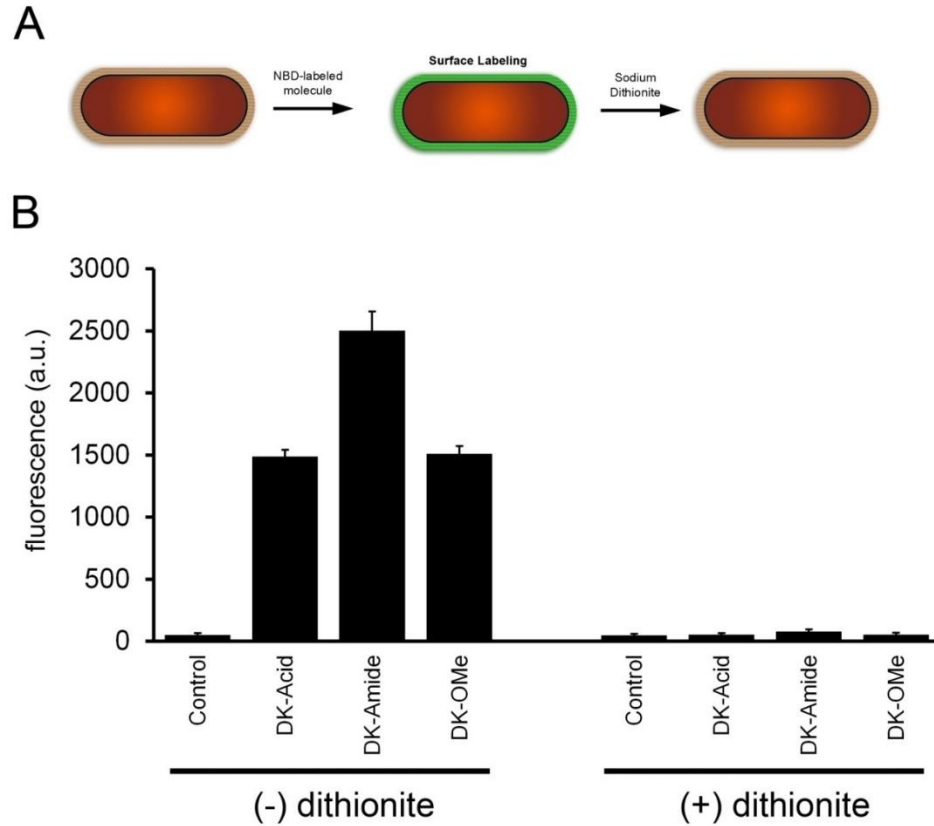


**Figure 3.4.** (A) Schematic representation of the quenching of surface exposed NBD moieties to the highly polar reductant dithionite. (B) *B. subtilis*  $\Delta dacA$  were labeled overnight with 100  $\mu\text{M}$  of D-amino acid derivative and analyzed by flow cytometry. Cellular fluorescence was quantified with and without a treatment of 5 mM sodium dithionite. Data are represented as mean + SD (n=3).

To delineate the localization of D-amino acid variants, *B. subtilis* were visualized using fluorescence microscopy following overnight labeling with DK-Amide and a variant displaying a larger tetramethylrhodamine fluorophore (DK-TAMRA-Amide). Cells displayed slightly elevated septal labeling with both variants, consistent with previous reports on peptidoglycan

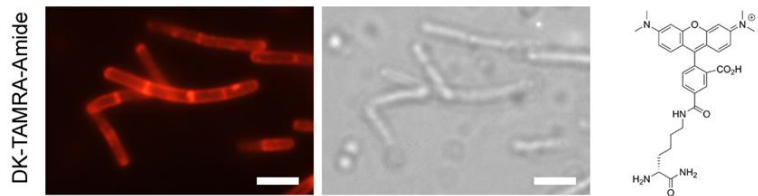


**Figure 3.5. Fluorescence and differential interference contrast (DIC) microscopy imaging of *B. subtilis* wildtype cells labeled overnight with 200  $\mu\text{M}$  DK-TAMRA-Amide. Scale bar represents 3  $\mu\text{m}$ .**

biosynthesis (Figure 3.5).

Finally, to further confirm that D-amino acid variants were indeed covalently attached to the peptidoglycan, we isolated and characterized the peptidoglycan from *B. subtilis* grown in the presence of DK-Amide. Following separation by RP-HPLC, the sample was analyzed by MALDI-TOF and was found to have a molecular weight consistent with the swapping of the terminal D-alanine by DK-Amide (Figure 3.6A). We also found that (using the NBD absorbance as a handle) isolated peptidoglycan displayed an absorbance profile consistent with the incorporation of DK-Amide (Figure 3.6B). These data confirm that the unnatural C-terminated DK-Amide is metabolically incorporated within the bacterial peptidoglycan.

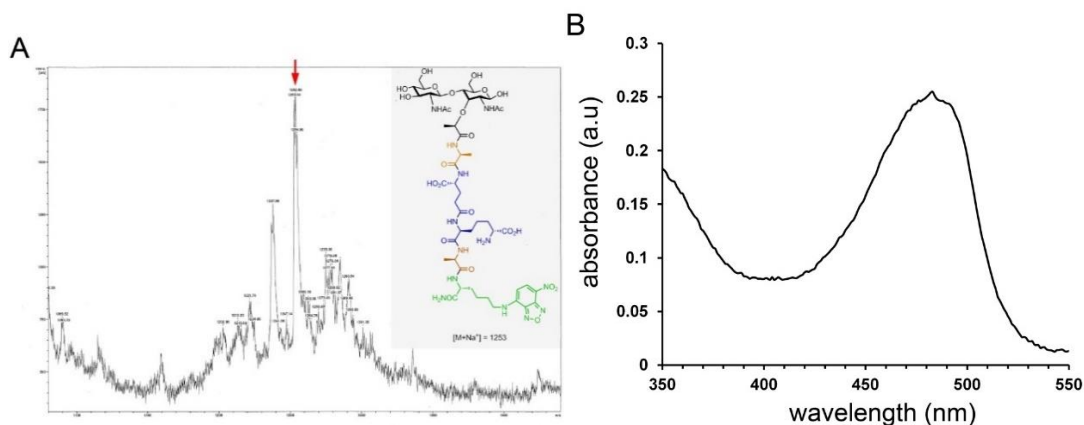


**Figure 3.6.** (A) MALDI-TOF analysis of peptidoglycan isolated from *B. subtilis* cells labeled with DK-Amide following RP-HPLC separation. Inset: structure of expected peptidoglycan repeating unit with the inclusion of DK-Amide and the expected molecular weight. (B) UV-Vis profile of the crude clarified peptidoglycan isolated from *B. subtilis* cells incubated with 500  $\mu$ M of DK-Amide.

Next, we set out to demonstrate that side-chains other than NBD modified lysine could be tolerated by transpeptidase. *B. subtilis* (wildtype and  $\Delta$ dacA) were incubated overnight in the presence of D-Cys-OH, D-Cys-NH<sub>2</sub>, and D-Cys-OMe (Figure 3.7). Surface-bound cysteine residues were then quantified via the reaction with maleimide

activated AlexaFluor 647. Cells labeled with all three cysteine variants displayed a considerable increase in fluorescence compared to control cells, a clear indication that these compounds also modify the surface of bacterial cells. In *B. subtilis*  $\Delta$ dacA, a trend reversal was observed in incorporation efficiency with the methyl ester derivative compared to the DK-OMe. The esterification of C-terminus D-cysteine led to a two-fold increase in labeling compared to D-Cys-OH and approximately a fifty percent increase compared to D-Cys-NH<sub>2</sub>. These results show that the recognition of the D-amino acid side chain does not entirely dictate the incorporation efficiency of unusually terminated D-amino acids. Therefore, our findings suggest that it is possible to modulate bacterial cell surface labeling of tailor-made D-amino acids via changes to the C-terminus.

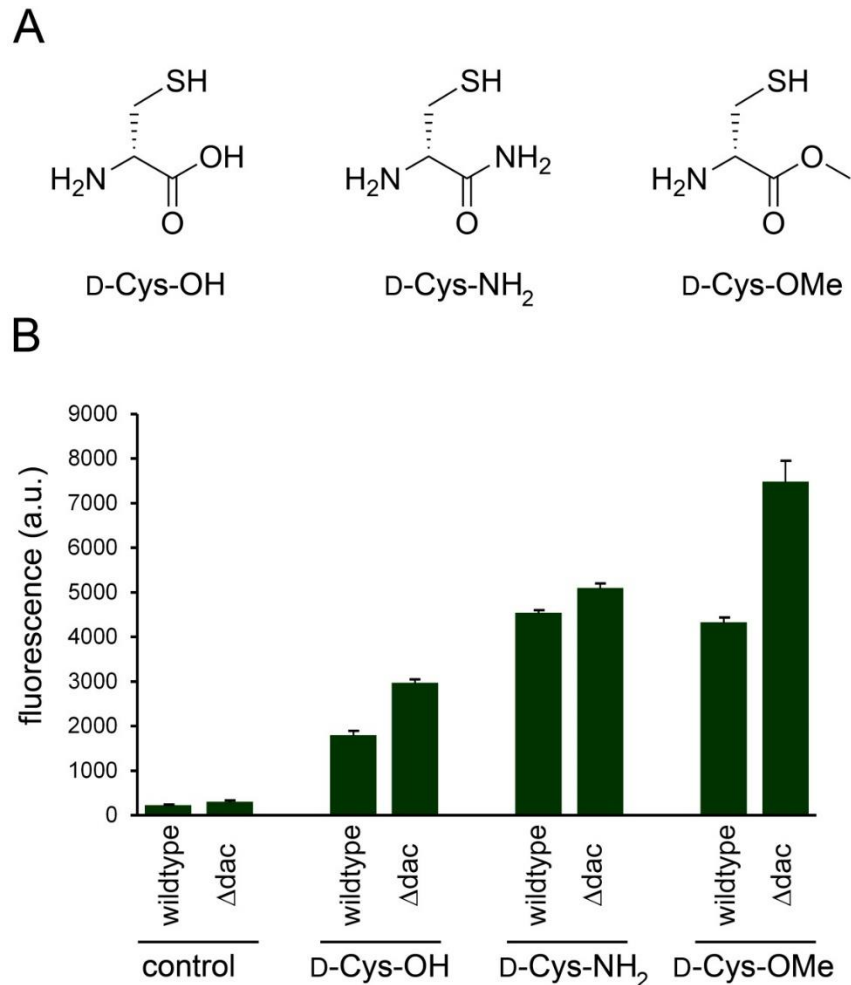


**Figure 3.7. Modification of the C-terminus of D-cysteine.** (A) Chemical structures of D-Cys-OH, D-Cys-NH<sub>2</sub>, and D-Cys-OMe. (B) *B. subtilis*  $\Delta$ dacA and wildtype were incubated with 1 mM of the specified D-cysteine derivative or without any added D-amino acid. The cells were subsequently labeled with 50  $\mu$ M of maleimide activated AlexaFluor 647 for 30 min and the fluorescence was quantified using flow cytometry. Data are represented as mean + SD (n=3).

### 3.3.3 Growth Phase effect of D-Amino Acid Incorporation

After establishing that bacterial surfaces can be labeled with unnaturally C-terminated D-amino acids, we set out to determine whether incorporation efficiency was linked to the bacterial growth phase. Bacteria possess a range of PBPs that must act in concert to respond to fluctuating environmental conditions such as nutrient availability and

life cycle stage. The expression of PBPs is highly regulated with both temporal and spatial control to coordinate peptidoglycan synthesis, maturation, and recycling. Likewise, the swapping of D-alanine from the peptidoglycan has been previously theorized to play a role in stationary phase cell wall remodeling.<sup>19</sup> We set out to probe these effects by using our panel of D-amino acid variants. The incorporation levels for *B. subtilis*  $\Delta$ dacA cells incubated with the compounds for the same amount of time either at stationary phase or at early log phase were measured (Figure 3.8). Consistent with the proposed role in stationary phase cell wall

remodeling, all D-amino acid variants (except DK-Amide) displayed similar (or better)

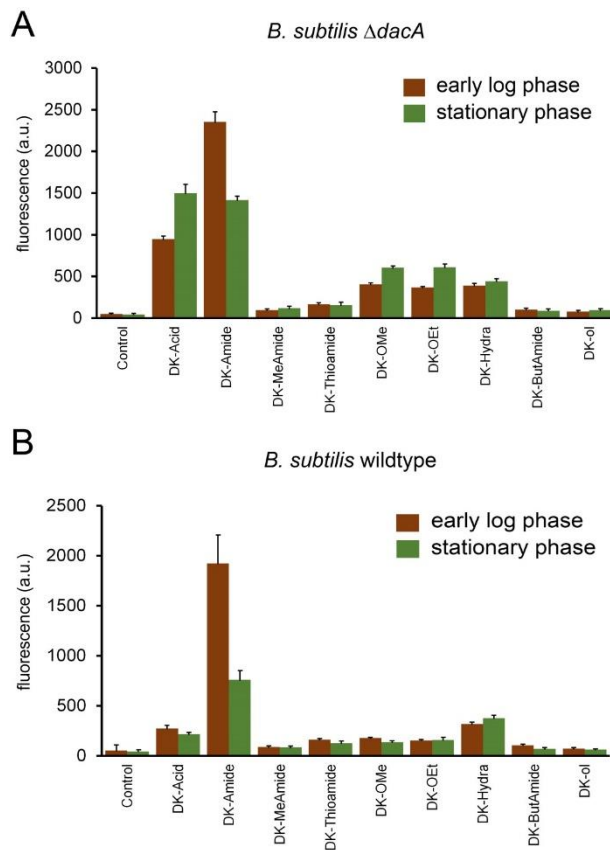


**Figure 3.8.** *B. subtilis*  $\Delta$ dacA (A) and *B. subtilis* wildtype (B) were labeled for 5 hours either at stationary phase or at early log phase. Data are represented as mean + SD (n=3).

incorporation in the stationary phase. The reversal in trend for DK-Amide could potentially be linked to its mimicry of amidated m-DAP, which would be a preferred pathway from the activated acyl-intermediate during the elevated peptidoglycan biosynthesis in the log phase. The  $\Delta$ dacA mutant strain of *B. subtilis* has proven to be a versatile organism for assessing the incorporation of unnatural D-amino acids since PBP carboxypeptidase can reduce overall signals by shortening the stem peptide. However, we reasoned that we could gain additional insight into the interplay between D-amino acid swapping, crosslinking, and hydrolysis by monitoring the incorporation in wildtype *B. subtilis*. Incubation of wildtype cells with the panel of variants demonstrated that there is a substantial difference in labeling between the two strains. For most of the variants, there was a considerable decrease in incorporation levels, except for DK-Amide and DK-Hydra, which remained virtually unchanged for the early log phase. In fact, DK-Hydra labeled wildtype cells at the same efficiency as DK-Acid. The change in relative incorporation between two strains of the same bacterial species indicates that modifying the C-terminus may be a feasible method for tuning the retention of the D-amino acid derivative once it is loaded on the stem peptide.

### **3.3.4 Amidation Effects on Crosslinking**

Next, we set out to determine the possible consequences of D-Ala-NH<sub>2</sub> mediated inhibition of transpeptidase crosslinking. We reasoned that inhibition of crosslinking by the incubation with D-Ala-NH<sub>2</sub> should modulate the overall porosity of the peptidoglycan and that this change could be monitored by a permeation probe. The overnight pre-incubation of *B. subtilis* cells with D-Ala-NH<sub>2</sub> followed by the exposure to FITC-labeled poly-L-lysine (hydrodynamic diameter of 2.5-7.5 nm) led to a marked increase in cell-

associated fluorescence compared to D-Ala-OH and control cells (Figure 3.9). The increase in fluorescence is consistent with a peptidoglycan structure that has greater accessibility to large macromolecules. The inhibition of peptidoglycan crosslinking by the conversion of the C-terminus to carboxamide has implications not only on surface porosity but it could potentially modulate the peptidoglycan stiffness as well.

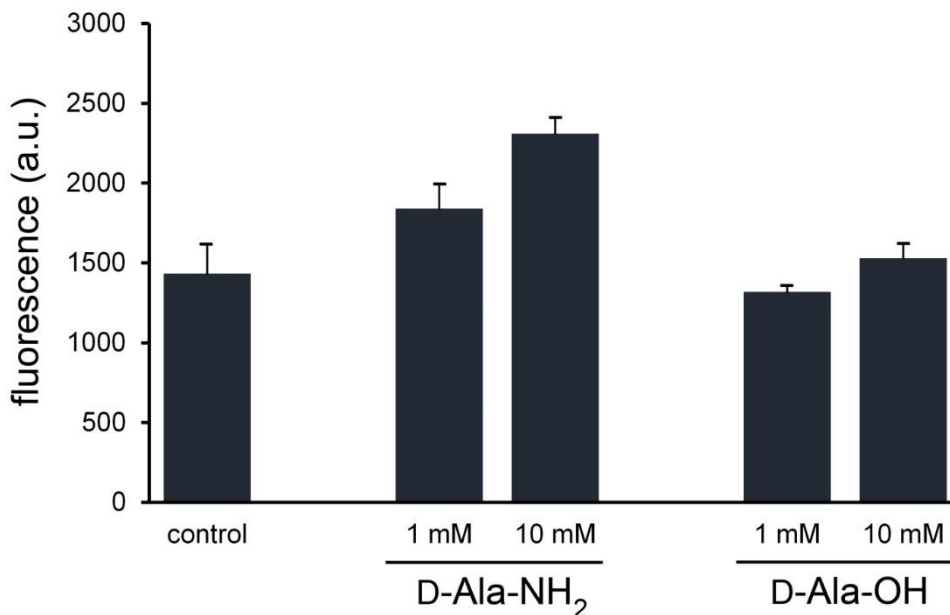


**Figure 3.9. Porosity of peptidoglycan.** *B. subtilis* wildtype cells first incubated overnight with either 1 mM or 10 mM of D-Ala-NH<sub>2</sub> or D-Ala-OH. Cells were then briefly incubated with 0.3  $\mu$ M of FITC-labeled poly-L-lysine. Association with the fluorescently labeled polymer was monitored using flow cytometry. Data are represented as mean + SD (n=3).

### **3.3.5 Kinetics of D-Amino Acid Incorporation**

The elevated incorporation levels observed with DK-Amide were explored next. Kinetics of incorporation and retention of labeling showed that DK-Amide is incorporated faster than DK-Acid and it was retained on the surface for hours after incorporation (Figure 3.10A and Figure 3.10B). These results suggest that amidation of the stem peptides by exogenous D-amino carboxamides may render them poor substrates for transpeptidase, thus effectively inhibiting subsequent swapping and cross-linking. Attenuation of cross-linking

levels can, in turn, reduce the overall stiffness of the peptidoglycan. We set out to probe the peptidoglycan of bacterial cells treated with DK-Amide using atomic force microscopy (AFM).<sup>20-23</sup> We acquired AFM force-indentation curves (Figure 3.11) from wildtype *B. subtilis* cells subjected to different growth conditions using either standard medium (control) or D-Ala-OH/D-Ala-NH<sub>2</sub> containing media.

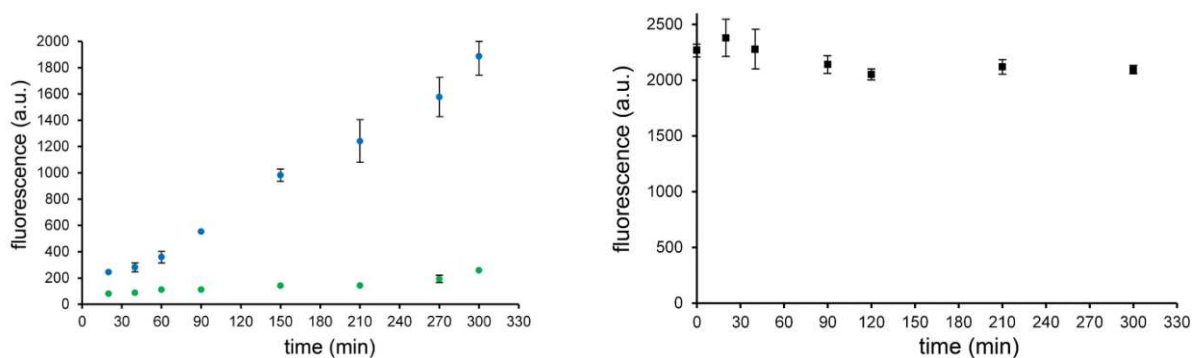


**Figure 3.10.** (A) Kinetics of incorporation of D-amino acid derivatives. Flow cytometry analysis of *B. subtilis* wildtype incubated at various times with 250  $\mu$ M of DK-Acid (green) and DK-Amide (blue). Data are represented as mean  $\pm$  SD ( $n=3$ ). (B) Retention of DK-Amide. *B. subtilis* wildtype cells incubated overnight with 100  $\mu$ M of DK-Amide. Next, cells were chased with fresh medium devoid of DK-Amide and fluorescence was monitored over time using flow cytometry. Data are represented as mean  $\pm$  SD ( $n=3$ ).

While the presence of D-Ala-OH resulted only in minor changes in the mechanical properties of bacteria, the incorporation of D-Ala-NH<sub>2</sub> had a profound effect on the bacterial cells response to external load. Since constructing quantitative models and obtaining proper data to extract absolute values of Young's modulus is complicated, we opted to perform a relative characterization of the mechanical properties of the bacterial cell wall by measuring effective stiffness of *B. subtilis* cells under low to moderate compressions (50–300 nm). Due to cell-to-cell variations, analysis of the cell population (we analyzed 6–12 cells per sample; Supporting Information, Table S1) was used to detect changes in mechanical properties of the cell wall from disruption of the peptidoglycan



cross-linking. We observed that effective stiffness of bacteria declined by about 25% when introducing D-Ala-NH<sub>2</sub> into the growth medium. The experimental stiffness values (with corresponding errors of the mean) for cells grown in as is (control), D-Ala-OH, and D-Ala-NH<sub>2</sub> spiked media were  $148 \pm 11 \text{ mN m}^{-1}$  ( $n = 9$ ),  $131 \pm 6 \text{ mN m}^{-1}$  ( $n = 11$ ), and  $109 \pm 13 \text{ mN m}^{-1}$  ( $n = 7$ ), respectively, for loads between 5 and 18 nN. These differences are even more pronounced at low loads, for example, another set of experiments with a different probe using loads under 5 nN showed a reduction in stiffness by about 45% from  $128 \pm 13 \text{ mN m}^{-1}$  ( $n = 5$ ) for normal peptidoglycan to  $69 \pm 5 \text{ mN m}^{-1}$  ( $n = 11$ ) for D-Ala-NH<sub>2</sub> modified peptidoglycan. The dramatic drop in the effective stiffness should be interpreted as a reduction of the Young's modulus of the peptidoglycan by approximately a third upon incorporation of D-Ala-NH<sub>2</sub>.

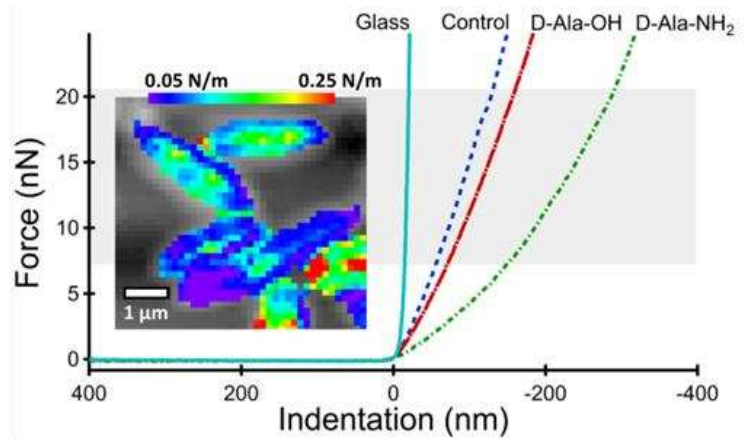


**Figure 3.11.** Typical force-indentation curves obtained on i) poly-L-Lysine (PLL) coated glass surface, ii) Wildtype *B. subtilis* cells grown in standard medium; iii) Wildtype *B. subtilis* incubated overnight in the presence of 10 mM of D-Ala-OH or D-Ala-NH<sub>2</sub>. Grayed out area indicates the region used in calculating the effective stiffness of a given cell for all force curves. The color overlay represents the apparent stiffness of the cell probed at a given location. Note greater apparent stiffness near midline of a bacterial cell.

### 3.3.6 Bacteria Profiling with D-Amino Acids

We measured cell labeling by D-amino acid variants with six additional types of bacteria aside from *B. subtilis* to profile the labelling of cell surfaces across different species (Figure 3.12). Contrary to all other Gram-positive bacteria assayed, DK-Amide failed to extensively label the surface of Gram-negative *E. coli* and only DK-Acid displayed significant incorporation. These differences could potentially reflect poor permeation of the molecules to the site of the transpeptidase and/or inherent differences in the *E. coli* PBPs. Similarly, the

Gram-negative human pathogen *Pseudomonas aeruginosa* (*P. aeruginosa*)

was labeled poorly with all the compounds evaluated. Of note, the decreased  $\beta$ -lactam sensitivity (same protein target as D-amino acid variants) by Gram-negative organisms has been proposed to be primarily caused by the lack of outer membrane permeability.<sup>23</sup> The incubation of Gram-positive *Listeria monocytogenes* (*L.*

*monocytogenes*) with our panel of variants resulted in a labeling profile clearly distinct

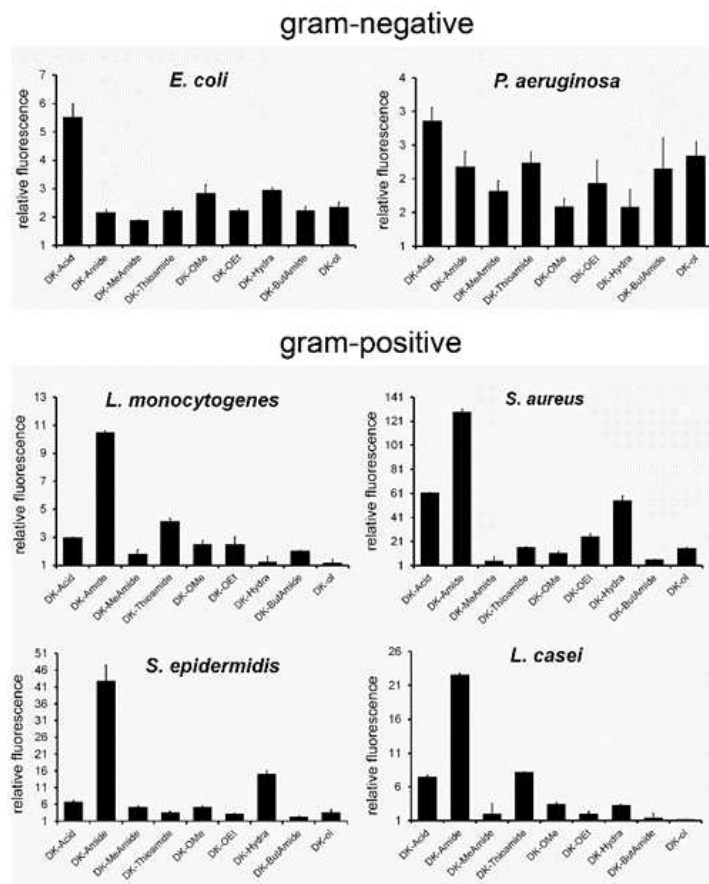


**Figure 3.12.** Differential profiling across several types of bacteria. Flow cytometry analysis of specified incubated overnight in the presence of 100  $\mu$ M of stated compounds. Relative fluorescence represents the fold increase over unlabeled cells. Data are represented as mean + SD (n=3).

from *B. subtilis*. While DK-Amide retained the ability to efficiently label *L. monocytogenes* cells, DK-Thioamide labeling was slightly more efficient than the carboxylic acid variant DK-Acid, while DK-Hydra showed almost no incorporation. The Gram-positive *Staphylococcus epidermidis* (*S. epidermidis*) showed overall lower levels of labeling compared to *S. aureus*. Unique to the set of bacteria evaluated, DK-Hydra showed a twofold increase in labeling of *S. epidermidis* compared to DK-Acid.

Next, we evaluated our panel of compounds against *Lactobacillus casei* (*L. casei*), a symbiotic gut microorganism.<sup>24</sup> Incubation with DK-Amide led to high incorporation levels in *L. casei*, while DK-Acid and DK-Thioamide also labeled these cells efficiently. These findings are intriguing considering that the fifth position in the peptidoglycan of *L. casei* is D-lactic acid, not D-alanine.<sup>25</sup> Furthermore, to our knowledge this is the first evaluation of peptidoglycan labeling of symbiotic bacteria via unnatural D-amino acids and it may have implications on potential therapeutic application of this technology. The Gram-positive human pathogen *Staphylococcus aureus* (*S. aureus*) displayed the largest absolute fluorescence signals among the set of bacteria tested. It was observed that *S. aureus* was labeled with DK-Amide about twice as efficiently as with DK-Acid or DK-Hydra. It is interesting to note that unlike vegetative *B. subtilis* cells, *S. aureus* cells do not contain amidated m-DAP. Therefore, it appears that the higher labeling efficiency of DK-Amide can only be partially explained by its m-DAP mimicry.

### **3.4 Conclusion**

In conclusion, we have shown that PBP transpeptidase exhibits remarkable flexibility in accepting unnatural D-amino acid derivatives as substrates for swapping surface-bound D-alanines. Most importantly, we demonstrate that subtle differences within

and between bacterial species could be profiled within our panel of compounds. The incorporation profile has the potential to form the basis of a novel bacterial detection method.

### **3.5 Materials and Methods**

All peptide related reagents (resin, coupling reagent, deprotection reagent, amino acids, and cleavage reagents) were purchased from ChemImpex. Alexa Fluor 647 C2 Maleimide was purchased from Life Technologies. All other reagents were purchased from Sigma and were used without further purification. Bacterial strains used for these experiments were *B. subtilis*  $\Delta$ dacA, *B. subtilis* NCIB 3610, *L. monocytogenes* 10403s, *S. Epidermidis* NRS101, *S. aureus* SCO1, *L. casei* ATCC 393, *P. aeruginosa* PAO1, and *E. coli* MG1655.

**Peptidoglycan Isolation.** *B. subtilis*  $\Delta$ dacA bacteria (50 mL) were grown at 37 °C OD<sub>600</sub> 0.6 in LB medium, at which point the medium was replaced with LB medium supplemented with 500  $\mu$ M of DK-Amide. The cells were allowed to incubate at 37 °C for 5 h in this medium before being harvested and washed with 1x phosphate buffer saline (PBS) (3  $\times$  50 mL each). The cells were then resuspended in 1x PBS and boiled for 7 min and then centrifuged at 14,000g for 8 min at 4°C. Cells were then placed in 25 mL of 5% (w/v) sodium dodecyl sulfate (SDS) and boiled for 25 min followed by centrifugation at 14,000g for 8 min at 4 °C. Following centrifugation, cells were boiled again in 25 mL of 4% (w/v) SDS for 15 min followed by centrifugation using same parameters as before. Cells were then washed 5 times with 60 °C DI water to remove all SDS. After washing, cells were incubated in 6 mL of 50 mM Tris HCl and 2 mg mL<sup>-1</sup> Proteinase K for 1 h at 60 °C, and then washed 3 times with DI water. The cell wall pellet was then resuspended and digested with 250  $\mu$ g/mL lysozyme in 25 mM sodium phosphate buffer pH 5.6 for 15

h at 37 °C. The digestion was then ceased by boiling for 3 min. The sample was then centrifuged at 14,000g for 8 min, the supernatant was retained and concentrated *in vacuo*. The labeled peptidoglycan was purified using PerkinElmer Series 200 HPLC. The purified DKAmide labeled peptidoglycan was analyzed using a Shimadzu UV-2101PC and Bruker Microflex MALDI-TOF MS. For the UV-Vis experiment, the peptidoglycan was dissolved in DI water and scanned from 350-550 nm.

**D-Cysteine Two-Step Labeling.** LB medium containing 1 mM D-Cys-OH, D-Cys-NH<sub>2</sub>, D-Cys- OMe, or dipeptides D-Ala-D-Cys-OH, D-Ala-D-Cys-NH<sub>2</sub> were prepared. *B. subtilis* ΔdacA or *B. subtilis* wildtype (NCIB 3610) were inoculated (1:100) in the corresponding medium and allowed to grow overnight at 37 °C with shaking in a 96-well plate. The labeled bacteria were harvested at 1,000g and washed three times with original culture volume with 1x PBS. The bacteria were then suspended in half the volume of the original culture with 50 μM Alexa Fluor 647 C2 Maleimide in 1x PBS. The bacteria were shaken for 30 min at room temperature. The bacteria were washed three times with 1x PBS followed by fixation with 2% formaldehyde in 1x PBS for 30 min at room temperature. The formaldehyde was removed with one wash of 1x PBS. Fluorescence of the samples were then analyzed using a BDFacs Canto II flow cytometer for cells were analyzed using a BDFacs Canto II flow cytometer (BD Biosciences, San Jose, CA) equipped with a 633nm HeNe laser (L1) and a 660/20 band-pass filter (FL5). A minimum of 10,000 events were counted for each data set. The data was analyzed using the FACSDivaversion 6.1.1 software.

**Bacterial D-Amino Acid Overnight Labeling.** LB medium containing 100 μM DK-Acid, DKAmide, DK-MeAmide, DK-Thioamide, DK-OMe, DK-OEt, DK-Hydra, DK-

ButAmide, DK-ol, were prepared. *B. subtilis*, *L. monocytogenes*, *S. aureus*, *S. epidermis*, *L. casei*, *E. coli*, or *P. aeruginosa* were inoculated (1:100) in the corresponding medias and allowed to grow overnight at 37 °C with shaking in a 96-well plate. *B. subtilis*, *S. aureus*, *S. epidermidis*, *E. coli*, *P. aeruginosa* were all grown in LB medium. *L. monocytogenes* was grown in Brain Heart Infusion (BHI) medium. *L. casei* were grown in MRS medium. The bacteria were harvested at 1,000g and washed three times with original culture volume with 1x PBS followed by fixation with 2% formaldehyde in 1x PBS for 30 min. at room temperature. The formaldehyde was removed with one wash of 1x PBS. Samples were then analyzed using a BDFacs Canto II flow cytometer using previously stated parameters for DK-Acid.

**Bacterial D-Amino Acid Stationary Phase Labeling.** *B. subtilis*  $\Delta$ dacA or *B. subtilis* wildtypewere grown at 37 °C to an OD600 1.0 in LB medium, at which point the medium was replaced with LB medium supplemented with 100  $\mu$ M DK-Acid, DK-Amide, DK-MeAmide, DK-Thioamide, DK-OMe, DK-OEt, DK-Hydra, DK-ButAmide, DK-ol. The bacteria were then incubated at 37 °C with shaking for 5 h in a 96-well plate. The bacteria were harvested at 1,000g and washed three times with original culture volume with 1x PBS followed by fixation with 2% formaldehyde in 1x PBS for 30 min at room temperature. The formaldehyde was removed with one wash of 1x PBS. Samples were then analyzed using a BDFacs Canto II flow cytometer cytometer using previously stated parameters for DK-Acid.

**Bacterial D-Amino Acid Logarithmic Phase Labeling.** LB medium solutions containing 100  $\mu$ M DK-Acid, DK-Amide, DK-MeAmide, DK-Thioamide, DK-OMe, DK-OEt, DK-Hydra, DK-ButAmide, DK-ol were prepared. *B. subtilis*  $\Delta$ dacA or *B. subtilis* wildtype

(NCIB 3610) were added to an OD600 0.1. The bacteria were then incubated at 37 °C with shaking for 5 h in a 96 well-plate. The bacteria were harvested at 1,000g and washed three times with original culture volume with 1x PBS followed by fixation with 2% formaldehyde in 1x PBS for 30 min. at room temperature. The formaldehyde was removed with one wash of 1x PBS. Samples were then analyzed using a BDFacs Canto II flow cytometer using previously stated parameters for DKAcid.

***B. subtilis* Wildtype (NCIB3610) Fluorescent Imaging.** LB medium containing 200 µM DK-Amide or DK-TAMRA-Amide were prepared. *B. subtilis* wildtype (NCIB 3610) were inoculated (1:100) in the corresponding medium and allowed to grow overnight at 37 °C. The bacteria were harvested at 1,000g and washed three times with original culture volume with 1x PBS. The bacteria were analyzed on a glass slide by fluorescence microscopy using a B-2E/C filter (ex 465-495/em 515-555) for bacteria labeled with DK-Amide and a G-2E/C filter (ex 528-553/em 590-650) for bacteria labeled with DK-TAMRA-Amide.

**FITC-Poly-L-lysine Permeation Assay.** LB medium containing 1 or 10 mM of either D-Ala-OH or D-Ala-NH<sub>2</sub> was prepared. *B. subtilis* wildtype (NCIB 3610) were inoculated (1:100) in the corresponding medium and allowed to grow overnight at 37 °C with shaking. The bacteria were harvested at 1,000g and washed three times with original culture volume with 1x PBS. The bacteria were then suspended in half the volume of the original culture with 0.3 µM FITC-Poly-L-lysine in 1x PBS for 15 min. at room temperature. The bacteria were washed three times with 1x PBS, one time with 1 M NaCl, followed by one wash again with 1x PBS. The bacteria were fixed with 2% formaldehyde in 1x PBS for 30 min at room temperature. The formaldehyde was removed with one wash of 1x PBS. Samples

were then analyzed using a BDFacs Canto II flow cytometer using previously stated parameters for DK-Acid.

***B. subtilis* Wildtype Incorporation Kinetics of DK-Acid/DK-Amide.** *B. subtilis* wildtype (NCIB 3610) was grown at 37 °C to an OD600 1.0 in LB medium, at which point the media was replaced with LB medium supplemented with 250 µM of DK-Acid or DK-Amide. A portion of the cells were taken at 0, 20, 40, 60, 90, 150, 210, 270, and 300 min. At each interval, the collected cells were washed three times with PBS followed by immediate fixation with 2% formaldehyde in 1x PBS for 30 min at room temperature. The formaldehyde was removed with one wash of 1x PBS. Samples were then analyzed using a BDFacs Canto II flow cytometer using the previously stated parameters for DK-Acid.

**Retention Assay of DK-Amide.** LB medium containing 100 µM DK-Amide was prepared. *B. subtilis* wildtype (NCIB 3610) were inoculated (1:100) in the media and allowed to grow overnight at 37 °C with shaking. The bacteria were harvested and washed three times with 1x PBS. The bacteria were then suspended in the same volume of the original culture with 1x PBS at 37 °C with shaking. A portion of the cells were taken at 0, 20, 40, 90, 120, 210, and 300 min. At each interval, the collected cells were immediately fixed with 2% formaldehyde in 1x PBS for 30 min at room temperature. The formaldehyde was removed with one wash of 1x PBS. Samples were then analyzed using a BDFacs Canto II flow cytometer using the previously stated parameters for DK-Acid.

**Measurements of Bacterial Stiffness with Atomic Force Microscope (AFM).** We prepared three types of samples using wildtype *B. subtilis* cells treated under different conditions: 1) cells (control sample) grown in standard LB medium; 2) cells grown in LB medium containing 10 mM D-Ala-OH, and 3) cells grown in LB medium containing 10



mM D-Ala-NH<sub>2</sub>. The glass slides used in the AFM fluid cell were coated by poly-L-lysine (PLL) to promote the adhesion of the bacteria. The slides were cleaned by exposure to air plasma (PDC-001, Harrick Plasma, Ithaca, NY) for 1 min, then 150  $\mu$ L of 0.01% solution of PLL in water were spread on the surface and dried overnight. The slides were baked at 100° C for 10 min before depositing cells. The overnight grown cell culture was diluted to an optical density at 600 nm (OD<sub>600</sub>) of 0.6 and suspended in LB broth. 150  $\mu$ L of cell suspension was deposited on the glass surface. After 20 min, the glass slide was rinsed gently 3 times with PBS buffer and assembled into the AFM's fluid cell with 3 mL of PBS. To assist in unambiguous interpretation of the force-indentation data a single contact mode AFM probe (either silicon nitride or silicon) was used on all cells in a series to ensure identical probe parameters. The spring constant of the probe was determined from the thermal noise spectrum in air (84 pN/nm for one probe and 110 pN/nm for another). We acquired several force-volume maps (force-distance measurements in a two-dimensional 40 $\times$ 40 array) from areas of the sample that were populated with bacteria using MFD-3D AFM (Asylum Research, Santa Barbara, CA). The maximum force applied to bacteria was 22 nN in one experimental series and 5 nN in another. In analyzing the force-volume maps, we considered only the extension (loading) part of the force-distance curves obtained near away from the edges. The curves were considered valid if they showed a featureless force-indentation curve; those with features indicating a slip of the probe near the edges of the cell were excluded. The effective stiffness of the cell was taken as the slope of the force-indentation curve between 5 nN and 18 nN of force for every bacteria sample in one experimental series and between 1 nN and 4 nN in another. The width of the distribution (standard deviation) of the stiffness values for individual cells was on average 25-30 %.

### 3.6 References

- (1) Sauvage, E.; Kerff, F.; Terrak, M.; Ayala, J. A.; Charlier, P. *FEMS Microbiol Rev* **2008**, *32*, 234.
- (2) Kohanski, M. A.; Dwyer, D. J.; Collins, J. J. *Nat Rev Microbiol* **2010**, *8*, 423.
- (3) Lam, H.; Oh, D. C.; Cava, F.; Takacs, C. N.; Clardy, J.; de Pedro, M. A.; Waldor, M. K. *Science* **2009**, *325*, 1552.
- (4) Cava, F.; de Pedro, M. A.; Lam, H.; Davis, B. M.; Waldor, M. K. *Embo J* **2011**, *30*, 3442.
- (5) Siegrist, M. S.; Whiteside, S.; Jewett, J. C.; Aditham, A.; Cava, F.; Bertozzi, C. R. *ACS Chem Biol* **2013**, *8*, 500.
- (6) Pilhofer, M.; Aistleitner, K.; Biboy, J.; Gray, J.; Kuru, E.; Hall, E.; Brun, Y. V.; VanNieuwenhze, M. S.; Vollmer, W.; Horn, M.; Jensen, G. J. *Nat Commun* **2013**, *4*, 2856.
- (7) Shieh, P.; Siegrist, M. S.; Cullen, A. J.; Bertozzi, C. R. *Proc Natl Acad Sci USA* **2014**, *111*, 5456.
- (8) Kuru, E.; Hughes, H. V.; Brown, P. J.; Hall, E.; Tekkam, S.; Cava, F.; de Pedro, M. A.; Brun, Y. V.; VanNieuwenhze, M. S. *Angew Chem Int Ed Engl* **2012**, *51*, 12519.
- (9) Lupoli, T. J.; Tsukamoto, H.; Doud, E. H.; Wang, T. S.; Walker, S.; Kahne, D. *J Am Chem Soc* **2011**, *133*, 10748.
- (10) Lebar, M. D.; May, J. M.; Meeske, A. J.; Leiman, S. A.; Lupoli, T. J.; Tsukamoto, H.; Losick, R.; Rudner, D. Z.; Walker, S.; Kahne, D. *J Am Chem Soc* **2014**, *136*, 10874.
- (11) Fura, J. M.; Sabulski, M. J.; Pires, M. M. *ACS Chem Biol* **2014**, *9*, 1480.
- (12) Bott, K. F. *Science* **1994**, *263*, 546.
- (13) Atrih, A.; Bacher, G.; Allmaier, G.; Williamson, M. P.; Foster, S. J. *J Bacteriol* **1999**, *181*, 3956.
- (14) Nemmara, V. V.; Adediran, S. A.; Dave, K.; Duez, C.; Pratt, R. F. *Biochemistry* **2013**, *52*, 2627.
- (15) Chen, I.; Howarth, M.; Lin, W.; Ting, A. Y. *Nat Methods* **2005**, *2*, 99.
- (16) Dutta, D.; Pulsipher, A.; Luo, W.; Yousaf, M. N. *J Am Chem Soc* **2011**, *133*, 8704.
- (17) Sletten, E. M.; Bertozzi, C. R. *Angew Chem Int Ed Engl* **2009**, *48*, 6974.
- (18) Mahal, L. K.; Yarema, K. J.; Bertozzi, C. R. *Science* **1997**, *276*, 1125.
- (19) Chittchang, M.; Alur, H. H.; Mitra, A. K.; Johnston, T. P. *J Pharm Pharmacol* **2002**, *54*, 315.
- (20) Dufrene, Y. F. *Nat Rev Microbiol* **2004**, *2*, 451.
- (21) Dufrene, Y. F. *J Bacteriol* **2002**, *184*, 5205.
- (22) Yao, X.; Jericho, M.; Pink, D.; Beveridge, T. *J Bacteriol* **1999**, *181*, 6865.
- (23) Delcour, A. H. *Biochim Biophys Acta* **2009**, *1794*, 808.
- (24) Scornec, H.; Tichit, M.; Bouchier, C.; Pedron, T.; Cavin, J. F.; Sansonetti, P. J.; Licandro-Seraut, H. *J Microbiol Methods* **2014**, *106*, 78.
- (25) Billot-Klein, D.; Legrand, R.; Schoot, B.; van Heijenoort, J.; Gutmann, L. *J Bacteriol* **1997**, *179*, 6208.

## Chapter 4

### Metabolic Remodeling of Bacterial Surfaces *via* Tetrazine Ligations

#### **4.1 Abstract**

Bioorthogonal click ligations are extensively used for the introduction of functional groups in biological systems. Tetrazine ligations are attractive in that they are catalyst-free and display favorable kinetics. We describe the efficient remodeling of bacterial cell surfaces using unnatural D-amino acids derivatized with tetrazine ligation handles. The metabolic incorporation of these unnatural D-amino acids onto bacterial cell surfaces resulted in a site-selective installation of fluorophores.

#### **4.2 Introduction**

Bioorthogonal chemical reactions have proven to be indispensable tools for probing and monitoring many biological processes with minimum sample interference.<sup>1-4</sup> These reactions have the advantage of being compatible with biological conditions (aqueous medium and physiological temperatures), typically induce minimal cytotoxicity, and display excellent selectivity. To date, a number of ligation strategies have been developed that are widely utilized.<sup>5</sup> One of the areas that has advanced the most since the introduction of bioorthogonal ligation reactions is the field of bio-imaging.<sup>6,7</sup> The ability to introduce tags that illuminate the localization and movement of biomacromolecules has completely revolutionized the way biological processes are monitored.<sup>4</sup> In this communication, we demonstrate for the first time the metabolic site-selective fluorescent labeling of bacterial cell surfaces using tetrazine-based ligation.

All bacteria are surrounded by a protective cell wall, where the major structural component is peptidoglycan.<sup>8</sup> Bacterial peptidoglycan is vital to all known bacteria, as it

provides resistance to unfavorable external conditions and counteracts internal osmotic pressure. The polymeric peptidoglycan resides on the exterior surface of bacterial cell membranes of Gram-positive organisms (inner membranes for Gram-negative organisms).<sup>9,10</sup> It is composed of repetitive sugar units linked to short oligopeptide chains. Of note, the oligopeptide unit contains several D-amino acids, a distinctive characteristic of bacteria. Nascent peptidoglycan is loaded onto the existing structure by penicillin binding proteins (PBPs). PBPs are a major class of bacterial enzymes that are important for bacterial growth and division.<sup>11-13</sup> In particular, transpeptidase domains of PBPs introduce crosslinks between neighboring oligopeptide strands by removing the terminal D-alanine to form an acyl intermediate. The PBP-anchored intermediate can be captured by a nearby nucleophilic *meso*-diaminopimelic acid (*m*-DAP) or L-lysine residue, resulting in the formation of a covalent crosslink. Recently, it was demonstrated that unnatural D-amino acids from the surrounding medium can also displace the acyl-intermediate, thus resulting in the swapping of the terminal D-

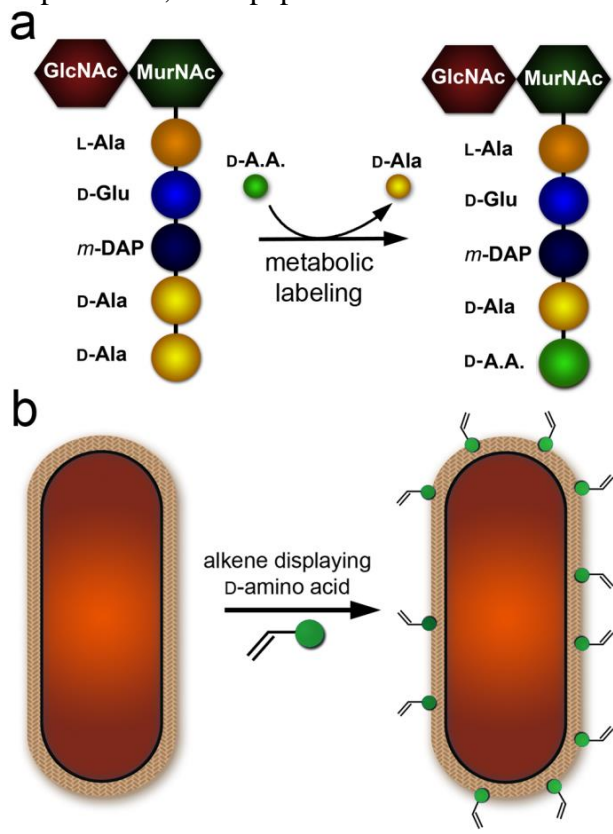


**Figure 4.1.** (A) Schematic diagram of the swapping of exogenous D-amino acid with terminal D-Alanine. (B) Metabolic incorporation decorates the bacterial cell surface with tetrazine ligation handles.

alanine with unnatural D-amino acids (Figure 4.1 A).<sup>14-23</sup> Metabolic swapping with exogenous D-amino acids is a facile method for remodeling bacterial cell surfaces.

The site-selective remodeling of bacterial surfaces can be a powerful way to introduce small epitopes or entirely non-native biomacromolecules.<sup>24</sup> Remodeled surfaces can, in turn, be leveraged for interrogation of endogenous biological processes (e.g., surface binding) or as potential therapeutic interventions. We recently exploited this methodology to induce the recruitment of endogenous antibodies to the surface of various bacteria, including the human pathogen *Staphylococcus aureus* (*S. aureus*), using unnatural D-amino acids conjugated to small antigenic epitopes.<sup>25,26</sup> Although unnatural D-amino acids represent a novel and promising strategy to decorate bacterial cell surfaces, lack of tolerability for large amino acid sidechains may prevent its wider utilization. During our development of antibody-recruiting D-amino acids, we observed a severe reduction in incorporation with increasing size of the sidechain of the D-amino acid. We propose to decouple the two components (surface modifications and epitope/macromolecule installation) by using a two-step process.

In this second generation remodeling strategy, the unnatural D-amino acid delivers a small biorthogonal handle to the bacterial cell surface with the goal of optimizing incorporation efficiency (Figure 4.1B). The remodeled cell surface is subsequently exposed to the complementary ligation handle to afford a covalent linkage. A major advantage of using bioorthogonal chemistry is that it should permit the introduction of larger molecules onto the cell surface, which may otherwise be prohibitive using a one-step strategy. D-amino acids displaying alkyne or azido handles on the side chain have been established as viable two-step methods of installing fluorophores onto bacterial peptidoglycans using

copper-catalyzed click reactions.<sup>17,18,27</sup> The Bertozzi laboratory has recently demonstrated the feasibility of using strain-promoted click chemistry to fluorescently label bacterial cell surfaces.<sup>19,20</sup> We identified tetrazine ligation as a prime candidate to implement our two-step strategy with the ultimate goal of efficiently installing highly antigenic molecules (some of which cannot be achieved using the one-step method) on bacterial cell surfaces *in vivo*.

Tetrazine ligation is a relatively new method in the repertoire of click reactions yet it has already attracted considerable attention due to the combination of its small size, fast kinetics, and established *in vivo* compatibility.<sup>28-31</sup> The reaction proceeds through an inverse-electron demand Diels-Alder reaction, releasing innocuous nitrogen gas as a byproduct (Figure 4.2A). Herein, we show for the first time that bacterial cell surfaces can be selectively remodeled using tetrazine click chemistry *via* transpeptidase mediated incorporation of D-amino acids. Most importantly, we show that this strategy affords live-cell peptidoglycan labeling of the human pathogen *S. aureus*.

## **4.3 Results and Discussion**

### **4.3.1 Alkene D-Amino Acid Incorporation**

We initially set out to probe the promiscuity of transpeptidase to tolerate D-amino acids derivatized with alkene functional groups. Previously, we had observed that a number of unnatural side chains could be accommodated in the swapping of exogenous D-amino acids with surface anchored terminal D-alanine. Yet, the incorporation efficiency appears to be highly dependent on the structure of the sidechain. A small panel of D-amino acids were synthesized using standard solid phase chemistry to probe (1) the structure of the alkene for tetrazine ligation, (2) transpeptidase restraints in the size/flexibility of the amino acid side chain, and (3) alkene displaying unnaturally C-terminated D-amino acids (Figure 4.2

B). Tetrazine ligation on bacterial cell surfaces was performed by overnight incubation of *S. aureus* in the presence of each unnatural D-amino acid variant. We chose to investigate ligations using Gram-positive *S. aureus* due to its prominent pathogenicity and potential for future application of this technology for immuno-modulation.<sup>32</sup> Successful incorporation of the D-amino acid leads to the covalent installation of alkene functional groups at the peptidoglycan (Figure 4.2B). For the optimization stage of our study, cells were fixed, treated with Cy5-methyl tetrazine, and fluorescence labeling was measured via flow cytometry.

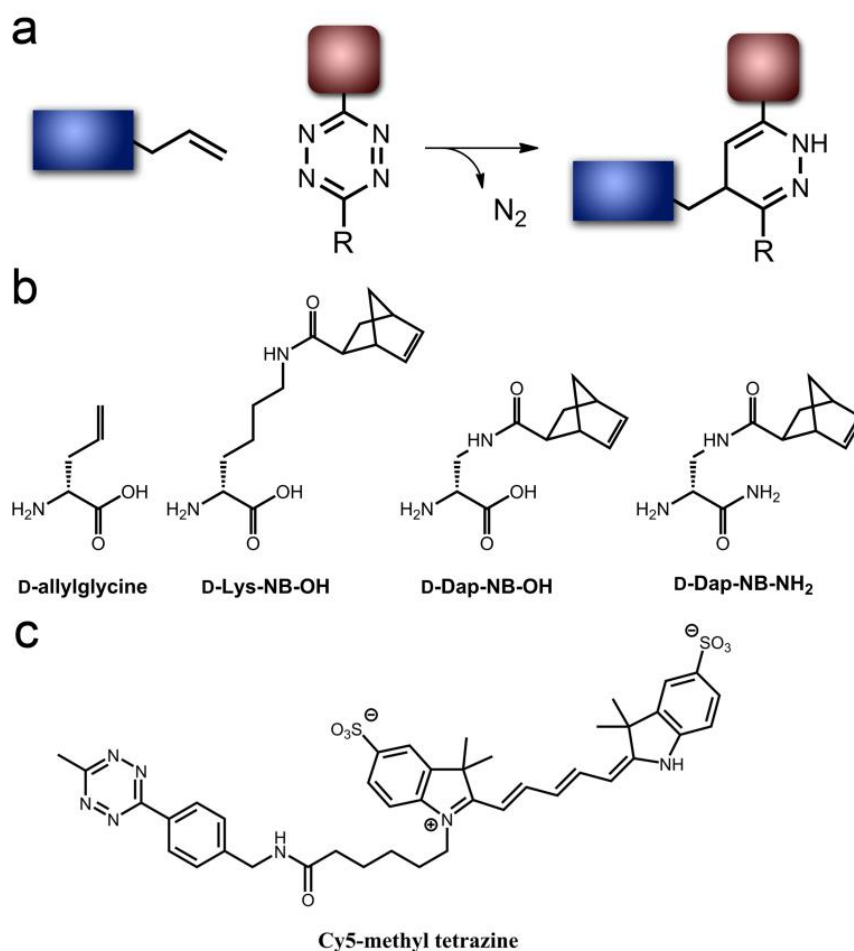


**Figure 4.2** (A) Tetrazine ligation. The boxes represent conjugated species to the tetrazine handles. (B) Chemical structure of 4 unnatural alkene-displaying D-amino acids. (C) Chemical structure of Cy5-methyl tetrazine.

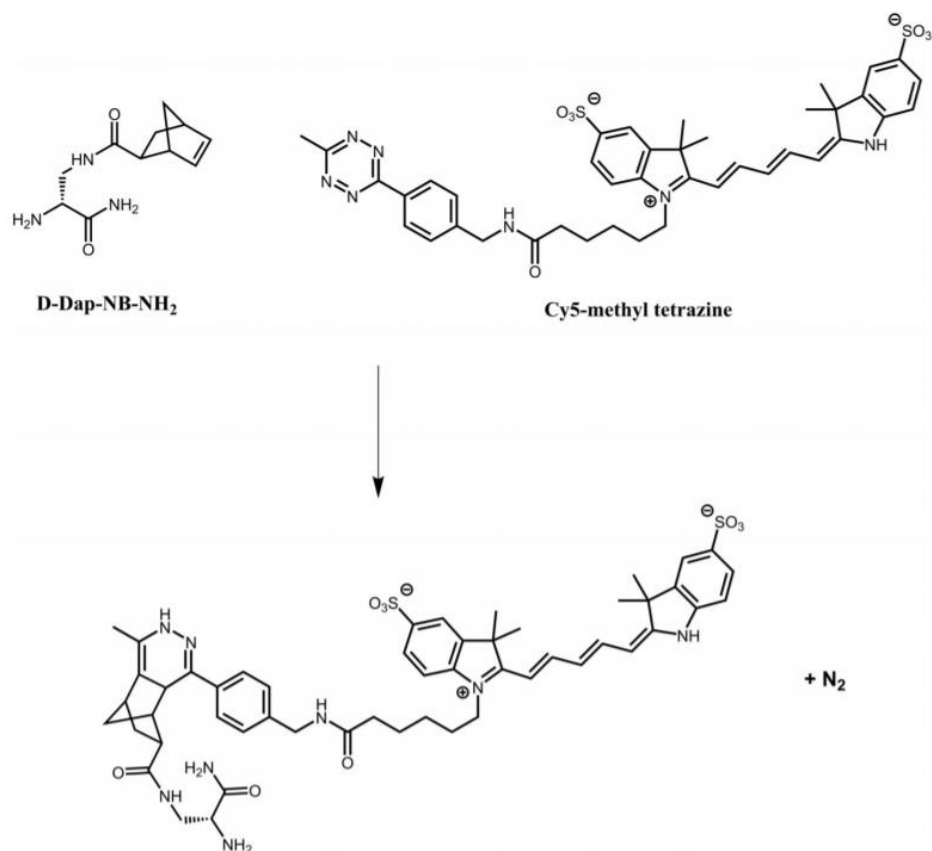
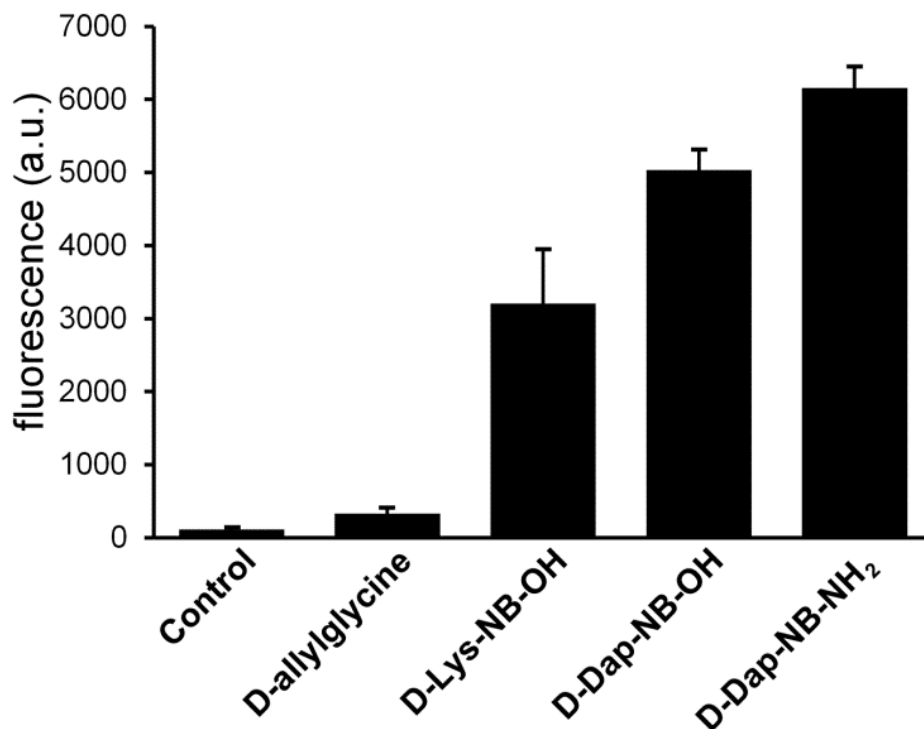


**Figure 4.3** Schematic diagram showing the reaction between the norbornene group and tetrazine conjugated to the fluorophore.

At first, we evaluated two unnatural D-amino acids for their compatibility with our strategy: D-allylglycine and D-Lys-NB-OH. D-allylglycine was chosen due to the small sidechain size and previously reported compatibility of this alkene configuration with tetrazine ligations.<sup>33</sup> The small sidechain is expected to lead to higher incorporation levels. D-Lys-NB-OH was built by conjugating a norbornene group to the  $\epsilon$ -amino group of D-Lysine. We had previously found that modified D-Lysine amino acids yielded satisfactory incorporation levels. The strained alkene within norbornene is expected to display increased reactivity compared to the allyl group and has been previously used in live cell imaging.<sup>34-36</sup> Surfaces of *S. aureus* cells remodeled with D-allylglycine resulted in a 3-fold increase in fluorescence compared to unmodified control cells (Figure 4.4). The incubation



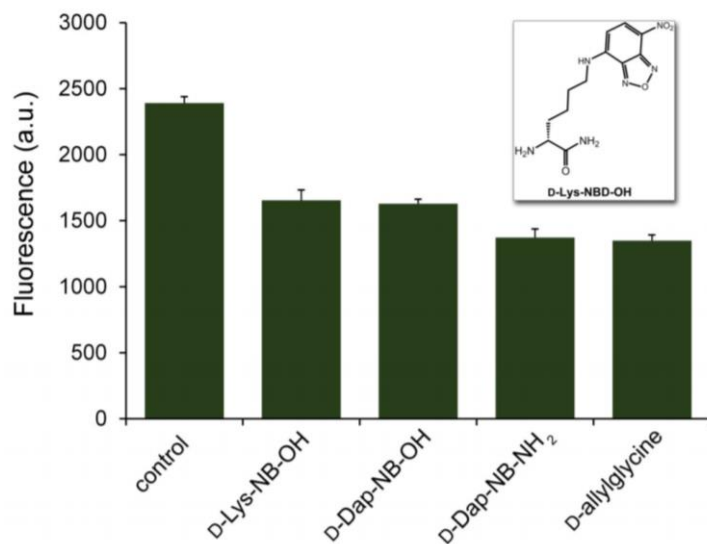
of the same cells with D-Lys-NB-OH resulted in a major increase (~30-fold) in fluorescence relative to control cells.



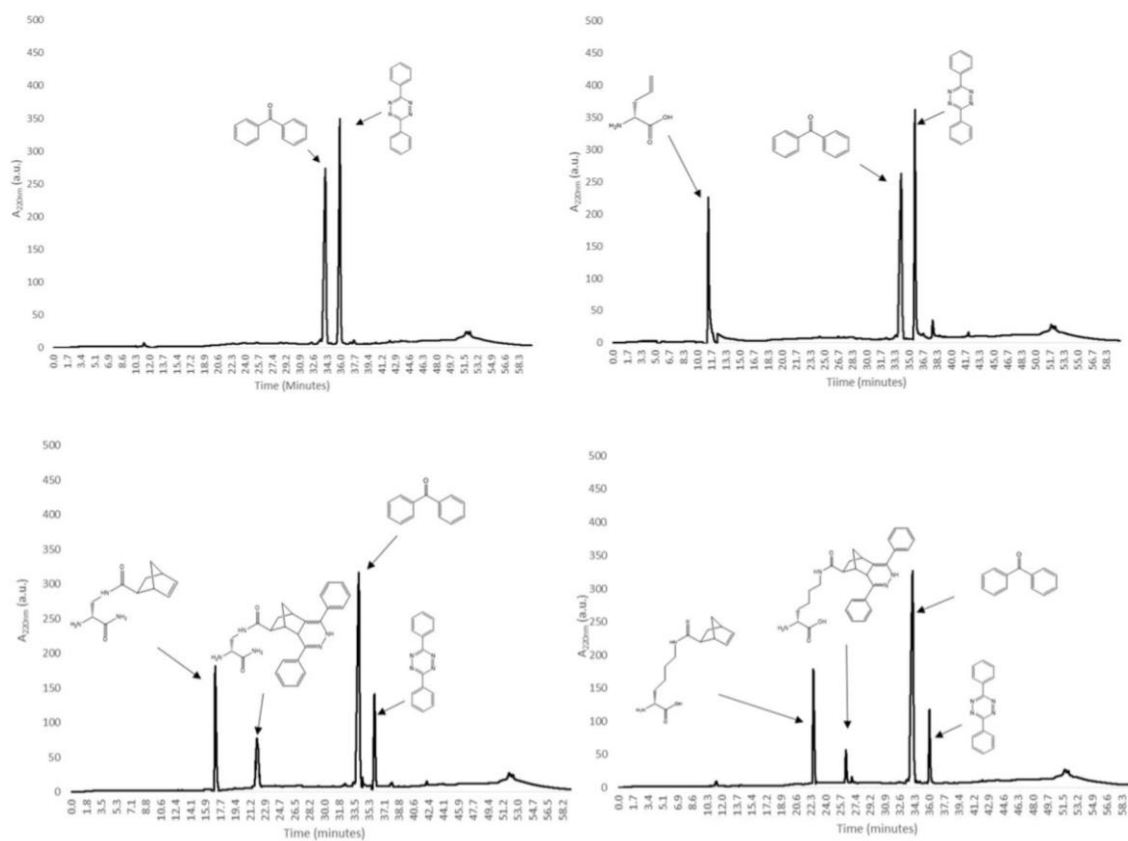
**Figure 4.4.** Flow cytometry analysis of tetrazine ligation on the surface of *S. aureus*. Cells were labeled overnight in the presence of unnatural D-amino acid variants or in media alone. Tetrazine reaction was then performed with Cy5-methyl tetrazine. Data are represented as mean

#### **4.3.2 Competition and Kinetics of Alkene D-Amino Acids**

We performed a fluorescence competition assay we recently developed to quantitatively establish incorporation efficiency of all alkene-displaying D-amino acid variants acids (Figure 4.5). As expected, D-allylglycine was incorporated onto cell surfaces to a higher extent than D-Lys-NB-OH. Furthermore, we observed much slower reaction kinetics with tetrazine for the unstrained alkene compared to the norbornene-bearing amino acid variants (Figure 4.6). Evidently, between the two opposing effects (incorporation efficiency and elevated strain-energy) the strained alkene is a more important overall feature.



**Figure 4.5.** Flow cytometry analysis of *S. aureus* co-incubated overnight in the presence of 500  $\mu$ M of D-allylglycine, D-Dap-NB-OH, D-Dap-NB-NH<sub>2</sub>, or D-Lys-NB-OH and 100  $\mu$ M D-Lys-NBD-OH. Data are represented as mean + SD (n=3). Inset: Chemical structure of D-Lys-NBD-



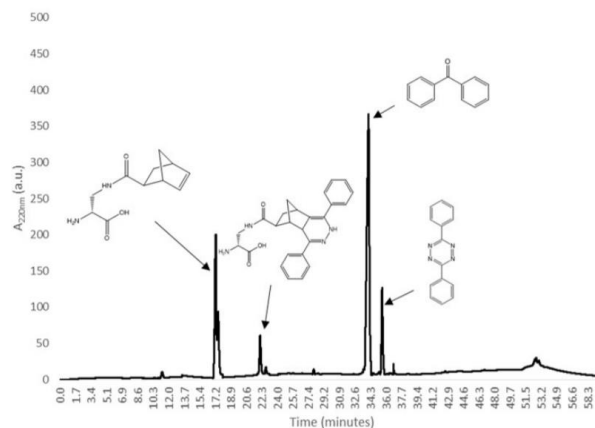


**Figure 4.6.** Reaction Analyses by Analytical RP-HPLC. Aliquots of D-allylglycine, D-Dap-NB-OH, D-Dap-NB-NH<sub>2</sub>, or D-Lys-NB-OH in MeOH were reacted with 3,6-Diphenyl-1,2,4,5-tetrazine (200  $\mu$ M) and internal standard benzophenone (400  $\mu$ M) in MeOH. The reactions were allowed to incubate for 6 h at 37  $^{\circ}$ C and then analyzed by RP-HPLC.

### **4.3.3 Amidation of Alkene D-Amino Acid**

Next, we evaluated the labeling efficiency of D-diaminopropionic acid modified with norbornene (D-Dap-NB-OH). Satisfactorily, the smaller D-Dap-NB-OH variant led to improved labeling levels relative to D-Lys-NB-OH (Figure 4.4). Cells remodeled with D-Dap-NB-OH led to ~45-fold increase in fluorescence relative to control cells. Finally, we set out to evaluate the possibility that we could further improve labeling by modifying the C-terminus carboxylic acid functional group into carboxamide. We and others had previously discovered that amidation of the C-terminus can increase loading and retention of the D-amino acid on the cell surface.<sup>37,38</sup> Consistent with our previous findings, we also showed that the carboxamide D-Dap-NB-NH<sub>2</sub> led to higher incorporation levels compared to its carboxylic acid counterpart. Cells labeled with the carboxamide D-Dap-NB-NH<sub>2</sub> led to a signal increase of ~55-fold compared to control cells. Together, we demonstrate that through structural optimization we were successful in using tetrazine ligation to site-specifically label the surface *S. aureus* cells.

#### 4.3.4 Live Cell Tetrazine Ligations and Stereospecificity

A major advantage of tetrazine is its compatibility with live cell ligation.<sup>30,33,39-42</sup> Next, we evaluated the tetrazine ligation reaction with live *S. aureus* cells metabolically remodeled with D-Dap-NB-NH<sub>2</sub> (Figure 4.7). A time course analysis of the labeling with Cy5-methyl tetrazine showed robust labeling as early as 30 minutes and the signal

continued to increase over the next several hours. The fast reaction kinetics of this ligation can potentially complement existing biocompatible reaction strategies. Fluorescence

microscopy analysis of cells labeled with D-Dap-NB-NH<sub>2</sub> showed delineated labeling at the septal region of the cells, consistent with the site of new peptidoglycan biosynthesis (Fig. 3, inset). In addition, we

performed two experiments to establish the mode of surface remodeling with D-Dap-NB-NH<sub>2</sub>. First, we isolated the peptidoglycan from cells labeled

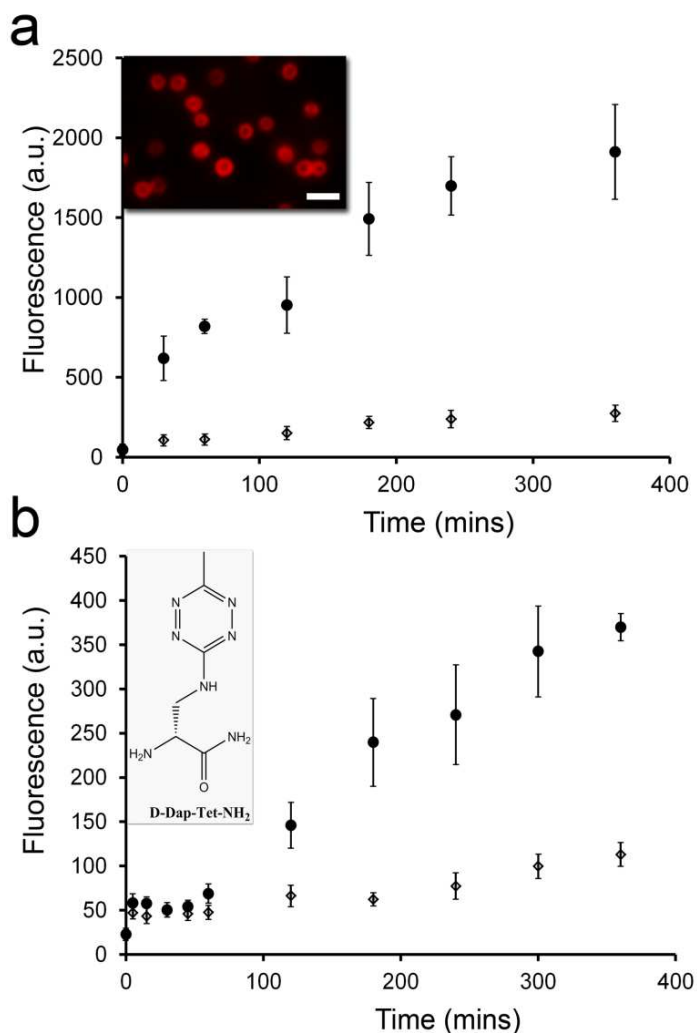


**Figure 4.7.** Flow cytometry analysis of live *S. aureus* labeled with (a) D-Dap-NB-NH<sub>2</sub> or (b) D-Dap-Tet-NH<sub>2</sub>. Data are represented as mean + SD (n = 3). Inset top, fluorescence microscopy imaging of *S. aureus*; scale bar is 2  $\mu$ m. Inset bottom, chemical structure of D-Dap-Tet-NH<sub>2</sub>.

with D-Dap-NB-NH<sub>2</sub>, analysed by mass spectrometry, and identified fragments consistent with covalent incorporation into the peptidoglycan monomeric structure (Figure 4.8). Second, the same cells incubated with the enantiomer L-Dap-NB-NH<sub>2</sub> led to near base line fluorescence signals, a result that points to the requirement for the D-stereochemistry (Fig. S4, ESI†).

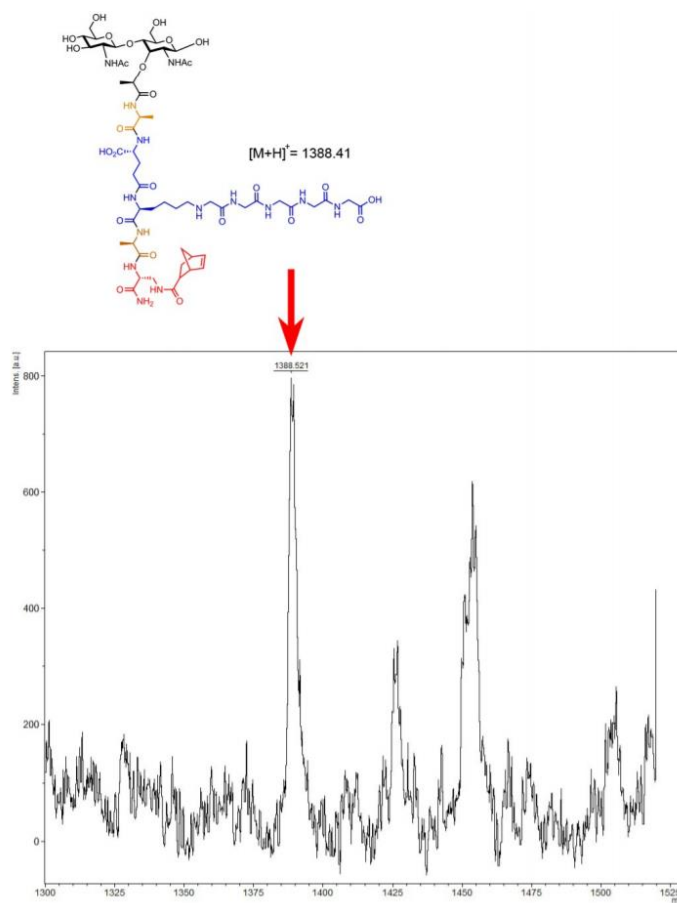


**Figure 4.8.** Peptidoglycan Isolation. (A) MALDI-TOF analysis of peptidoglycan isolated from *S. aureus* cells labeled with D-Dap-NB-NH<sub>2</sub> following RP-HPLC separation. (B) Structure of expected peptidoglycan repeating unit with the inclusion of D-Dap-NB-NH<sub>2</sub> and the expected

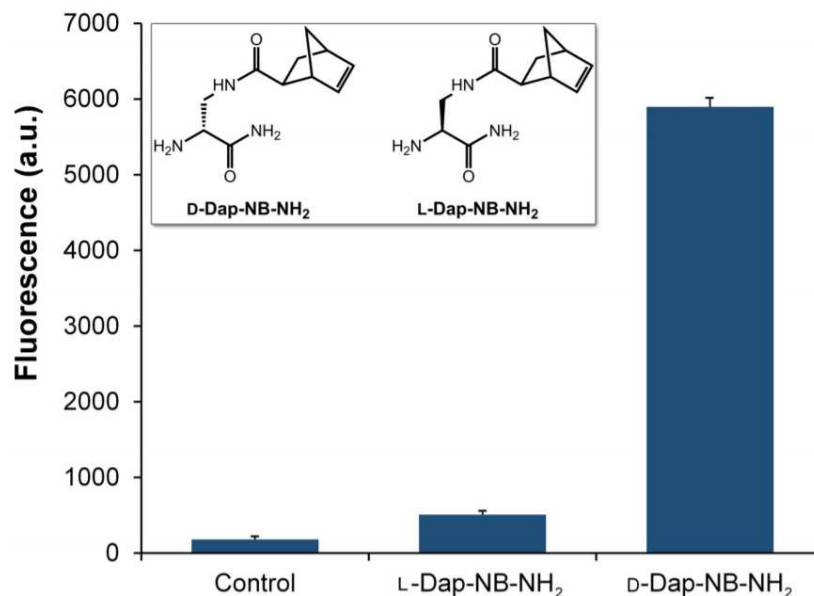


**Figure 4.9.** Stereospecificity of incorporation. Flow cytometry analysis of *S. aureus* incubated overnight in the presence of 3 mM of L-Dap-NB-NH<sub>2</sub> and D-Dap-NB-NH<sub>2</sub>. Data are represented as mean + SD (n=3). Inset: Chemical structures of L-Dap-NB-NH<sub>2</sub> and D-Dap-NB-

#### **4.3.5 Trans-cyclooctene-Tetrazine Live Cell Ligation**

Ring strain of the alkene species has significant influence on reaction kinetics with the tetrazine ligation partner. The highly strained *trans*-cyclooctene (TCO) has been reported to accelerate the reaction between 2 to 3 orders of magnitude.<sup>33</sup> We reasoned that the installation of TCO onto the sidechain of a D-amino acid would lead to minimal incorporation due to its large size. Instead, we explored the possibility of switching the ligation partners. We designed and synthesized D-Dap-Tet-NH<sub>2</sub>, in which the tetrazine was conjugated to the amino sidechain of D-Dap. In this scheme, the tetrazine is metabolically loaded onto the bacterial surface and TCO-conjugates can be used to further decorate the bacterial surface.

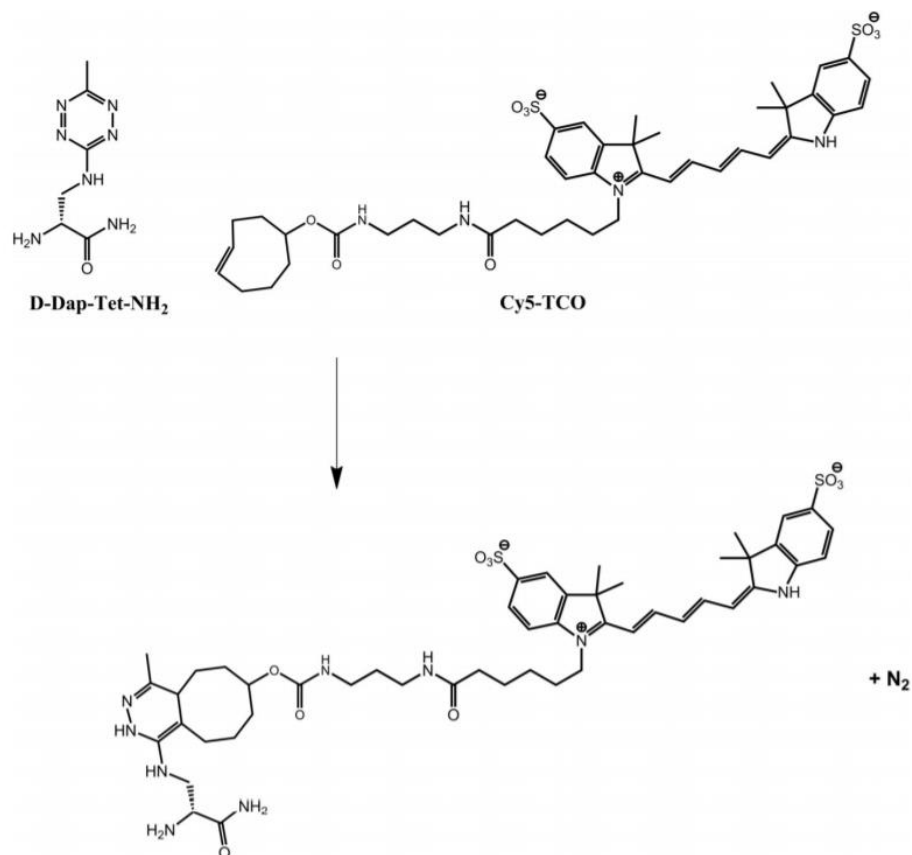


**Figure 4.10.** Schematic diagram showing the reaction between the tetrazine group and trans-cyclooctene

*S. aureus* cells surfaces were remodeled with D-Dap-Tet-NH<sub>2</sub>, followed by the incubation with TCO-Cy5, and analyzed by flow cytometry. Specific labeling in the presence of the tetrazine-displaying D-amino acid was observed (Fig. 3b). However, the reaction was slower compared to D-Dap-NB-NH<sub>2</sub>. Presumably, the incorporation levels may have been lower than desired or the amino group adjacent to the tetrazine may deactivate the diene. Finally, we showed that the unnatural D-amino acid displayed no significant reduction in cellular viability (Fig. S5, ESI†). Future re-designs will be evaluated to optimize the neighboring groups to the tetrazine to accelerate reaction rates, while preserving design features that increase incorporation efficiency.

#### **4.4 Conclusion**

In conclusion, we established a new peptidoglycan labeling approach using alkene-tetrazine biorthogonal chemistry. We have shown that norbornene containing D-amino acids are viable coupling tools to link a tetrazine fluorophore on the surface of bacterial cells. This can provide an alternative method of installing molecules of interest to the exterior of the cell. Peptidoglycan labeling of live bacteria through this ligation approach can pave the way for future *in vivo* studies due to its non-toxic effects and proven biocompatibility. Tetrazine ligation will be considered our primary target for future development of our D-amino acid Recruitment Therapy (DART) strategy.

#### **4.6 Materials and Methods**

All peptide related reagents (resin, coupling reagent, deprotection reagent, amino acids, and cleavage reagents) were purchased from ChemImpex. D-allylglycine was purchased directly from ChemImpex. Cy5-Methyl Tetrazine and Cy5-TCO were purchased from Click Chemistry Tools. 5-norbornene-2-carboxylic acid was purchased from Alfa Aesar. All other reagents were purchased from Sigma and were used without further purification. The bacterial strain used for the experiments was *Staphylococcus aureus* (*S. aureus*) SCO1.

**Bacterial Peptidoglycan Labeling.** Lysogeny broth (LB) containing 3 mM D-allylglycine, D-Dap-NB-OH, D-Dap-NB-NH<sub>2</sub>, or D-Lys-NB-OH were prepared. *S. aureus* was inoculated (1:100) in the corresponding medias and allowed to grow overnight at 37 °C with shaking in a 96-well plate. The bacteria were harvested at 1,000g for 3 min. and washed three times with original culture volume with 1x phosphate buffered saline (PBS) followed by fixation with 2% formaldehyde in 1x PBS for 30 min. at room temperature. The formaldehyde was removed with three washes of 1x PBS. The bacteria were then



suspended in half the volume of the original culture with 20  $\mu$ M Cy5-Methyl Tetrazine in 1x PBS. The bacteria were shaken for 15 hr at 37 °C, harvested at 1,000g for 3 min., and washed three times with 1x PBS. Fluorescence of the samples were then analyzed using a BDFacs Canto II flow cytometer for cells were analyzed using a BDFacs Canto II flow cytometer (BD Biosciences, San Jose, CA) equipped with a 633nm HeNe laser (L1) and a 660/20 band-pass filter (FL5). A minimum of 10,000 events were counted for each data set. The data was analyzed using the FACSDiva version 6.1.1 software. Fluorescent imaging of the D-Dap-NB-NH<sub>2</sub> labeled bacteria was analyzed on a glass slide using a Cy5 HYQ (Nikon 96324; Exc.590- 650/Em.663-738) filter.

**Tetrazine-Cy5 Live-Cell Peptidoglycan Labeling.** LB medium containing 3 mM D-Dap-NBNH<sub>2</sub> was prepared. *S. aureus* was inoculated (1:100) in the corresponding medium and allowed to grow overnight at 37 °C with shaking in a 96-well plate. The bacteria were harvested at 1,000g for 3min. and washed three times with original culture volume with 1x PBS. The cells were then immediately suspended in half the volume of the original culture with 20  $\mu$ M Cy5-Methyl Tetrazine in 1x PBS. A portion of the cells were taken at 30, 60, 120, 180, 240, and 360 min. At each interval, the collected cells were washed three times with 1x PBS followed by immediate fixation with 2% formaldehyde in 1x PBS for 30 min at room temperature. The formaldehyde was removed with three washes of 1x PBS. Samples were then analyzed using a BDFacs Canto II flow cytometer using the previously stated parameters.

**TCO-Cy5 Live-Cell Peptidoglycan Labeling.** LB medium containing 3 mM D-Dap-Tet-NH<sub>2</sub> was prepared. *S. aureus* was inoculated (1:100) in the corresponding medium and allowed to grow overnight at 37 °C with shaking in a 96-well plate. The bacteria were

harvested at 1,000g for 3 min. and washed three times with original culture volume with 1x PBS. The cells were then immediately suspended in half the volume of the original culture with 50  $\mu$ M TCO-Cy5 in 1x PBS. A portion of the cells were taken at 5, 15, 30, 45, 60, 120, 180, 240, 300, and 360 min. At each interval, the collected cells were washed three times with 1x PBS followed by immediate fixation with 2% formaldehyde in 1x PBS for 30 min at room temperature. The formaldehyde was removed with three washes of 1x PBS. Samples were then analyzed using a BDFacs Canto II flow cytometer using the previously stated parameters.

**Stereospecificity of incorporation.** LB medium containing 3 mM D-Dap-NB-NH<sub>2</sub> or L-Dap-NBNH<sub>2</sub> was prepared. *S. aureus* was inoculated (1:100) in the corresponding medium and allowed to grow overnight at 37 °C with shaking in a 96-well plate. The bacteria were harvested at 1,000g for 3 min. and washed three times with original culture volume with 1x phosphate buffered saline (PBS) followed by fixation with 2% formaldehyde in 1x PBS for 30 min. at room temperature. The formaldehyde was removed with three washes of 1x PBS. The bacteria were then suspended in half the volume of the original culture with 20  $\mu$ M Cy5-Methyl Tetrazine in 1x PBS. The bacteria were shaken for 15 hr at 37 °C, harvested at 1,000g for 3 min., and washed three times with 1x PBS. Samples were then analyzed using a BDFacs Canto II flow cytometer using the previously stated parameters.

**Competition Assay.** LB medium containing 500  $\mu$ M D-allylglycine, D-Dap-NB-OH, D-Dap-NB-NH<sub>2</sub>, or D-Lys-NB-OH were prepared. To each sample, D-lysine-nitrobenzoxadiazole (D-Lys-NBD-OH) was added for a final concentration of 100  $\mu$ M. *S. aureus* was inoculated (1:100) in the corresponding medias and allowed to grow overnight at 37 °C with shaking in a 96-well plate. The bacteria were harvested at 1,000g for 3 min.

and washed three times with original culture volume with 1x phosphate buffered saline (PBS) followed by fixation with 2% formaldehyde in 1x PBS for 30 min. at room temperature. The formaldehyde was removed with three washes of 1x PBS. Samples were then analyzed using a BDFacs Canto II flow cytometer using a 488nm argon laser (L1) and a 530/30 band-pass filter (FL1). A minimum of 10,000 events were counted for each data set.

**Peptidoglycan Isolation.** *S. aureus* SCO1 bacteria (50 mL) were grown at 37 °C OD600 0.6 in LB medium, at which point the medium was replaced with LB medium supplemented with 3 mM of D-Dap-NB-NH<sub>2</sub>. The cells were allowed to incubate at 37 °C overnight in this medium before being harvested and washed with 1x phosphate buffer saline (PBS) (3 × 50 mL each). The cells were then resuspended in 1x PBS and boiled for 7 min and then centrifuged at 14,000g for 8 min at 4 °C. Cells were then placed in 25 mL of 5% (w/v) sodium dodecyl sulfate (SDS) and boiled for 25 min followed by centrifugation at 14,000g for 8 min at 4 °C. Following centrifugation, cells were boiled again in 25 mL of 4% (w/v) SDS for 15 min followed by centrifugation using same parameters as before. Cells were then washed 5 times with 60 °C DI water to remove all SDS. After washing, cells were incubated in 6 mL of 50 mM Tris HCl and 2 mg mL<sup>-1</sup> Proteinase K for 1 h at 60 °C, and then washed 3 times with DI water. The cell wall pellet was then resuspended and digested with 250 µg/mL lysozyme in 25 mM sodium phosphate buffer pH 5.6 for 15 h at 37 °C. The digestion was then ceased by boiling for 3 min. The sample was then centrifuged at 14,000g for 8 min, the supernatant was retained and concentrated in vacuo. The labeled peptidoglycan was purified using PerkinElmer Series

200 HPLC. The purified D-Dap-NB-NH<sub>2</sub> labeled peptidoglycan was analyzed using a Bruker Microflex MALDI-TOF MS.

**Reaction Analyses by Analytical RP-HPLC.** The specified amino acid derivatives were analyzed using a PerkinElmer Series 200 reverse phase HPLC on a Phenomenex C4 column with an eluent consisting of solvent A (H<sub>2</sub>O /0.01% TFA) and solvent B (CH<sub>3</sub>CN /0.01% TFA) with a 60 minute gradient consisting of 5 to 100 % B, a flow rate of 3 mL/min and monitoring at 220 nm. ( $\lambda$ 220). The standard solution was 3,6-Diphenyl-1,2,4,5-tetrazine (200  $\mu$ M) and internal standard benzophenone (400  $\mu$ M) in MeOH. 50 mM D-allylglycine, D-Dap-NB-OH, D-Dap-NB-NH<sub>2</sub>, or D-Lys-NB-OH in MeOH were reacted with 3,6-Diphenyl-1,2,4,5-tetrazine (200  $\mu$ M) and internal standard benzophenone (400  $\mu$ M) in MeOH. The reactions were stirred for 6 hr at 37 oC and then analyzed by RP-HPLC.

## **4.6 References**

- (1) Sletten, E. M.; Bertozzi, C. R. *Angew Chem Int Ed Engl* **2009**, *48*, 6974.
- (2) Kolb, H. C.; Finn, M. G.; Sharpless, K. B. *Angew Chem Int Ed Engl* **2001**, *40*, 2004.
- (3) Lim, R. K.; Lin, Q. *Chem Commun (Camb)* **2010**, *46*, 1589.
- (4) Prescher, J. A.; Bertozzi, C. R. *Nat Chem Biol* **2005**, *1*, 13.
- (5) Patterson, D. M.; Nazarova, L. A.; Prescher, J. A. *ACS Chem Biol* **2014**, *9*, 592.
- (6) Baskin, J. M.; Prescher, J. A.; Laughlin, S. T.; Agard, N. J.; Chang, P. V.; Miller, I. A.; Lo, A.; Codelli, J. A.; Bertozzi, C. R. *Proc Natl Acad Sci U S A* **2007**, *104*, 16793.
- (7) Chan, J.; Dodani, S. C.; Chang, C. J. *Nat Chem* **2012**, *4*, 973.
- (8) Silhavy, T. J.; Kahne, D.; Walker, S. *Cold Spring Harb Perspect Biol* **2010**, *2*, a000414.
- (9) Lovering, A. L.; Safadi, S. S.; Strynadka, N. C. *Annu Rev Biochem* **2012**, *81*, 451.
- (10) Vollmer, W.; Blanot, D.; de Pedro, M. A. *FEMS Microbiol Rev* **2008**, *32*, 149.
- (11) Waxman, D. J.; Strominger, J. L. *Annu Rev Biochem* **1983**, *52*, 825.
- (12) Sauvage, E.; Kerff, F.; Terrak, M.; Ayala, J. A.; Charlier, P. *FEMS Microbiol Rev* **2008**, *32*, 234.
- (13) Rothfield, L.; Justice, S.; Garcia-Lara, J. *Annu Rev Genet* **1999**, *33*, 423.
- (14) Lupoli, T. J.; Tsukamoto, H.; Doud, E. H.; Wang, T. S.; Walker, S.; Kahne, D. *J Am Chem Soc* **2011**, *133*, 10748.
- (15) Cava, F.; de Pedro, M. A.; Lam, H.; Davis, B. M.; Waldor, M. K. *EMBO J* **2011**, *30*, 3442.
- (16) Lam, H.; Oh, D. C.; Cava, F.; Takacs, C. N.; Clardy, J.; de Pedro, M. A.; Waldor, M. K. *Science* **2009**, *325*, 1552.
- (17) Kuru, E.; Tekkam, S.; Hall, E.; Brun, Y. V.; Van Nieuwenhze, M. S. *Nat Protoc* **2015**, *10*, 33.
- (18) Kuru, E.; Hughes, H. V.; Brown, P. J.; Hall, E.; Tekkam, S.; Cava, F.; de Pedro, M. A.; Brun, Y. V.; VanNieuwenhze, M. S. *Angew Chem Int Ed Engl* **2012**, *51*, 12519.
- (19) Siegrist, M. S.; Whiteside, S.; Jewett, J. C.; Aditham, A.; Cava, F.; Bertozzi, C. R. *ACS Chem Biol* **2013**, *8*, 500.
- (20) Shieh, P.; Siegrist, M. S.; Cullen, A. J.; Bertozzi, C. R. *Proc Natl Acad Sci U S A* **2014**, *111*, 5456.
- (21) Siegrist, M. S.; Swarts, B. M.; Fox, D. M.; Lim, S. A.; Bertozzi, C. R. *FEMS Microbiol Rev* **2015**, *39*, 184.
- (22) Jacquier, N.; Frandi, A.; Pillonel, T.; Viollier, P. H.; Greub, G. *Nat Commun* **2014**, *5*, 3578.
- (23) Liechti, G. W.; Kuru, E.; Hall, E.; Kalinda, A.; Brun, Y. V.; VanNieuwenhze, M.; Maurelli, A. T. *Nature* **2014**, *506*, 507.
- (24) Gautam, S.; Gniadek, T. J.; Kim, T.; Spiegel, D. A. *Trends Biotechnol* **2013**, *31*, 258.

- (25) Fura, J. M.; Sabulski, M. J.; Pires, M. M. *ACS Chem Biol* **2014**, *9*, 1480.
- (26) Fura, J. M.; Pires, M. M. *Biopolymers* **2015**.
- (27) Pilhofer, M.; Aistleitner, K.; Biboy, J.; Gray, J.; Kuru, E.; Hall, E.; Brun, Y. V.; VanNieuwenhze, M. S.; Vollmer, W.; Horn, M.; Jensen, G. J. *Nat Commun* **2013**, *4*, 2856.
- (28) Blackman, M. L.; Royzen, M.; Fox, J. M. *J Am Chem Soc* **2008**, *130*, 13518.
- (29) Knall, A. C.; Slugovc, C. *Chem Soc Rev* **2013**, *42*, 5131.
- (30) Devaraj, N. K.; Weissleder, R.; Hilderbrand, S. A. *Bioconjug Chem* **2008**, *19*, 2297.
- (31) Devaraj, N. K.; Weissleder, R. *Acc Chem Res* **2011**, *44*, 816.
- (32) Lowy, F. D. *N Engl J Med* **1998**, *339*, 520.
- (33) Rieder, U.; Luedtke, N. W. *Angew Chem Int Ed Engl* **2014**, *53*, 9168.
- (34) Han, H. S.; Devaraj, N. K.; Lee, J.; Hilderbrand, S. A.; Weissleder, R.; Bawendi, M. G. *J Am Chem Soc* **2010**, *132*, 7838.
- (35) Lang, K.; Davis, L.; Wallace, S.; Mahesh, M.; Cox, D. J.; Blackman, M. L.; Fox, J. M.; Chin, J. W. *J Am Chem Soc* **2012**, *134*, 10317.
- (36) Lang, K.; Davis, L.; Torres-Kolbus, J.; Chou, C.; Deiters, A.; Chin, J. W. *Nat Chem* **2012**, *4*, 298.
- (37) Pidgeon, S. E.; Fura, J. M.; Leon, W.; Birabaharan, M.; Vezenov, D.; Pires, M. M. *Angew Chem Int Ed Engl* **2015**, *54*, 6158.
- (38) Lebar, M. D.; May, J. M.; Meeske, A. J.; Leiman, S. A.; Lupoli, T. J.; Tsukamoto, H.; Losick, R.; Rudner, D. Z.; Walker, S.; Kahne, D. *J Am Chem Soc* **2014**, *136*, 10874.
- (39) Chung, H. J.; Reiner, T.; Budin, G.; Min, C.; Liong, M.; Issadore, D.; Lee, H.; Weissleder, R. *ACS Nano* **2011**, *5*, 8834.
- (40) Liong, M.; Fernandez-Suarez, M.; Issadore, D.; Min, C.; Tassa, C.; Reiner, T.; Fortune, S. M.; Toner, M.; Lee, H.; Weissleder, R. *Bioconjug Chem* **2011**, *22*, 2390.
- (41) Devaraj, N. K.; Upadhyay, R.; Haun, J. B.; Hilderbrand, S. A.; Weissleder, R. *Angew Chem Int Ed Engl* **2009**, *48*, 7013.
- (42) Seitchik, J. L.; Peeler, J. C.; Taylor, M. T.; Blackman, M. L.; Rhoads, T. W.; Cooley, R. B.; Refakis, C.; Fox, J. M.; Mehl, R. A. *J Am Chem Soc* **2012**, *134*, 2898.

## Chapter 5

### Cell Wall Remodeling of *Staphylococcus aureus* in Live Hosts

#### **5.1 Abstract**

Peptidoglycan (PG) scaffolds are critical components of bacterial cell walls. They counter internal turgor pressure to prevent lysis and protect against external insults. It was recently discovered that various types of bacteria release large quantities of PG building blocks (D-amino acids) into their surrounding medium. Contrarily, cultured bacteria were also found to incorporate D-amino acids (both natural and synthetic) from the medium directly into their PG scaffold. These two processes may potentially function, in concert, to metabolically remodel PG in live host organisms. Yet, demonstration that bacteria can decorate their cell surfaces with exogenous D-amino acids was limited to *in vitro* culture conditions. We present the first evidence that bacteria remodel their PG with exogenous D-amino acids in a live host animal. A tetrazine click partner was conjugated onto the sidechain of a D-amino acid to capture incorporation into the bacterial PG scaffold using a complementary click-reactive fluorophore. *Staphylococcus aureus* infected *Caenorhabditis elegans* treated with exogenous D-amino acids readily revealed *in vivo* PG labeling. These results suggest that extracellular D-amino acids may provide pathogens with a mode of late-stage *in vivo* cell surface remodeling.

#### **5.2 Introduction**

The adaptation of bacteria to their surrounding environment is vital to their survival. As a prominent example, bacteria must adequately respond to challenges encountered during colonization of their host organisms. There is increasing evidence that structural remodeling of bacterial cell surfaces is a powerful mode of promoting colonization.<sup>1,2</sup> For

example, *Staphylococcus aureus* (*S. aureus*) cells decorate their surfaces to establish host adhesion and evade immune response.<sup>3</sup> Surface-bound sortases anchor full length proteins onto the peptidoglycan (PG) scaffold for their display to the host organism. Similarly, the PG structure can be chemically altered in response to environmental cues, including challenges with antibiotics and host immune system.<sup>4-12</sup>

Recently, it was discovered that diverse species of bacteria grown in culture release PG building blocks (D-amino acids) into the surrounding medium;<sup>13</sup> in turn, released D-amino acids modulated PG amount and strength (Figure 5.1). These findings were further extended to live host animals, which provided direct evidence that D-amino acid release may be integral to host-microbiome relationships.<sup>14</sup> Conversely, bacteria (both Gram-positive and -negative) incorporate extracellular D-amino acids within their own PG scaffolds.<sup>13,15</sup>

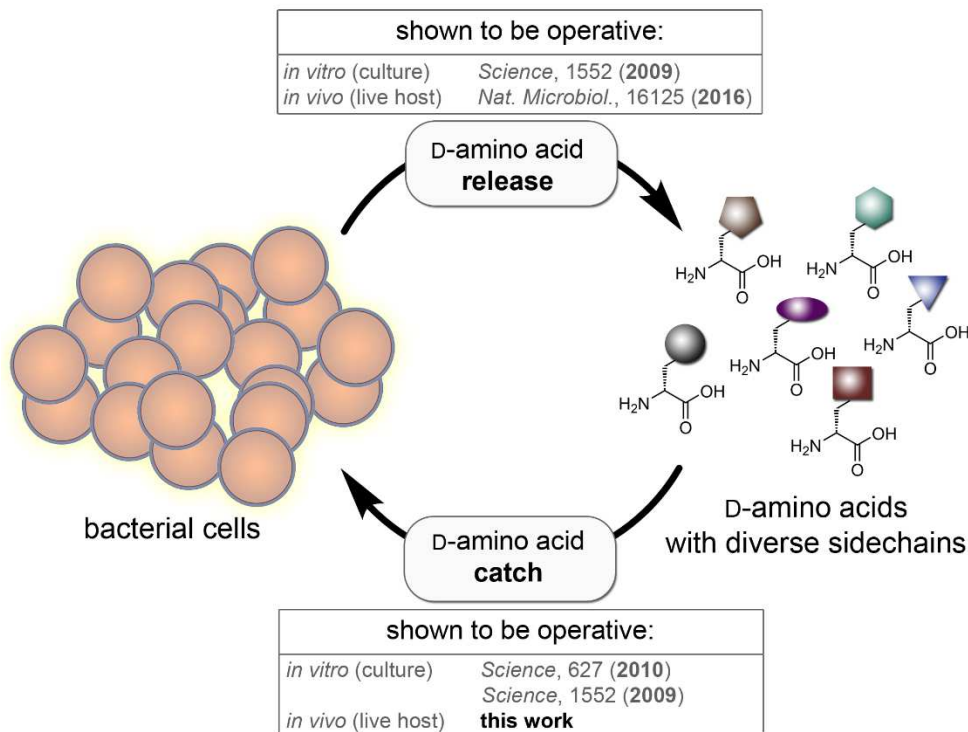


**Figure 5.1.** Scheme showing the two processes (D-amino acid release and incorporation) by bacterial cells both *in vitro* and *in vivo*.



D-amino acids are found within stem peptides from PG chains, which is a distinctive characteristic of bacteria. Bacteria incorporate exogenous D-amino acids into their expanding PG scaffold during cellular growth *via* surface bound transpeptidases such as Penicillin Binding Proteins (PBPs) and L,D-transpeptidases.<sup>13,15,16</sup> More specifically, exogenous D-amino acids supplemented in the surrounding medium replace D-alanine residues on PG stem peptides during crosslinking (Figure 5.2A). In addition to naturally produced D-amino acids, swapping of surface bound D-alanine was also established with entirely unnatural synthetic D-amino acids.<sup>17,18</sup> A striking feature of cell wall remodeling with synthetic D-amino acids is the vast promiscuity displayed by surface anchored transpeptidases in tolerating entirely unnatural sidechains.

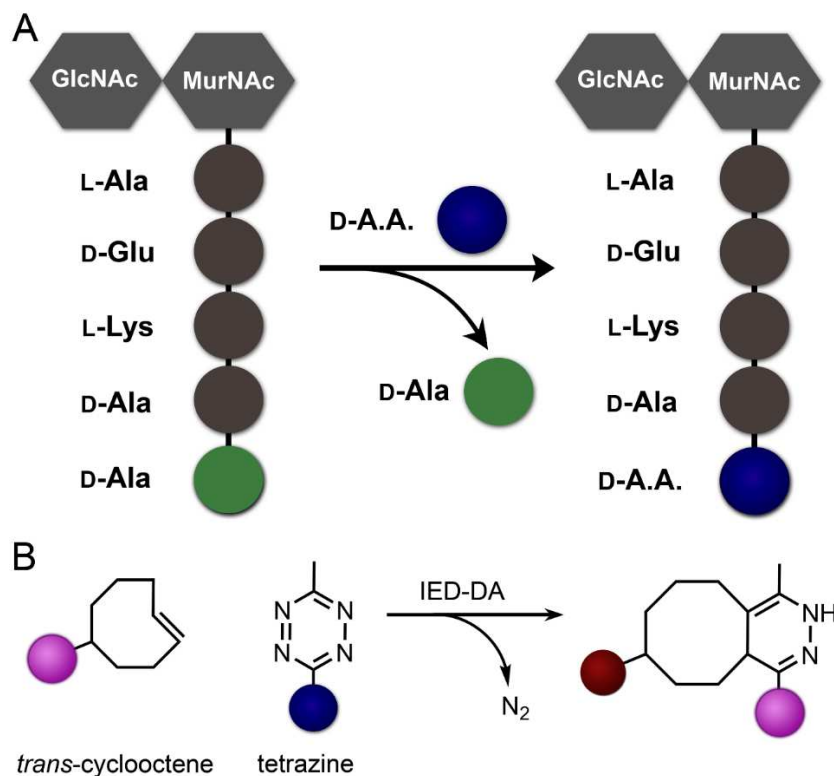


**Figure 5.2.** (A) Representation of PG remodeling in *S. aureus*. PBP transpeptidases catalyze the swapping of the 5<sup>th</sup> position amino acid on the stem peptide (D-Ala) with exogenous D-amino acids (D-A.A.). (B) Inverse electron demand-Diels Alder (IED-DA) results in the covalent ligation of a TCO and a tetrazine-modified fragment.

Metabolic PG labeling with synthetic D-amino acids provides a unique mode of installing handles (e.g., fluorophores) within the growing cell wall. In turn, fluorescent D-amino acids have become invaluable PG probes and have underpinned important new findings related to cell wall biosynthesis.<sup>19-25</sup> Similarly, our research group has leveraged relaxed substrate specificity by PG biosynthetic enzymes to graft unnatural handles onto bacterial cell surfaces.<sup>26-34</sup> Incorporation and release (“catch and release”) of D-amino acids potentially provide mechanisms to modulate the composition of the surrounding environment and remodel PG scaffolds. Yet, incorporation of exogenous D-amino acids into bacterial PG scaffolds in live host animals has not been demonstrated. Here, we designed a D-amino acid reporter probe that captured PG incorporation of exogenous D-amino acids in live *Caenorhabditis elegans* (*C. elegans*).

## **5.3 Results and Discussion**

### **5.3.1 Tetrazine D-Amino Acid Incorporation**

Selectivity, minimal cytotoxicity, diverse chemistries, and compatibility with complex biomacromolecules make bioorthogonal reactions powerful chemical tools to study biology.<sup>35-37</sup> Bertozzi and co-workers have previously shown that D-amino acids displaying copper-mediated (azide-alkyne) and copper-free (strained alkyne) click chemistry handles are tolerated by several Gram-positive bacteria.<sup>18,38,39</sup> More recently, we demonstrated that alkene- and tetrazine-displaying D-amino acids are readily incorporated onto bacterial PG scaffolds.<sup>34</sup> The tetrazine-*trans*-cyclooctene ligation is a rapid method for the assembly of biomolecular constructs (Figure 5.2B).<sup>40</sup> With rate constants up to  $10^6 \text{ M}^{-1}\text{s}^{-1}$ , this inverse electron demand Diels-Alder (IED-DA) reaction provides exceptional versatility and compatibility with *in vivo* ligations.<sup>41,42</sup>

In our original design, we reasoned that either the alkene handle or tetrazine handle could be conjugated onto the sidechain of a D-amino acid. We were concerned that the large size of *trans*-cyclooctene (TCO) would dramatically lower labeling efficiency, having previously shown that the sidechain size can have an inverse relationship with incorporation efficiency.<sup>29</sup> Therefore, the smaller norbornene was chosen in the place of TCO. Unfortunately, low ring strain in norbornene had a deleterious effect on conjugation efficiency with tetrazine-conjugated fluorophores. The reactive partners were swapped in a second set of D-amino acids, which were modified to display the tetrazine handle. A small tetrazine was assembled onto the sidechain of D-propionic acid. Although cell surface labeling was observed, the electron donating effect of the amino group dramatically reduced IED-DA efficiency.

The slow reaction rates from our previous alkene-tetrazine strategy, which required several hours of treatment for observable ligation, became a significant impediment in capturing PG remodeling in live organisms. We set out to improve on this design by using optimized handles that result in fast ligation without compromising incorporation efficiency. Towards this goal, we synthesized D-TetPG, a tetrazine derivative flanked by a phenyl substituent (Figure 5.3A). Its enantiomer was recently shown to display high reactivity and stability when incorporated into recombinant green fluorescent protein (GFP).<sup>43</sup> Electron-withdrawing by the phenyl ring led to diene activation with minimal increase in structural size. Ligation with TCO-modified handles was exceedingly fast with product formation complete within ~2 min.

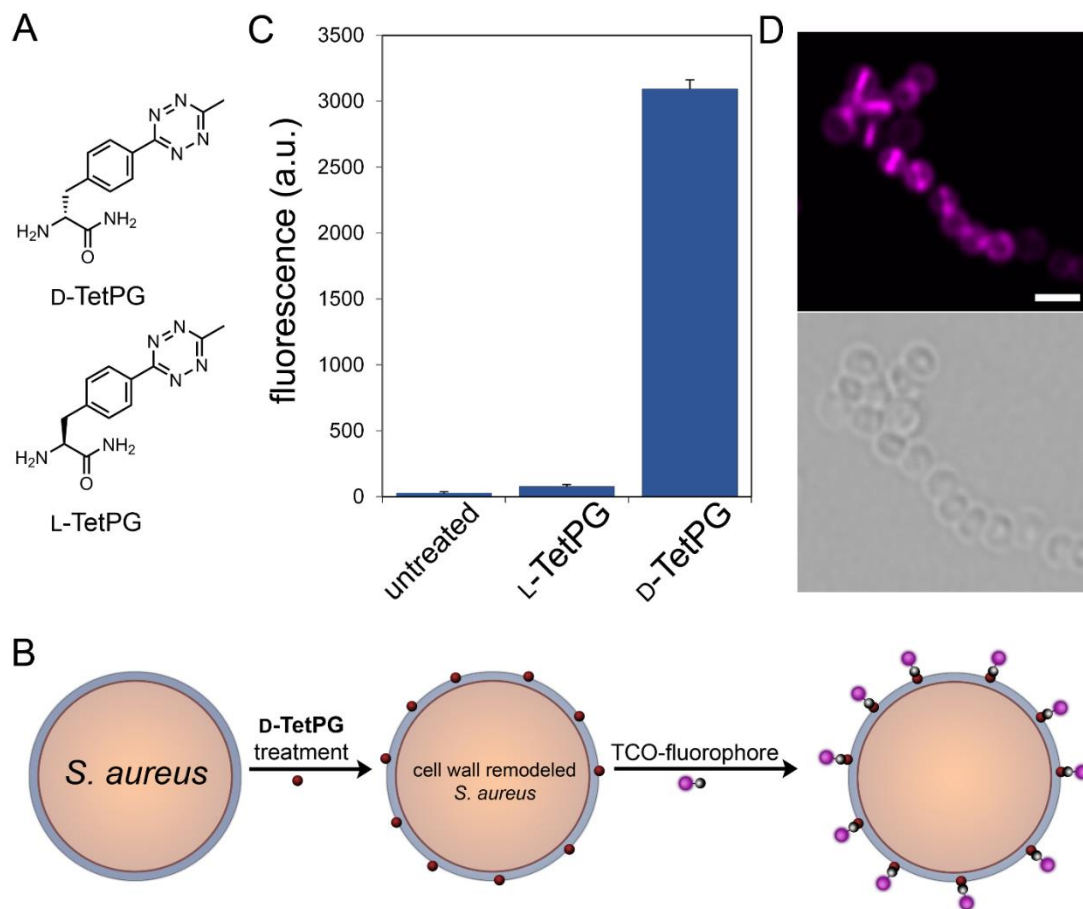


**Figure 5.3.** (A) Chemical structures of D-TetPG and L-TetPG. (B) Schematic representation of PG labeling of *S. aureus* by D-TetPG and its ligation with a TCO-fluorophore. (C) *S. aureus* cells were treated with D-TetPG (1 mM), L-TetPG (1 mM), or untreated media overnight followed by incubation with 50  $\mu$ M Cy5-TCO (30 min) and analyzed using flow cytometry. Data are represented as mean + SD (n =3). (D) Fluorescence microscopy (top) and phase contrast (bottom) imaging of *S. aureus* treated with D-TetPG from (C). Scale bar represents 2  $\mu$ m.

Synthesis of D-TetPG was initiated by reacting Boc-4-cyano-D-Phenylalanine with anhydrous hydrazine and nickel triflate catalyst, followed by oxidation with sodium nitrite. Conversion to the C-terminus carboxamide form was performed by using standard solid phase peptide coupling to Rink Amide resin, followed by global release and deprotection. We, and others, have found that C-terminus amidation improves incorporation and retention of exogenous D-amino acids in Gram-positive bacteria relative to its carboxylic acid counterpart.<sup>25,30</sup> The final D-TetPG was purified by RP-HPLC and characterized by

NMR and HRMS. The control enantiomeric L-TetPG was synthesized using a similar route with the exception of the starting building block, which was the L-stereocenter.

The ability of D-TetPG to label bacterial PG was first assessed in cultured *S. aureus* (Figure 5.3B). *S. aureus* is an excellent model Gram-positive pathogen due to its high clinical burden and emerging drug-resistant strains. *S. aureus* cells were treated overnight with D-TetPG, formaldehyde fixed, incubated with the fluorophore conjugate Cy5-TCO, and labeling was quantified *via* flow cytometry (Figure 5.3C). A marked increase in fluorescence levels (>100-fold) was observed for cells treated with D-TetPG relative to untreated cells. In contrast, treatment of *S. aureus* with the enantiomeric L-TetPG led to a 2-fold increase in fluorescence levels compared to untreated cells. These results are consistent with the requirement of D-stereocenters for incorporation into PG scaffolds. Confocal microscopy analysis of D-TetPG treated *S. aureus* revealed concentrated signals at the septal region, which is the primary site of new PG biosynthesis (Figure 5.3D). In addition, a labeling competition experiment was performed by co-incubation of D-TetPG with D-Ala, which resulted in a significant decrease in cellular fluorescence (Figure 5.4). These results clearly suggest that D-TetPG is readily accommodated by bacterial cells to reveal *in vitro* PG remodeling.

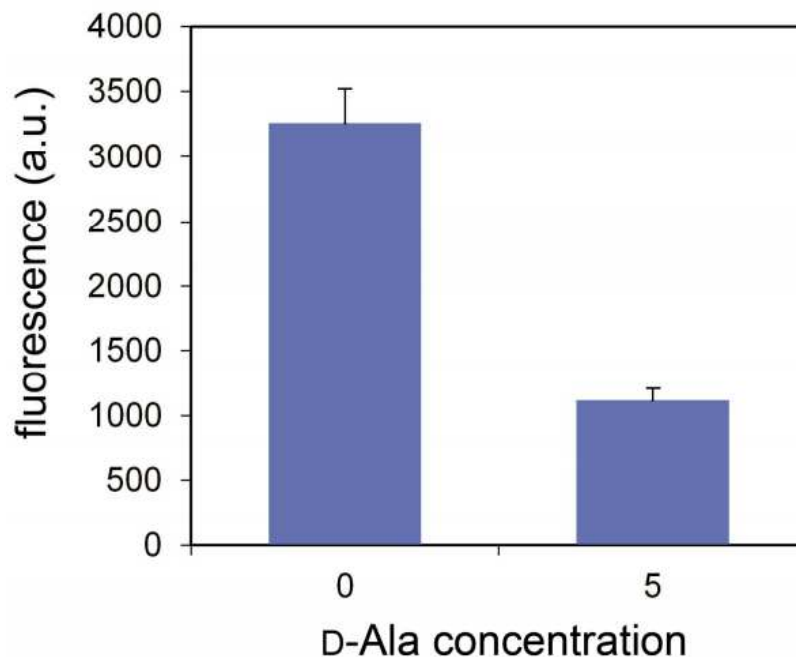


**Figure 5.4.** *S. aureus* cells were treated with D-TetPG (1 mM) in the presence of no D-Ala or 5 mM D-Ala overnight followed by incubation with 50  $\mu$ M Cy5-TCO and analyzed using flow cytometry. Data are represented as mean + SD (n =3).

### **5.3.2 Kinetics of Tetrazine D-Amino Acids**

Next, the kinetics of surface-bound tetrazine-TCO ligation was evaluated using live bacterial cells. Ligation between phenyl-flanked tetrazine and TCO was previously found to be extremely fast using model proteins.<sup>43</sup> However, tetrazine handles are imbedded within the PG matrix in D-TetPG labeled cells, which can potentially alter reaction kinetics. To test this concept, *S. aureus* cells were once again treated with D-TetPG, incubated with Cy5-TCO, and samples were periodically analyzed for fluorescence levels for 180 min (Figure 5.5). By the first time point (5 min), fluorescence levels were nearly 100-fold over background and reached a plateau level within 15 min. From these results, it was evident that PG-anchored tetrazine handles are readily reacted with Cy5-TCO and the ligation is mostly complete within a few minutes.

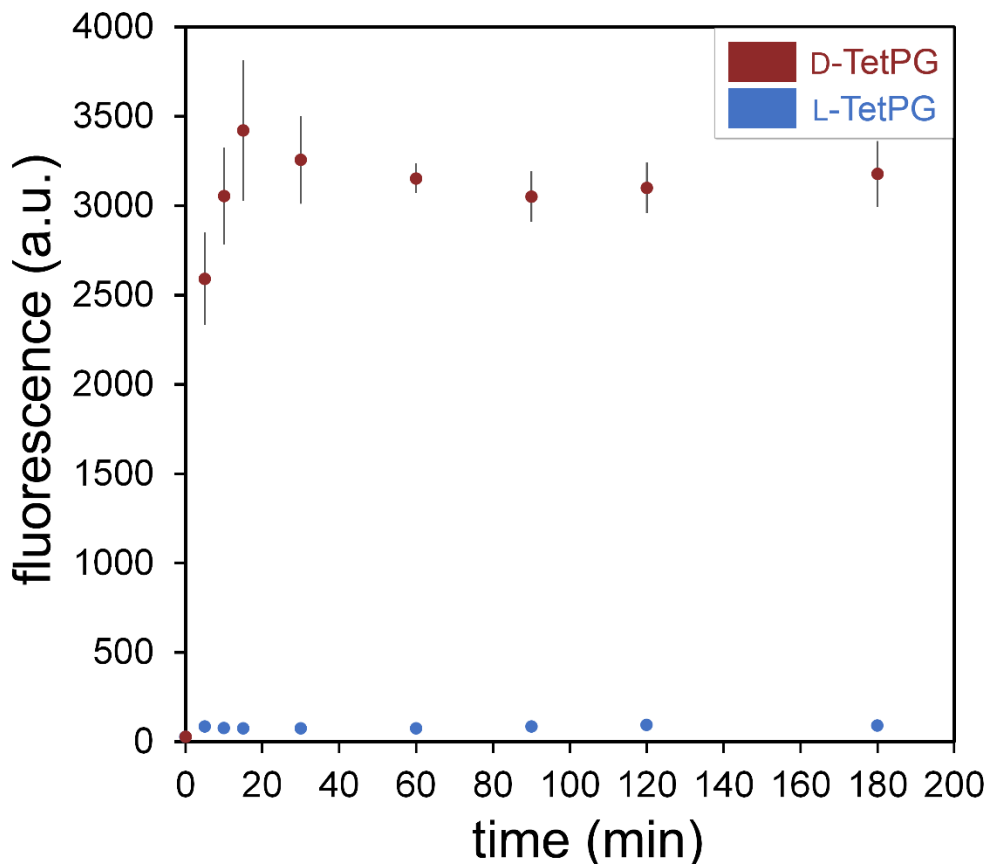


**Figure 5.5.** *S. aureus* cells were treated with D-TetPG (1 mM) or L-TetPG (1 mM) overnight followed by incubation with 50  $\mu$ M Cy5-TCO and analyzed at various time points using flow cytometry. Data are represented as mean + SD (n =3).

### **5.3.3 In vivo D-Amino Acid Labeling**

With a synthetic D-amino acid in hand operating in a time-scale compatible with *in vivo* studies, we turned our attention to capturing PG remodeling in live host organisms. The nematode *C. elegans* has proven to be a highly valuable animal model for studying host-pathogen interactions.<sup>44-46</sup> We had anticipated that direct monitoring of PG remodeling with fluorescently-labeled D-amino acids would suffer from two severe drawbacks: (1) low incorporation efficiency due to the large sidechain and (2) high background fluorescence levels. The high background fluorescence was expected due to the high concentrations required for robust PG labeling by unnatural D-amino acids – a

product of the inherent high  $K_M$  of PBPs for its substrates. Nonetheless, we tested the possibility of directly capturing PG remodeling in *C. elegans* with FITC-modified D-Lysine, D-Lys(FITC). *S. aureus*-infected *C. elegans* were treated with D-Lys(FITC) and analyzed by fluorescence microscopy. mCherry-expressing *S. aureus* were observed in various compartments of *C. elegans* (Figure 5.6). However, green fluorescence signal from D-Lys(FITC) was observed indiscriminately throughout the inner cavity of *C. elegans*. The high fluorescence background highlights the need for a two-step ligation that optimizes incorporation and signal-to-noise levels.

We next evaluated the compatibility of tetrazine-TCO ligations in live *C. elegans* by pre-labeling bacterial

cells with the PG probe D-TetPG (*ex vivo* labeling, Figure 5.7). GFP-expressing *S. aureus* cells were used to visualize co-localization of bacteria

and D-TetPG labels on bacterial PG. After overnight treatment with D-TetPG, *S. aureus* cells were washed and transferred to a liquid culture of *C. elegans* (infection period). After a 4 h incubation period, non-colonized bacteria were removed, followed by treatment with Cy5-TCO for 20 min. Confocal microscopy imaging showed prominent PG labeling co-

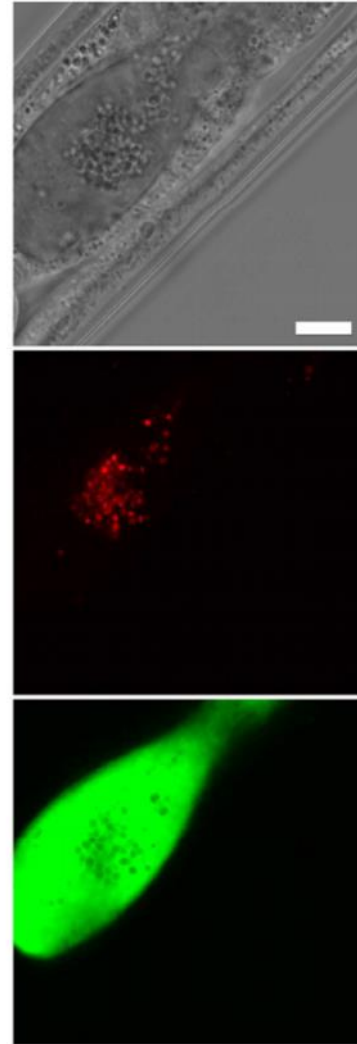


**Figure 5.6.** *S. aureus* labeling with D-Lys (FITC). *S. aureus* were introduced into *C. elegans* for 4 h, washed to remove uncolonized bacteria, treated with 1 mM D-Lys (FITC) for 3 h. *C. elegans* were washed, anesthetized, mounted on a bed of agarose, and imaged using confocal microscopy. Scale bar represents 10  $\mu$ m.



localized with GFP-expressing *S. aureus* (Figure 5.8). Bacterial treatment with the control L-TetPG led to no discernible Cy5 fluorescence signals (Figure 5.9). These results establish the constructive ligation of tetrazine-TCO handles within PG scaffolds in the host organism *C. elegans*. In the future, we plan to explore this facile mode of grafting unnatural handles onto bacterial cell surfaces with the goal of revealing key aspects of host-pathogen interactions.

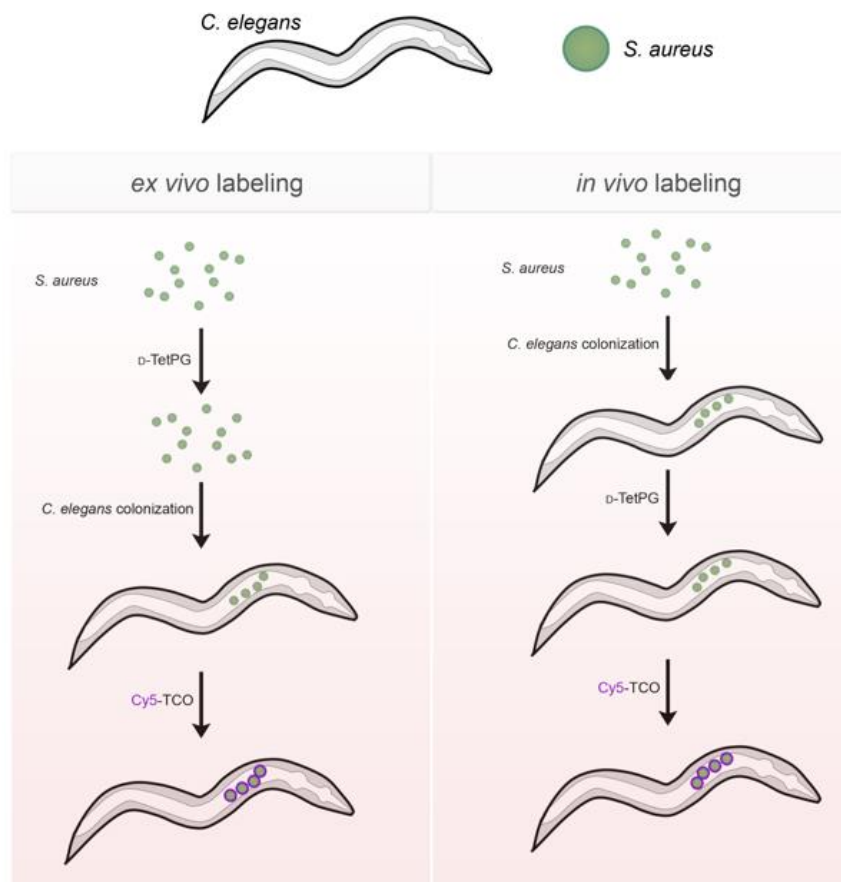


**Figure 5.7.** Schematic representation of PG labeling of *S. aureus* by D-TetPG *ex vivo* and *in vivo* with *C. elegans*. *Ex vivo* labeling corresponds to labeling of *S. aureus* cells with D-TetPG prior to infection. *In vivo* corresponds to labeling of *S. aureus* cells with D-TetPG within *C. elegans* followed by Cy5-TCO ligation.

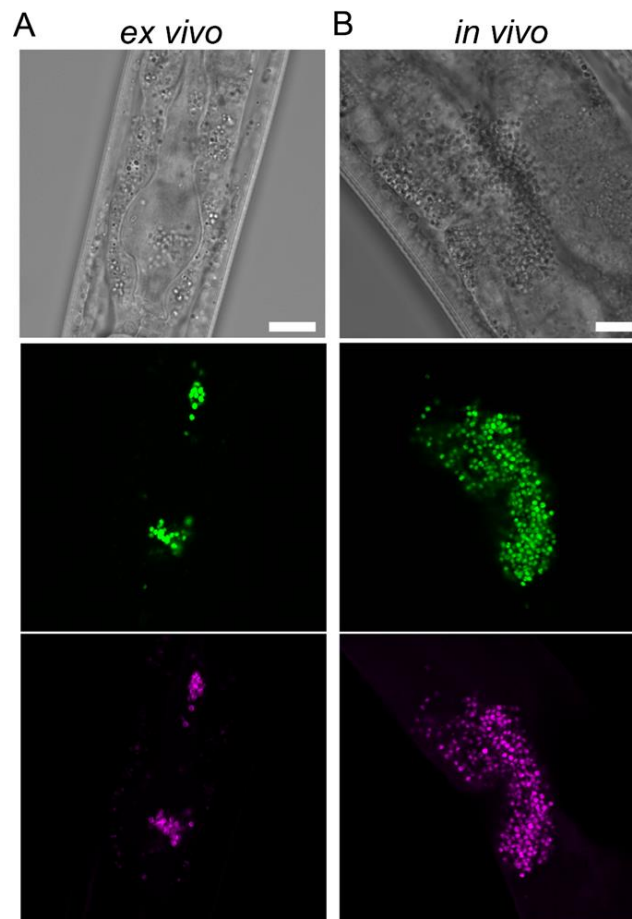


**Figure 5.8.** (A) *S. aureus* cells were treated overnight with D-TetPG (1 mM), transferred to a liquid culture of *C. elegans* (infection period) for 4 h, washed to remove non-colonized bacteria, and incubated with Cy5-TCO for 20 min. (B) *S. aureus* were introduced into *C. elegans*, washed to remove uncolonized bacteria, treated with D-TetPG (1 mM) for 3 h, and Cy5-TCO for 20 min. For (A) and (B), *C. elegans* were anesthetized, mounted on a bed of agarose, and imaged using confocal microscopy. Scale bar presents 10  $\mu\text{m}$ .

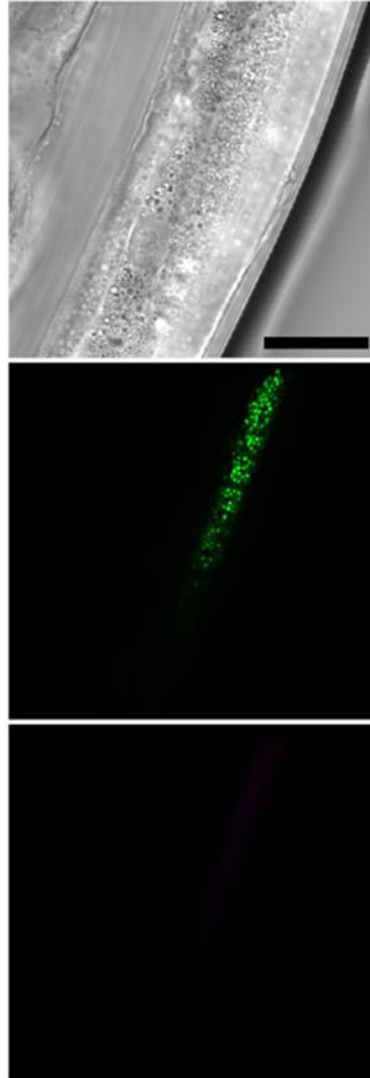


**Figure 5.9.** *S. aureus* were introduced into *C. elegans* for 4 h, washed to remove uncolonized bacteria, treated with L-TetPG (1 mM) for 3 h, and then Cy5-TCO for 20 min. *C. elegans* were anesthetized, mounted on a bed of agarose, and imaged using confocal microscopy. Scale bar presents 10  $\mu$ m.

Finally, we evaluated PG remodeling by exogenous D-amino acids in *S. aureus* infected *C. elegans* (*in vivo* labeling, Figure 5.7). Untreated bacterial cells were first introduced into *C. elegans* to initiate colonization. Consistent with previous reports, *C. elegans* infected with *S. aureus* cells showed distention of the lumen, suggestive of *S. aureus* pathogenicity.<sup>47</sup> After which point, *C. elegans* were treated with D-TetPG for 3 h to induce PG remodeling and ligation was performed with Cy5-TCO in live hosts.

Remarkably, clear co-localization of Cy5-fluorescence signals and GFP-expressing *S. aureus* was observed, which is indicative of *in vivo* PG remodeling (Figure 5.8). To our knowledge, this represents the first example of exogenous D-amino acids incorporation by bacteria in a live host organism.

#### **5.4 Conclusion**

In conclusion, we have demonstrated that a D-amino acid conjugated with an optimized tetrazine led to PG remodeling of bacterial cells. We showed that a complimentary click partner led to rapid ligation onto PG-anchored tetrazine handles in cultured bacteria and in *S. aureus* infected *C. elegans*. Our results close the loop on the D-amino acid “catch & release” phenomenon observed for bacteria both *in vitro* and *in vivo*. Going forward, we will investigate the functional consequence of PG remodeling by both pathogenic and commensal bacteria in *C. elegans*.

#### **5.5 Materials and Methods**

All peptide related reagents (resin, coupling reagent, amino acids, and cleavage reagents) were purchased from ChemImpex. Cy5-trans-cyclooctene (Cy5-TCO) was purchased from Click Chemistry Tools. All other reagents were purchased from Sigma and were used without further purification. Bacterial strain used for the experiments were: Strain Growth Media *Staphylococcus aureus* AH2547 = *S. aureus* HG001 (AH2183) + pCM29 (P<sub>sarA</sub>\_sGFP, camR) BBL Trypticase Soy Broth (TSB), *Staphylococcus aureus* SC01 LB Broth (Lennox)

**Stereospecificity of transpeptidase.** LB broth containing 1 mM D-Tet or L-Tet were prepared. *Staphylococcus aureus* SC01 from an overnight growth was added to the medium (1:100 dilution) and allowed to grow overnight at 37 °C with shaking. The bacteria were

harvested at 6,000g and washed three times with original culture volume of 1x PBS followed by fixation with 2% formaldehyde in 1x PBS for 30 min at ambient temperature. Cells were washed once more to remove the formaldehyde and the cells were then suspended in 50 uM Cy5-TCO in 1x PBS and shaken at ambient temperature for 30 min. The bacteria were washed three times with 1x PBS and samples analyzed using a BDFacs Canto II flow cytometer with a 633nm HeNe laser (L1) and a 660/20 band-pass filter (FL5). A minimum of 10,000 events were counted for each data set.

**Live Cell TCO Kinetics.** LB broth containing 1 mM D-Tet was prepared. *Staphylococcus aureus* SC01 from an overnight growth was added to the medium (1:100 dilution) and allowed to grow overnight at 37 oC with shaking. The bacteria were harvested at 6,000g and washed three times with original culture volume of 1x PBS. Cells were then suspended in 50 uM Cy5-TCO in 1x PBS and shaken at ambient temperature and various time points were collected. At each time point, the cells were fixed with 2% formaldehyde in 1x PBS for 30 min at ambient temperature. Cells were washed once more to remove the formaldehyde and samples analyzed by flow cytometry using previously stated parameters. For confocal microscopy, the cells were analyzed on a glass slide using a Nikon Eclipse Ti-E with Cy5 filter.

***Ex vivo* Cy5-TCO Click Chemistry in *C. elegans*.** N2 *Caenorhabditis elegans* were maintained by standard protocol using nematode growth agar with bacterial lawns of *E.coli* OP50 on a 60mm x 15mm cell culture dish. *C. elegans* were grown to contain primarily L4 larval stage nematodes by incubation at ambient temperature for ~48-52 h, washed off the plates with M9 buffer, and washed three times with M9 buffer. For washing steps, the *C. elegans* were pelleted at 1000g. The *C. elegans* were resuspended in 450 uL of M9 buffer

containing 10% LB broth and transferred to a sterile 24 multiwell plate. *Staphylococcus aureus* GFP (50 uL) pre-labeled overnight in 1 mM D-Tet and washed was added to the 450 uL suspension of *C. elegans*. The *C. elegans* were incubated at ambient temperature for 4 hrs, harvested at 1000g and washed three times with M9 buffer to remove bacteria on the outside of the *C. elegans*. The *C. elegans* were then resuspended in 500 uL of M9 buffer containing 10% LB broth and 50 uM Cy5-TCO and incubated for 20 min at ambient temperature. The *C. elegans* were harvested at 1000g, and washed three times with M9 buffer, and put into a final suspension of 10mM sodium azide in M9 buffer and analyzed by confocal microscopy.

***In Vivo* D-Tet Labeling and Cy5-TCO Click Chemistry in *C. elegans*.** N2 *Caenorhabditis elegans* were maintained by standard protocol using nematode growth agar with bacterial lawns of *E. coli* OP50 (source) on a 60mm x 15mm cell culture dish. *C. elegans* were grown to contain primarily L4 larval stage nematodes by incubation at ambient temperature for ~48-52 h, washed off the plates with M9 buffer, and washed three times with M9 buffer. For washing steps, the *C. elegans* were pelleted at 1000g. The *C. elegans* were resuspended in 450 uL of M9 buffer containing 10% LB broth and transferred to a sterile 24 multiwell plate. *Staphylococcus aureus* GFP (50 uL) from an overnight culture was washed and added to the 450 uL suspension of *C. elegans*. The *C. elegans* were incubated at ambient temperature for 2 hrs, harvested at 1000g and washed three times with M9 buffer to remove bacteria on the outside of the *C. elegans*. The *C. elegans* were then resuspended in 500 uL of M9 buffer containing 10% LB broth and 1 mM D-Tet or L-Tet, and incubated at ambient temperature for 3 hrs. The *C. elegans* were harvested at 1000g and washed three times with M9 buffer and resuspended in 50 uM Cy5-TCO and incubated

for 20 min at ambient temperature. The *C. elegans* were harvested at 1000g, and washed three times with M9 buffer, and put into a final suspension of 10mM sodium azide in M9 buffer and analyzed by confocal microscopy.

## 5.6 References

- (1) Ribet, D.; Cossart, P. *Microbes Infect* **2015**, *17*, 173.
- (2) King, J. E.; Roberts, I. S. *Adv Exp Med Biol* **2016**, *915*, 129.
- (3) Hendrickx, A. P.; Budzik, J. M.; Oh, S. Y.; Schneewind, O. *Nat Rev Microbiol* **2011**, *9*, 166.
- (4) Alvarez, L.; Espaillet, A.; Hermoso, J. A.; de Pedro, M. A.; Cava, F. *Microb Drug Resist* **2014**, *20*, 190.
- (5) Horcajo, P.; de Pedro, M. A.; Cava, F. *Microb Drug Resist* **2012**, *18*, 306.
- (6) Lavollay, M.; Arthur, M.; Fourgeaud, M.; Dubost, L.; Marie, A.; Veziris, N.; Blanot, D.; Gutmann, L.; Mainardi, J. L. *J Bacteriol* **2008**, *190*, 4360.
- (7) Pisabarro, A. G.; Canada, F. J.; Vazquez, D.; Arriaga, P.; Rodriguez-Tebar, A. *J Antibiot (Tokyo)* **1986**, *39*, 914.
- (8) Boneca, I. G.; Dussurget, O.; Cabanes, D.; Nahori, M. A.; Sousa, S.; Lecuit, M.; Psylinakis, E.; Bouriotis, V.; Hugot, J. P.; Giovannini, M.; Coyle, A.; Bertin, J.; Namane, A.; Rousselle, J. C.; Cayet, N.; Prevost, M. C.; Balloy, V.; Chignard, M.; Philpott, D. J.; Cossart, P.; Girardin, S. E. *Proc Natl Acad Sci U S A* **2007**, *104*, 997.
- (9) Vollmer, W.; Tomasz, A. *J Biol Chem* **2000**, *275*, 20496.
- (10) Zipperle, G. F., Jr.; Ezzell, J. W., Jr.; Doyle, R. J. *Can J Microbiol* **1984**, *30*, 553.
- (11) Bera, A.; Biswas, R.; Herbert, S.; Kulauzovic, E.; Weidenmaier, C.; Peschel, A.; Gotz, F. *J Bacteriol* **2007**, *189*, 280.
- (12) Singh, M.; Chang, J.; Coffman, L.; Kim, S. J. *Sci Rep* **2016**, *6*, 31757.
- (13) Lam, H.; Oh, D. C.; Cava, F.; Takacs, C. N.; Clardy, J.; de Pedro, M. A.; Waldor, M. K. *Science* **2009**, *325*, 1552.
- (14) Sasabe, J.; Miyoshi, Y.; Rakoff-Nahoum, S.; Zhang, T.; Mita, M.; Davis, B. M.; Hamase, K.; Waldor, M. K. *Nat Microbiol* **2016**, *1*, 16125.
- (15) Kolodkin-Gal, I.; Romero, D.; Cao, S.; Clardy, J.; Kolter, R.; Losick, R. *Science* **2010**, *328*, 627.
- (16) Squeglia, F.; Marchetti, R.; Ruggiero, A.; Lanzetta, R.; Marasco, D.; Dworkin, J.; Petoukhov, M.; Molinaro, A.; Berisio, R.; Silipo, A. *J Am Chem Soc* **2011**, *133*, 20676.
- (17) Kuru, E.; Hughes, H. V.; Brown, P. J.; Hall, E.; Tekkam, S.; Cava, F.; de Pedro, M. A.; Brun, Y. V.; VanNieuwenhze, M. S. *Angew Chem Int Ed Engl* **2012**, *51*, 12519.
- (18) Siegrist, M. S.; Whiteside, S.; Jewett, J. C.; Aditham, A.; Cava, F.; Bertozzi, C. R. *ACS Chem Biol* **2013**, *8*, 500.
- (19) Bisson-Filho, A. W.; Hsu, Y. P.; Squyres, G. R.; Kuru, E.; Wu, F.; Jukes, C.; Sun, Y.; Dekker, C.; Holden, S.; VanNieuwenhze, M. S.; Brun, Y. V.; Garner, E. C. *Science* **2017**, *355*, 739.
- (20) Pilhofer, M.; Aistleitner, K.; Biboy, J.; Gray, J.; Kuru, E.; Hall, E.; Brun, Y. V.; VanNieuwenhze, M. S.; Vollmer, W.; Horn, M.; Jensen, G. J. *Nat Commun* **2013**, *4*, 2856.
- (21) Fleurie, A.; Lesterlin, C.; Manuse, S.; Zhao, C.; Cluzel, C.; Laverge, J. P.; Franz-Wachtel, M.; Macek, B.; Combet, C.; Kuru, E.; VanNieuwenhze, M. S.; Brun, Y. V.; Sherratt, D.; Grangeasse, C. *Nature* **2014**, *516*, 259.
- (22) Liechti, G. W.; Kuru, E.; Hall, E.; Kalinda, A.; Brun, Y. V.; VanNieuwenhze, M.; Maurelli, A. T. *Nature* **2014**, *506*, 507.
- (23) Faure, L. M.; Fiche, J. B.; Espinosa, L.; Ducret, A.; Anantharaman, V.; Luciano, J.; Lhospice, S.; Islam, S. T.; Treguier, J.; Sotes, M.; Kuru, E.; Van Nieuwenhze, M. S.; Brun, Y. V.; Theodoly, O.; Aravind, L.; Nollmann, M.; Mignot, T. *Nature* **2016**, *539*, 530.
- (24) Qiao, Y.; Lebar, M. D.; Schirner, K.; Schaefer, K.; Tsukamoto, H.; Kahne, D.; Walker, S. *J Am Chem Soc* **2014**, *136*, 14678.
- (25) Lebar, M. D.; May, J. M.; Meeske, A. J.; Leiman, S. A.; Lupoli, T. J.; Tsukamoto, H.; Losick, R.; Rudner, D. Z.; Walker, S.; Kahne, D. *J Am Chem Soc* **2014**, *136*, 10874.
- (26) Pires, M. M.; Pidgeon, S. E. *Angew Chem Int Ed Engl* **2017**.



- (27) Fura, J. M.; Pidgeon, S. E.; Birabaharan, M.; Pires, M. M. *ACS Infect Dis* **2016**, *2*, 302.
- (28) Sarkar, S.; Libby, E. A.; Pidgeon, S. E.; Dworkin, J.; Pires, M. M. *Angew Chem Int Ed Engl* **2016**, *55*, 8401.
- (29) Fura, J. M.; Kearns, D.; Pires, M. M. *J Biol Chem* **2015**, *290*, 30540.
- (30) Pidgeon, S. E.; Fura, J. M.; Leon, W.; Birabaharan, M.; Vezenov, D.; Pires, M. M. *Angew Chem Int Ed Engl* **2015**, *54*, 6158.
- (31) Sarkar, S.; Pires, M. M. *PLoS One* **2015**, *10*, e0117613.
- (32) Fura, J. M.; Sabulski, M. J.; Pires, M. M. *ACS Chem Biol* **2014**, *9*, 1480.
- (33) Pidgeon, S. E.; Pires, M. M. *ACS Chem Biol* **2017**.
- (34) Pidgeon, S. E.; Pires, M. M. *Chem Commun (Camb)* **2015**, *51*, 10330.
- (35) Prescher, J. A.; Dube, D. H.; Bertozzi, C. R. *Nature* **2004**, *430*, 873.
- (36) Agard, N. J.; Prescher, J. A.; Bertozzi, C. R. *J Am Chem Soc* **2004**, *126*, 15046.
- (37) Dehnert, K. W.; Baskin, J. M.; Laughlin, S. T.; Beahm, B. J.; Naidu, N. N.; Amacher, S. L.; Bertozzi, C. R. *Chembiochem* **2012**, *13*, 353.
- (38) Shieh, P.; Siegrist, M. S.; Cullen, A. J.; Bertozzi, C. R. *Proc Natl Acad Sci U S A* **2014**, *111*, 5456.
- (39) Ngo, J. T.; Adams, S. R.; Deerinck, T. J.; Boassa, D.; Rodriguez-Rivera, F.; Palida, S. F.; Bertozzi, C. R.; Ellisman, M. H.; Tsien, R. Y. *Nat Chem Biol* **2016**, *12*, 459.
- (40) Blackman, M. L.; Royzen, M.; Fox, J. M. *J Am Chem Soc* **2008**, *130*, 13518.
- (41) Devaraj, N. K.; Weissleder, R. *Acc Chem Res* **2011**, *44*, 816.
- (42) Devaraj, N. K.; Thurber, G. M.; Keliher, E. J.; Marinelli, B.; Weissleder, R. *Proc Natl Acad Sci U S A* **2012**, *109*, 4762.
- (43) Blizzard, R. J.; Backus, D. R.; Brown, W.; Bazewicz, C. G.; Li, Y.; Mehl, R. A. *J Am Chem Soc* **2015**, *137*, 10044.
- (44) Alegado, R. A.; Campbell, M. C.; Chen, W. C.; Slutz, S. S.; Tan, M. W. *Cell Microbiol* **2003**, *5*, 435.
- (45) Garcia-Lara, J.; Needham, A. J.; Foster, S. J. *FEMS Immunol Med Microbiol* **2005**, *43*, 311.
- (46) Arvanitis, M.; Glavis-Bloom, J.; Mylonakis, E. *Curr Opin Pharmacol* **2013**, *13*, 769.
- (47) Sifri, C. D.; Baresch-Bernal, A.; Calderwood, S. B.; von Eiff, C. *Infect Immun* **2006**, *74*, 1091.

## Chapter 6

# Vancomycin-dependent Response in Live Drug-Resistant Bacteria via Metabolic Labeling

### 6.1 Abstract

The surge in drug-resistant bacterial infections threatens to overburden healthcare systems worldwide. Bacterial cell walls are essential to bacteria – making them unique targets for the development of antibiotics. We describe a cellular reporter to directly monitor the phenotypic switch in drug resistant bacteria with temporal resolution. Vancomycin-resistant Enterococci (VRE) escape the bactericidal actions of vancomycin by chemically modifying their cell wall precursors, which renders them drug insensitive. A synthetic cell wall analog was developed to hijack the biosynthetic rewiring for drug resistant cells in response to antibiotics. Our work provides the first *in vivo* VanX reporter agent that responds to cell wall alteration in drug resistant bacteria. Cellular reporters that reveal mechanisms related to antibiotic resistance can potentially have a significant impact on the fundamental understanding of cellular adaption to antibiotics.

### 6.2 Introduction

Vancomycin, and related glycopeptides, disrupt PG assembly by binding to the terminal D-alanyl-D-alanine (D-Ala-D-Ala) of Lipid II, sequestering peptidoglycan (PG) building blocks (Figure 6.1A).<sup>1,2</sup> The most prevalent form of vancomycin resistance occurs when the last amino acid on Lipid II is chemically modified from D-Alanine (D-Ala) to D-Lactic acid (D-Lac) (Figure 6.1B).<sup>3-6</sup> Metabolic re-engineering of Lipid II in VRE cells is controlled by a set of antibiotic inducible genes: *vanR*, *vanS*, *vanH*, *vanA*, and *vanX* genes (*vanRSHAX*).<sup>7,8</sup> In order for VRE cells to reach high levels of resistance they must vastly

reduce the cytoplasmic pool of D-Ala-D-Ala. To accomplish this, VRE cells express D,D-dipeptidase VanX to hydrolyze D-Ala-D-Ala, which allows D-Ala-D-Lac to accumulate in its place (Figure 6.1C).<sup>9-11</sup> We hypothesized that synthetic analogs of D-Ala-D-Ala would enable the *in vivo* interrogation of VanX activity, thus providing a platform for the first direct phenotypic assay for VanX in VRE cells. Non-native analogs of D-Ala-D-Ala were recently shown to be tolerated by MurF.<sup>12-16</sup> Maurelli and co-workers applied this strategy to confirm the presence of PG in *Chlamydia trachomatis* – settling a 50 year debate.<sup>12,15</sup> We anticipated that dipeptide analogs could be leveraged to track the *in vivo* Lipid II processing associated with vancomycin resistant bacteria (Figure 6.2A).

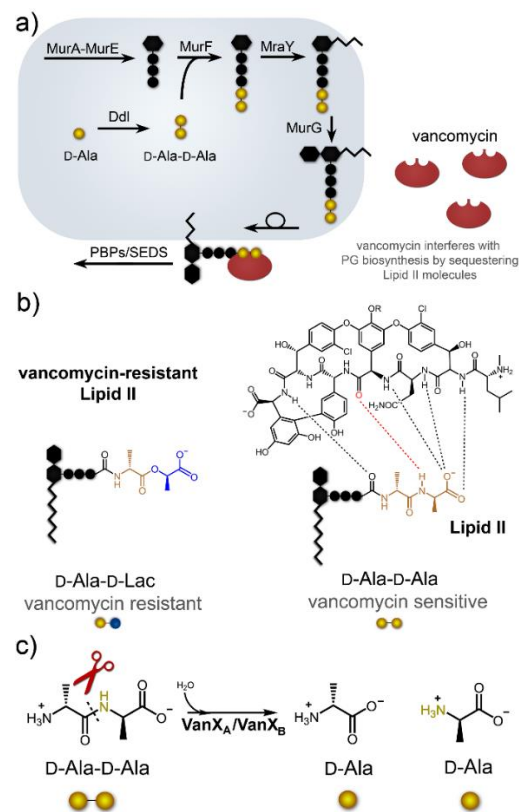


**Figure 6.1.** (A) Schematic representation of the intracellular biosynthesis of PG building blocks. Vancomycin sequestration of Lipid II molecules halts PG polymerization. (B) Structure of terminal end of Lipid II in drug-sensitive and -resistant organisms with vancomycin. (C) VanX-mediated hydrolysis of the vancomycin susceptible D-Ala-D-Ala dipeptide building blocks.

Previous reports had demonstrated VanX substrate plasticity in accommodating non-native dipeptides *in vitro*.<sup>17</sup> As such, we predicted that analogs of D-Ala-D-Ala containing reporter handles could potentially be suitable substrates of VanX (Figure 6.2B). In the absence of VanX activity, reporter dipeptides were expected to be processed intracellularly, loaded onto Lipid II molecules, and become imbedded within the mature PG. Once analogs are PG-anchored, reporter fluorophores can be installed *via* copper-catalyzed azide-alkyne cycloaddition (CuAAC) reactions (Figure 6.2C).<sup>18,19</sup> In cells displaying high levels of VanX activity, intracellular hydrolysis of reporter dipeptides were expected to reduce the dipeptide pool available for Lipid II production. VanX-mediated hydrolysis of D-Ala-D-Ala generates the corresponding single amino acids, which are not substrates for MurF, to drive the utilization of D-Ala-D-Lac (Figure 6.2A). Elevated cellular levels of VanX activity should result in attenuated levels of cell wall labeling, affording access to the adaptation dynamics of live VRE cells.

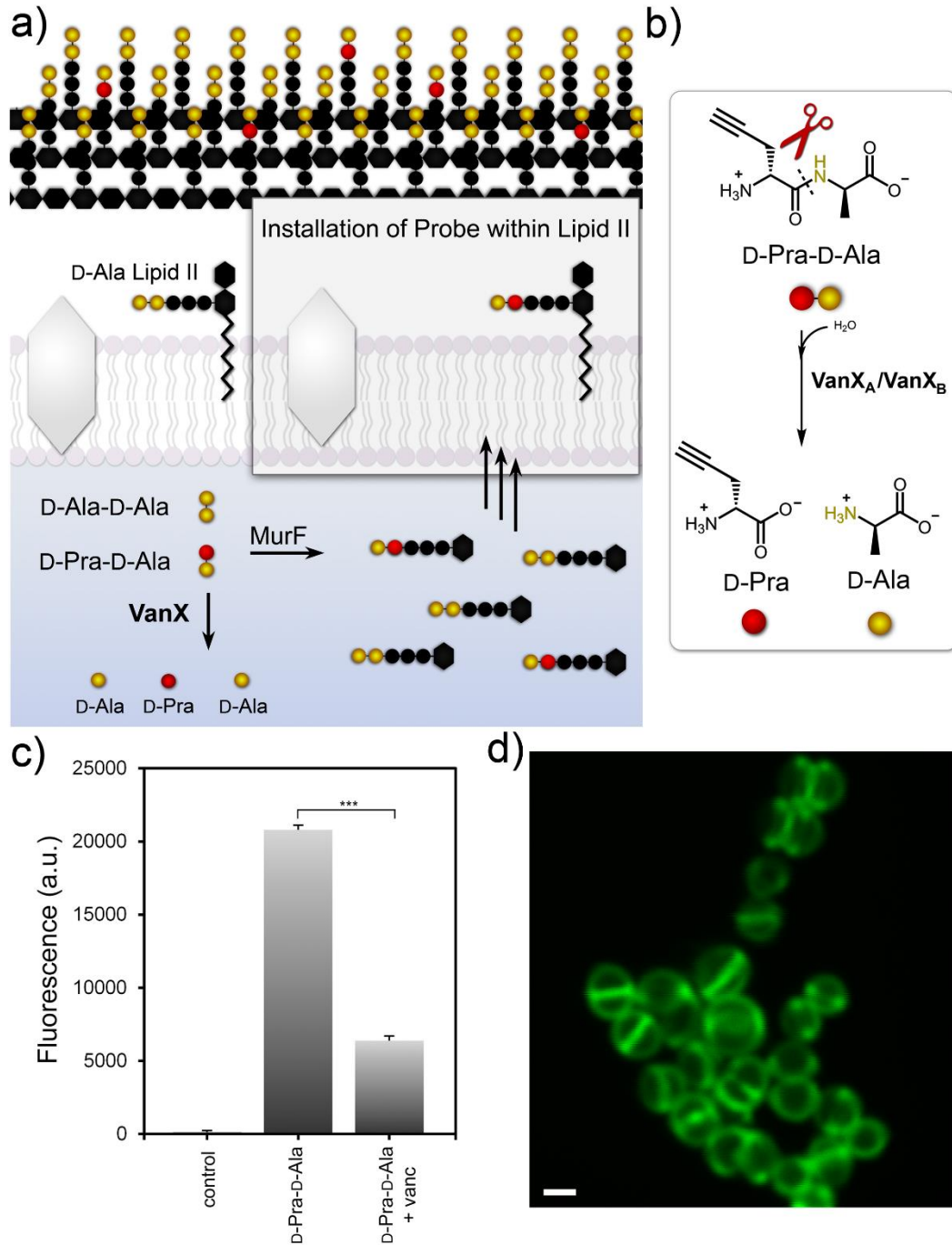


**Figure 6.2.** (A) VanX dipeptidase activity hydrolyzes D-Ala-D-Ala and its analogs. (B) Proposed dipeptidase hydrolysis of synthetic analogs of D-Ala-D-Ala by VanX. (C) Analysis of *E. faecium* (VanA) treated overnight with 1 mM D-Pra-D-Ala (+/- 16  $\mu\text{g}/\text{mL}$  vancomycin) followed by CuAAC with 6-FAM azide. Data are represented as mean + SD ( $n = 3$ ).  $P$  values were generated by an unpaired, two-sided  $t$ -test using GraphPad Prism 5 and  $P$  values are indicated (\* $P \leq 0.05$ , \*\* $P \leq 0.01$ , \*\*\* $P \leq 0.001$ , \*\*\*\* $P \leq 0.0001$ , and NS, not significant). (D) Confocal microscopy imaging of *E. faecium* (VanA) treated overnight with 1 mM D-Pra-D-Ala followed by CuAAC with 6-FAM azide. Scale = 2  $\mu\text{m}$ .

## **6.3 Results and Discussion**

### **6.3.1 Alkyne Dipeptide Incorporation**

We first evaluated two dipeptides, D-Ala-D-Pra and D-Pra-D-Ala, both structural analogs of the endogenous VanX substrate displaying an alkyne handle on the sidechain (Figure 6.3B).<sup>12,13</sup> A terminal alkyne was selected as the click chemistry partner due to its small size. Adequate processing of D-Pra-D-Ala by VanX<sub>A</sub> (the VanX in VanA-typed VRE cells) was anticipated based on our modeling of the VanX<sub>A</sub> active site using its crystal structure information (Figure 6.4).<sup>20</sup> The alkyne handle on the sidechain of D-Pra can be readily accommodated within the VanX<sub>A</sub> binding pocket. Treatment of *Bacillus subtilis* (*B. subtilis*), a model Gram-positive organism that can be readily cultured and lacks pathogenicity cells, with D-Pra-D-Ala led to a ~ 100-fold increase in cellular fluorescence compared to unlabeled cells, suggestive of the metabolic utilization of this dipeptide probe (Figure 6.3C). A much smaller (~ 7-fold) increase was observed in cells treated with the similar reporter dipeptide D-Ala-D-Pra. It was anticipated that reduced cellular fluorescence might be attributed to PG processing by surface-bound carboxypeptidases (including DacA) during cell wall maturation.<sup>21,22</sup> Consistently, genetically modified *B. subtilis* cells lacking *dacA* treated with D-Ala-D-Pra displayed a nearly 10-fold increase in fluorescence levels, consistent with DacA being partly responsible for signal reduction.

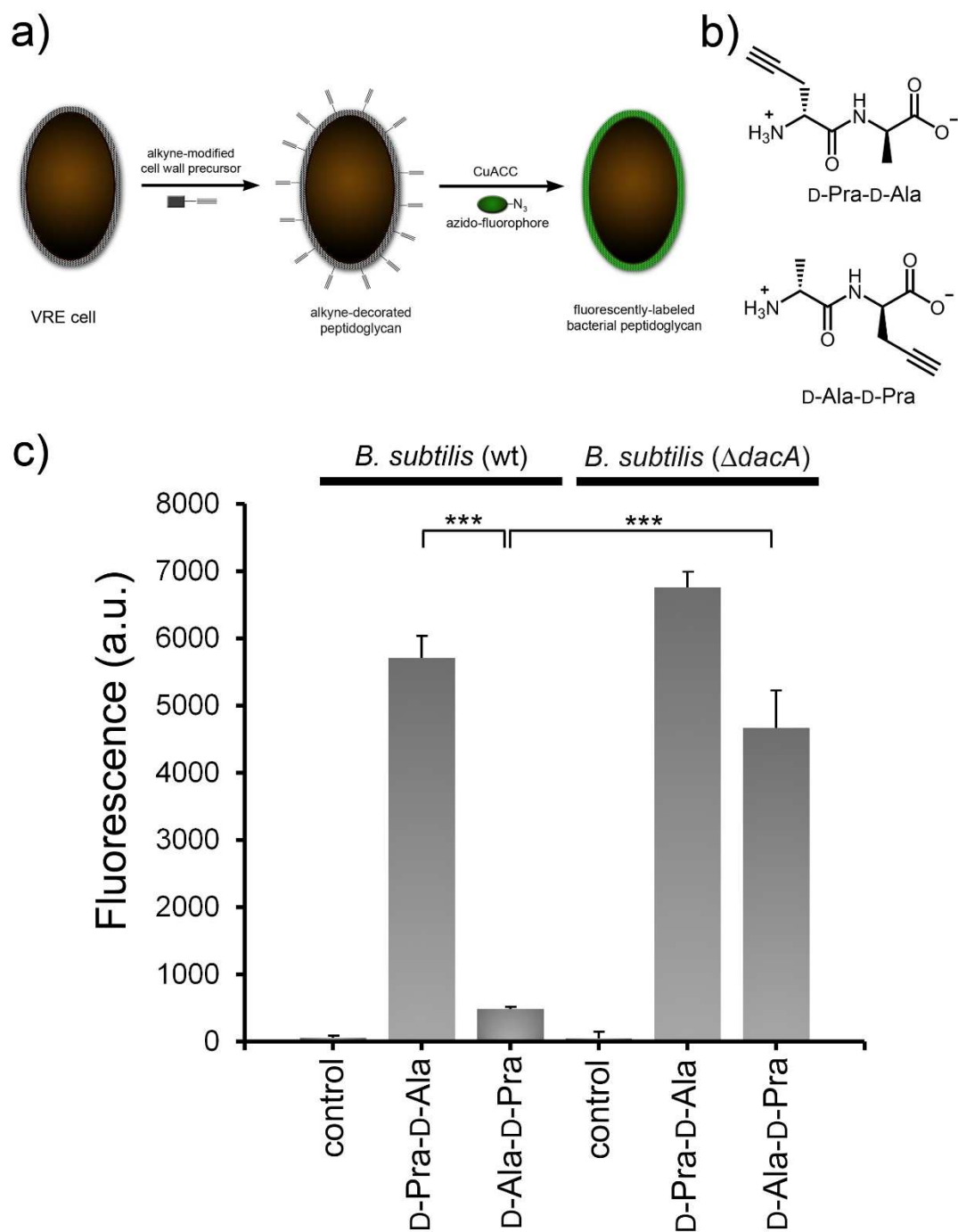


**Figure 6.3.** (A) Schematic diagram delineating incorporation of synthetic PG precursors displaying alkyne handles, followed by click chemistry (CuAAC) to fluorescently label bacterial PG. (B) Chemical structures of D-Pra-D-Ala and D-Ala-D-Pra dipeptides. (C) Flow cytometry analysis of *B. subtilis* (wild-type and  $\Delta dacA$ ), incubated overnight in the presence of 1 mM D-Pra-D-Ala or D-Ala-D-Pra followed by CuAAC with 6-FAM azide. Data are represented as mean + SD ( $n = 3$ ).  $P$  values were generated by an unpaired, two-sided  $t$ -test using GraphPad Prism 5 and  $P$  values are indicated (\* $P \leq 0.05$ , \*\* $P \leq 0.01$ , \*\*\* $P \leq 0.001$ , \*\*\*\* $P \leq 0.0001$ , and NS, not significant).

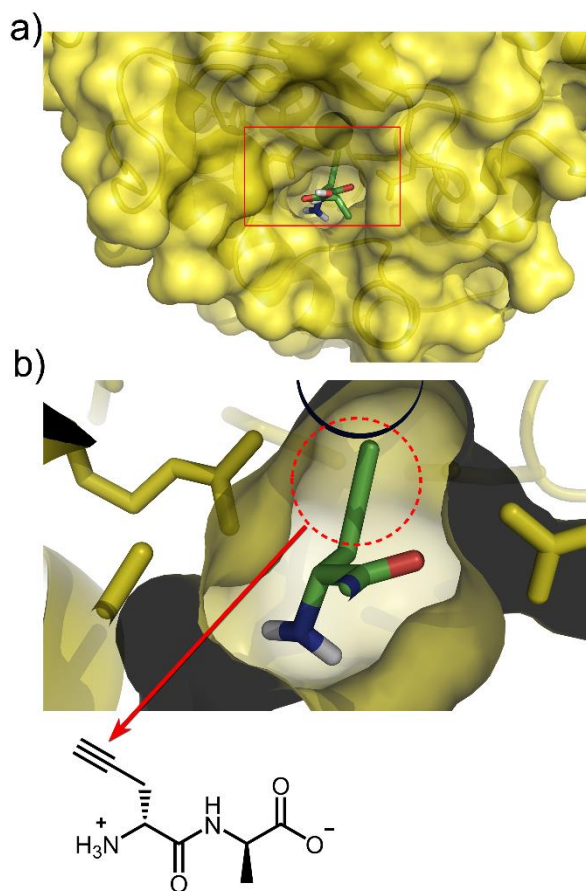


**Figure 6.4** (A) Structure of the dipeptidase VanX in complex with dipeptide substrate D-alanyl-D-alanine (D-Ala-D-Ala).<sup>23</sup> (B) Detailed view of interaction between VanX and D-Ala-D-Ala. Modeling shows a large pocket-space around the methyl group of D-alanyl, suggesting promiscuity for unnatural dipeptide D-Pra-D-Ala.

Subsequently, we set out to confirm the entry of the reporter dipeptides into the intracellular PG biosynthetic pathway. Cells exposed to synthetic analogs of D-Ala-D-Ala are expected to afford late stage (beyond the MurF ligation step) alkyne displaying PG precursors in the bacterial cytosolic space. PG precursors were harvested from cells treated with D-Pra-D-Ala. Subsequently, the UDP-MurNAc-pentapeptide (the penultimate intermediate to Lipid II) was isolated and characterized by LC-MS (Figure 6.5). Based on these findings, it was evident that reporter dipeptides entered the PG biosynthetic pathway.



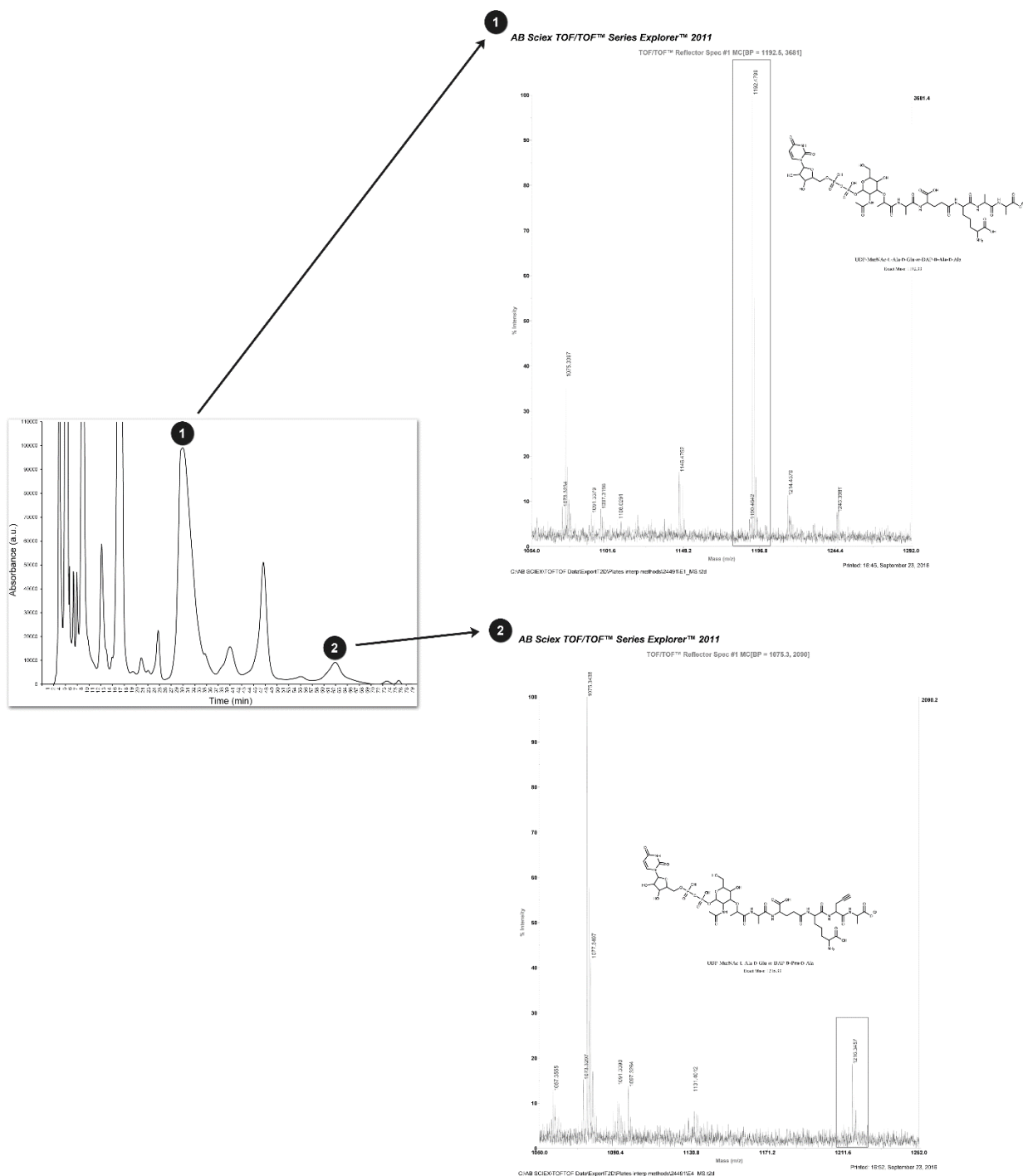


**Figure 6.5.** UDP-MurNac-pentapeptide precursor isolation. RP-HPLC chromatogram of cytosolic contents of *Bacillus subtilis*  $\Delta$ dacA incubated with 10 mM D-Pra-D-Ala, followed by treatment with chloramphenicol and vancomycin. Peak 1 corresponds to endogenous UDP-MurNac-pentapeptide with terminal D-Ala-D-Ala analyzed by MALDI-ToF (1192.4799 m/z). Peak 2 corresponds to modified UDP-MurNac-pentapeptide with terminal D-Pra-D-Ala analyzed by MALDI-ToF (1216.3457 m/z).

### 6.3.2 Dipeptide Incorporation with Diverse Bacteria

The compatibility of D-Pra-D-Ala in metabolically labeling diverse types of bacteria was also evaluated. Four additional bacteria were chosen, namely *Lactobacillus casei* (*L. casei*), *Lactobacillus plantarum* (*L. plantarum*), *Enterococcus faecium* (*E. faecium*), and *Enterococcus faecalis* (*E. faecalis*). Interestingly, both lactobacilli bacteria that naturally utilize the dipeptide D-Ala-D-Lac were labeled to significant extents with the exogenous dipeptide D-Pra-D-Ala (Figure 6.6). These findings indicate a lack of tight selectivity by MurF on its substrate backbone (ester vs. amide). Indeed, no dedicated MurF-like ligase exists in VRE that joins D-Ala-D-Lac to form the UDP-MurNAc-pentadepsipeptide, which highlights the substrate plasticity by MurF.<sup>3</sup> Nonetheless, this represents the first direct observation that MurF from lactobacilli bacteria tolerate dipeptide substrates in live organisms. Most importantly, treatment of two types of drug-sensitive Enterococci bacteria with the reporter dipeptide led to high levels of cellular labelling – a finding that set the stage for the potential monitoring of VanX in live VRE cells.

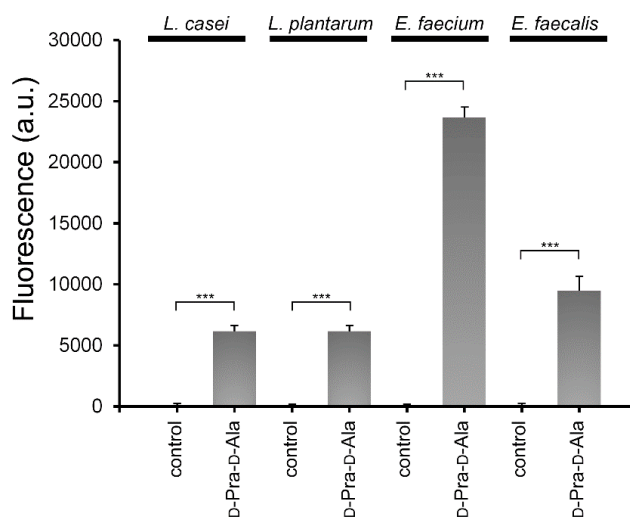


**Figure 6.6** Analysis of D-Pra-D-Ala incorporation with various bacterial strains. Flow cytometry of *Lactobacillus casei* ATCC 393, *Lactobacillus plantarum* ATCC 21028, and vancomycin sensitive strains of *Enterococcus faecium* ATCC BAA-2127, and *Enterococcus faecalis* ATCC 29212 incubated overnight with 1 mM D-Pra-D-Ala followed by CuAAC with 6-FAM azide. All

data are represented as mean +SD (n = 3). *P* values were generated by an unpaired, two-sided *t*-test using GraphPad Prism 5 and *P* values are indicated (\**P*≤0.05, \*\**P*≤0.01, \*\*\**P*≤0.001, \*\*\*\**P*≤0.0001, and NS, not significant).

### **6.3.3 VanX Dipeptide Hydrolysis**

We next focused on establishing the ability of exogenous D-Pra-D-Ala to enter the PG biosynthetic pathway of VanA-type *E. faecium* cells, which are extremely resistant to vancomycin and part of the highly problematic ESKAPE class of pathogens.<sup>24</sup> Similar to drug-sensitive *E. faecium*, significant cellular fluorescence was observed in *E. faecium* BAA-2317 measured by flow cytometry (Figure 6.2C). *E. faecium* (VanA) responds to vancomycin exposure by depleting cytosolic D-Ala-D-Ala via VanX<sub>A</sub>-mediated dipeptidase activity. Consistently, a 3.2-fold decrease in cellular fluorescence was observed for *E. faecium* (VanA) challenged with vancomycin, which could also be readily visualized within 4 h of treatment (Figure 6.7).

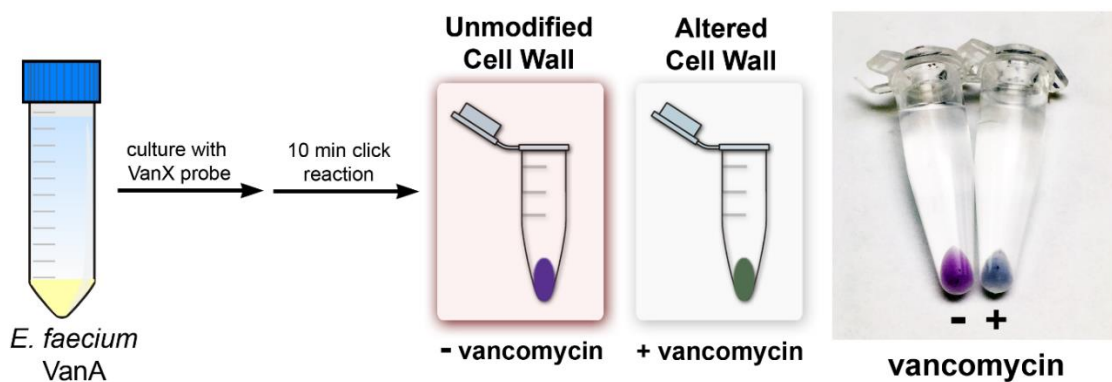


**Figure 6.7** Schematic representation showing how VRE cells can be labeled with synthetic cell wall precursors to reveal resistant phenotype. Cells were incubated with 500 μM D-Pra-D-Ala for 4 h, then CuAAC was performed with sulfocyanine5 azide.

Labelling of the same cells with the single amino acid D-Pra did not decrease in the presence of vancomycin, an indication that the fluorescence decrease in D-Pra-D-Ala labelled VRE cells is not linked to PG transpeptidase activity (Figure 6.8). Accentuated labelling was clearly visible at the septal ring, which is the primary site of Lipid II pools

(Figure 6.2D and Figure 6.9). In addition, PG digestion from VRE cells by lysozyme was consistent with probe installment within the PG scaffold (Figure 6.10).

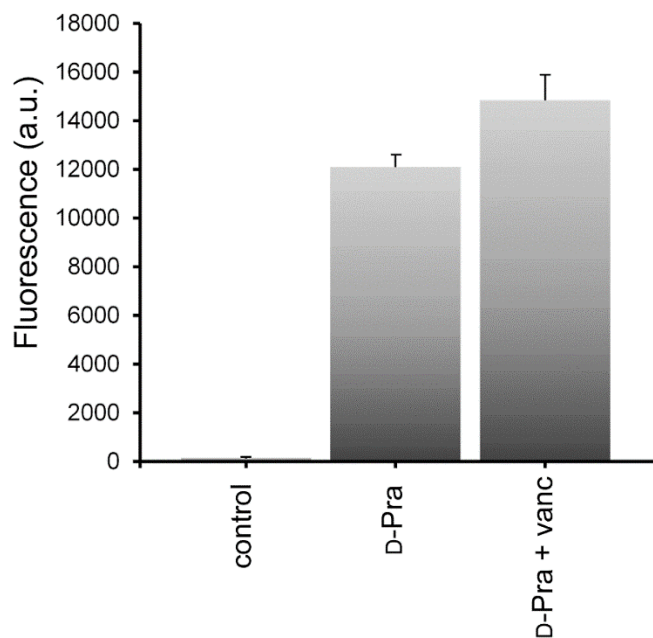


**Figure 6.8.** Flow cytometry analysis of *E. faecium* (VanA) incubated overnight with 1 mM D-Pra (+/- 16  $\mu\text{g}/\text{mL}$  vancomycin) followed by CuAAC with 6-FAM azide. All data are represented as mean +SD (n = 3).

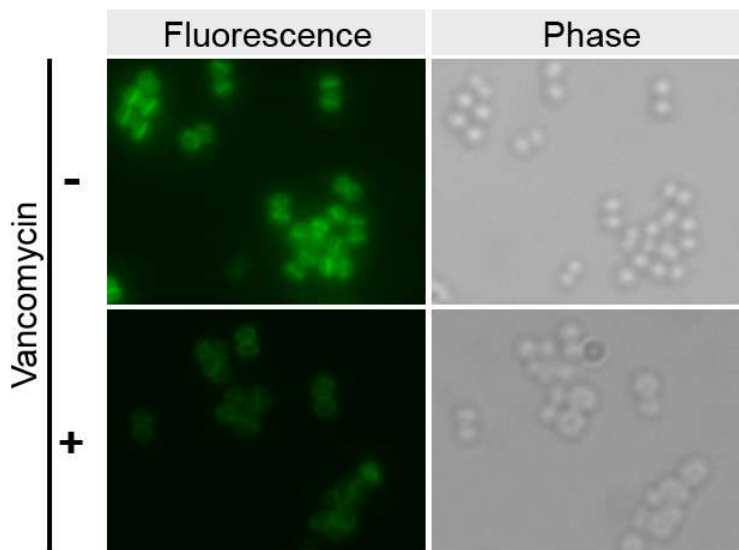


**Figure 6.9** Microscopy imaging of *E. faecium* (VanA) treated overnight with 1 mM D-Pra-D-Ala (+/- 16  $\mu\text{g}/\text{mL}$  vancomycin) followed by CuAAC with 6-FAM azide.

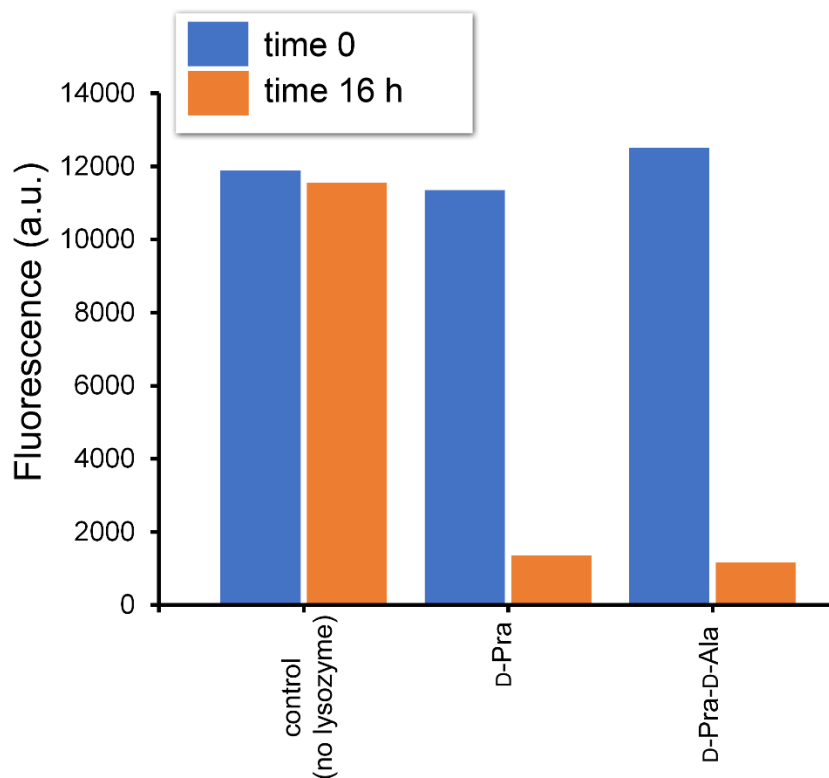


**Figure 6.10** PG digestion was measured using flow cytometry by the loss of fluorescence upon treatment with lysozyme of VRE cells pre-treated with specific PG analogs (1 mM) followed by CuAAC with 6-FAM azide. Measurements were made at time 0 and after 16 h incubated at 37 °C.

Despite the continuous supply and replenishment of reporter dipeptides from the surrounding media, VanX<sub>A</sub> sufficiently reduces the intracellular D-Pra-D-Ala concentration to significantly reduce PG labeling in the presence of vancomycin.<sup>17,25</sup> Titration of *E. faecium* (VanA) cells with increasing concentrations of vancomycin led to the corresponding attenuation of cellular fluorescence (Figure 6.11). Moreover, vancomycin-dependent fluorescence attenuation by vancomycin was observed in a wide range of dipeptide probe concentrations (Figure 6.12). Crucially, cellular fluorescence in drug-sensitive *E. faecium* remained unchanged upon exposure to vancomycin (Figure 6.13). Next, a series of control dipeptides were synthesized and examined in *E. faecium* (VanA) cells. Three of the dipeptides were stereochemical controls (2 diastereomers and 1

enantiomer) of D-Pra-D-Ala (Figure 6.14). Minimal cellular labelling was observed with L-amino acid based dipeptides and dipeptide acetylation (NAc-D- Pra-D-Ala), which effectively renders the *N*-terminus amino group incompatible with MurF ligation.

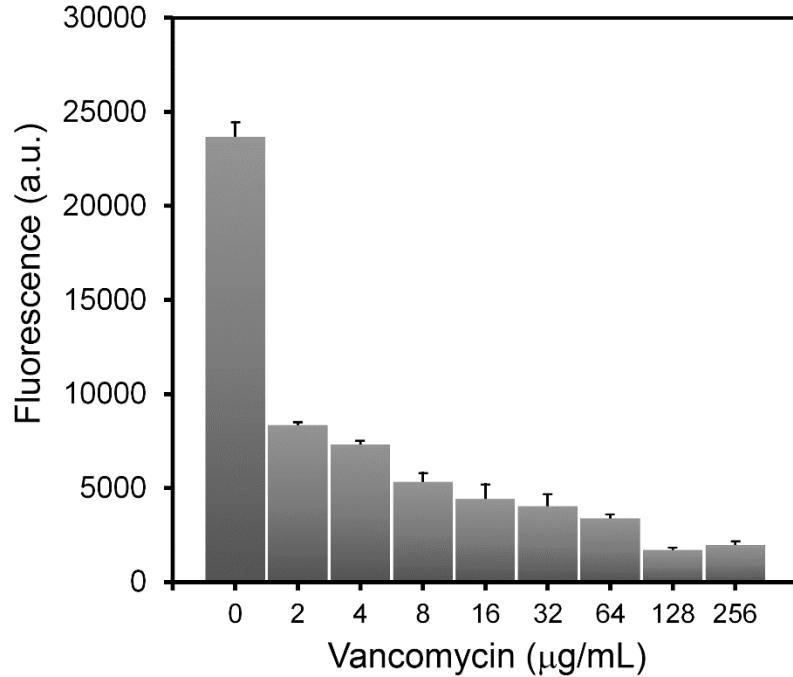


**Figure 6.11** Flow cytometry analysis of *E. faecium* (VanA) incubated overnight with 1 mM D-Pra-D-Ala and various concentrations of vancomycin. All data are represented as mean +SD (n = 3).

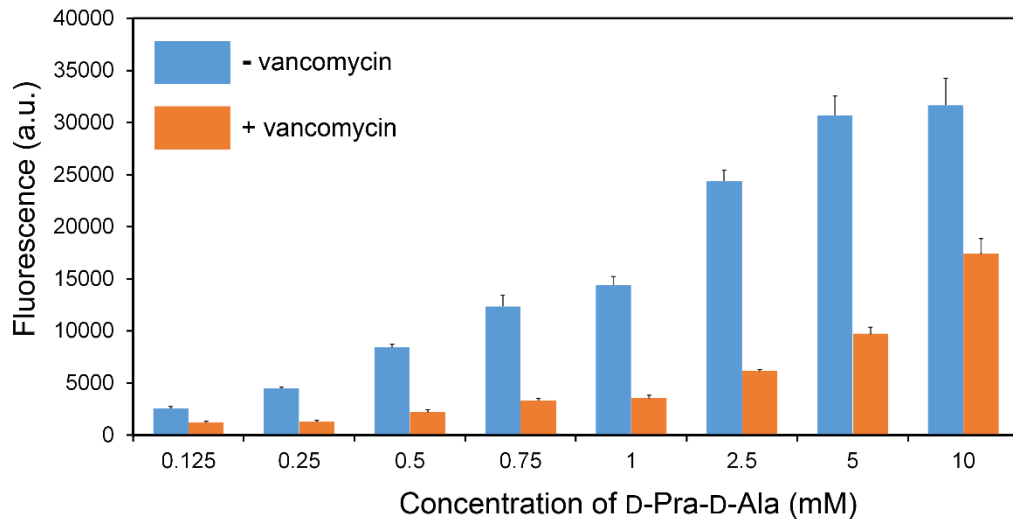


**Figure 6.12** Flow cytometry analysis of *E. faecium* (VanA) incubated overnight with stated concentrations of D-Pra-D-Ala (+/- 16 µg/mL vancomycin) followed by CuAAC with 6-FAM azide. All data are represented as mean +SD (n = 3).

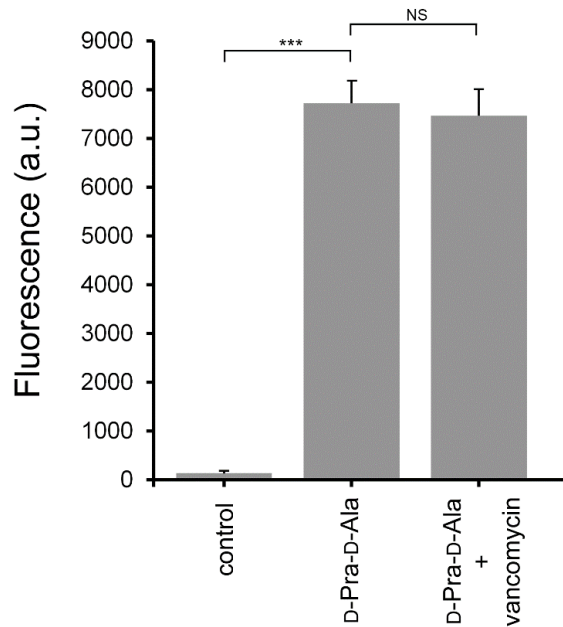


**Figure 6.13** Flow cytometry analysis of drug-sensitive *E. faecium* ATCC BAA-2127 incubated overnight with 1 mM D-Pra-D-Ala (+/- 0.1 µg/mL vancomycin). All data are represented as mean + SD ( $n = 3$ ).  $P$  values were generated by an unpaired, two-sided  $t$ -test using GraphPad Prism 5 and  $P$  values are indicated (\* $P \leq 0.05$ , \*\* $P \leq 0.01$ , \*\*\* $P \leq 0.001$ , \*\*\*\* $P \leq 0.0001$ , and NS, not significant).

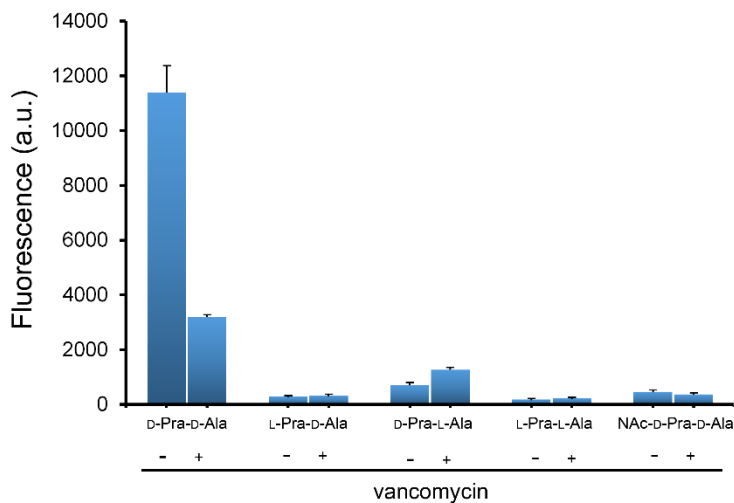
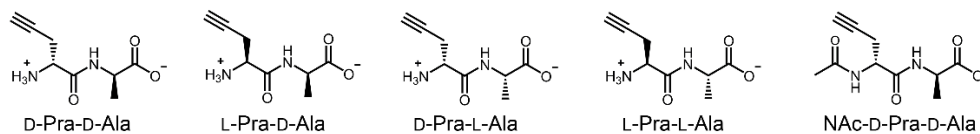


**Figure 6.14** Flow cytometry analysis of *E. faecium* ATCC BAA-2127 (VanA) incubated overnight with 1 mM dipeptide variants. All data are represented as mean + SD ( $n = 3$ ).

We next evaluated the effect of the click chemistry reaction in vancomycin-dependent cellular response in VRE cells. Two additional dipeptides (D-Cys-D-Ala and D-Ala-D-Cys) were synthesized and examined for their ability to enter the PG biosynthetic pathway and report on VanX<sub>A</sub> activity (Figure 6.15). VRE cells treated with D-Cys-D-Ala and D-Ala-D-Cys displayed similar vancomycin-dependent labelling profiles. These results suggest that the chemistry involved in the fluorophore tagging step does not play a significant role. An additional dipeptide, D-Pra-D-Lac, was also synthesized to assess *in vivo* VanX<sub>A</sub> substrate specificity (Figure 6.16). The ester backbone found in D-Pra-D-Lac should make it a poor substrate for VanX<sub>A</sub>, forming the basis for the preferential accumulation of D-Ala-D-Lac over D-Ala-D-Ala in the metabolic rewiring of induced VRE.<sup>17</sup> Treatment of *E. faecium* (VanA) cells with D-Pra-D-Lac resulted in cellular labeling that was independent of

vancomycin. These results suggest that, as expected, the expression of VanX<sub>A</sub> does not significantly alter the pool of D-Ala-D-Lac in VRE. Moreover, they provide evidence for

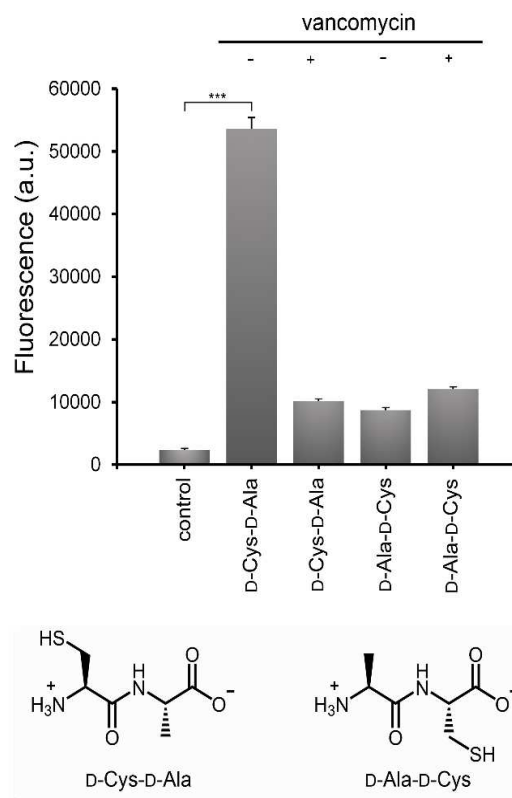


**Figure 6.15** Analysis of vanX activity with cysteine handle dipeptides in *E. faecium* (vanA) ATCC BAA-2317. Flow cytometry of *E. faecium* incubated overnight with 1 mM D-Cys-D-Ala or D-Ala-D-Cys (+/- 16 µg/mL vancomycin) followed by maleimide conjugation to Alexa Fluor 488 C5 maleimide. All data are represented as mean +SD (n = 3). P values were generated by an unpaired, two-sided *t*-test using GraphPad Prism 5 and P values are indicated (\* $P \leq 0.05$ , \*\* $P \leq 0.01$ , \*\*\* $P \leq 0.001$ , \*\*\*\* $P \leq 0.0001$ , and NS, not significant).



the VanXA selectivity for dipeptides relative to dipeptide in live VRE cells and illustrate the insight provided by synthetic cell wall analogs in PG metabolism.

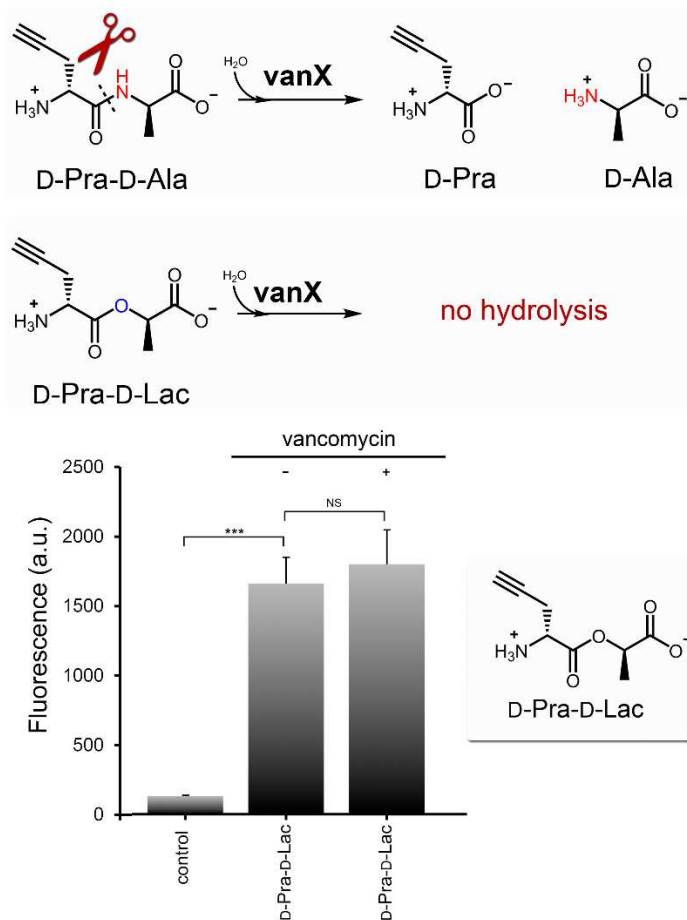


**Figure 6.16** Analysis of VanX substrate specificity in *E. faecium* (VanA) ATCC BAA-2317. Flow cytometry of *E. Faecium* incubated overnight with 1 mM D-Pra-D-Lac (+/- 16  $\mu$ g/mL vancomycin) followed by CuAAC with 6-FAM azide. All data are represented as mean +SD (n = 3). *P* values were generated by an unpaired, two-sided *t*-test using GraphPad Prism 5 and *P* values are indicated (\**P*≤0.05, \*\**P*≤0.01, \*\*\**P*≤0.001, \*\*\*\**P*≤0.0001, and NS, not significant).

We next examined vancomycin resistance in VanB-type VRE cells. More specifically, we set out to monitor VanXB activity in *E. faecalis* organisms using D-Pra-D-Ala. Considerable cellular labeling of *E. faecalis* ATCC 51299 (VanB) was observed at similar levels to *E. faecium* (Figure 6.17). In contrast to VanA-typed VRE, fluorescence signals remained unchanged when challenged with increasing levels of vancomycin. These results

are suggestive of insufficient dipeptidase activity by VanX<sub>B</sub> in reducing the intracellular pool of the reporter dipeptide. Consistently, previous *in vitro* analysis of VanX<sub>B</sub> from *E. faecalis* showed that it possesses ~ 10-fold lower specific activity relative to *E. faecium* VanX<sub>A</sub>.<sup>26</sup> Moreover, unlike *E. faecalis* (VanB), *E. faecium* (VanA) have exclusively UDP-MurNAc-pentadepsipeptide PG precursors in the cytosolic space. Together, our findings suggest that high VanX<sub>A</sub> activity is a primary driver for the extreme levels of vancomycin-resistance found in VanA-typed VRE.

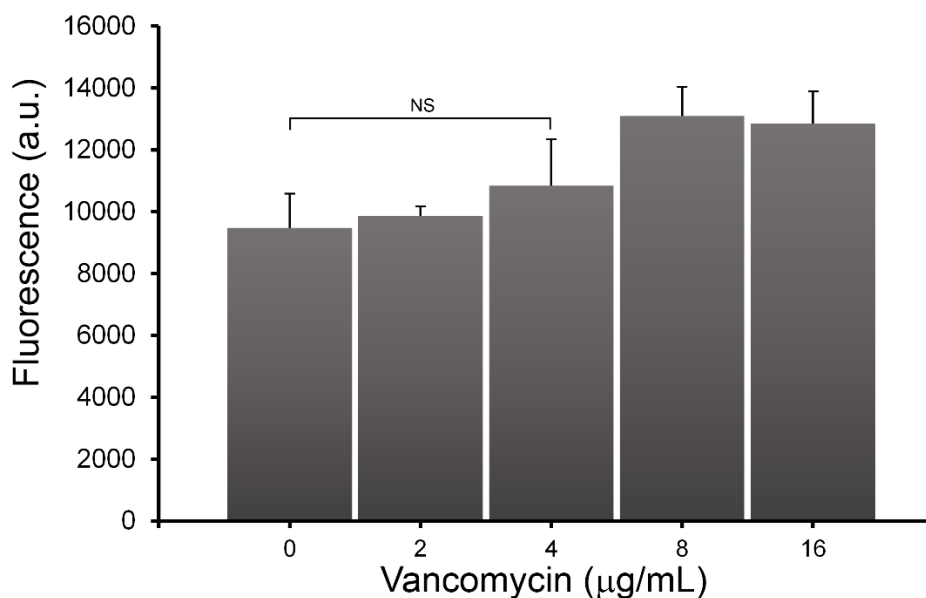


**Figure 6.17** Analysis of vanX activity in *Enterococcus faecalis* (vanB) ATCC 51299. Flow cytometry analysis of *E. faecalis* incubated overnight with 1 mM D-Pra-D-Ala with various concentrations of vancomycin followed by CuAAC with 6-FAM azide. All data are represented as mean +SD (n = 3). *P* values were generated by an unpaired, two-sided *t*-test using GraphPad Prism 5 and *P* values are indicated (\**P*≤0.05, \*\**P*≤0.01, \*\*\**P*≤0.001, \*\*\*\**P*≤0.0001, and NS, not significant).

### **6.3.4 Kinetics of Cell Wall Remodelling**

Having established a platform to monitor changes to cell wall composition in VRE cells, we reasoned that our probe could be leveraged to empirically determine the kinetics in cell wall remodeling by determining the induction and persistence phases (Figure 6.18).<sup>27,28</sup>

The induction phase reflects the kinetics in cell wall alteration upon vancomycin exposure, whereas the persistence phase reflects the kinetics in reverting back to D-Ala based PG. VRE cells were exposed to vancomycin and collected every 15 minutes to analyse for cellular fluorescence (Figure 3d). Shortly after (45 minutes) vancomycin exposure, there was a statistically significant difference in the cell wall composition and this difference became more prominent over the next several hours. Likewise, the persistence phase was relatively short-lived. The rapid kinetics in induction and persistence point to a fitness cost associated with maintaining D-Lac-based PG phenotype.<sup>29</sup> Expression of VanX<sub>A</sub> closes a loop in the production and degradation cycle of D-Ala-D-Ala (Figure 3f). In the process, VRE exposed to vancomycin enter a futile cycle that is energetically costly. Our results illustrate the ability of VRE cells to quickly adapt to the presence of vancomycin by shifting the chemical composition of their cell walls.

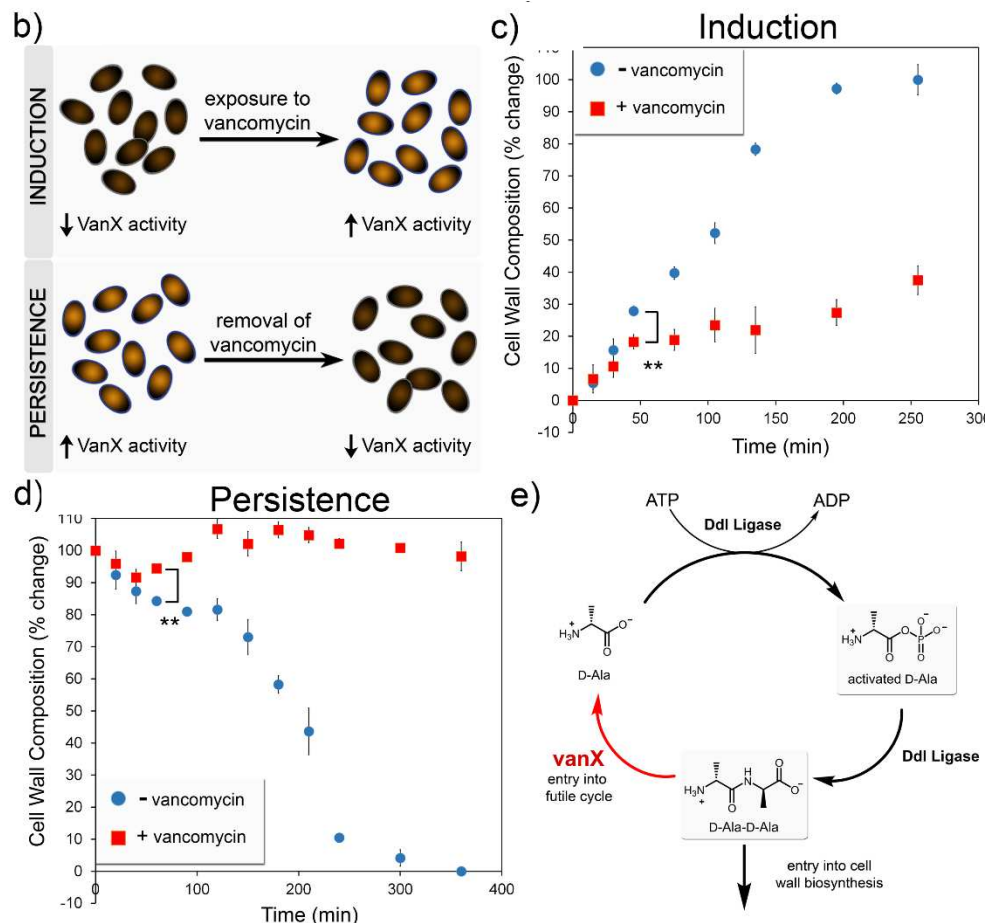


**Figure 6.18** (A) Schematic representation of the two phases monitored with the VanX probe. Flow cytometry analysis of *E. faecium* (VanA) VanX dipeptidase induction (B) and persistence (C) in response to vancomycin. *E. faecium* cells were treated with D-Pra-D-Ala (1 mM) and collected at various time points and fluorescently labeled with 6-FAM azide by CuAAC. Data are represented as mean + SD (n = 3). D) VanX expression closes a futile cycle in the production/degradation of D-Ala-D-Ala.

### 6.3.5 Vancomycin Variants and Pathway Activation

Finally, structural variants of vancomycin were evaluated for resistance induction (Figure 6.19A). VRE cells assayed with aglycon-vanc responded similarly to the parent vancomycin molecule (Figure 6.19B).<sup>30</sup> On the other hand, desleucyl-vanc – a vancomycin derivative missing the crucial leucine residue that participates in the association to D-Ala-D-Ala on Lipid II molecules – showed minimal decrease in labelling levels.<sup>31</sup> Next, we evaluated six additional antibiotics encompassing a range of mechanisms of action related

to PG biosynthesis inactivation for their ability to induce cell wall alteration in VRE cells (Figure 6.19C). From these results, it is clear that teicoplanin is a more potent inducer than vancomycin.<sup>32</sup> Interestingly, bacitracin showed strong induction despite not having a proposed association with D-Ala-D-Ala, contrary to previous reports using cell lysates.<sup>33</sup> On the other hand, flavomycin treatment did not induce a signal change even though it had been previously shown to induce gene expression of the *vanRSHAX* cluster.<sup>33</sup> Notably, this assay should be compatible with a high-throughput platform to analyse potential drug leads for their ability to either inhibit induction or circumvent sensing by VRE.

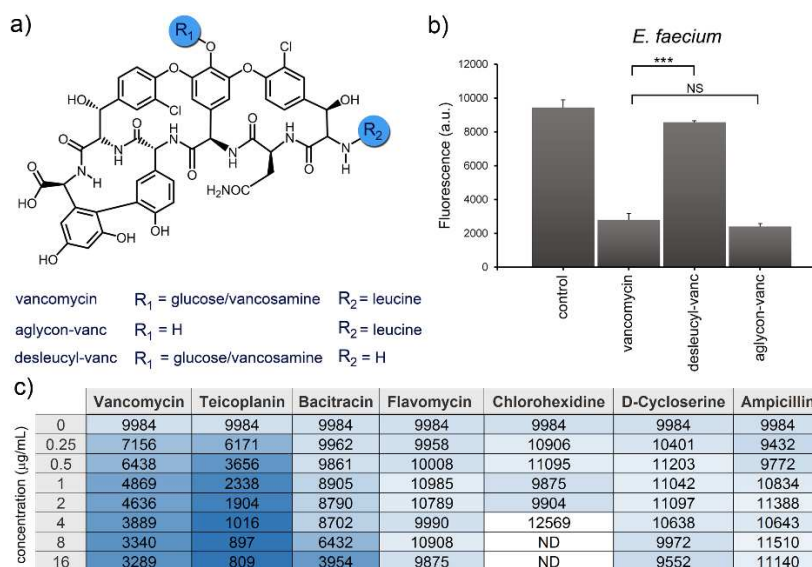


**Figure 6.19** (A) Chemical structure of vancomycin and two of its synthetic derivatives. Flow cytometry analysis of *E. faecium* incubated overnight with D-Pra-D-Ala (1 mM) and treated with the (B) vancomycin derivatives and (C) cell wall antibiotics. Data are represented as mean + SD (n = 3). *P* values were generated by an unpaired, two-sided *t*-test using GraphPad Prism 5 and *P* values are indicated (\**P* ≤ 0.05, \*\**P* ≤ 0.01, \*\*\**P* ≤ 0.001, \*\*\*\**P* ≤ 0.0001, and NS, not significant). Shading was internally normalized to represent the varying levels of activation. The darker the blue shade, the lower cell labelling was observed. ND = Not determined due to toxicity.

## 6.4 Conclusions

In conclusion, a cell wall analog was developed to reveal PG remodeling in drug resistant bacteria in response to glycopeptide antibiotics. Our results showed that a simple cell wall mimic can be a powerful tool to monitor the dynamic changes upon induction of

vancomycin-linked genes. We demonstrated subtle differences in VanX activities in two different VRE types, the selectivity of VanX between dipeptides and didepsipeptides in live cells, and a new modality for tracking the induction of the drug resistant phenotype in VRE.

### **6.5 Materials and Methods**

All peptide related reagents (resin, coupling reagent, deprotection reagent, amino acids, and cleavage reagents) were purchased from ChemImpex. FAM (fluorescein) azide 6-isomer and sulfo-cyanine5 azide were purchased from Lumiprobe. Alexa Fluor 488 C5-maleimide was purchased from Life Technologies. Vancomycin hydrochloride was purchased from AK Scientific. All other reagents were purchased from Sigma and were used without further purification. Bacterial strains used for these experiments were:

	Strain	Growth Media
Vancomycin Resistant	<i>Enterococcus faecium</i> ATCC BAA-2317 (VanA)	BBL Trypticase Soy Broth (TSB)
	<i>Enterococcus faecalis</i> ATCC 51299 (VanB)	Brain Heart Infusion Broth (BHI)
Vancomycin Sensitive	<i>Enterococcus faecium</i> ATCC BAA-2127	BBL Trypticase Soy Broth (TSB)
	<i>Enterococcus faecalis</i> ATCC 29212	Brain Heart Infusion Broth (BHI)
	<i>Lactobacillus casei</i> ATCC 393 (03)	Difco Lactobacilli MRS Broth
	<i>Lactobacillus plantarum</i> ATCC 21028 (KY 3648)	Difco Lactobacilli MRS Broth
	<i>Bacillus Subtilis</i> NCIB 3610	Lysogeny Broth (LB)
	<i>Bacillus Subtilis</i> $\Delta$ dacA	Lysogeny Broth (LB)

**Copper-catalyzed azide-alkyne cycloaddition (CuAAC) cell surface labeling.** For all experiments with azide-alkyne click chemistry, the following fluorophore labeling protocol was used after fixation of cells. Cells were suspended in half the volume of the original

culture with 1x PBS. The reagents were added in the following order for final concentrations of 1 mM CuSO<sub>4</sub>, 128 uM THPTA, 1.2 mM L-ascorbic acid (freshly prepared) and 30 uM fluorescein azide 6-isomer. The reactions were performed at ambient temperature for 1 h with shaking. After washing, samples were analyzed using a BDFacs Canto II flow cytometer using a 488nm argon laser (L1) and a 530/30 band-pass filter (FL1). A minimum of 10,000 events were counted for each data set. The data was analyzed using the FACSDiva version 6.1.1.

***Bacillus subtilis* D-Pra-D-Ala / D-Ala-D-Pra labeling.** Lysogeny broth containing 1 mM D-Pra-D-Ala or D-Ala-D-Pra were prepared. *Bacillus Subtilis*  $\Delta$ dacA or *Bacillus Subtilis* NCIB 3610 (WT) from an overnight culture were added to the corresponding medium (1:100) and allowed to grow overnight at 37 °C with shaking. The bacteria were harvested at 6,000g and wash three times with original culture volume of 1x PBS followed by fixation with 2% formaldehyde in 1x PBS for 30 min at ambient temperature. The cells were washed once more to remove the formaldehyde and CuAAC was performed. The cells were washed three times with 1x PBS and analyzed using a BDFacs Canto II flow cytometer using the previously stated parameters.

**Intracellular accumulation of cell wall precursor UDP-N-acetyl-muramic acid pentapeptide and precursor modified with D-Pra-D-Ala.** Analysis of the cytoplasmic peptidoglycan nucleotide precursor was examined using *Bacillus Subtilis*  $\Delta$ dacA grown in 50 mL LB with or without 10 mM D-Pra-D-Ala. *B. Subtilis*  $\Delta$ dacA were added to the corresponding medium (1:100) and allowed to grow at 37 °C with shaking. At an optical density (OD<sub>600</sub>) of 0.6, chlorpamphenicol was added to the bacterial growth containing 10 mM D-Pra-D-Ala for a final concentration of 130 µg/mL. The cells were incubated for an

additional 15 min. Vancomycin was then added to the bacterial growth containing 10 mM D-Pra-D-Ala for a final concentration of 100 µg/mL, and the cells were incubated for an additional 30 min. Cells were harvested at 4,000g, and boiled in water for 15 min. The cell extract was centrifuged at 4,000g and the supernatant lyophilized. UDP-linked cell wall precursors were analyzed by reverse-phase HPLC using a phenomenex nucleosil 5µ C18 120A, 250 x 320 mm column. Isocratic conditions were 50 mM ammonium acetate pH 4.2 at a flow rate of 0.5 mL/min monitoring at 254 nm. Precursors were confirmed by negative mode MALDI-ToF mass spectrometry using 1 mg/mL 6-aza-2-thiothymine dissolved in 50% (vol/vol) ethanol-20 mM ammonium acetate as the matrix.

**D-Pra-D-Ala labeling with diverse bacteria.** LB, MRS, BHI, or TSB broth were prepared containing 1 mM D-Pra-D-Ala were prepared. *Lactobacillus casei* ATCC 393 (03) and *Lactobacillus plantarum* ATCC 21028 (KY 3648) were added to the corresponding MRS medium (1:100). *Enterococcus faecium* ATCC BAA-2127 was added to the corresponding TSB medium (1:100), and *Enterococcus faecalis* ATCC 29212 was added to the corresponding BHI medium (1:100). The bacteria were allowed to grow overnight at 37 °C with shaking. The bacteria were harvested at 6,000g and wash three times with original culture volume of 1x PBS followed by fixation with 2% formaldehyde in 1x PBS for 30 min at ambient temperature. The cells were washed once more to remove the formaldehyde and CuAAC was performed. The cells were washed three times with 1x PBS and analyzed using a BDFacs Canto II flow cytometer using the previously stated parameters.

**Vancomycin Concentration Scan with D-Pra-D-Ala.** TSB or BHI medium containing 1 mM D-Pra-D-Ala was prepared. To the TSB medium was added vancomycin hydrochloride for final concentrations of 2, 4, 8, 16, 32, 64, 128, or 256 µg/mL. To the BHI



medium was added vancomycin hydrochloride for final concentrations of 0.5, 1, 2, 4, 8, 10, 12, 14, or 16 ug/mL *Enterococcus faecium* ATCC BAA-2317 (VanA) was added to the TSB medium (1:100) and *Enterococcus faecalis* ATCC 51299 (VanB) to the BHI medium and allowed to grow overnight at 37 °C with shaking. The bacteria were harvested at 6,000g and wash three times with original culture volume of 1x PBS followed by fixation with 2% formaldehyde in 1x PBS for 30 min at ambient temperature. The cells were washed once more to remove the formaldehyde and CuAAC was performed. The cells were washed three times with 1x PBS and analyzed using a BDFacs Canto II flow cytometer using the previously stated parameters. For fluorescent imaging, the cells were analyzed on a glass slide using a B-2E/C filter (ex 465-495/em 515-555).

**Visual Inspection of VanX Activity.** TSB medium containing 500 uM D-Pra-D-Ala with or without 16 ug/mL vancomycin was prepared. *Enterococcus faecium* ATCC BAA-2317 (VanA) was added to the medium for an optical density (OD<sub>600</sub>) of 0.6. The bacteria were grown at 37 °C with shaking for 3.5 hrs. The bacteria were harvested at 6,000g and wash three times with original culture volume of 1x PBS and CuAAC was performed at double the previous click concentrations for 10 min, using sulfo-cyanine5 azide. The bacteria were washed three times with 1x PBS and images were taken of the cell pellets.

**Vancomycin Incubation with D-Pra-D-Ala for sensitive *E. faecium*.** TSB medium containing 500 uM D-Pra-D-Ala was prepared. To the TSB medium was added vancomycin hydrochloride for a final concentrations of 0.1 ug/mL *Enterococcus faecium* ATCC BAA-2127 was added to the TSB medium (1:100) and allowed to grow overnight at 37 °C with shaking. The bacteria were harvested at 6,000g and wash three times with original culture volume of 1x PBS followed by fixation with 2% formaldehyde in 1x PBS

for 30 min at ambient temperature. The cells were washed once more to remove the formaldehyde and CuAAC was performed. The cells were washed three times with 1x PBS and analyzed using a BDFacs Canto II flow cytometer using the previously stated parameters.

**Control Dipeptides.** TSB medium containing 1 mM D-Pra-D-Ala, D-Pra-L-Ala, L-Pra-D-Ala, L-Pra-L-Ala, D-Pra-N-Me-D-Ala, or NAc-D-Pra-D-Ala were prepared with or without 16 ug/mL vancomycin hydrochloride. *Enterococcus faecium* ATCC BAA-2317 (VanA) was added to the corresponding medium (1:100) and allowed to incubate overnight at 37 °C with shaking. The bacteria were harvested at 6,000g and wash three times with original culture volume of 1x PBS followed by fixation with 2% formaldehyde in 1x PBS for 30 min at ambient temperature. The cells were washed once more to remove the formaldehyde and CuAAC was performed. The cells were washed three times with 1x PBS and analyzed using a BDFacs Canto II flow cytometer using the previously stated parameters.

**D-Cys-D-Ala / D-Ala-D-Cys Labeling.** TSB medium containing 1 mM D-Cys-D-Ala or D-Ala-D-Cys were prepared with or without 16 ug/mL vancomycin hydrochloride. *Enterococcus faecium* ATCC BAA-2317 (VanA) was added to the corresponding medium (1:100) and allowed to incubate overnight at 37 °C with shaking. The bacteria were harvested at 6,000g and wash three times with original culture volume of 1x PBS with 5 mM dithiothreitol (DTT) and washed another three times with 1x PBS. The cells were incubated with 50 uM Alexa 488 C5-maleimide in 1x PBS for 30min at 37 °C. The cells were washed three times with 1x PBS followed by fixation with 2% formaldehyde in 1x

PBS for 30 min. The cells were washed three times with 1x PBS and analyzed using a BDFacs Canto II flow cytometer using the previously stated parameters.

**Induction of vanX dipeptidase.** TSB medium containing 1 mM D-Pra-D-Ala was prepared. *Enterococcus faecium* ATCC BAA-2317 (VanA) was added to the corresponding medium for an initial optical density (OD<sub>600</sub>) of 0.2. The cells were incubated at 37 °C with shaking. A portion of the cells were taken at 0, 15, 30, 45, 60, and 105 min. At 105 min (OD<sub>600</sub> = 0.6) the culture was split in half and to one sample was added vancomycin hydrochloride for a final concentration of 16 ug/mL. A portion of the cells were collected at 120, 135, 150, 180, 210, 240, 300, and 360 min. At each of the intervals, the collected cells were washed three times with 1x PBS followed by immediate fixation with 2% formaldehyde in 1x PBS for 30 min at ambient temperature. The cells were washed once more to remove the formaldehyde and CuAAC was performed. The cells were washed three times with 1x PBS and analyzed using a BDFacs Canto II flow cytometer using the previously stated parameters.

**Persistence of vanX dipeptidase.** TSB medium containing 1 mM D-Pra-D-Ala was prepared with 16 ug/mL vancomycin hydrochloride. *Enterococcus faecium* ATCC BAA-2317 (VanA) was added to the corresponding medium (1:100) and allowed to incubate overnight at 37 °C with shaking. The next day, the cells were washed to remove the vancomycin and resupplemented with TSB medium containing 1 mM D-Pra-D-Ala with or without 16 ug/mL vancomycin hydrochloride. A sample of cells were collected at various time points. At each of the intervals, the collected cells were washed three times with 1x PBS followed by immediate fixation with 2% formaldehyde in 1x PBS for 30 min at ambient temperature. The cells were washed once more to remove the formaldehyde and

CuAAC was performed. The cells were washed three times with 1x PBS and analyzed using a BDFacs Canto II flow cytometer using the previously stated parameters.

**Vancomycin derivative scan with D-Pra-D-Ala.** TSB medium containing 1 mM D-Pra-D-Ala and BHI medium containing 1 mM D-Laclick were prepared. The the medium was added 16 ug/mL vancomycin, desleucyl-vancomycin, or aglycon-vancomycin. *Enterococcus faecium* ATCC BAA-2317 (VanA) was added (1:100) to the TSB medium and allowed to grow overnight at 37 °C with shaking. The bacteria were harvested at 6,000g and wash three times with original culture volume of 1x PBS followed by fixation with 2% formaldehyde in 1x PBS for 30 min at ambient temperature. The cells were washed once more to remove the formaldehyde and CuAAC was performed. The cells were washed three times with 1x PBS and analyzed using a BDFacs Canto II flow cytometer using the previously stated parameters.

**Antibiotic scan with D-Pra-D-Ala.** TSB containing 1 mM D-Pra-D-Ala was prepared. Various antibiotics (vancomycin, teicoplanin, bacitracin, flavomycin, chlorohexidine, D-cycloserine, and ampicillin) were added for final concentrations of 0.25, 0.50, 1, 2, 4, 8, or 16 ug/mL. *Enterococcus faecium* ATCC BAA-2317 (VanA) was added (1:100) to the medium and allowed to grow overnight at 37 °C with shaking. The bacteria were harvested at 6,000g and wash three times with original culture volume of 1x PBS followed by fixation with 2% formaldehyde in 1x PBS for 30 min at ambient temperature. The cells were washed once more to remove the formaldehyde and CuAAC was performed. The cells were washed three times with 1x PBS and analyzed using a BDFacs Canto II flow cytometer using the previously stated parameters.

**Peptidoglycan digestion with Lysozyme.** TSB containing 1 mM D-Pra-D-Ala or D-Pra was prepared. *Enterococcus faecium* ATCC BAA-2317 (VanA) was added (1:100) to the medium and allowed to grow overnight at 37 °C with shaking. The bacteria were harvested at 6,000g and wash three times with original culture volume of 1x PBS followed by fixation with 2% formaldehyde in 1x PBS for 30 min at ambient temperature. The cells were washed once more to remove the formaldehyde and CuAAC was performed. The cells were washed three times with 1x PBS and then incubated at 37 °C with 500 µg/mL lysozyme (MP-Biomedicals) overnight. The cells were washed two times with 1x PBS, then once with 4 % formaldehyde in 1x PBS (quench lysozyme reaction) and analyzed using a BD FACS Canto II flow cytometer using the previously stated parameters.

**Isolation of Modified Peptidoglycan Muropeptide with D-Pra-D-Ala.** TSB medium (50 mL) containing 10 mM D-Pra-D-Ala was prepared. *Enterococcus faecium* ATCC BAA-2317 (VanA) was added (1:100) to the medium and allowed to grow overnight at 37 °C with shaking. The cells were harvested at 4000g and washed three times with 1x PBS. The cells were then resuspended in 1x PBS and boiled for 10 min and then centrifuged at 14,000g for 10 min at 4 °C. Cells were then placed in 25 mL of 5% (w/v) sodium dodecyl sulfate (SDS) and boiled for 25 min followed by centrifugation at 14,000g for 10 min at 4 °C. Following centrifugation, cells were boiled again in 25 mL of 4% (w/v) SDS for 15 min followed by centrifugation using same parameters as before. Cells were then washed five times with 60 °C DI water to remove all SDS. After washing, cells were incubated in 10 mL of 50 mM Tris (pH 7.2) containing 2 mg/mL Proteinase K for 1 h at 60 °C, and then washed 3 times with DI water. The cell wall pellet was then resuspended and digested with 250 µg/mL lysozyme in 25 mM sodium phosphate buffer pH 5.6 for 16 h at 37 °C. The

digestion was then ceased by boiling for 3 min. The sample was then centrifuged at 14,000g for 8 min, the supernatant was retained and concentrated *in vacuo*. The sample was then analyzed by a Shimadzu LC-MS 2020 using a phenomenex nucleosil 5 $\mu$  C18 120A, 250 x 320 mm column. Solvents were A: H<sub>2</sub>O (0.1% formic acid) and B: Acetonitrile (0.1% formic acid) using the following gradient condition, 0-10 min (0% B), and then ramping to 100% B from 10-50 min. Mass spectrometry was analyzed in the positive mode.

## **6.6 References**

- (1) Barna, J. C. J.; Williams, D. H. *Annu Rev Microbiol* **1984**, *38*, 339.
- (2) Smith, T. L.; Pearson, M. L.; Wilcox, K. R.; Cruz, C.; Lancaster, M. V.; Robinson-Dunn, B.; Tenover, F. C.; Zervos, M. J.; Band, J. D.; White, E.; Jarvis, W. R. *The New England journal of medicine* **1999**, *340*, 493.
- (3) Bugg, T. D.; Wright, G. D.; Dutka-Malen, S.; Arthur, M.; Courvalin, P.; Walsh, C. T. *Biochemistry* **1991**, *30*, 10408.
- (4) Arthur, M.; Molinas, C.; Bugg, T. D.; Wright, G. D.; Walsh, C. T.; Courvalin, P. *Antimicrob Agents Chemother* **1992**, *36*, 867.
- (5) Hubbard, B. K.; Walsh, C. T. *Angew Chem Int Ed Engl* **2003**, *42*, 730.
- (6) Kahne, D.; Leimkuhler, C.; Lu, W.; Walsh, C. *Chem Rev* **2005**, *105*, 425.
- (7) Koteva, K.; Hong, H. J.; Wang, X. D.; Nazi, I.; Hughes, D.; Naldrett, M. J.; Buttner, M. J.; Wright, G. D. *Nat Chem Biol* **2010**, *6*, 327.
- (8) Evers, S.; Courvalin, P. *J Bacteriol* **1996**, *178*, 1302.
- (9) Arthur, M.; Depardieu, F.; Snaith, H. A.; Reynolds, P. E.; Courvalin, P. *Antimicrob Agents Chemother* **1994**, *38*, 1899.
- (10) Arthur, M.; Depardieu, F.; Cabanie, L.; Reynolds, P.; Courvalin, P. *Mol Microbiol* **1998**, *30*, 819.
- (11) Reynolds, P. E.; Depardieu, F.; Dutka-Malen, S.; Arthur, M.; Courvalin, P. *Mol Microbiol* **1994**, *13*, 1065.
- (12) Liechti, G. W.; Kuru, E.; Hall, E.; Kalinda, A.; Brun, Y. V.; VanNieuwenhze, M.; Aurelli, A. T. *Nature* **2014**, *506*, 507.
- (13) Sarkar, S.; Libby, E. A.; Pidgeon, S. E.; Dworkin, J.; Pires, M. M. *Angew Chem Int Ed Engl* **2016**, *55*, 8401.
- (14) Fura, J. M.; Pidgeon, S. E.; Birabaharan, M.; Pires, M. M. *ACS Infect Dis* **2016**, *2*, 302.
- (15) Liechti, G.; Kuru, E.; Packiam, M.; Hsu, Y. P.; Tekkam, S.; Hall, E.; Rittichier, J. T.; VanNieuwenhze, M.; Brun, Y. V.; Aurelli, A. T. *PLoS Pathog* **2016**, *12*, e1005590.
- (16) Schouten, J. A.; Bagga, S.; Lloyd, A. J.; de Pascale, G.; Dowson, C. G.; Roper, D. I.; Bugg, T. D. *Mol Biosyst* **2006**, *2*, 484.
- (17) Lessard, I. A.; Pratt, S. D.; McCafferty, D. G.; Bussiere, D. E.; Hutchins, C.; Wanner, B. L.; Katz, L.; Walsh, C. T. *Chemistry & Biology* **1998**, *5*, 489.
- (18) Siegrist, M. S.; Whiteside, S.; Jewett, J. C.; Aditham, A.; Cava, F.; Bertozzi, C. R. *ACS Chem Biol* **2013**, *8*, 500.
- (19) Ngo, J. T.; Adams, S. R.; Deerinck, T. J.; Boassa, D.; Rodriguez-Rivera, F.; Palida, S. F.; Bertozzi, C. R.; Ellisman, M. H.; Tsien, R. Y. *Nat Chem Biol* **2016**, *12*, 459.
- (20) Bussiere, D. E.; Pratt, S. D.; Katz, L.; Severin, J. M.; Holzman, T.; Park, C. H. *Mol Cell* **1998**, *2*, 75.
- (21) Despreaux, C. W.; Manning, R. F. *Gene* **1993**, *131*, 35.
- (22) Atrih, A.; Bacher, G.; Allmaier, G.; Williamson, M. P.; Foster, S. J. *J Bacteriol* **1999**, *181*, 3956.
- (23) Bussiere, D. E.; Pratt, S. D.; Katz, L.; Severin, J. M.; Holzman, T.; Park, C. H. *Mol Cell* **1998**, *2*, 75.

- (24) Boucher, H. W.; Talbot, G. H.; Bradley, J. S.; Edwards, J. E.; Gilbert, D.; Rice, L. B.; Scheld, M.; Spellberg, B.; Bartlett, J. *Clinical Infectious Diseases* **2009**, *48*, 1.
- (25) Matthews, M. L.; Periyannan, G.; Hajdin, C.; Sidgel, T. K.; Bennett, B.; Crowder, M. W. *J Am Chem Soc* **2006**, *128*, 13050.
- (26) Hill, C. M.; Krause, K. M.; Lewis, S. R.; Blais, J.; Benton, B. M.; Mammen, M.; Humphrey, P. P.; Kinana, A.; Janc, J. W. *Antimicrob Agents Chemother* **2010**, *54*, 2814.
- (27) Baptista, M.; Rodrigues, P.; Depardieu, F.; Courvalin, P.; Arthur, M. *Mol Microbiol* **1999**, *32*, 17.
- (28) Reynolds, P. E. *Cell Mol Life Sci* **1998**, *54*, 325.
- (29) Foucault, M. L.; Depardieu, F.; Courvalin, P.; Grillot-Courvalin, C. *Proc Natl Acad Sci U S A* **2010**, *107*, 16964.
- (30) Kaplan, J.; Korty, B. D.; Axelsen, P. H.; Loll, P. J. *J Med Chem* **2001**, *44*, 1837.
- (31) Goldman, R. C.; Baizman, E. R.; Longley, C. B.; Branstrom, A. A. *FEMS Microbiol Lett* **2000**, *183*, 209.
- (32) Dutka-Malen, S.; Leclercq, R.; Coutant, V.; Duval, J.; Courvalin, P. *Antimicrob Agents Chemother* **1990**, *34*, 1875.
- (33) Baptista, M.; Depardieu, F.; Courvalin, P.; Arthur, M. *Antimicrob Agents Chemother* **1996**, *40*, 2291.



## Chapter 7

### **Cell Wall Piracy by a Synthetic Analog Reveals Metabolic Adaptation in Vancomycin Resistant Enterococci**

#### **7.1 Abstract**

Drug-resistant bacterial infections threaten to overburden our healthcare system and disrupt modern medicine. A large class of potent antibiotics, including vancomycin, operate by interfering with bacterial cell wall biosynthesis. Vancomycin-resistant Enterococci (VRE) evade the blockage of cell wall biosynthesis by altering cell wall precursors, rendering them drug insensitive. Herein, we reveal the phenotypic plasticity and cell wall remodeling of VRE in response to vancomycin in live bacterial cells *via* a metabolic probe. A synthetic cell wall analog was designed and constructed to monitor cell wall structural alterations. Our results demonstrate that the biosynthetic pathway for vancomycin-resistant precursors can be hijacked by synthetic analogs to track the kinetics of phenotype induction. In addition, we leveraged this probe to interrogate the response of VRE cells to vancomycin analogs and a series of cell wall-targeted antibiotics. Finally, we describe a proof-of-principle strategy to visually inspect drug resistance induction. Based on our findings, we anticipate that our metabolic probe will play an important role in further elucidating the interplay among the enzymes involved in the VRE biosynthetic rewiring.

#### **7.2 Introduction**

Today, vancomycin-resistant enterococci (VRE) are considered a major public health problem.<sup>1</sup> Vancomycin imparts its antimicrobial activity by inhibiting peptidoglycan (PG) biosynthesis. PG is an essential biopolymer composed of monomeric units of disaccharides connected to pentapeptide chains. By binding and sequestering the critical lipid-anchored

intermediate Lipid II, vancomycin prevents the transport of PG building blocks to the growing PG scaffold. Vancomycin association to Lipid II is mediated by a series of hydrogen bonds to the terminal dipeptide D-alanyl-D-alanine (D-Ala-D-Ala) unit on the PG stem peptide (Figure 7.1A).<sup>2-4</sup> VRE cells gain resistance to vancomycin by synthesizing D-alanyl-D-lactate (D-Ala-D-Lac) terminated PG precursors.<sup>5-8</sup>

The two main variations of VRE (VanA and VanB) are mediated by the acquisition of a resistance plasmid.<sup>9</sup> VRE cells displaying the VanA phenotype are resistant to both vancomycin and teicoplanin. In contrast, VRE cells displaying the VanB phenotype remain sensitive to teicoplanin. Resistance is driven by the polycistronic expression of the *vanR*, *vanS*, *vanH*, *vanA/vanB*, *vanY* and *vanX* genes (*vanRSHAX*). VanS, a membrane receptor, binds vancomycin and induces expression of *vanH*, *vanA*, *vanX* by the response regulator VanR.<sup>10,11</sup> In the absence of an inducible antibiotic in VRE cells, Lipid II molecules are primarily composed of terminal D-Ala. Exposure to vancomycin induces a shift in cell wall biosynthesis towards the intracellular production of D-Lac and PG building blocks displaying D-Lac at the terminal position.<sup>6</sup> Biosynthesis is initiated by VanH conversion of pyruvate to D-Lac, which is ligated onto D-Ala by the ligases VanA/VanB to afford the D-Ala-D-Lac

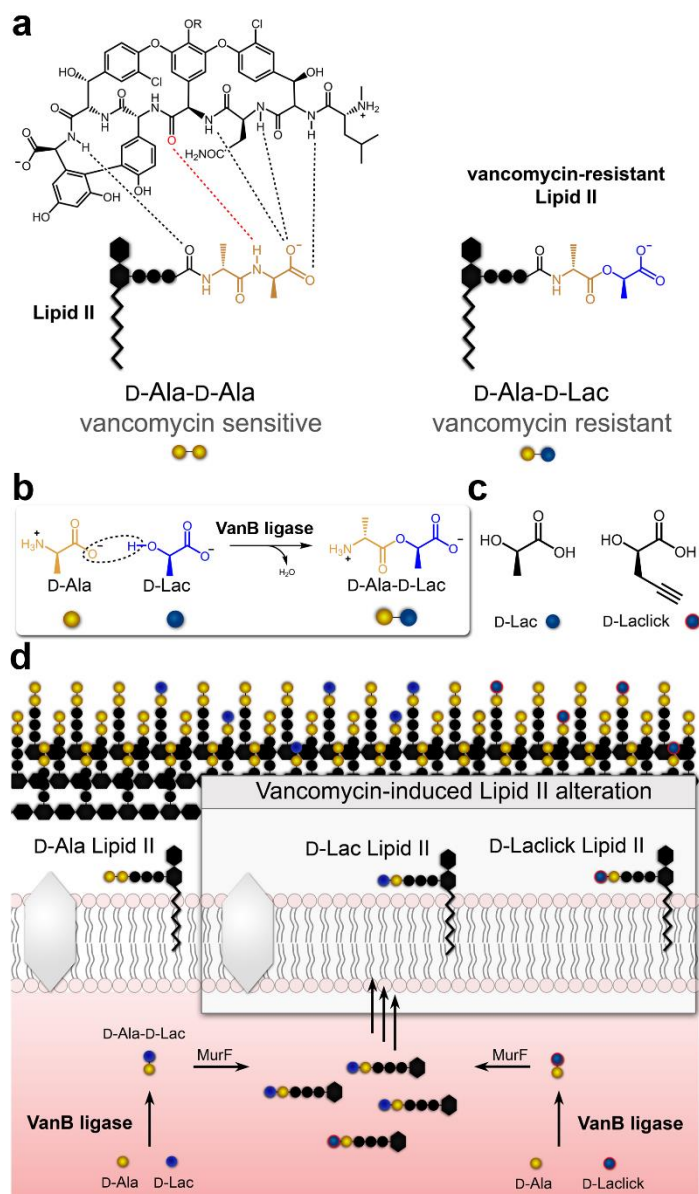


**Figure 7.1** Vancomycin binding to Lipid II and dipeptide metabolic alteration. (A) Structure of vancomycin and its hydrogen bond network mediating association to D-Ala-D-Ala terminus of Lipid II. (B) VanB ligates D-Ala to D-Lac to generate the vancomycin insensitive building block D-Ala-D-Lac. (C) Chemical structures of D-Lac and its analog D-Laclick. (D) Schematic representation of VanB ligase in the assembly of D-Ala-D-Lac building blocks that are PG precursors.

dipeptide (Figure 7.1B). This building block is joined onto a tripeptide by MurF to yield the full PG pentadepsipeptide precursor, which is subsequently loaded onto the lipid carrier. To ensure that primarily D-Lac terminated Lipid II molecules are assembled, a D,D-

dipeptidase (VanX) is encoded on the endogenous resistance plasmid along with the carboxypeptidase VanY.<sup>12</sup> VanX is tasked with the proteolysis of the dipeptide D-Ala-D-Ala, thus greatly reducing the production of D-Ala terminated Lipid II molecules. Through the concerted actions of these enzymes, VRE cells continue to grow and proliferate in the presence of high concentrations of vancomycin.

Seminal contributions from the Walsh, Courvalin, Kahne, and Walker laboratories have established the suite of genes required for the wholesale alteration of Lipid II in VRE and the structural requirement for glycopeptide binding to Lipid II.<sup>13-16</sup> At the protein level, elegant *in vitro* characterization studies of VanA/VanB and VanX<sub>A</sub>/VanX<sub>B</sub> (the ligases and dipeptidases from VanA- and VanB-type VRE cells, respectively) have established their catalytic function and substrate specificities.<sup>17-21</sup> However, no methods have been described to directly monitor and quantify PG structural plasticity linked to drug resistance in live VRE cells. We hypothesized that a deeper understanding of the metabolic processes involved in drug resistance could be achieved by gaining access to the cell wall biosynthetic machinery *in vivo*. Herein, we describe a synthetic analog (D-Laclck, Figure 7.1C) that mimics the substrate for the VRE-linked VanB ligase. A reporter handle was included at a strategic point within this PG precursor to generate a resistance-specific output signal. We anticipated that monitoring cell wall alterations during drug evasion with temporal resolution will reveal insight into adaptation dynamics and kinetics.

Although all five genes in VRE play specific roles in vancomycin sensing and biosynthesis of altered PG precursors, fundamentally the net change is the introduction of a D-Lac at the terminal position within Lipid II. Production of D-Lac in the intracellular space is triggered upon sensing of vancomycin in VRE cells, which is subsequently

incorporated into PG-precursors to establish the buildup of vancomycin-insensitive Lipid II molecules. We set out to examine the contribution of resistance-linked ligases by mimicking the critical D-Lac. More specifically, we focused on VanB ligases from VanB-typed VRE cells. Following its biosynthesis from pyruvate, D-Lac is assembled into D-Ala-D-Lac by the VanB ligase (Figure 7.1D). This didepsipeptide is processed further by a series of enzymes to yield Lipid II and eventually becomes imbedded within the extracytoplasmic PG scaffold. We synthesized an analog of D-Lac that displayed a click chemistry compatible alkyne handle called D-Laclick. We anticipated that proper mimicry of the endogenous D-Lac by D-Laclick should lead to its utilization by VanB ligases, yielding an intracellular pool of D-Ala-D-Laclick didepsipeptides (Figure 7.1D). Once D-Laclick units are PG-anchored, reporter fluorophores can be installed *via* copper-catalyzed azide-alkyne cycloaddition (CuAAC) reactions (Figure 7.2A).<sup>22,23</sup> Hijacking of the biosynthetic pathway of VRE responsible for the assembly of drug-resistant building blocks by activity-based probes should reveal, for the first time, how ligases operate in response to vancomycin in live bacteria.

## **7.3 Results and Discussion**

### **7.3.1 D-Laclick Incorporation**

Initially, *E. faecalis* (VanB-type VRE) cells were treated with D-Laclick and metabolic labeling was revealed by a click chemistry step to install reporter fluorophores onto surface-bound PG. Flow cytometry analysis of VRE cells probed with D-Laclick showed minimal labeling in the absence of vancomycin but a marked 30-fold increase upon the co-incubation with the antibiotic (Figure 7.2B; see Figure 7.3 for a secondary VanB strain). Further analysis of the response of VRE cells to vancomycin demonstrated that

cellular fluorescence intensities were highly dependent on the concentration of the antibiotic (Figure 7.2C). Interestingly, an approximate linear correlation with the vancomycin concentration was evident within the range of its minimum inhibitor

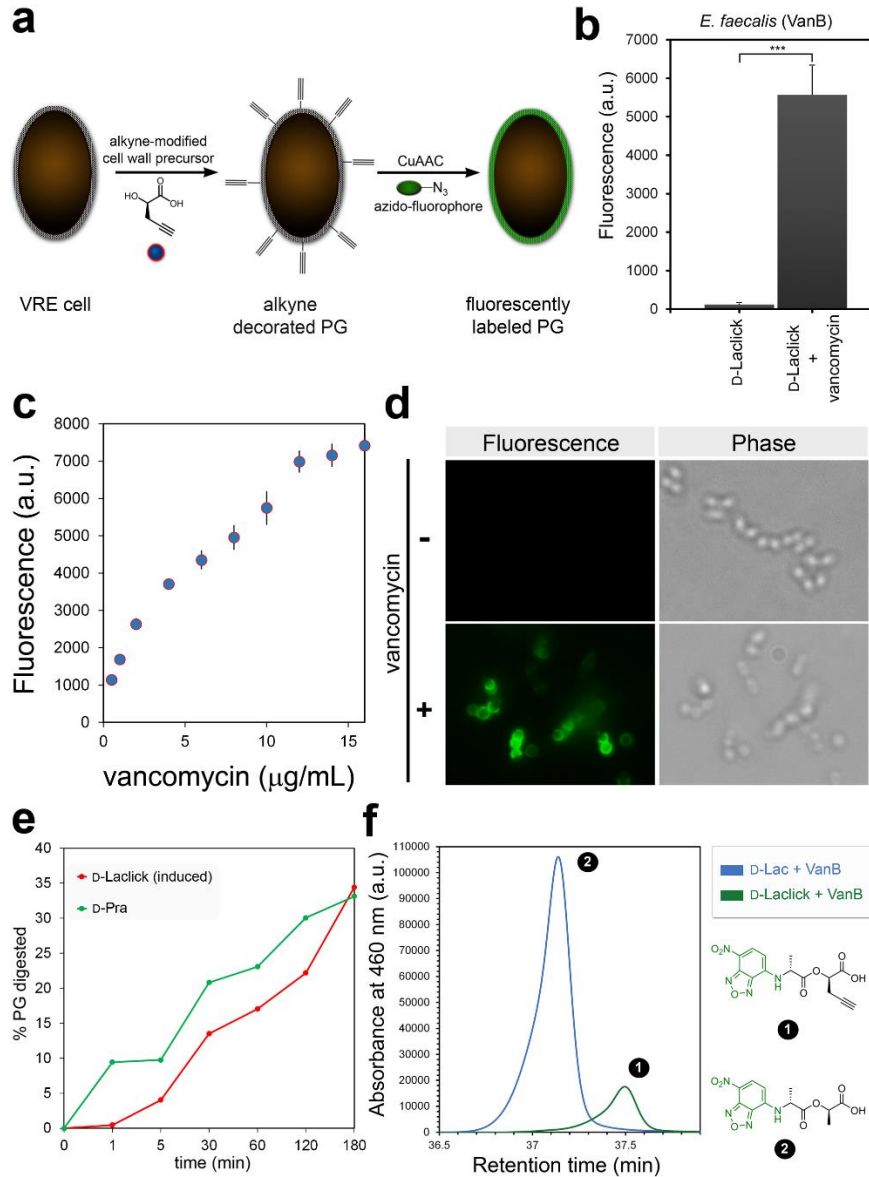


**Figure 7.2** Bacterial cell surface labeling in vancomycin resistant bacteria. (A) Schematic diagram delineating incorporation of synthetic PG precursors displaying alkyne handles, followed by click chemistry (CuAAC) to fluorescently label bacterial PG. (B) Flow cytometry analysis of *E. faecalis* ATCC 51299 (VanB) incubated overnight with 1 mM D-Laclick (+/- 16  $\mu\text{g/mL}$  vancomycin) followed by CuAAC with 6-FAM azide. (C) Flow cytometry analysis of *E. faecalis* (VanB) incubated overnight with 1 mM D-Laclick with various concentrations of vancomycin. Data are represented as mean + SD ( $n = 3$ ).  $P$  values were generated by an unpaired, two-sided t-test using GraphPad Prism 5 and  $P$  values are indicated ( $*P \leq 0.05$ ,  $**P \leq 0.01$ ,  $***P \leq 0.001$ ,  $****P \leq 0.0001$ ,

and NS, not significant). (D) Microscopy imaging of *E. faecalis* ATCC 51299 (VanB) incubated overnight with 1 mM D-Laclick (+/- 16 µg/mL vancomycin) and imaged using fluorescence and phase microscopy. (E) PG digestion was measured by the loss of fluorescence upon treatment with lysozyme of VRE cells pre-treated with specific probes. (F) HPLC profile of the reaction products using recombinant VanB ligase with D-Lac or D-Laclick.

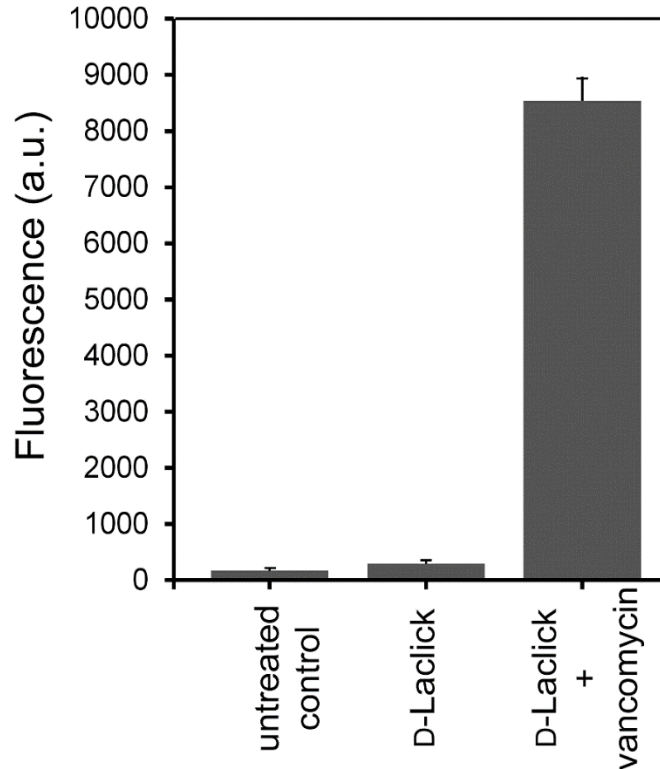


**Figure 7.3** Flow cytometry analysis of *E. faecalis* ATCC 51575 (VanB) incubated overnight with 1 mM D-Laclick (+/- 16 µg/mL vancomycin) followed by CuAAC with 6- FAM azide. All data are represented as mean +SD (n = 3).

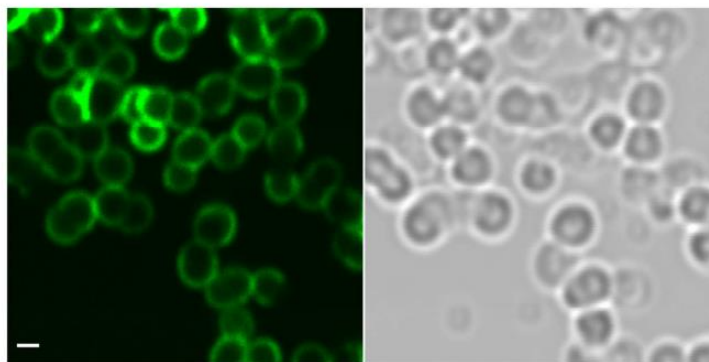


**Figure 7.4** Fluorescence and brightfield confocal microscopy of *E. faecalis* ATCC51575 (VanB) incubated overnight with 1 mM D-Laclick (+ 16 µg/mL vancomycin) followed by CuAAC with 6- FAM azide. Scale bar = 1 µm.

concentration (~ 16 µg/mL) – a feature that was previously shown for the induction of VanX.<sup>24,25</sup> The same cell treatment was further evaluated using epi-fluorescence microscopy. Consistently, in the absence of vancomycin, minimal fluorescence was observed (Figure 7.2D; see Figure 7.4 for confocal imaging). The exposure of VRE cells to vancomycin led to a visible increase in cell surface fluorescence. Next, a series of experiments were performed to establish the localization of the PG probe and the possible mode of installation. PG-associated fluorescence from D-Laclick treated VRE cells decreased upon release by lysozyme (Figure 7.2E and Figure 7.5). As a control, PG digestion from VRE cells treated with D-Propargylglycine (D-Pra),<sup>26</sup> which was previously shown to metabolically label PG *via* transpeptidases, was also monitored. We also found that, in contrast to D-Laclick, labeling levels of VRE cells treated with D-Pra did not increase upon vancomycin exposure. These results suggest that VRE labeling results in PG incorporation in a mode distinct from PG-linked transpeptidases.

VanB 51575	Fluorescence (a.u.)			VanB 51299	Fluorescence (a.u.)		
time (min)	D-Laclick Uninduced	D-Laclick Induced	D-Pra	time (min)	D-Laclick Uninduced	D-Laclick Induced	D-Pra
0	274	9568	13195	0	266	7458	7674
1	321	8755	11384	1	274	7426	6978
5	310	8350	10033	5	307	7169	6954
30	360	7786	9466	30	278	6491	6138
60	234	7684	9125	60	248	6238	5972
120	276	6944	7865	120	248	5870	5456
180	227	5844	6615	180	268	4992	5230

**Figure 7.5** Peptidoglycan digestion of *E. faecalis* ATCC 51575 and ATCC 51299. Cells were incubated overnight with 1 mM D-Laclick (+/- 16 µg/mL vancomycin) or 1 mM D-propargylglycine followed by CuAAC with 6-FAM azide. The cells were then incubated at 37°C with 500 µg/mL lysozyme, various time points collected and cells analyzed by flow cytometry.

### **7.3.2 In vitro Ligation**

Next, we set out to demonstrate that VanB ligase tolerates the unnatural substrate D-Laclick in place of the endogenous D-Lac. Recombinant VanB ligase was expressed in *E. coli* and



purified to homogeneity (Figure 7.6). We developed a facile assay to monitor depsidipeptide formation by LC-MS to circumvent the need for a radioactive assay (Figure 7.7). Subsequently, we showed that VanB processed D-Laclick to yield D-Ala-D-Laclick (Figure 7.2F). Moreover, no product was observed in the absence of VanB or in the presence of heat-denatured VanB (Figure 7.8). In addition, we synthesized D-Ala-D-Laclick to show the tolerance of VRE cells with the modified depsidipeptide (Figure 7.9). As expected, fluorescence levels were minimally affected by vancomycin exposure and were stereoselective.<sup>22</sup> Enterococci processing of D-Laclick was expected to be reserved for vancomycin-resistance strains. Consistently, treatment of drug sensitive *E. faecalis* with D-Laclick led to minimal cellular fluorescence in the absence and at sub-lethal levels of vancomycin (Figure 7.10).

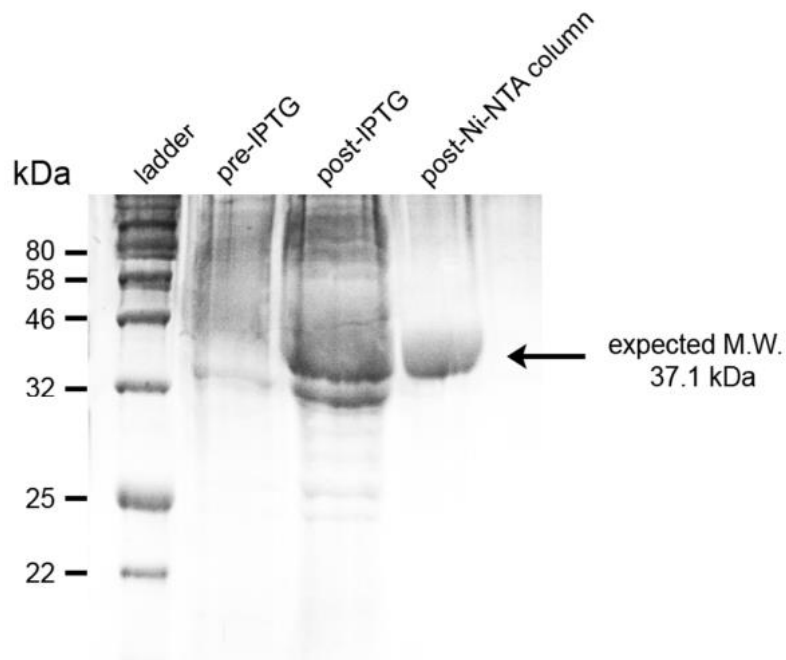
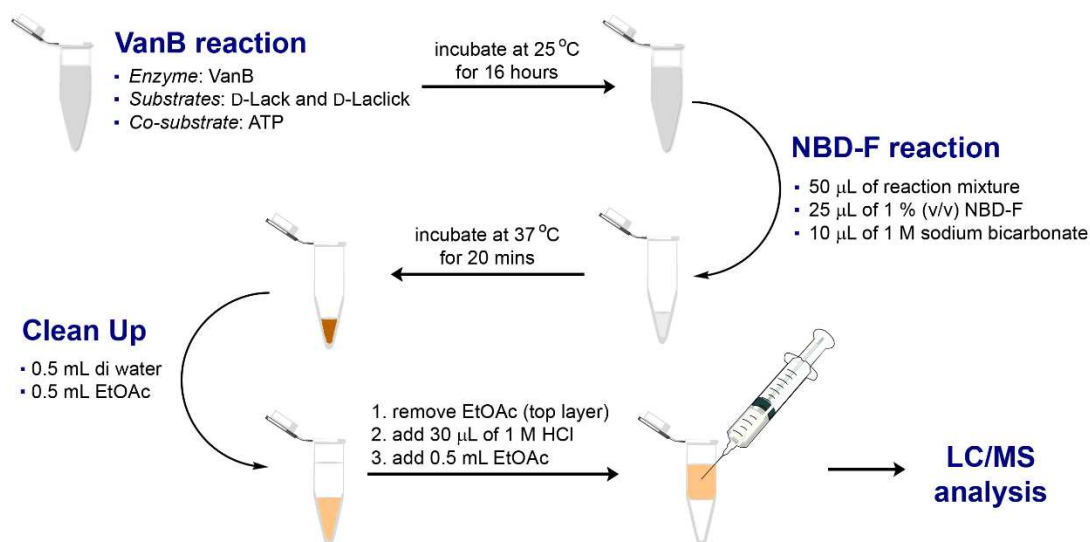


**Figure 7.6** SDS/15% polyacrylamide gel stained with Coomassie Blue with pre-IPTG, post-IPTG, and purified VanB ligase (~37.1 kDa) using a Ni-NTA column.



### Expected Products:

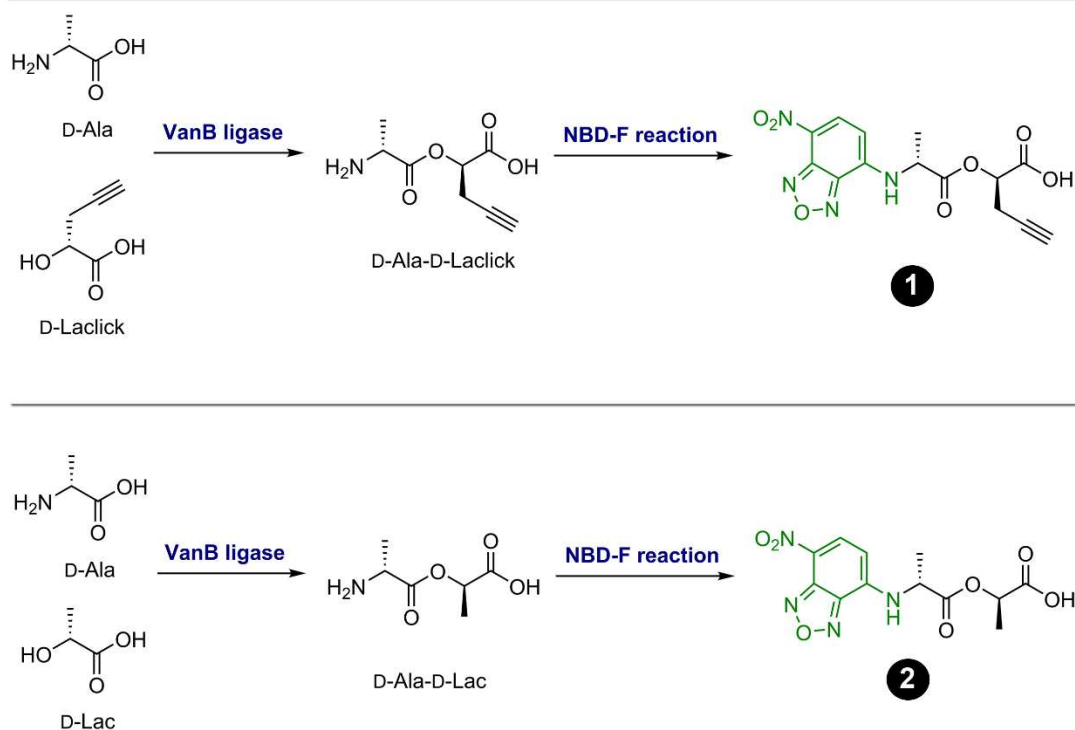


**Figure 7.7** VanB ligase *in vitro* assay to analyze product formation. The VanB enzyme was incubated at 25°C with D-Ala, ATP, and D-Lac or D-Laclick for 16 h. Mixture was incubated with NBD-F, cleaned up with dH<sub>2</sub>O/EtOAc, acidified, and then extracted with EtOAc and analyzed by LC-MS for VanB ligase product formation. Compound (1) and (2) correspond to VanB ligase product of D-Ala-D-Laclick and D-Ala-D-Lac after NBD-F treatment, respectively.

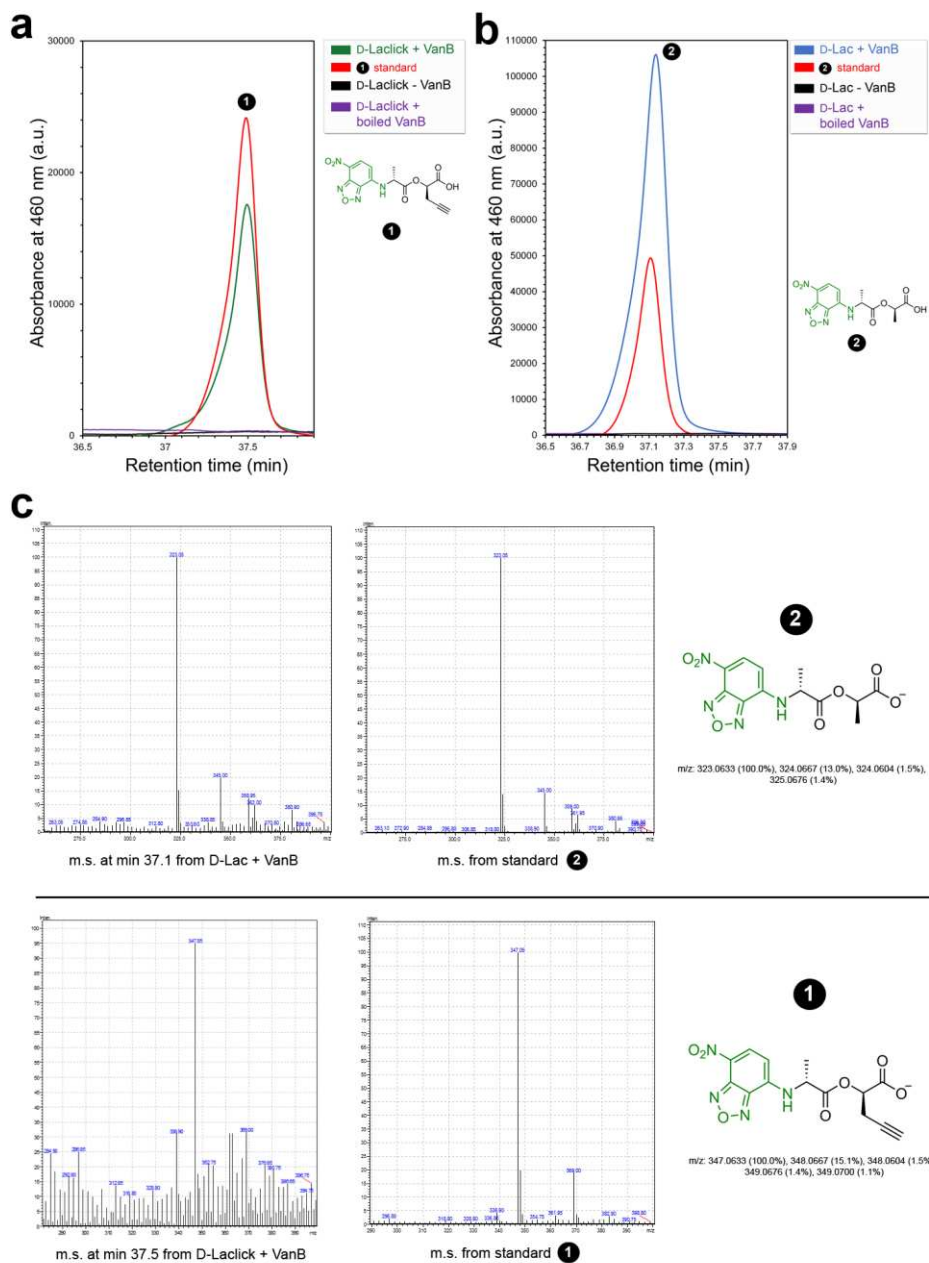


**Figure 7.8** LC-MS analysis of *in vitro* VanB ligase products. (a) LC monitored at 460 nm of VanB ligase D-Ala-D-Laclck and D-Ala-D-Lac after NBD-F treatment. (b) Mass spectrometry of D-Ala-D-Lac VanB ligase product and synthesized standard after NBD-F treatment. (c) Mass spectrometry of D-Ala-D-Laclck VanB ligase product and synthesized standard after NBD-F treatment.

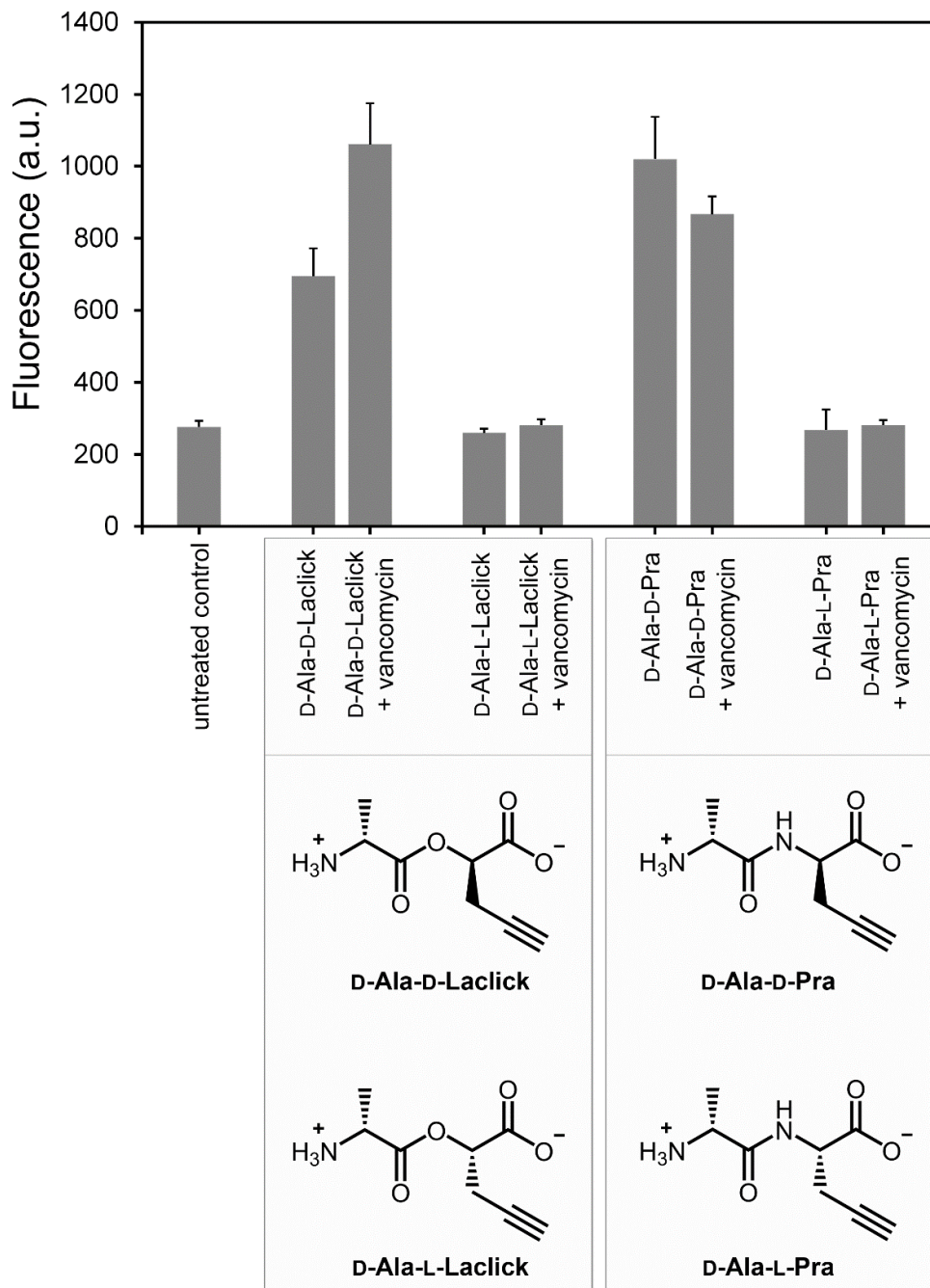


**Figure 7.9** Flow cytometry analysis of *E. faecalis* ATCC 51575 (VanB) incubated overnight with 1 mM D-Ala-D-Laclick, D-Ala-L-Laclick, D-Ala-D-Pra, or D-Ala-L-Pra with varying vancomycin concentrations followed by CuAAC with 6-FAM azide. All data are represented as mean + SD (n = 3).

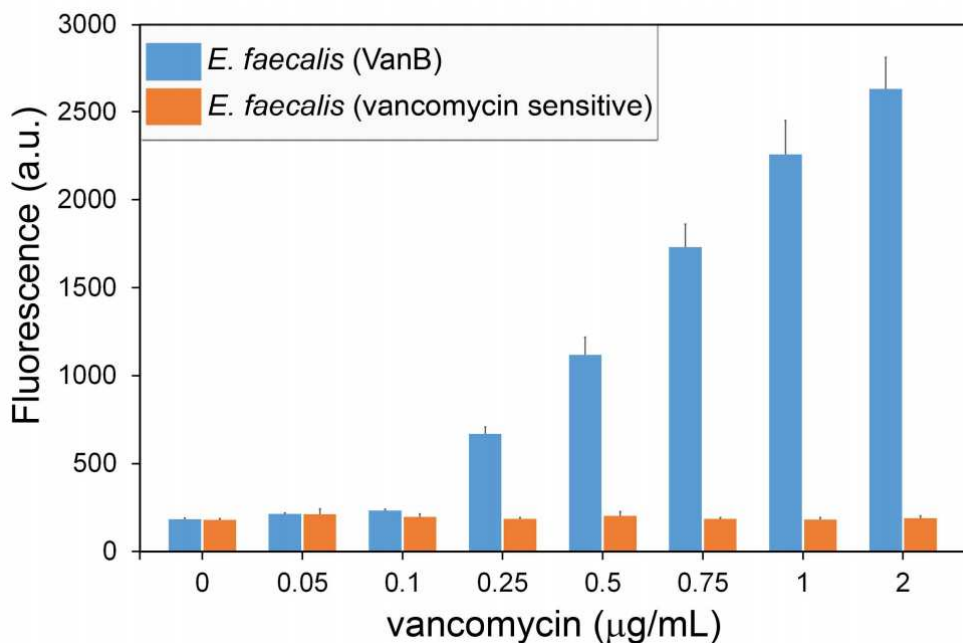


**Figure 7.10** Flow cytometry analysis of *E. faecalis* ATCC 29212 (drug sensitive) and *E. faecalis* ATCC 51299 (VanB) incubated overnight with 1 mM D-Laclick with varying vancomycin concentrations followed by CuAAC with 6-FAM azide. All data are represented as mean +SD (n = 3).

### **7.3.3 Analysis of D-Laclick in *E. Faecium***

We next examined the ability of D-Laclick to probe cell wall remodeling in the VanA-typed enterococci. Interestingly, *E. faecium* (VanA-typed VRE) cells treated with D-Laclick labeled poorly in the absence and presence of vancomycin (Figure 7.11). We hypothesize that the low fluorescence signals in D-Laclick-treated *E. faecium* (VanA) was a result of carboxypeptidase activity (surface-bound carboxypeptidases or VanY-mediated hydrolysis), which can release the terminal position on the PG stem peptide. Hydrolysis of the terminal D-Lac (and D-Laclick) on the PG precursor or mature PG would, consequently, function to reduce handles for fluorophore conjugation. It has been previously shown that VanA-typed VRE have reduced levels of pentapeptides/pentadepsipeptide (59% in total) intracellular PG precursors compared to

VanB-typed VRE (94% in total).<sup>27</sup> Next, we deduced that our synthetic cell wall analogs could provide a unique opportunity to readily visualize VRE induction. For facile interpretation of the results, we modified our assay to include bright chromophores in the labeling step with the goal of facilitating visual inspection. Following a similar labeling procedure as before, a marked color difference was observed in *E. faecalis* (VanB) cells in a vancomycin-dependent manner (Figure 7.12).

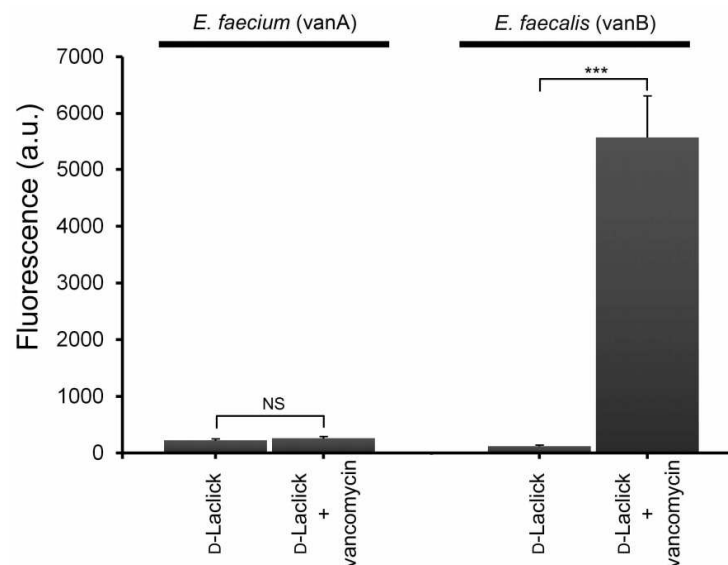


**Figure 7.11** Flow cytometry analysis of *E. faecium* ATCC BAA-2317 (VanA) and *E. faecalis* ATCC 51299 (VanB) incubated overnight with 1 mM D-Laclick (+/- 16 µg/mL vancomycin) followed by CuAAC with 6-FAM azide. All data are represented as mean +SD (n = 3). P values were generated by an unpaired, two-sided t-test using GraphPad Prism 5 and P values are indicated (\*P≤0.05, \*\*P≤0.01, \*\*\*P≤0.001, \*\*\*\*P≤0.0001, and NS, not significant).

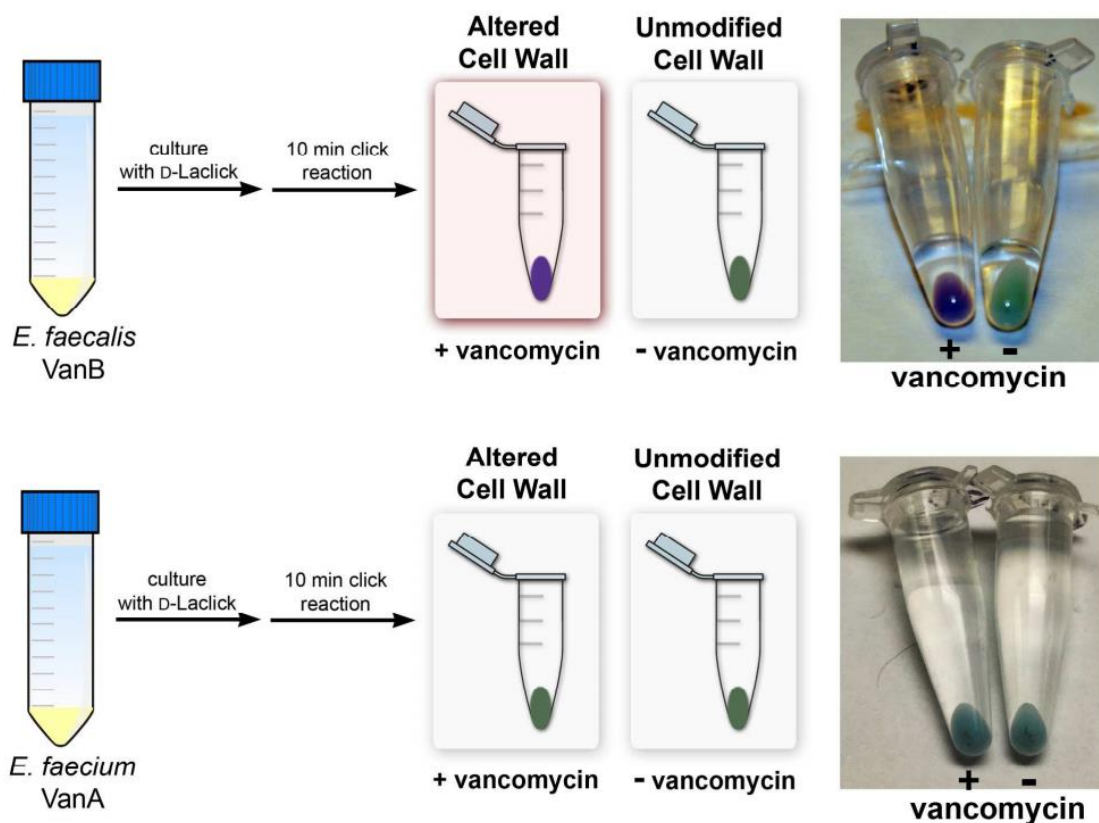


**Figure 7.12** Cartoon representation showing how VRE cells can be metabolically labeled with synthetic cell wall precursors to reveal resistance induction to vancomycin.

### **7.3.4 Kinetics of Cell Wall Remodeling**

The role of the stereochemistry of D-Lac was evaluated by synthesizing the enantiomeric L-Laclick. As expected, VRE cells treated with L-Laclick displayed 8-fold lower cellular fluorescence relative to D-Laclick treated cells upon exposure to vancomycin (Figure 7.13A). To gain further insight into the cell wall remodeling dynamics in VRE, we focused on two critical phases in VRE cellular response to vancomycin: induction and persistence of cell wall remodeling (Figure 7.13B). Induction refers to the time it takes for bacteria to shift their PG biosynthesis towards vancomycin-insensitive building blocks, while persistence is the time it takes for the drug-resistant phenotype to revert back to a vancomycin-sensitive state. Specifically, we set out to empirically



determine the kinetics in these two phases using live VRE cells. Based on our PG piracy strategy, we anticipated that it would be possible to monitor VRE cell wall alteration with unprecedented temporal resolution. Genetic methods were previously employed to monitor transcription activation<sup>28</sup>, GFP production,<sup>29</sup> and PG precursor composition.<sup>30</sup> *E. faecalis* (VanB) cells were treated with D-Laclick and allowed to grow and divide in order to preload cells with reporter D-Lac. Vancomycin was supplemented to the culture media and cellular fluorescence was measured every fifteen minutes for several hours (Figure 7.13C). Within 75 minutes following treatment, statistically significant differences in fluorescence labeling were observed. From these results, it was evident that VRE cells have evolved to alter PG composition rapidly when challenged with the antibiotic vancomycin. The persistence phase is similarly short-lived as

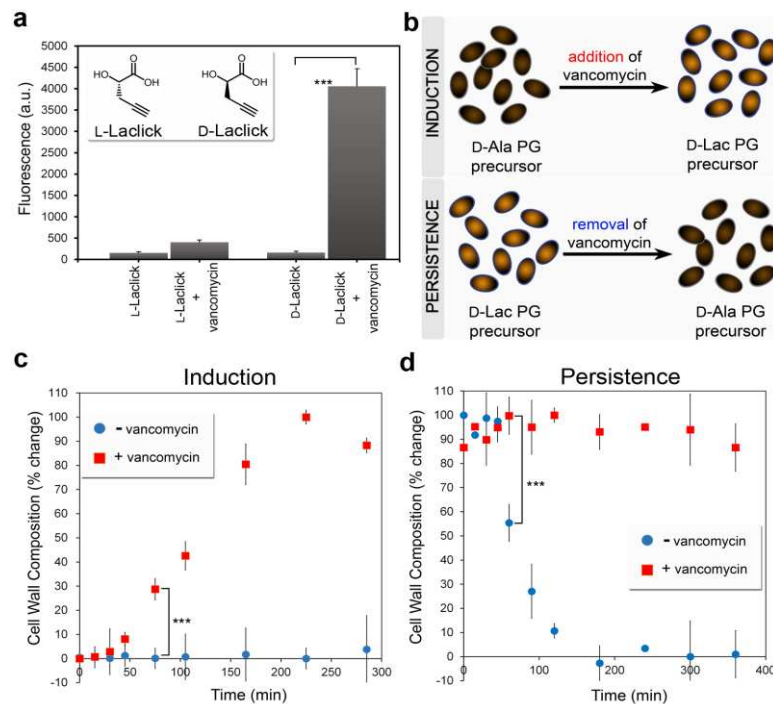


**Figure 7.13** Stereochemistry, induction, and persistence kinetic analysis. (a) Flow cytometry analysis of *E. faecalis* (VanB) incubated overnight with 1 mM D-Laclick or 1 mM L-Laclick (+/- 16  $\mu$ g/mL vancomycin) followed by CuAAC with 6-FAM azide. (b) Schematic diagram showing the two phases analyzed of VRE in response to vancomycin. Flow cytometry analysis of *E. faecalis* VanB induction (c) and persistence (d) in response to vancomycin. *E. faecalis* cells were treated



with D-Laclick (1 mM) and collected at various time points and fluorescently labeled with 6-FAM azide by CuAAC. Data are represented percent change from time of vancomycin addition and obtained as mean +/- SD ( $n = 3$ ).

demonstrated by the change in cellular labeling within 60 minutes following removal of vancomycin (Figure 7.13D). Kinetics of PG alterations were consistent with those found for gene activation, protein production, and precursor levels, an indication that these processes are tightly linked to streamline the wholesale phenotypic change. Together, these results highlight the dynamic nature of cell wall remodeling in response to an external stimuli and the rapid response in the wholesale alteration of a key cellular building block.

### **7.3.5 Vancomycin Variants and Pathway Activation**

With a VRE probe in hand operating within a specific resistance-phenotype, we set out to evaluate D-Lac induction using chemically altered vancomycin derivatives (Figure 7.14A). Aglycon-vanc is devoid of the disaccharide moiety, which does not participate in D-Ala-D-Ala binding and maintains antimicrobial activity.<sup>31</sup> Desleucyl-vanc is chemically stripped of the crucial binding motif for D-Ala-D-Ala but retains the ability to inhibit transglycosylation.<sup>32</sup> *E. faecalis* (VanB) exposed to vancomycin derivatives were probed for VanB activity induction using D-Laclick (Figure 7.14B). Only vancomycin and aglycon-vanc (the two variants that retain D-Ala-D-Ala binding) exposure led to a significant reduction in cellular fluorescence, consistent with findings by Kahne and co-workers.<sup>33</sup> These results indicate that D-Ala-D-Ala binding by vancomycin- like agents may be a requirement for vanS-dependent induction in VanB, as previously suggested.<sup>34</sup> To examine induction by antibiotics further, an additional panel of seven antibiotics was assessed that encompassed a range of PG biosynthesis inactivators (Figure 7.14C). From this set, vancomycin was the only antibiotic to induce cell wall remodeling, in agreement

with the elevated susceptibility of VanB organisms to the other six agents and in agreement with previous reports.<sup>24,35,36</sup> These results demonstrate that D-Laclick represents a reliable and quantitative phenotypic readout on cell wall remodeling in VanB-type VRE. Unlike minimal inhibitory concentration examinations, which are sensitive to

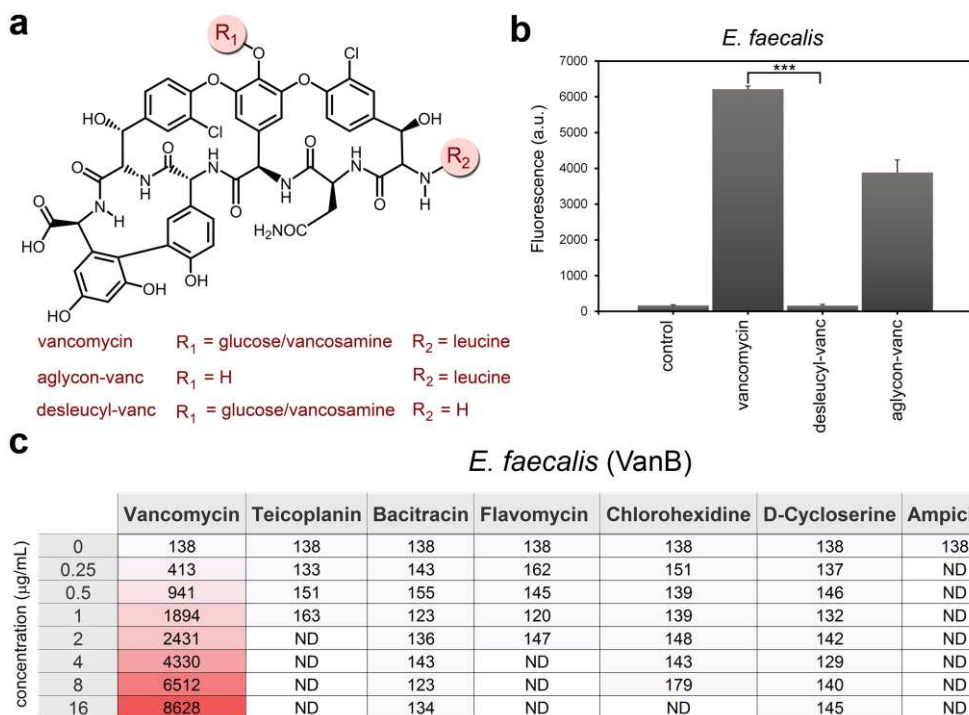


**Figure 7.14.** Induction of VanB ligase with vancomycin derivatives. (A) Chemical structure of vancomycin and chemical derivatives. (B) Flow cytometry analysis and VanB ligase activity of *E. faecalis* (VanB) incubated overnight with 1 mM D-Laclick (+/- 16  $\mu$ g/mL vancomycin variants) followed by CuAAC with 6-FAM azide. All data are represented as mean + SD ( $n = 3$ ). Flow cytometry analysis of *E. faecalis* (VanB) incubated overnight with D-Laclick with various concentrations of antibiotics, followed by CuAAC with 6-FAM azide. Shading is internally calibrated within each set with darker red representing elevated induction. ND = not determined due to lack of cell viability.

any mode of cellular disruption, our probe directly reports on the structural alteration in live VRE cells in response to agents that induce the resistant-phenotype. We anticipate that this strategy could prove useful in dissecting structural components of antibiotics responsible for VanB-activation. Finally, we deduced that our synthetic cell wall analogs could provide a unique opportunity to readily visualize VRE induction.

## **7.4 Conclusions**

We have designed and synthesized an unnatural cell wall precursor to gain access to the PG biosynthesis of VRE. This reporter molecule mimics the substrate of a key ligase that operates in altering the chemical structure of Lipid II. Our results showed that the reporter molecule D-Laclick can be leveraged to reveal cell wall remodeling dynamics in live VRE cells. We anticipate that the development of chemical tools to systematically characterize cell wall biogenesis in drug-resistant bacteria will directly contribute to our understanding of the molecular mechanisms underpinning bacterial pathogenesis and drug resistance. Most significantly, these activity-based probes may pave the way for the design of novel antibiotic and diagnostic modalities. In the future, we will target additional enzymatic pathways that work in concert with ligases in VRE to formulate a complementary tool to study drug resistance.

## **7.5 Materials and Methods**

All peptide related reagents (resin, coupling reagent, deprotection reagent, amino acids, and cleavage reagents) were purchased from ChemImpex. FAM (fluorescein) azide 6-isomer, sulfo-cyanine3 azide and were purchased from Lumiprobe. Vancomycin hydrochloride was purchased from AK Scientific. All other reagents were purchased from Sigma and were used without further purification. Bacterial strains used for these experiments were:

	Strain	Growth Media
Vancomycin Resistant	<i>Enterococcus faecalis</i> ATCC 51299 (VanB)	Brain Heart Infusion Broth (BHI)
	<i>Enterococcus faecium</i> ATCC BAA-2317 (VanA)	BBL Trypticase Soy Broth (TSB)
	<i>Enterococcus faecalis</i> ATCC 51575 (VanB)	Brain Heart Infusion Broth (BHI)
Vancomycin Sensitive	<i>Enterococcus faecalis</i> ATCC 29212	Brain Heart Infusion Broth (BHI)

**Copper-catalyzed azide-alkyne cycloaddition (CuAAC) cell surface labeling.** For all experiments with azide-alkyne click chemistry, the following fluorophore labeling protocol was used after fixation of cells. Cells were suspended in half the volume of the original culture with 1x PBS. The reagents were added in the following order for final concentrations of 1 mM CuSO<sub>4</sub>, 128 uM THPTA, 1.2 mM L-ascorbic acid (freshly prepared) and 30 uM fluorescein azide 6-isomer. The reactions were performed at ambient temperature for 1 h with shaking. After washing, samples were analyzed using a BDFacs Canto II flow cytometer using a 488nm argon laser (L1) and a 530/30 band-pass filter (FL1). A minimum of 10,000 events were counted for each data set. The data was analyzed using the FACSDiva version 6.1.1.

**D-Laclick/L-Laclick Labeling.** TSB or BHI medium containing 1 mM D-Laclick or L-Laclick were prepared with or without 16 ug/mL vancomycin hydrochloride. *Enterococcus faecalis* ATCC-51299 (VanB) or *Enterococcus faecalis* ATCC-51575 (VanB) were added to the BHI medium (1:100) and *Enterococcus faecium* ATCC BAA-2317 (VanA) to the TSB medium and allowed to grow overnight at 37 °C with shaking. The bacteria were harvested at 6,000g and wash three times with original culture volume of 1x PBS followed by fixation with 2% formaldehyde in 1x PBS for 30 min at ambient temperature. The cells were washed once more to remove the formaldehyde and CuAAC was performed. The

cells were washed three times with 1x PBS and analyzed using a BDFacs Canto II flow cytometer using the previously stated parameters.

**Vancomycin Concentration Scan with D-Laclick.** BHI medium containing 1 mM D-Laclick was prepared. To that medium was added vancomycin hydrochloride for final concentrations of 0.5, 1, 2, 4, 8, 10, 12, 14, or 16 ug/mL. *Enterococcus faecalis* ATCC 51299 (VanB) was added to the corresponding medium (1:100) and allowed to grow overnight at 37 °C with shaking. The bacteria were harvested at 6,000g and wash three times with original culture volume of 1x PBS followed by fixation with 2% formaldehyde in 1x PBS for 30 min at ambient temperature. The cells were washed once more to remove the formaldehyde and CuAAC was performed. The cells were washed three times with 1x PBS and analyzed using a BDFacs Canto II flow cytometer using the previously stated parameters. For fluorescent imaging confocal microscopy, the cells were analyzed on a glass slide using a B-2E/C filter (ex 465-495/em 515-555). For confocal microscopy, a Nikon Eclipse Ti-E was used with 488nm-excitation and 505-550 band pass emission filter for FITC.

**Peptidoglycan Digestion/Lysozyme Treatment of Labeled Peptidoglycan.** BHI medium containing 1 mM D-Laclick with or without 16 ug/mL vancomycin hydrochloride, along with BHI medium containing 1 mM D-propargylglycine (D-Pra) were prepared. *Enterococcus faecalis* ATCC-51299 (VanB) or *Enterococcus faecalis* ATCC-51575 (VanB) were added to the BHI medium (1:100) and allowed to grow overnight at 37 °C with shaking. The bacteria were harvested at 6,000g and wash three times with original culture volume of 1x PBS followed by fixation with 2% formaldehyde in 1x PBS for 30 min at ambient temperature. The cells were washed once more to remove the formaldehyde

and CuAAC was performed. The cells were washed three times with 1x PBS. The bacteria were resuspended in 1x PBS containing 500 ug/mL lysozyme (MP biomedical) and incubated at 37°C. A portion of the cells were taken at 1, 5, 30, 60, 120, and 180 min. At each time point, the collected bacteria were washed three times with 1x PBS and resuspended in a final solution of 1x PBS containing 4% formaldehyde to quench the lysozyme reaction. The cells were analyzed using a BDFacs Canto II flow cytometer using the previously stated parameters.

**D-Pra vs D-Laclick labeling of Enterococci.** BHI medium containing 1 mM D-propargylglycine (D-Pra) or D-Laclick with or without 16 ug/mL vancomycin hydrochloride were prepared. *Enterococcus faecalis* ATCC-51299 (VanB) or *Enterococcus faecalis* ATCC-51575 (VanB) were added to the BHI medium (1:100) and allowed to grow overnight at 37 °C with shaking. The bacteria were harvested at 6,000g and wash three times with original culture volume of 1x PBS followed by fixation with 2% formaldehyde in 1x PBS for 30 min at ambient temperature. The cells were washed once more to remove the formaldehyde and CuAAC was performed. The cells were washed three times with 1x PBS and analyzed using a BDFacs Canto II flow cytometer using the previously stated parameters.

**VanB Ligase Protein Purification.** Purification of VanB ligase was performed in BL21 E. coli containing plasmid VanB\_pET-28a(+) encoding the His-tagged VanB ligase. The BL21 E. coli were grown at 37°C in LB broth (2 L) containing 50 ug/mL kanamycin until the OD<sub>600nm</sub> was 0.6. At that point, isopropyl-D-thiogalactopyranoside (IPTG) was added for a final concentration of 1 mM, and incubated for an additional 2 h. Bacteria were harvested at 4000g, washed two times with 1x phosphate buffered saline (PBS), and

resuspended in 100 mL lysis buffer (50 mM Na<sub>2</sub>HPO<sub>4</sub>, 300 mM NaCl, 1 mM Imidazole, 1 mM DTT, 1x Halt Protease inhibitor cocktail, pH 8.0). The sample was sonicated for 15 min at 4°C. Lysed cells were centrifuged at 20,000g for 30 min at 4°C. All the following steps were performed at 4°C. The supernatant was applied to a 1 mL agarose Ni-NTA column equilibrated with lysis buffer. The column was washed with 25 mL of buffer containing 50 mM Na<sub>2</sub>HPO<sub>4</sub>, 300 mM NaCl, 1 mM Imidazole (pH 8.0), followed by 25 mL of each of the following four buffers containing 50 mM Na<sub>2</sub>HPO<sub>4</sub>, 300 mM NaCl (pH 8.0) with increasing concentrations of imidazole (5, 10, 50, 250 mM). His-tagged VanB ligase was eluted with buffer containing 250 mM imidazole. The purified protein was dialyzed with an Amicon Ultra Centrifugal Filter Unit with a 30 kDa molecular weight cutoff at 4000g against the ligase assay buffer containing 50 mM HEPES, 10 mM MgCl<sub>2</sub>, 10 mM KCl (pH 7.5). The final protein stock was stored at -20°C in 20% glycerol. Sodium dodecyl sulfate-polyacrylamide (SDS) gel electrophoresis was carried out on a 15% polyacrylamide gel with standard proteins (11-245 kDa, New England Biolabs). Proteins were stained with 0.25% Coomassie blue in 50% methanol-10% acetic acid for 30 min at room temperature, destained with 50% methanol-10% acetic acid for 2 h, and imaged using a Bio-Rad imaging system.

***In Vitro* VanB Ligase Reaction and Analysis.** VanB ligase conditions were performed at 10 mM D-alanine, 100 mM D-lactic acid or D-Lallick, 50 mM adenosine triphosphate (ATP), and 50 uM purified VanB ligase in buffer condition of 50 mM HEPES, 10 mM MgCl<sub>2</sub> and 10 mM KCl (pH 7.5). Controls for ligase activity were the absence of VanB and VanB ligase boiled for 15 min prior to incubation to inactivate the enzyme. The reactions were shaken for 16 h at room temperature. Analysis of the reaction was done by

product fluorophore conjugation and LC-MS. After 16 h, a portion of the reaction (50 uL) was collected and added 25 uL 4-Fluoro-7-Nitrobenzofurazan (NBD-F) (1% in acetonitrile) and 10 uL of 1 M sodium bicarbonate. The mixture was incubated at 37 °C for 20 min. After 20 min, dH<sub>2</sub>O (500 uL) and ethyl acetate (500 uL) were added and mixed. The aqueous layer was retained and acidified with 30 uL of 1 M HCl, followed by addition of ethyl acetate (500 uL) and mixing. The organic layer was concentrated *in vacuo*, residue resuspended in dH<sub>2</sub>O, and analyzed by a Shimadzu LCMS-2020. Product analysis was done using a phenomenex nucelosil, 5u C18 120A, 250 x 3.20 mm column using solvent A-H<sub>2</sub>O (0.05% formic acid) and solvent B-acetonitrile (0.05% formic acid) at a flow rate of 0.20 mL/min monitoring at 460 nm. The following gradient condition was used: 0-10 min 0% B, then ramped to 100% B from 10 to 50 min. All mass spectrometry was analyzed in the negative mode.

**Dipeptide Labeling of Peptidoglycan.** BHI medium containing 1 mM D-Ala-D-Laclick, D-Ala-L-Laclick, D-Ala-D-Pra, or D-Ala-L-Pra with or without 16 ug/mL vancomycin hydrochloride were prepared. *Enterococcus faecalis* ATCC-51575 (VanB) was added to the BHI medium (1:100) and allowed to grow overnight at 37 °C with shaking. The bacteria were harvested at 6,000g and wash three times with original culture volume of 1x PBS followed by fixation with 2% formaldehyde in 1x PBS for 30 min at ambient temperature. The cells were washed once more to remove the formaldehyde and CuAAC was performed. The cells were washed three times with 1x PBS and analyzed using a BDFacs Canto II flow cytometer using the previously stated parameters.

**Induction of VanB ligase.** BHI medium containing 1 mM D-Laclick was prepared. *Enterococcus faecalis* ATCC-51299 (VanB) was added to the corresponding medium for



an initial optical density ( $OD_{600}$ ) of 0.2. The cells were incubated at 37 °C with shaking. A portion of the cells were taken at 0, 15, 30, 45, and 60 min. At 60 min ( $OD_{600} = 0.6$ ) the culture was split in half and to one sample was added vancomycin hydrochloride for a final concentration of 4 ug/mL. A portion of the cells were collected at 75, 90, 105, 120, 150, 180, 240, 300, and 360 min. At each of the intervals, the collected cells were washed three times with 1x PBS followed by immediate fixation with 2% formaldehyde in 1x PBS for 30 min at ambient temperature. The cells were washed once more to remove the formaldehyde and CuAAC was performed. The cells were washed three times with 1x PBS and analyzed using a BDFacs Canto II flow cytometer using the previously stated parameters.

**Persistence of VanB ligase.** BHI medium containing 1 mM D-Laclick was prepared with 16 ug/mL vancomycin hydrochloride. *Enterococcus faecalis* ATCC-51299 (VanB) was added to the corresponding medium (1:100) and allowed to incubate overnight at 37 °C with shaking. The following day, the cells were washed to remove the vancomycin and diluted to optical density ( $OD_{600}$ ) of 0.2 with BHI medium containing 1 mM D-Laclick with or without 16 ug/mL vancomycin hydrochloride. A sample of cells were collected at various time points. At each of the intervals, the collected cells were washed three times with 1x PBS followed by immediate fixation with 2% formaldehyde in 1x PBS for 30 min at ambient temperature. The cells were washed once more to remove the formaldehyde and CuAAC was performed. The cells were washed three times with 1x PBS and analyzed using a BDFacs Canto II flow cytometer using the previously stated parameters.

**Vancomycin Resistant vs Sensitive Enterococci D-Laclick Labeling.** BHI medium containing 1 mM D-Laclick was prepared. To that medium was added vancomycin

hydrochloride for final concentrations of 0.05, 0.10, 0.25, 0.50, 0.75, 1.0, or 2.0 ug/mL. *Enterococcus faecalis* ATCC-51299 (VanB) or *Enterococcus faecalis* ATCC 29212 was added to the BHI medium (1:100). The bacteria were allowed to grow overnight at 37 °C with shaking. The bacteria were harvested at 6,000g and wash three times with original culture volume of 1x PBS followed by fixation with 2% formaldehyde in 1x PBS for 30 min at ambient temperature. The cells were washed once more to remove the formaldehyde and CuAAC was performed. The cells were washed three times with 1x PBS and analyzed using a BDFacs Canto II flow cytometer using the previously stated parameters.

**Vancomycin derivative scan with D-Laclick.** BHI medium containing 1 mM D-Laclick was prepared. The medium was added 16 ug/mL vancomycin, desleucyl-vancomycin, or aglycon-vancomycin. *Enterococcus faecalis* ATCC-51299 (VanB) was added to the BHI medium (1:100). The bacteria were allowed to grow overnight at 37 °C with shaking. The bacteria were harvested at 6,000g and wash three times with original culture volume of 1x PBS followed by fixation with 2% formaldehyde in 1x PBS for 30 min at ambient temperature. The cells were washed once more to remove the formaldehyde and CuAAC was performed. The cells were washed three times with 1x PBS and analyzed using a BDFacs Canto II flow cytometer using the previously stated parameters.

**Antibiotic scan with D-Laclick.** BHI medium 1 mM D-Laclick was prepared. Various antibiotics (vancomycin, teicoplanin, bacitracin, flavomycin, chlorohexidine, D-cycloserine, and ampicillin) were added for final concentrations of 0.25, 0.50, 1, 2, 4, 8, or 16 ug/mL. *Enterococcus faecalis* ATCC-51299 (VanB) was added to the BHI medium (1:100). The bacteria were allowed to grow overnight at 37 °C with shaking. The bacteria were harvested at 6,000g and wash three times with original culture volume of 1x PBS

followed by fixation with 2% formaldehyde in 1x PBS for 30 min at ambient temperature. The cells were washed once more to remove the formaldehyde and CuAAC was performed. The cells were washed three times with 1x PBS and analyzed using a BDFacs Canto II flow cytometer using the previously stated parameters.

**Visualization VanB Ligase Induction.** BHI medium containing 1 mM D-Laclick was prepared with or without 16 ug/mL vancomycin hydrochloride. *Enterococcus faecalis* ATCC-51299 (VanB) was added to the BHI medium (1:100). The bacteria were allowed to grow overnight at 37 °C with shaking. The bacteria were harvested at 6,000g and wash three times with original culture volume of 1x PBS and CuAAC was performed using sulfo-cyanine3-azide. The bacteria were washed three times with 1x PBS and images were taken of the cell pellets.

## 7.6 References

- (1) Ventola, C. L. *P T* **2015**, *40*, 277.
- (2) Barna, J. C. J.; Williams, D. H. *Annu Rev Microbiol* **1984**, *38*, 339.
- (3) Breukink, E.; Wiedemann, I.; van Kraaij, C.; Kuipers, O. P.; Sahl, H. G.; de Kruijff, B. *Science* **1999**, *286*, 2361.
- (4) Breukink, E.; de Kruijff, B. *Nat Rev Drug Discov* **2006**, *5*, 321.
- (5) Bugg, T. D.; Dutka-Malen, S.; Arthur, M.; Courvalin, P.; Walsh, C. T. *Biochemistry* **1991**, *30*, 2017.
- (6) Arthur, M.; Molinas, C.; Bugg, T. D.; Wright, G. D.; Walsh, C. T.; Courvalin, P. *Antimicrob Agents Chemother* **1992**, *36*, 867.
- (7) Hubbard, B. K.; Walsh, C. T. *Angew Chem Int Ed Engl* **2003**, *42*, 730.
- (8) Kahne, D.; Leimkuhler, C.; Lu, W.; Walsh, C. *Chem Rev* **2005**, *105*, 425.
- (9) Leclercq, R.; Derlot, E.; Duval, J.; Courvalin, P. *N Engl J Med* **1988**, *319*, 157.
- (10) Arthur, M.; Molinas, C.; Courvalin, P. *J Bacteriol* **1992**, *174*, 2582.
- (11) Koteva, K.; Hong, H. J.; Wang, X. D.; Nazi, I.; Hughes, D.; Naldrett, M. J.; Buttner, M. J.; Wright, G. D. *Nat Chem Biol* **2010**, *6*, 327.
- (12) Arthur, M.; Depardieu, F.; Cabanie, L.; Reynolds, P.; Courvalin, P. *Mol Microbiol* **1998**, *30*, 819.
- (13) Eggert, U. S.; Ruiz, N.; Falcone, B. V.; Branstrom, A. A.; Goldman, R. C.; Silhavy, T. J.; Kahne, D. *Science* **2001**, *294*, 361.
- (14) Marshall, C. G.; Lessard, I. A.; Park, I.; Wright, G. D. *Antimicrob Agents Chemother* **1998**, *42*, 2215.
- (15) van Wageningen, A. M.; Kirkpatrick, P. N.; Williams, D. H.; Harris, B. R.; Kershaw, J. K.; Lennard, N. J.; Jones, M.; Jones, S. J.; Solenberg, P. J. *Chemistry & Biology* **1998**, *5*, 155.
- (16) Wright, G. D. *Nat Rev Microbiol* **2007**, *5*, 175.
- (17) Bugg, T. D.; Wright, G. D.; Dutka-Malen, S.; Arthur, M.; Courvalin, P.; Walsh, C. T. *Biochemistry* **1991**, *30*, 10408.
- (18) Fan, C.; Moews, P. C.; Walsh, C. T.; Knox, J. R. *Science* **1994**, *266*, 439.
- (19) Reynolds, P. E.; Depardieu, F.; Dutka-Malen, S.; Arthur, M.; Courvalin, P. *Molecular Microbiology* **1994**, *13*, 1065.
- (20) McCafferty, D. G.; Lessard, I. A.; Walsh, C. T. *Biochemistry* **1997**, *36*, 10498.
- (21) Meziane-Cherif, D.; Badet-Denisot, M. A.; Evers, S.; Courvalin, P.; Badet, B. *FEBS Lett* **1994**, *354*, 140.
- (22) Siegrist, M. S.; Whiteside, S.; Jewett, J. C.; Aditham, A.; Cava, F.; Bertozzi, C. R. *ACS Chem Biol* **2013**, *8*, 500.
- (23) Ngo, J. T.; Adams, S. R.; Deerinck, T. J.; Boassa, D.; Rodriguez-Rivera, F.; Palida, S. F.; Bertozzi, C. R.; Ellisman, M. H.; Tsien, R. Y. *Nat Chem Biol* **2016**, *12*, 459.
- (24) Baptista, M.; Depardieu, F.; Courvalin, P.; Arthur, M. *Antimicrob Agents Chemother* **1996**, *40*, 2291.
- (25) Baptista, M.; Depardieu, F.; Reynolds, P.; Courvalin, P.; Arthur, M. *Mol Microbiol* **1997**, *25*, 93.

- (26) Siegrist, M. S.; Whiteside, S.; Jewett, J. C.; Aditham, A.; Cava, F.; Bertozzi, C. R. *ACS Chem Biol* **2013**, *8*, 500.
- (27) Hill, C. M.; Krause, K. M.; Lewis, S. R.; Blais, J.; Benton, B. M.; Mammen, M.; Humphrey, P. P.; Kinana, A.; Janc, J. W. *Antimicrob Agents Chemother* **2010**, *54*, 2814.
- (28) Kwun, M. J.; Hong, H. J. *Antimicrob Agents Chemother* **2014**, *58*, 6306.
- (29) Baptista, M.; Rodrigues, P.; Depardieu, F.; Courvalin, P.; Arthur, M. *Mol Microbiol* **1999**, *32*, 17.
- (30) Reynolds, P. E. *Cell Mol Life Sci* **1998**, *54*, 325.
- (31) Kaplan, J.; Korty, B. D.; Axelsen, P. H.; Loll, P. J. *J Med Chem* **2001**, *44*, 1837.
- (32) Goldman, R. C.; Baizman, E. R.; Longley, C. B.; Branstrom, A. A. *FEMS Microbiol Lett* **2000**, *183*, 209.
- (33) Dong, S. D.; Oberthur, M.; Losey, H. C.; Anderson, J. W.; Eggert, U. S.; Pecuh, M. W.; Walsh, C. T.; Kahne, D. *J Am Chem Soc* **2002**, *124*, 9064.
- (34) Kwun, M. J.; Novotna, G.; Hesketh, A. R.; Hill, L.; Hong, H. J. *Antimicrob Agents Chemother* **2013**, *57*, 4470.
- (35) Arthur, M.; Quintiliani, R., Jr. *Antimicrob Agents Chemother* **2001**, *45*, 375.
- (36) Arthur, M.; Depardieu, F.; Reynolds, P.; Courvalin, P. *Mol Microbiol* **1996**, *21*, 33.

## Chapter 8

# **L,D-transpeptidase Specific Probe Reveals Spatial Organization of Peptidoglycan Crosslinking**

### **8.1 Abstract**

Peptidoglycan (PG) is a crosslinked, mesh-like scaffold endowed with the strength to withstand the internal turgor pressure of bacteria. Crosslinking of peptide chains within PG is an essential process and its disruption thereof underpins the potency of several classes of antibiotics. Two primary crosslinking modes have been identified that are carried out by D,D-transpeptidases and L,D-transpeptidases (Ldts). The nascent PG from each enzymatic class is structurally unique, which results in different crosslinking configurations. Recent advances in PG cellular probes have been powerful in advancing the understanding of D,D-transpeptidation by Penicillin Binding Proteins (PBPs). In contrast, no cellular probes have been previously described to directly interrogate Ldt function in live cells. Herein, we describe a new class of Ldt-specific probes composed of structural analogs of nascent PG, which are metabolically incorporated into the PG scaffold by Ldts. With a panel of tetra- and penta-peptide PG stem mimics, we demonstrated that subtle modifications such as amidation of iso-Glu can control PG crosslinking. Ldt-probes were applied to quantify and track the localization of Ldt activity in *Enterococcus faecium*, *Mycobacterium smegmatis*, and *Mycobacterium tuberculosis*. Most importantly, simultaneous labeling of bacterial cells with D,D- and L,D-specific markers revealed spatial distribution of Ldt and PBP crosslinking across the PG scaffold. These results suggest that Ldt crosslinking may have distinct functions that work in concert with PBP crosslinking to assemble the PG scaffold. We anticipate that unraveling the interplay between Ldts and PBP crosslinking may guide drug regimen and establish new drug targets.

## **8.1 Introduction**

Bacterial cell walls are the frontline in controlling how bacteria interact with their environment (or host organisms) and serve to counter high internal turgor pressure. Peptidoglycan (PG), a primary component of bacterial cell walls, is an essential scaffold that provides physical and mechanical stability to bacterial cells (Figure 8A) <sup>1-3</sup>. Despite the large diversity in bacterial shapes and cell wall configurations, the overall primary PG structure remains relatively constant by having two major structural components. The backbone glycan chain is assembled with disaccharide building blocks that are composed of *N*-acetyl-glucosamine (GlcNAc) and *N*-acetyl muramic acid (MurNAc). A pentapeptide chain (stem peptide) is attached to MurNAc via its *N*-terminus. Although there are variations within the stem peptide sequence between bacteria, the canonical sequence is L-Ala-D-Glx-(L-Lys/*m*-DAP)-D-Ala-D-Ala.

A growing body of evidence points to the fact that PG undergoes extensive chemical remodeling – both in the glycan and peptide segments – in order to refine its chemical and physical properties <sup>4-6</sup>. Modifications include the *N*-glycolylation of muramic acid in the glycan backbone <sup>7</sup>, *O*-acetylation <sup>8,9</sup>, or amidation of D-glutamate and -DAP in the peptide side chain <sup>10</sup>. These modifications are critical for the proper integrity and architecture of the PG scaffold. In addition, PG remodeling can have significant influences on drug sensitivity <sup>11-14</sup>, interaction with PG sensors on cell surfaces <sup>15,16</sup>, and host-microbiota interaction <sup>17-20</sup>. The most prominent chemical change to nascent PG scaffold involves covalent crosslinking of neighboring stem peptides by membrane-anchored transpeptidases. Cell wall crosslinking is essential to bacteria as its inhibition represents a primary mode of action for some of the most potent antibiotics in clinical use. Covalent

PG crosslinks greatly enhance cell wall strength and define the porosity of this scaffold. Crosslinking levels can vary considerably, ranging from 20-90% depending on the organism<sup>21,22</sup>.

The primary function of PG transpeptidation is to generate an amide bond between the sidechain of a stem peptide to the C-terminus of an adjacent stem peptide. Two main classes of enzymes are responsible for PG crosslinking: D,D-transpeptidases and L,D-transpeptidases (Ldts). D,D-transpeptidation reactions are carried out by various Penicillin Binding Proteins (PBPs) and are considered to be the predominant mode of PG crosslinking for several classes of bacteria (Figure 8.1A)<sup>1</sup>. A new class of PG transpeptidases, Ldts, was initially identified in *Enterococcus hirae*<sup>23</sup> but the enzyme itself was first characterized more recently in *Enterococcus faecium*<sup>24,25</sup>. Since its discovery, Ldts have been shown to be operative in a large number of organisms including *Bacillus subtilis*<sup>26</sup>, *Mycobacterium tuberculosis*<sup>27</sup>, *Clostridium difficile*<sup>28</sup>, and *Escherichia coli*<sup>29</sup>.

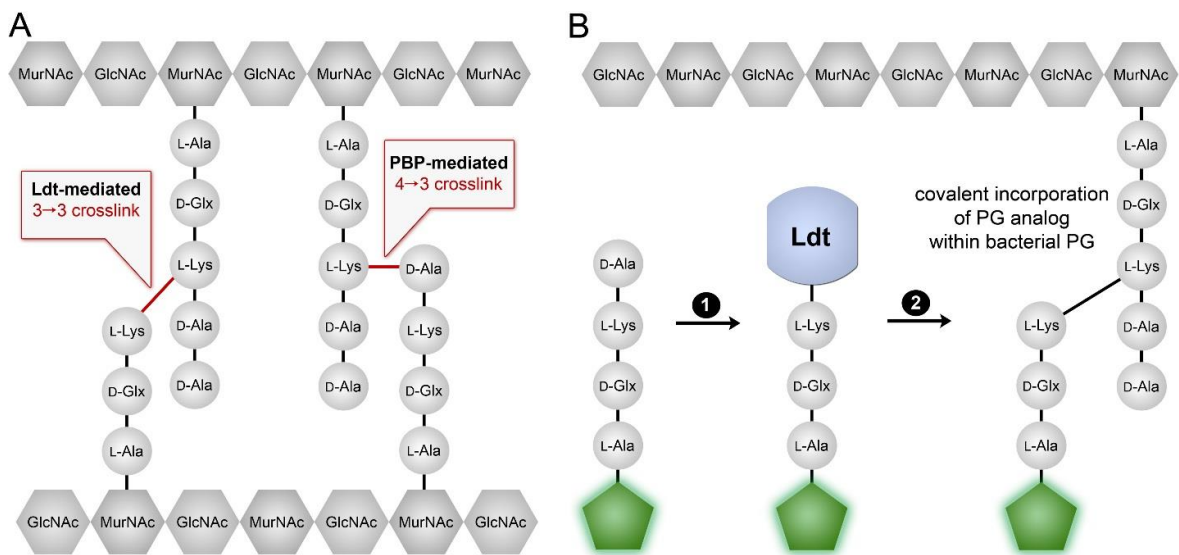


**Figure 8.1** (A) PG crosslinking modes associated with Ldts and PBPs. (B) A synthetic mimic of the stem peptide modified with a fluorescent handle (green hexagon) is covalently incorporated within growing PG scaffold. First, a terminal D-Ala residue is removed by Ltd, leading a covalent intermediate. Second, this acyl-donor is captured by the 3<sup>rd</sup> position amino acid within existing PG thus leading to its crosslinking with PG and generating a measurable fluorescent signal.



There are structurally subtle but functionally important differences between PBP TPs and Ldts. Despite having similar enzymatic functions, the two enzymes have no primary sequence homology. Indeed, Ldts have no similarity to proteins currently in the protein database<sup>14</sup>. PBP TPs crosslink PG stem peptides by first removing terminal D-Ala residues on penta-peptide substrates to form covalent intermediates (Figure 8.2). A neighboring nucleophilic amino group from the 3<sup>rd</sup> position (L-Lys or *m*-DAP, depending on the bacterial class) captures the acyl intermediate to generate a 4-3 crosslink. The main variation between PBPs and Ldts is that Ldts generate 3-3 crosslinks between PG stem peptides because its substrates are tetra-peptides (Figure 8.1B). As the enzyme name implies, Ldts substrates are not terminated as D,D-stereocenters, but instead as L,D-stereocenters<sup>14,25,30</sup>. A majority of bacterial PGs are composed of mostly 4-3 crosslinks, with some organisms having a minor component of 3-3 crosslinks. A prominent exception is mycobacterial PG, which is composed of mostly 3-3 crosslinks<sup>31-34</sup>. In the case of drug-sensitive *E. faecium*, the PG scaffold is composed of mostly 4-3 crosslinks yet both PBPs and Ldts are expressed<sup>35</sup>. Exposure of *E. faecium* to either ampicillin or vancomycin results in a shift to 3-3 crosslinks for two different reasons. In vancomycin resistant enterococci (VRE) cells, vancomycin treatment leads to the truncation of the penta-peptide on lipid II<sup>36-38</sup>. Tetra-peptide is a substrate for Ldts but not PBPs, resulting in higher levels of 3-3 crosslinks. In ampicillin-resistant *E. faecium*, inactivation of PBPs is compensated by shifting crosslinking substrates from penta-peptide to tetra-peptide<sup>25,39</sup>.

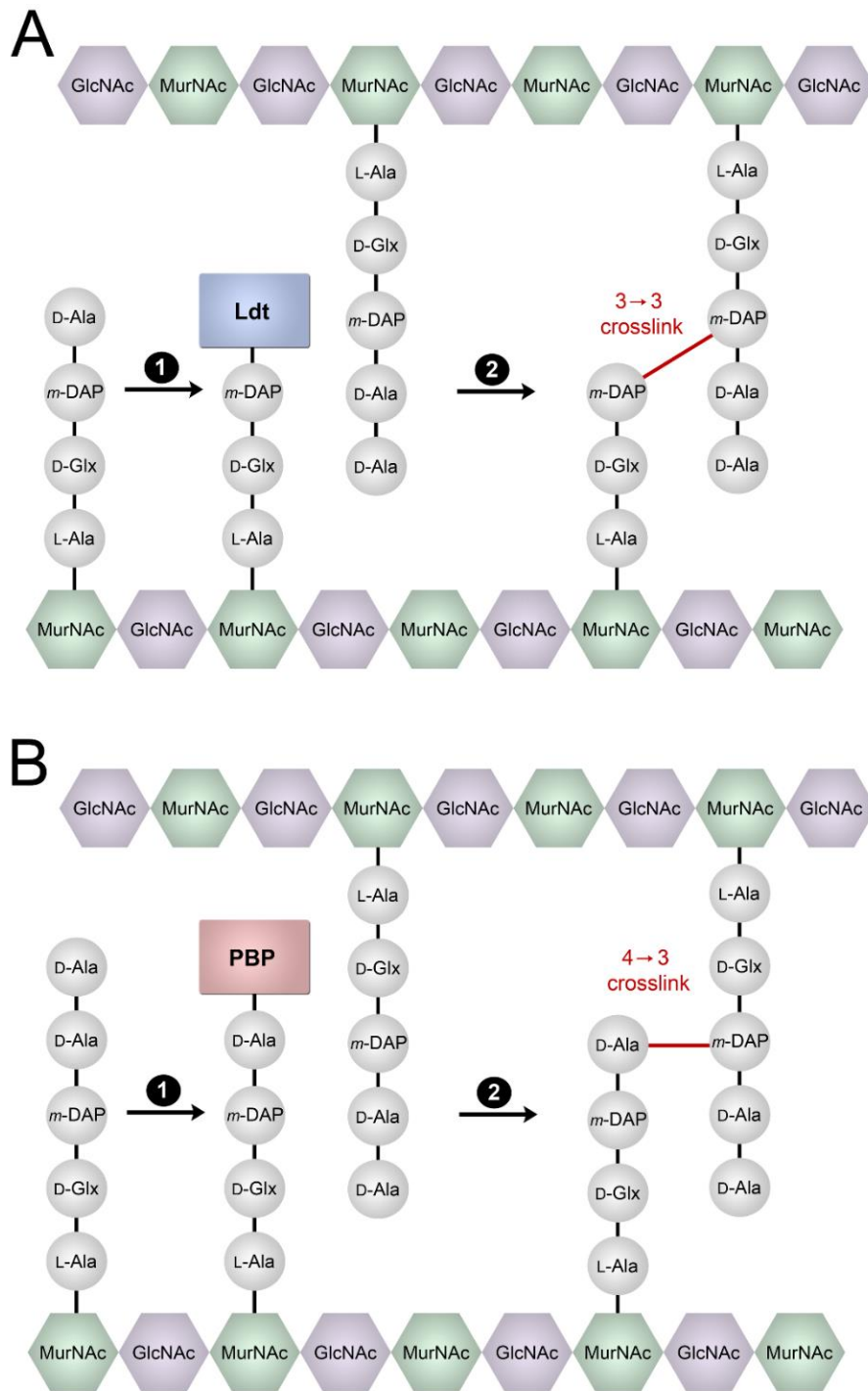


**Figure 8.2** L,D-transpeptidase (Ldt) vs D,D-transpeptidase (DD-TPs) crosslinking reactions (A). A neighboring amino group from the 3<sup>rd</sup> position (ex. *m*-Dap) captures the acyl intermediate created by the tetrapeptide substrate of Ldts to generate a 3-3 crosslink. (B) A neighboring amino group from the 3<sup>rd</sup> position (ex. *m*-Dap) captures the acyl intermediate created by the pentapeptide substrate of DD-TPs to generate a 4-3 crosslink.

PG biosynthesis is initiated in the cytosolic space where a series of enzymatic transformations produce lipid II, a lipid-linked disaccharide penta-peptide precursor<sup>2,30</sup>. Lipid II is then translocated across the cytoplasmic membrane and nascent PG is integrated into the existing cell wall by the combination of transglycosylases and TPs. Both steps are critical for proper PG assembly as evidenced by the fact that disruption of these processes can be lethal to bacterial cells. There are two major classes of PG TPs, namely PBPs TPs and Ldts. Both classes play important roles in the assembly of the PG scaffold, although it is unclear whether they are functionally redundant or assume specialized roles. The emergence of single D-amino acid PG probes has been fundamental in advancing live cell PG fluorescence analysis<sup>40-45</sup>. As examples of these advances, the presence of PG in *Chlamydia trachomatis* was established<sup>46</sup> and treadmilling by FtsZ filaments was shown to drive PG synthesis<sup>47-49</sup>. Prior studies have demonstrated that structural mimicry of nascent PBP substrates result in PG incorporation *in vitro*<sup>50</sup> and in live bacterial cells<sup>51,52</sup>. Also, during the preparation of our manuscript it was shown, *in vitro*, that Ldts mediate crosslinking of synthetic Ldt substrates<sup>53</sup>. In contrast, there are currently no probes to tag and visualize Ldts in live cells. We assembled synthetic substrate of Ldt to specifically interrogate Ldt activity and isolate this crosslinking mode from PBP TPs.

Despite the fundamental importance of PG crosslinking to the growth and division of bacterial cells, key questions remain unanswered about specific processes. These questions include: Are both modes of TP operative at the same time in certain organisms? How are PBP TPs and Ldts organized spatially within a cell? How do structural modifications within the stem peptide control PG crosslinking? Answers to these questions can greatly enhance our current understanding of PG biosynthetic control and dynamics.

Towards these goals, we hypothesized that we can disentangle the two primary modes of cell wall crosslinking in live bacterial cells using synthetic nascent PG analogs. We built mimics of the substrate stem peptides for both PBP TPs and Ldts that could serve as surrogates for the endogenous PG substrate in PG crosslinking, thereby becoming covalently imbedded within the PG scaffold in live bacteria (Figure 8.1B). Structural mimicry of the substrates for both TPs served to reveal patterns of PG crosslinking in live cells that were previously unknown and may be implications of the role that Ldts play in complementing the PG-biosynthetic machinery.

### **8.3 Results and Discussion**

#### **8.3.1 Incorporation of Tetra- and Penta-peptide Probes**

We anticipated that Ldt crosslinking of PG could be quantified by conjugating a fluorescent handle onto the *N*-terminus of the tetra-peptide PG mimic. Treatment of bacterial cells with the fluorescently tagged stem peptides should lead to their covalent incorporation into the expanding PG scaffold during cell growth (Figure 8.2A). Cellular fluorescence is subsequently quantified using flow cytometry and fluorescence levels should correlate with PG crosslinking of synthetic stem peptide mimics. At first, two synthetic stem peptide mimics were synthesized: **TetraFl** and **PentaFl** (Figure 8.2B). Both peptides are structurally similar except for the additional terminal D-Ala in **PentaFl**, which mimics the endogenous substrates of PBP TPs. Drug-sensitive *E. faecium* cells (WT) at low cell densities ( $OD_{600} \sim 0.05$ ) were treated with either **TetraFl** or **PentaFl** and fluorescence levels were measured after 16 h. In the absence of synthetic stem peptides, background cellular fluorescence levels were low (Figure 8.2C). Cellular treatment with **TetraFl** led to a ~210-fold fluorescence increase over background and ~5.5-fold over

**PentaFl**. Higher labeling levels for **TetraFl** relative to **PentaFl** in *E. faecium* (WT) likely reflects either a higher overall catalytic efficiency by Ldts or a greater flexibility by Ldts in tolerating synthetic stem peptide mimics. No apparent effect on cell growth and morphology was observed. These initial results represent the first example of live cell imaging of Ldt activity.

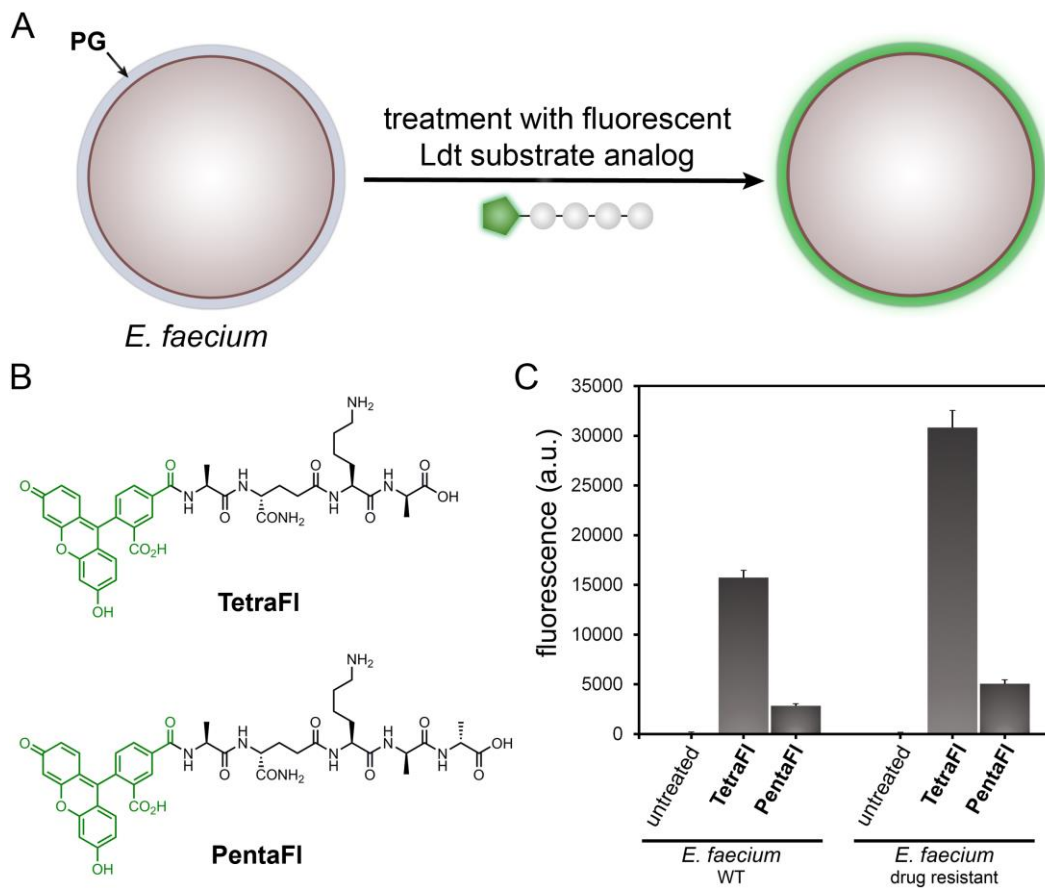


**Figure 8.3** (A) Schematic diagram delineating incorporation of synthesized fluorescent Ldt substrate and incorporation into bacterial PG. (B) Chemical structure of fluorescein-modified tetra-peptide (**TetraFl**) and penta-peptide (**PentaFl**) PG stem mimics. (C) Flow cytometry analysis of *E. faecium* (WT and drug resistant strain) treated overnight with 100 μM **TetraFl** or **PentaFl**. Data are represented as mean + SD (n = 3).

Interestingly, Ldt-mediated labeling was detected despite the expected low (<2 %) abundance of 4-3 crosslinks in drug-sensitive *E. faecium*<sup>25</sup>. In contrast, PG from drug-

resistant *E. faecium* was previously shown to be composed almost entirely of 3-3 crosslinks (99%). The difference in PG composition between drug resistant and drug sensitive *E. faecium* is controlled entirely at the substrate level, not by the expression of Ldts<sup>54</sup>. In fact, Ldt was previously shown to be constitutively expressed in both drug-resistant and -sensitive strains to similar levels<sup>35</sup>. Fluorescence levels were higher for both probes in the drug-resistant strain, which may reflect additional controls in TP crosslinking modalities besides protein expression levels (Figure 8.2C). Similar trends were found for an additional drug-sensitive and drug-resistant strain of *E. faecium* further confirming our general strategy of labeling cell surfaces with Ldt analogs (Figure 8.3).

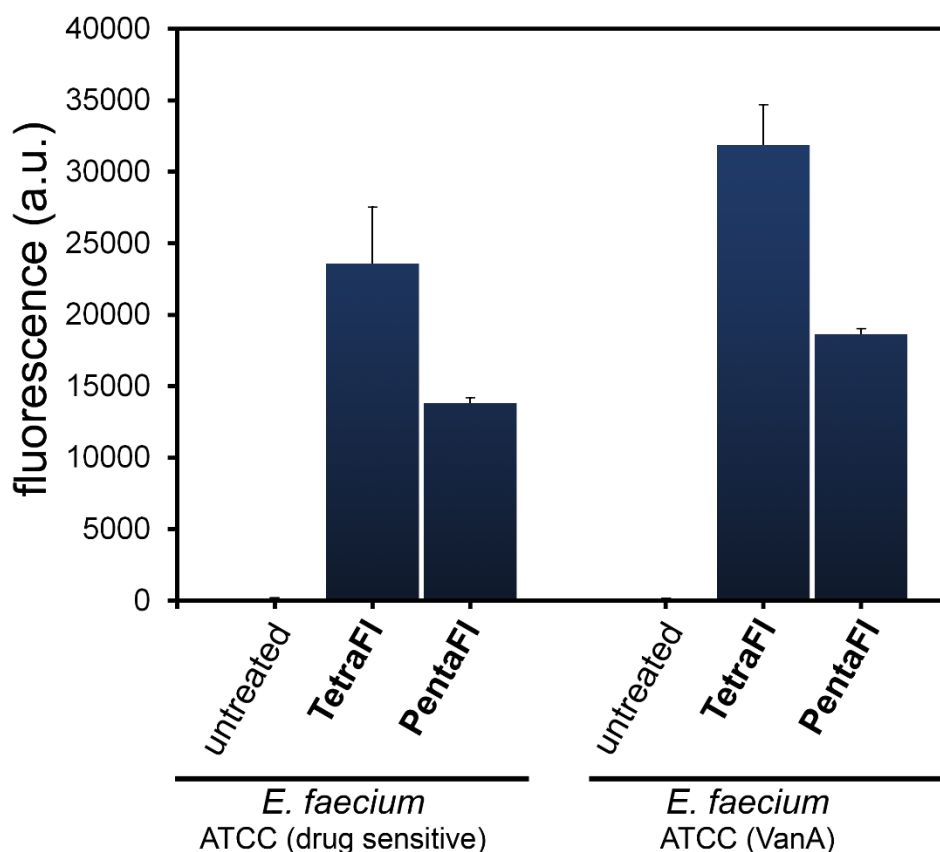


**Figure 8.4** Flow cytometry analysis of additional *E. Faecium* strains ATCC BAA-2317 (VanA) and ATCC BAA-2127 (drug sensitive) incubated overnight with 100  $\mu$ M **TetraFl** or **PentaFl**. Data are represented as mean + SD (n = 3).

### **8.3.2 Structural Variations of Stem Peptide**

Having established the feasibility of labeling cell surfaces with synthetic stem peptide analogs of Ldt substrates, we set out to extensively map how structural variations can impact crosslinking by surface-bound TPs. Variations of the tetra-peptide sequence were installed within four strategic sites: C-terminus (acid/amide), terminal residue(s) (D-Ala/L-Ala), second position (iso-Gln/iso-Glu), and third position (L-Lys/acetylated L-Lys). Each variation was designed to interrogate specific aspects of substrate recognition by TPs. For the tetra-peptide series, the stereospecificity was evaluated first by cell treatment with **TetraFl-2** – a variant that has a terminal L-Ala (Figure 8.4A). Cellular fluorescence levels were reduced to near background levels, thus indicating a strong selection for the correct stereocenter at the terminal Ala position. In **TetraFl-3**, the 3<sup>rd</sup> position Lys residue is acetylated to block any potential acyl-transfer reaction to this nucleophilic site. While there was a ~2.3-fold decrease in fluorescence, labeling levels suggest contribution of the synthetic stem peptide as an acyl-acceptor. The introduction of a carboxylic acid at the second position iso-Glu (**TetraFl-4**), instead of iso-Gln, resulted in a 4.5-fold decrease in surface labeling, a finding that is consistent with recent *in vitro* analysis that showed reduction in crosslinking<sup>53</sup>. Amidation of the C-terminus (**TetraFl-5**) also led to decreased levels of cell surface labeling, which points to a preference for the endogenous carboxylate at the stem peptide terminus.

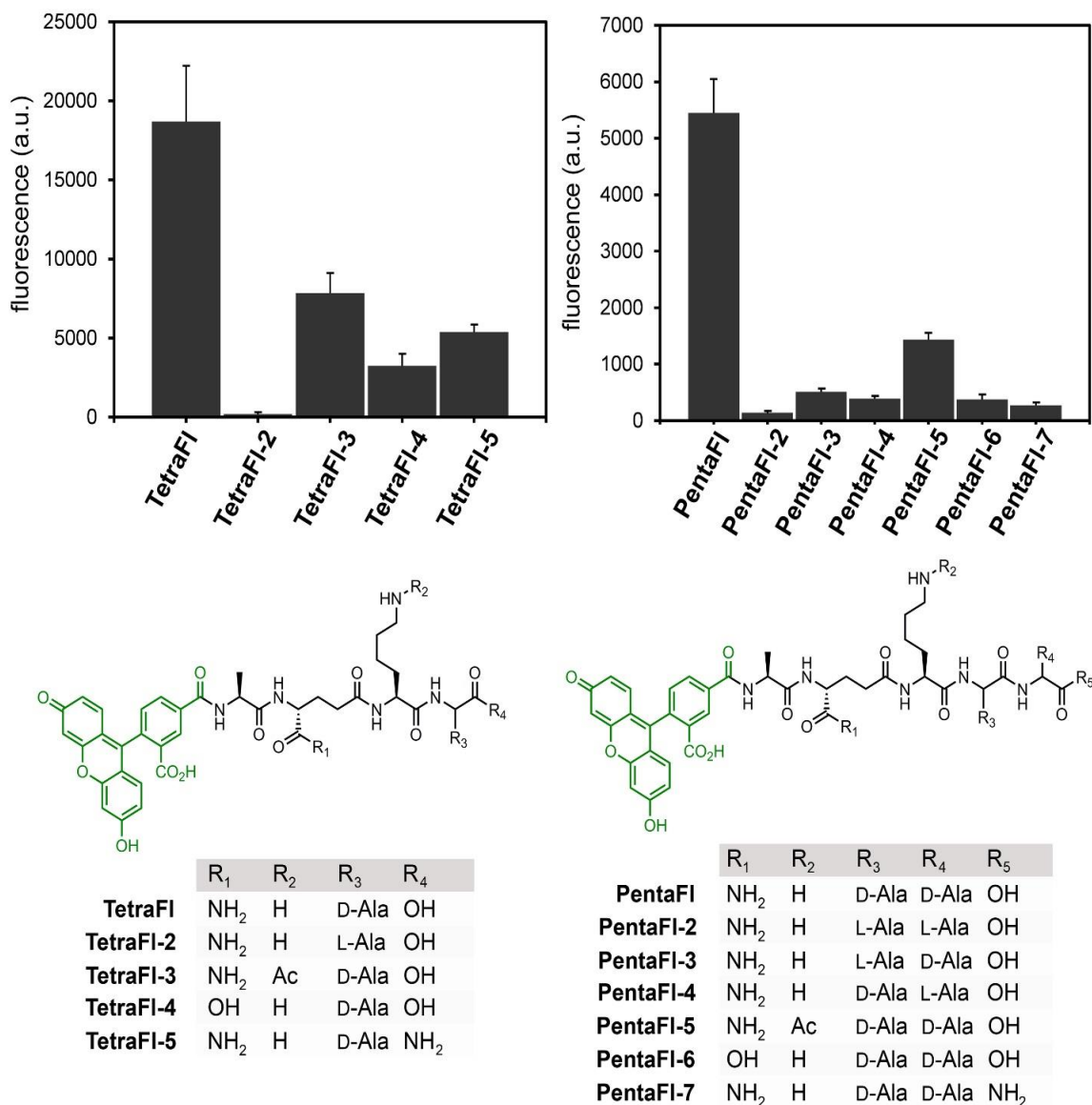


**Figure 8.5** Flow cytometry analysis of *E. faecium* (drug resistant) treated overnight with 100  $\mu$ M of tetra-peptide or penta-peptide with variations. Data are represented as mean + SD (n = 3). Chemical series of tetra-peptides and penta-peptides with variations at the C-terminus (acid/amide), terminal residue(s) (D-Ala/L-Ala), second position (iso-Gln/iso-Glu), and third position (L-Lys/acetylated L-Lys).

A similar panel of stem peptide variants was built for the penta-peptide probes (Figure 8.4B). Overall, the trends were mostly consistent with the tetra-peptide probes including the stereoselectivity at both the fourth and fifth position. It is interesting that these trends are similar despite the lack of structural similarities between PBP TPs and



Ldts. It is worth noting that we were able to recapitulate in *E. faecium* the *in vitro* demonstration that the lack of amidation of iso-Glu results in greatly diminished crosslinking by PBPs from *Enterococcus faecalis*, *Streptococcus pneumoniae*, and *Staphylococcus aureus* (*S. aureus*) (**PentaFI-6**)<sup>31,50,55</sup>. Identical patterns of cellular labeling were observed in a second strain of *E. faecium* across the panels of tetra- and penta-peptide probes (Figure 8.5), thus reconfirming the necessity for amidation at iso-Glu. A recent CRISPRi phenotype screen identified that deletion of the enzymes responsible for the amidation of iso-Glu (MurT/GatD) is lethal, which may reflect the lack of PG crosslinking in the absence of iso-Glu amidation<sup>56</sup>. Together, these results reveal how subtle changes to the stem peptide structure can potentially control PG crosslinking levels in live bacterial cells and confirm that MurT/GatD may be a promising antibiotic target.

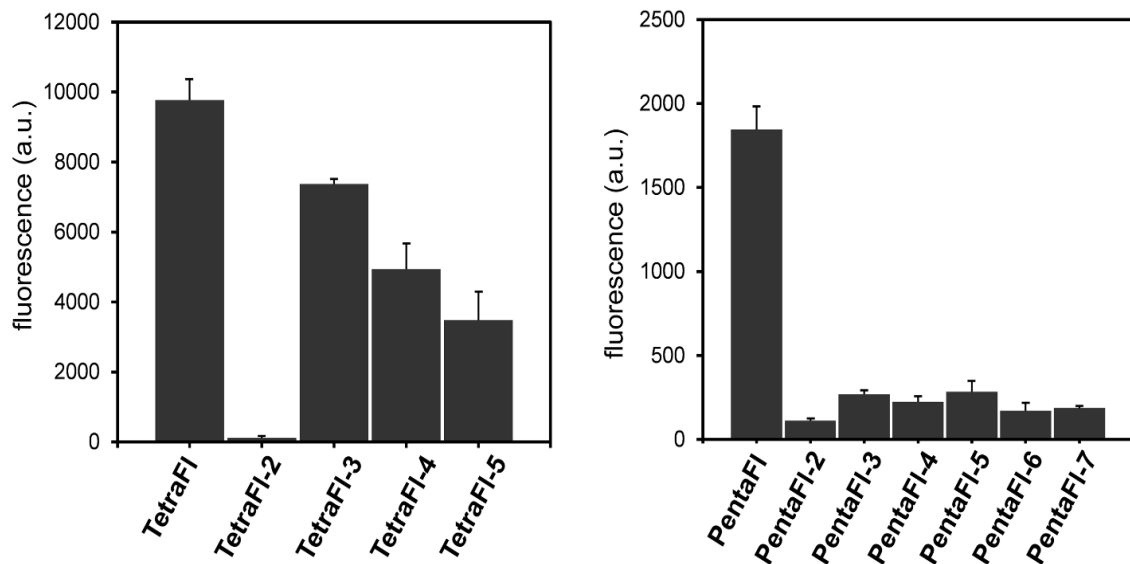


**Figure 8.6** Flow cytometry analysis of *E. Faecium* (D344s) incubated overnight with 100  $\mu$ M tetrapeptide or pentapeptide with variations (see Figure 8.5). Data are represented as mean + SD (n = 3).

### **8.3.3 Antibiotic Effects of Crosslinking**

Next, we set out to evaluate how PG crosslinking modes may be affected by various antibiotics in M9 (a multi-drug resistant strain of *E. faecium*) (Figure 8.6). Initially, we evaluated two  $\beta$ -lactam agents: ampicillin and meropenem. Whereas ampicillin is not known to inhibit Ldts, meropenem (along with other carbapenems) has been shown to inhibit both PBPs and Ldts<sup>57,58</sup>. At low concentrations (0.05  $\mu\text{g/mL}$ ) of meropenem no change in cellular fluorescence was observed. As expected, treatment at higher concentrations (16  $\mu\text{g/mL}$ ) led to reduction in both **TetraFl** and **PentaFl** cell labeling. Despite the reduction in cellular fluorescence to basal fluorescence levels, bacterial cells grew similar to untreated cells (MIC  $\sim$ 18  $\mu\text{g/mL}$ ). Most interestingly, there was a near 2-fold increase in **TetraFl**-labeling upon treatment with 16  $\mu\text{g/mL}$  of ampicillin. A similar trend was also observed in a VanA-resistant *E. faecium* strain. Inclusion of asparagine onto the lysine sidechain of **TetraFl**, which is a closer mimic of *E. faecium* PG, also demonstrated an ampicillin-induction in surface labeling (Figure 8.7). These results suggest that there may be an adaptation response by *E. faecium* cells when challenged with ampicillin. Bacteria are armed with a number of strategies that allow them to respond to potentially toxic agents, which can be the basis for drug-resistant phenotypes<sup>59</sup>. In fact, inducible antibiotic responses have been previously described in enterococci<sup>60-64</sup>.

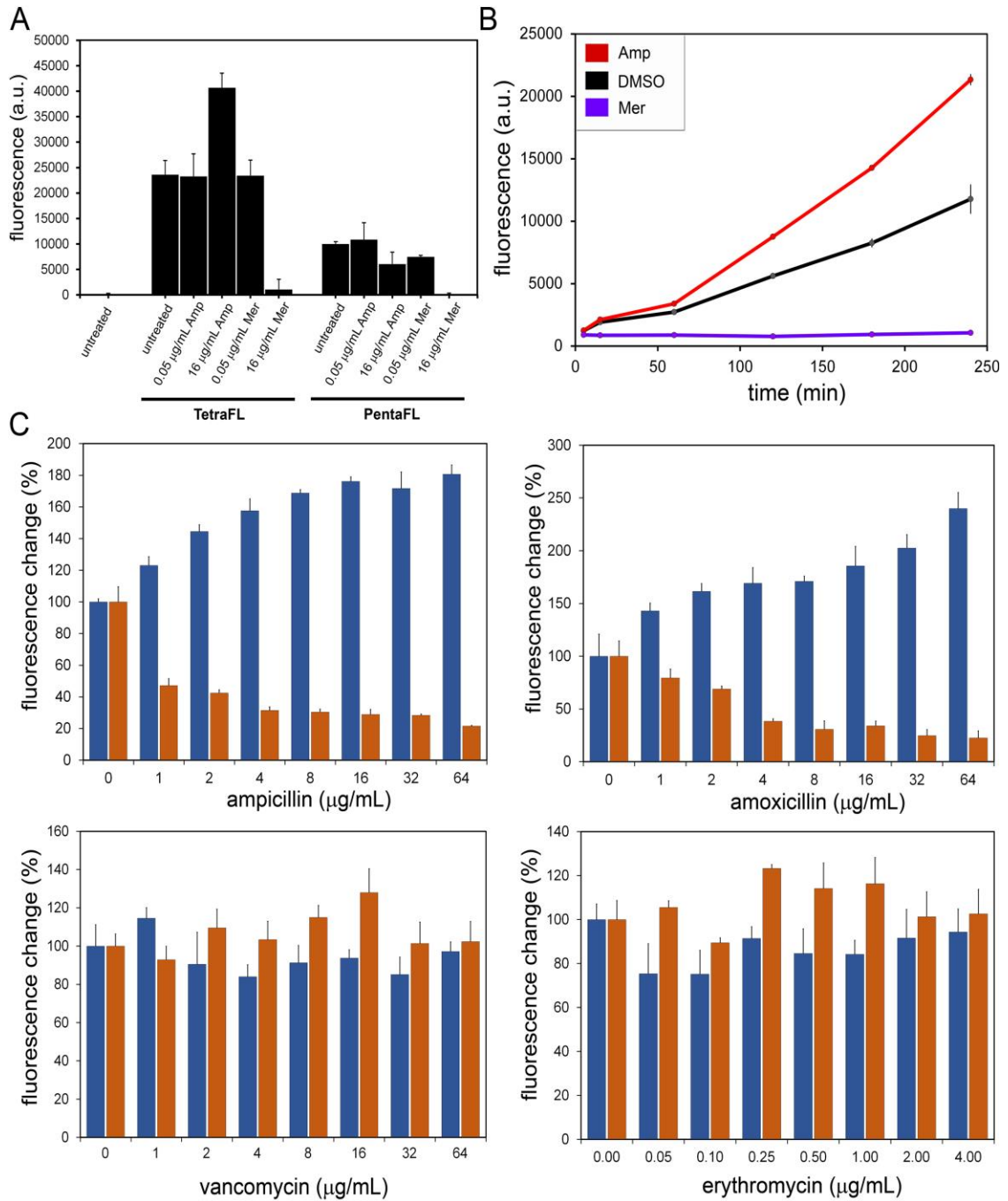


**Figure 8.7** (A) Flow cytometry analysis of *E. faecium* (M9) treated overnight with 100  $\mu$ M TetraFl or PentaFl with or without ampicillin/meropenem. Data are represented as mean + SD (n = 3). (B) *E. faecium* (M9) treated with 100  $\mu$ M TetraFl with 16  $\mu$ g/mL ampicillin, 8  $\mu$ g/mL meropenem, or DMSO at early log phase. Cells were collected at various time points and analyzed by flow cytometry. Data are represented as mean + SD (n = 3). (C) Flow cytometry analysis of *E. faecium* (M9) treated overnight with 100  $\mu$ M TetraFl (blue bars) or PentaFl (orange bars) and increasing concentrations of ampicillin, amoxicillin, vancomycin, or erythromycin. Data are represented as mean + SD (n = 3).

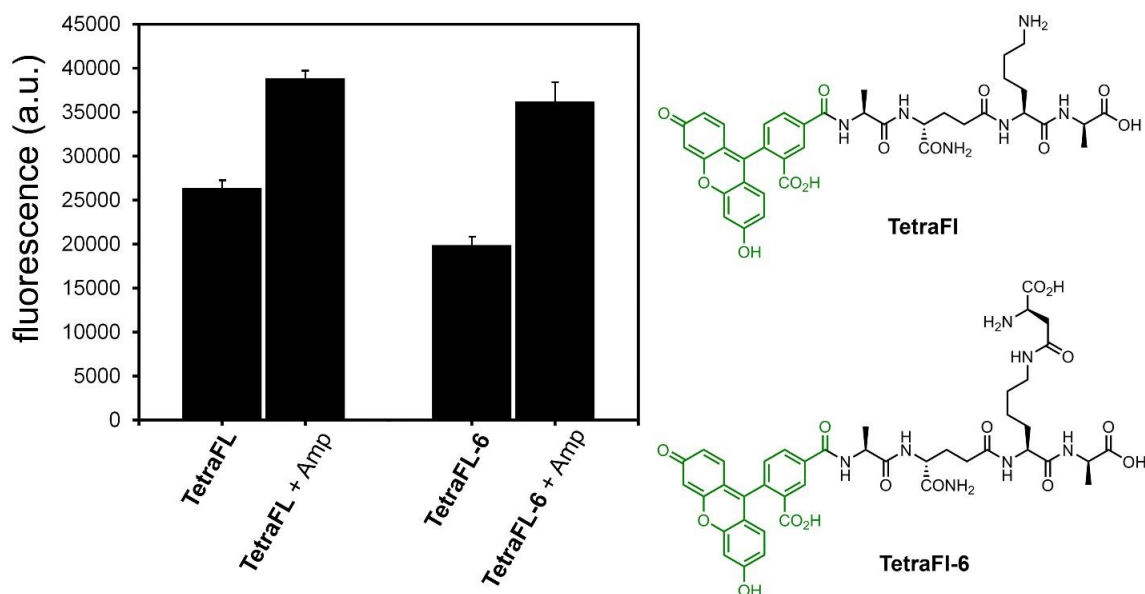


**Figure 8.8** Flow cytometry analysis of *E. Faecium* BAA-2317 (VanA) incubated overnight with 100  $\mu$ M TetraFl or TetraFl-6 with or without 16 mg/mL ampicillin. Data are represented as mean + SD (n = 3).

### 8.3.4 Kinetics of Stem Peptide Probe Incorporation

To gain further insight into the induction of **TetraFl**-labeling, a time-course analysis was performed (Figure 8.6B). *E. faecium* cells from early log ( $OD_{600} \sim 0.05$ ) were treated with ampicillin, meropenem, or DMSO and co-incubated with **TetraFl**. Within 60 minutes, there was a significant difference in fluorescence between DMSO and ampicillin treated cells that became greater over the next three hours. These results suggest that induction of **TetraFl**-labeling was observable through the log phase of growth. Finally, we performed a comprehensive concentration-dependency analysis of both **TetraFl** and **PentaFl** in the presence of eight antibiotics (Figure 8.6C and Figure 8.8). Two agents from the penicillin-class of  $\beta$ -lactams (ampicillin and amoxicillin) yielded similar patterns of response: a concentration-dependent increase in **TetraFl** labeling and decrease in **PentaFl** labeling. Critically, reduction in fluorescence levels of bacteria treated with **PentaFl** suggests that **PentaFl** is not being processed by Ldts. Treatment with two antibiotics that

are not  $\beta$ -lactams (vancomycin and erythromycin) led to no significant change in fluorescence across all sub-MIC concentrations. Moreover, both carbapenems tested (meropenem and imipenem) led to a reduction of both **TetraFl** and **PentaFl** labeling (Figure 8.8). Likewise, there was a decrease upon treatment with a cephalosporin agent (ceftriaxone), which was previously shown to inhibit Ldt *in vitro*<sup>58</sup>, but no change with a monobactam (aztreonam). Together, these results confirm the induction in **TetraFl** labeling and also show the sensitivity of **PentaFl** labeling the majority of  $\beta$ -lactams tested. We are currently investigating possible response elements that may be responsible for the observed increase in **TetraFl** labeling.

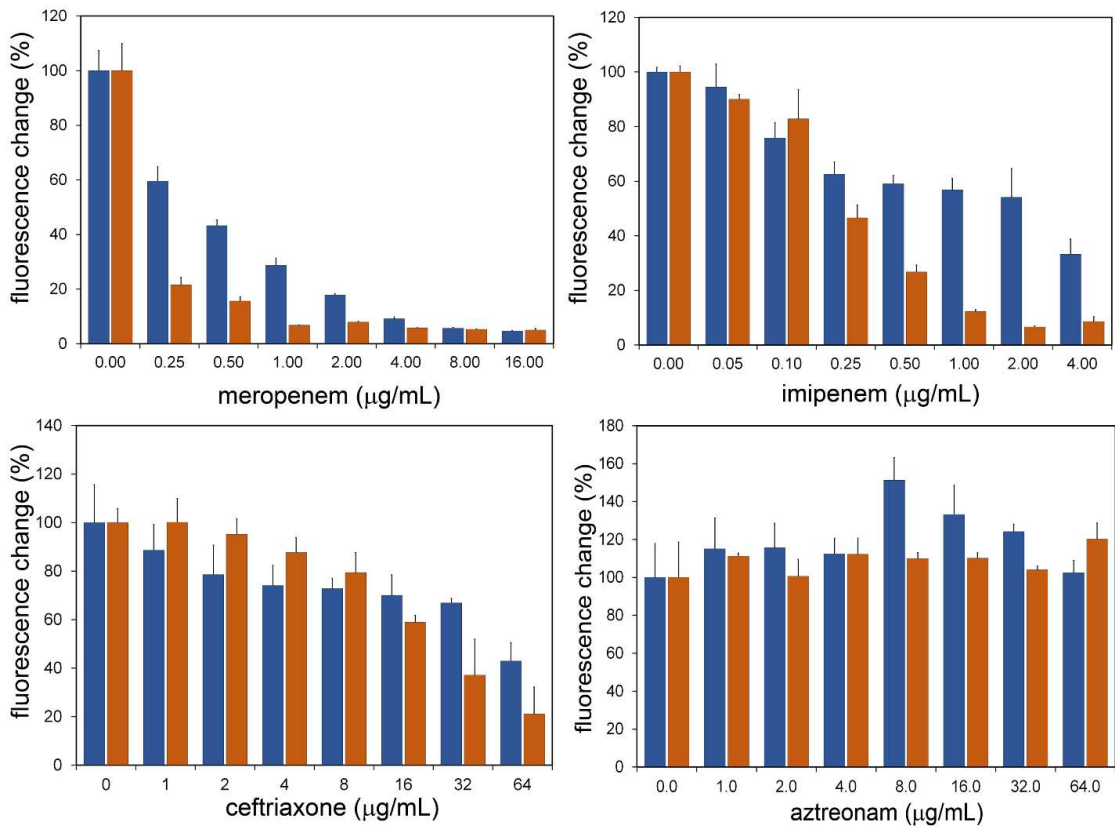


**Figure 8.9** Flow cytometry analysis of *E. faecium* (M9) treated overnight with 100  $\mu$ M **TetraFl** (blue bars) or **PentaFl** (orange bars) and increasing concentrations of meropenem, imipenem, ceftriaxone, or aztreonam. Data are represented as mean + SD (n = 3).

### 8.3.5 Localization of Crosslinking Modes

Localization studies were performed next with the two cellular probes that mimic the substrates of the two primary TPs in bacteria. To differentiate the fluorescence signals between the tetra- and penta-peptide probes, the fluorescent moiety in **TetraFl** was replaced with rhodamine (**TetraRh**). In addition, a single D-amino acid derivative was synthesized that yielded Diethyl-Amino-coumarin-D-Alanine (**DADA**, Figure 8.9). Live cell treatment of bacterial cells with unnatural D-amino acids results in site specific labeling of PG<sup>40,42,44,46,49,65-68</sup>. Similarly, we had also established how relaxed substrate specificity by PG biosynthetic enzymes can be hijacked to install non-native handles onto bacterial cell surfaces<sup>69-78</sup>. Treatment of *E. faecium* cells with unnatural D-amino acids results in the swapping of the terminal D-Ala on the 5<sup>th</sup> position of the penta-peptide, presumably by PBP TPs<sup>79</sup>.

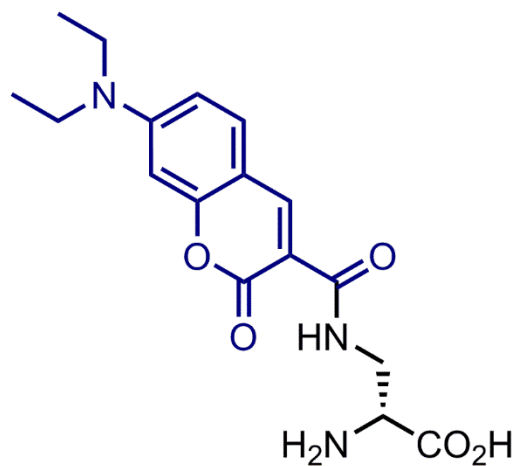


**Figure 8.10** Structure of single D-amino acid derivative Diethyl-Amino-coumarin-D-Alanine (**DADA**).

The goal of this experiment was to establish how PG crosslinking modes are spatially organized within bacterial cells. For these pulse-treatments, all three probes (**TetraRh**, **PentaFl**, and **DADA**) were simultaneously incubated with *E. faecium* cells. Cells from early log phase ( $OD_{600} \sim 0.1$ ) were labeled for 5 minutes and subsequently imaged by confocal microscopy (Figure 8.10A). **PentaFl** and **DADA** labeling were almost exclusively observed at the septal region of cells. **DADA** clearly showed septal and split

equatorial ring labeling<sup>80,81</sup>. Quite strikingly, Ldt activity showed a clear difference in labeling pattern compared to PBP TP activity. **TetraRh** labeling was prominent at the septal region but also evenly distributed throughout the entire cell surface. These results may reflect difference in localization of Ldt activity relative to PBP TP activity in *E. faecium*.

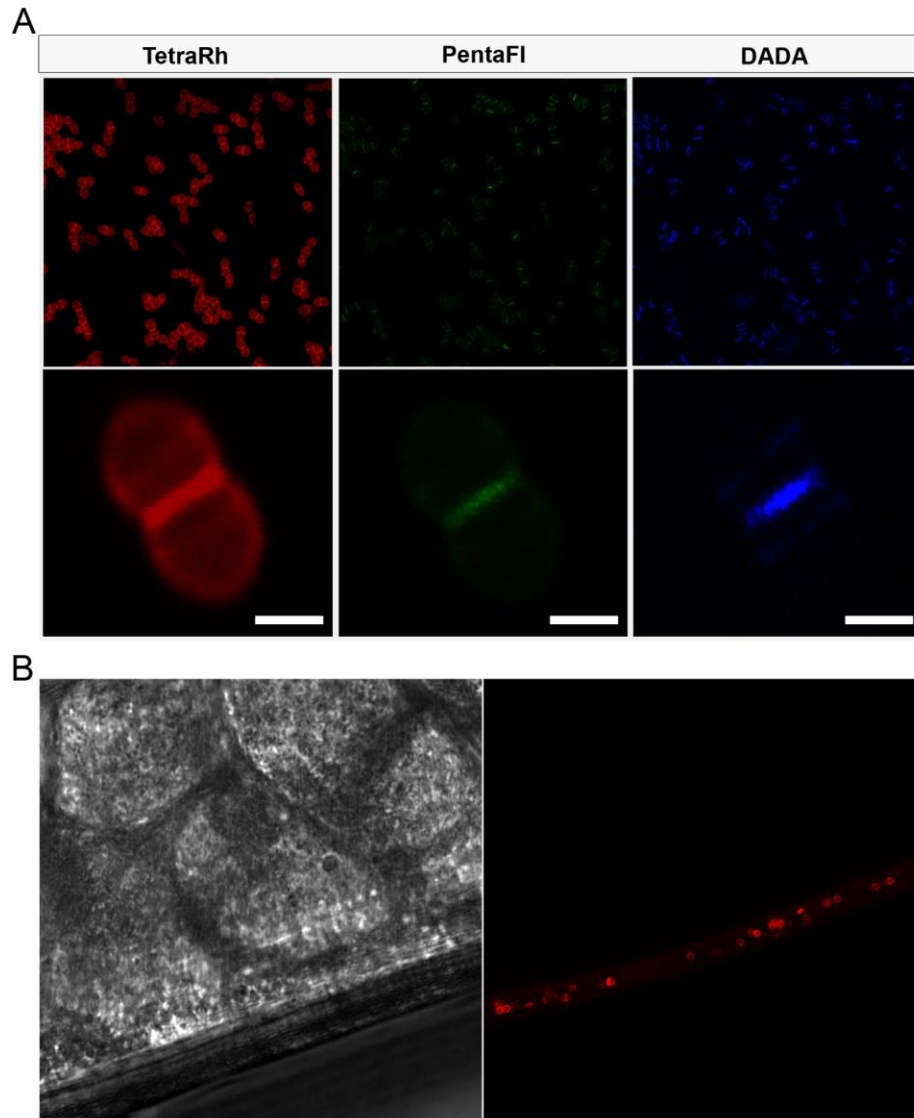


**Figure 8.11** (A) Confocal microscopy image of *E. faecium* (WT) treated with 5-minute pulse of 500  $\mu$ M **TetraRh**, 500  $\mu$ M **PentaFl**, and 5 mM **DADA**. (Scale bar: 1  $\mu$ m). (B) *In vivo* labeling of *E. faecium* in model host. *C. elegans* were infected with *E. faecium* for 4 h, washed to remove noncolonized bacteria, and incubated with 50  $\mu$ M **TetraRh** for 2 h. The *C. elegans* were washed, anesthetized, mounted on a bed of agarose, and imaged using confocal microscopy.

### **8.3.6 In vivo Labeling of Stem Peptide Probes**

PG remodeling can be a potentially advantageous adaptation displayed by pathogens invading their hosting organisms. This concept is exemplified by the finding that PG remodeling in *Vibrio cholera* leads to curvature changes that promote pathogenesis in mice <sup>82</sup>. Likewise, it is reasonable to consider that PG crosslinking by Ldts can alter bacterial virulence. Towards the goal of assessing Ldt activity in living host animals, we investigated whether **TetraRh** can label in *Caenorhabditis elegans* (*C. elegans*). *C. elegans* are powerful model animals for studying bacterial pathogenesis <sup>83-85</sup>. As an example, *C. elegans* were recently used to establish how a PG hydrolase from *E. faecium* can protect *C. elegans* against Salmonella pathogenesis <sup>17</sup>. Moreover, it was previously established that *S. aureus* cells can be metabolically labeled in live *C. elegans* by sortase substrates analogs <sup>86,87</sup>. For our current work, *C. elegans* (~L4 stage) were incubated with *E. faecium* to establish bacterial colonization. After removing non-colonized bacteria, *E. faecium* infected *C. elegans* were incubated with **TetraFl** for 2 h. Following a washing step, *C. elegans* were visualized using confocal microscopy (Figure 8.10B). Remarkably, we were able to specifically label the PG of colonized bacteria in live *C. elegans*. These results may pave the way to establishing how PG crosslinking is controlled by external factors, including a host response to bacterial infection.

### **8.3.7 Mycobacteria Labeling with Stem Peptide Probes**

Having established the ability to track Ldt activity in *E. faecium*, we turned our attention to a different class of pathogens. PG from mycobacteria are surrounded by highly impermeable mycomembranes that endows these organisms with intrinsic resistance to



vast types of antibiotics. PG crosslinking in mycobacteria is unique in that 3-3 crosslinking levels can reach levels close to 80 %. At first, we evaluated the panel of tetra- and penta-peptides for their ability to tag PG of *Mycobacterium smegmatis* (*M. smegmatis*) using similar conditions as *E. faecium* (Figure 8.11A). Remarkably, high labeling levels were observed for both **TetraFl** and **PentaFl**, albeit with lower levels for **PentaFl**. High labeling levels are unusual considering the well-established permeability barrier imposed by the mycomembranes. Transport via an outer membrane pore may explain the high levels of probe penetration past the mycomembrane layer, a feature that we are currently investigating. The specificity of PG labeling was confirmed by the terminal L-Ala control for both **TetraFl** and **PentaFl**. In addition, iso-Glu amidation was also found to be important for PG incorporation as demonstrated by the reduced fluorescence levels in cells treated with **TetraFl-4**. These results confirmed that amidation of the stem peptide by MurT/GatD may play a pivotal role in dictating PG crosslinking levels by Ldts.

We next used Ldt-deletion mutant *M. smegmatis* strains to establish the contribution of Ldts to cell labeling by tetra-peptide probes. Strains of *M. smegmatis* were treated with a subset of three tetra-peptides (**TetraFl**, **TetraFl-2**, and **TetraFl-5**) (Figure 8.11B). A clear reduction in labeling levels was observed in the single Ldt deletion mutant ( $\Delta ldtC$ ) across both **TetraFl** and **TetraFl-5** suggestive of this enzyme being involved in incorporation of Ldt probes. Further deletion of Ldts led to a greater than 5-fold reduction<sup>31</sup>. The retention of cellular labeling in the triple-deletion strain is most likely a result of the three ldt genes encoded in the *M. smegmatis* genome. As expected, treatment with the stereocontrol **TetraFl-2** led to basal cell surface labeling levels across all strains. Together,

these results implicate Ldts as being the primary mode of PG incorporation by tetra-peptide probes.

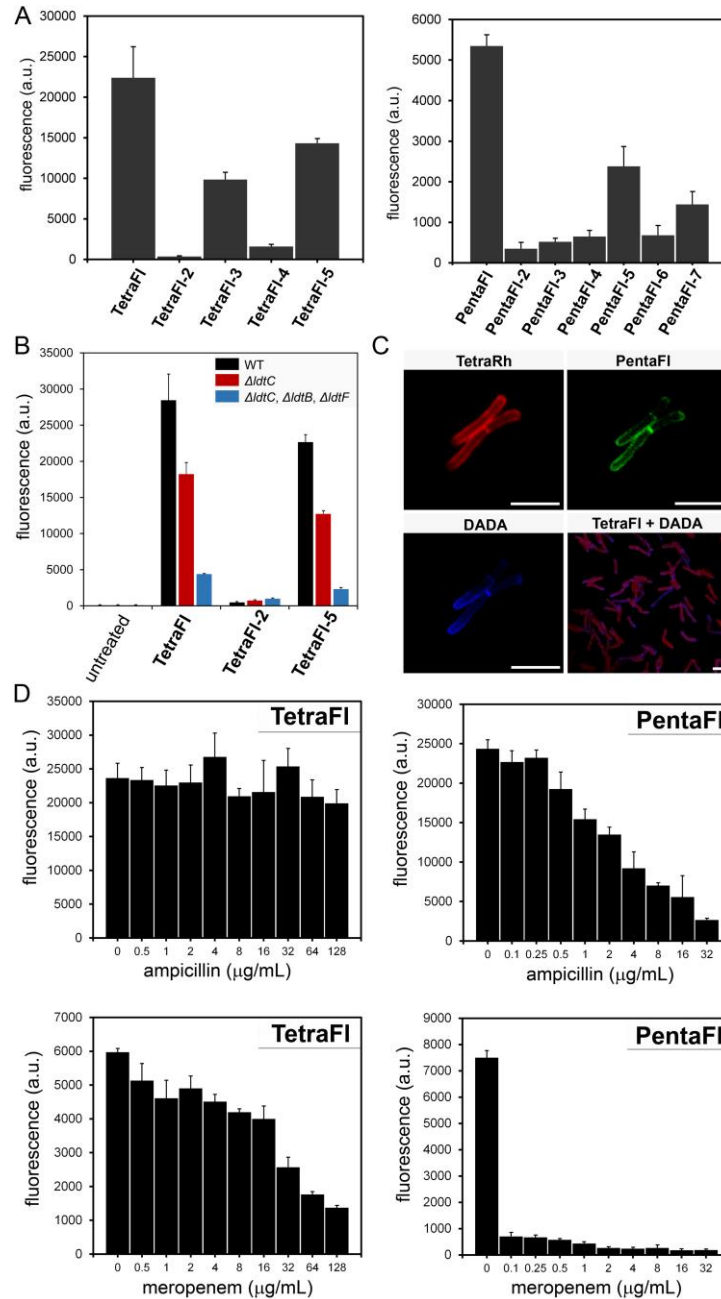


**Figure 8.12** (A) Flow cytometry analysis of *M. smegmatis* (WT) treated overnight with 100  $\mu\text{M}$  tetra-peptide or penta-peptide with variations (see Fig. 3). Data are represented as mean + SD ( $n = 3$ ). (B) Flow cytometry analysis of *M. smegmatis* (WT) and Ldt knockout mutants treated overnight with 100  $\mu\text{M}$  **TetraFI**, **TetraFI-2**, or **TetraFI-5**. Data are represented as mean + SD ( $n = 3$ ). (C) Confocal microscopy image of *M. smegmatis* (WT) treated with 30-minute pulse of 500  $\mu\text{M}$  **TetraRh**, 500  $\mu\text{M}$  **PentaFI**, and 5 mM **DADA**. (Scale bar: 2  $\mu\text{m}$ ) (D) Flow cytometry analysis of

*M. smegmatis* (WT) treated overnight with 100  $\mu$ M **TetraFl** or **PentaFl** with increasing concentrations of ampicillin or meropenem. Data are represented as mean + SD (n = 3).

The localization of PG crosslinking by the two primary TP modes in *M. smegmatis* was visualized using confocal microscopy (Figure 8.11C). Strikingly, clear spatial separation was observed between **TetraRh** and **DADA**. **DADA**-labeling was observed primarily at the pole and **TetraRh**-labeling was extensive throughout the cell sidewalls. Pole labeling observed with **DADA** is similar to single-amino acid probes previously reported for mycobacteria<sup>88</sup>. More specifically, a single pole within a dividing cell was labeled more prominently with **DADA** than the other pole. Co-incubation of *M. smegmatis* cells with both **TetraRh** and **DADA** revealed that primary labeling sites with **DADA** are mostly devoid of **TetraRh** labeling. The interplay between crosslinking modes may have specific roles in dictating cell elongation relative to cell division. It is possible that 4-3 linkages have a more primary role in polar and septal growth, and 3-3 linkages serve to structurally reinforce the wall throughout the entire cell, since the PG is the anchor for the entire mycolyl-arabinogalactan portion of the mycobacterial cell envelope.

The sensitivity of the tetra- and penta-peptide probes against a range of antibiotics was also measured in *M. smegmatis* (Figure 8.11D). In contrast to our observations with *E. faecium*, titration of the  $\beta$ -lactam ampicillin led to no observable change in fluorescence levels for **TetraFl** treated *M. smegmatis* cells. As expected, ampicillin treatment led to a concentration-dependent decrease in fluorescence in *M. smegmatis* incubated with **PentaFl**. Treatment with a carbapenem antibiotic (meropenem) led to reductions in cellular fluorescence in cells treated with either **TetraFl** or **PentaFl**. Together, these results show a lack of response to ampicillin in **TetraFl** labeling of *M. smegmatis* and the inhibition of

TPs results in reduced labeling levels. The role of iso-Glu amidation in the incorporation of PG probes, and hence PG crosslinking, was also confirmed by treatment of *M. smegmatis* cells with **PentaRh** and **PentaRh-6** and visualized by fluorescence microscopy (Figure 8.12). Unmodified iso-Glu in the second position of the stem peptide resulted in background labeling levels. Labeling was shown to be mediated by enzymatic processes as heat-killed *M. smegmatis* cells did not show any labeling in the presence of **PentaRh**.

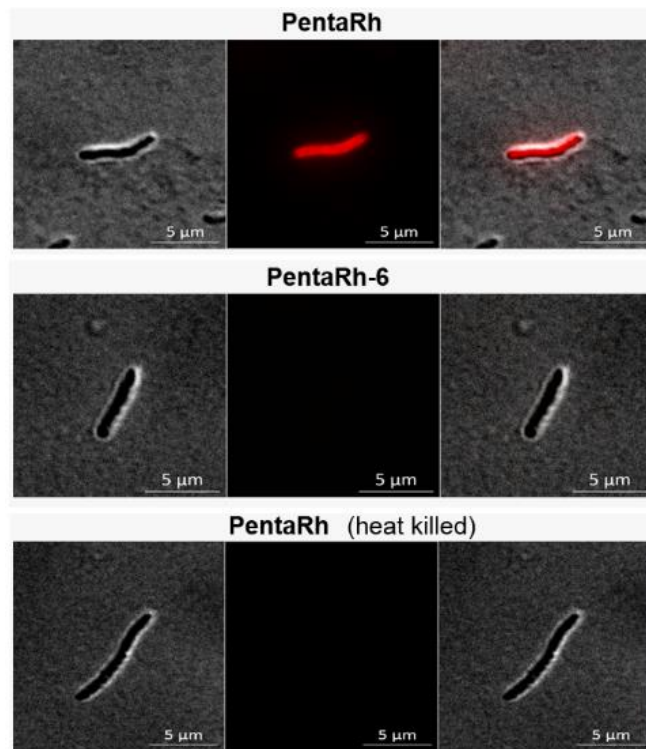


**Figure 8.13** Confocal microscopy image of *M. smegmatis* mc<sup>2</sup>155 treated for 3 h with 50 μM **PentaRh** or **PentaRh-6**. (Scale bar: 5 μm).

Finally, labeling experiments were extended to *M. tuberculosis*, the causative agent of tuberculosis. First, *M. tuberculosis* cells were incubated with **TetraRh** and imaged using confocal microscopy at various times points to analyze the progression of surface labeling (Figure 8.13). Within 30 minutes, there was a unique labeling pattern that was contained within segments of cells. At longer incubation times, there was complete labeling

throughout the sidewalls of most cells analyzed. Interestingly, treatment with sub-lethal concentrations of meropenem resulted in morphological changes that caused bulging of the pole and more accentuated polar labeling (Figure 8.14). As in the case for both *M. smegmatis* and *E. faecium*, two other organisms that express Lts, labeling of *M. tuberculosis* cells with **TetraRh** resulted in higher cellular fluorescence levels than **PentaRh** (Figure 8.15). In addition, it was confirmed that amidation of iso-Glu plays a determinant role in PG crosslinking in *M. tuberculosis* (Figure 8.17).

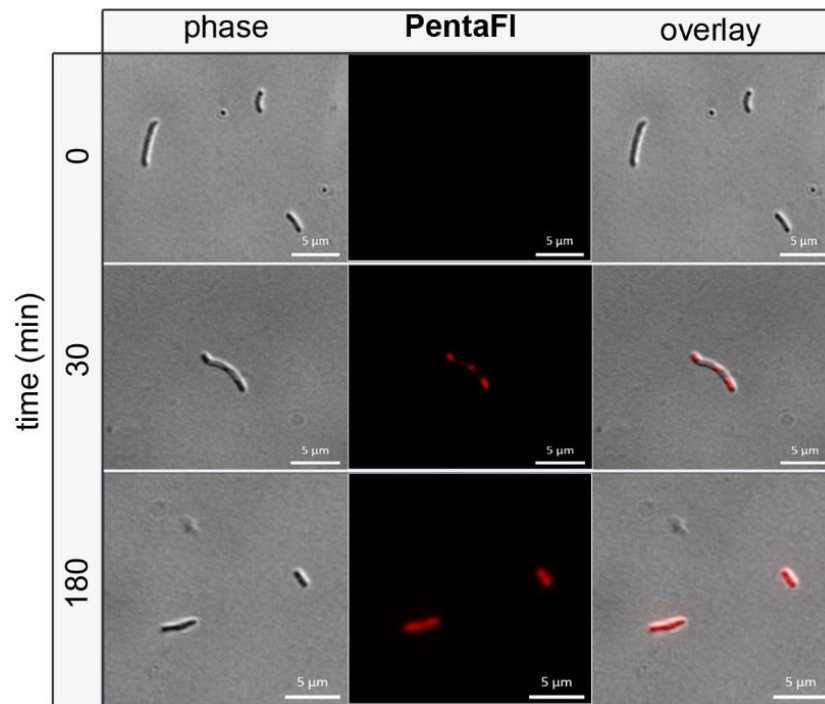


**Figure 8.14** Confocal microscopy image of *M. tuberculosis* treated with 50 μM **TetraRh** for 30 min and 3 h. (Scale bar: 5 μm).

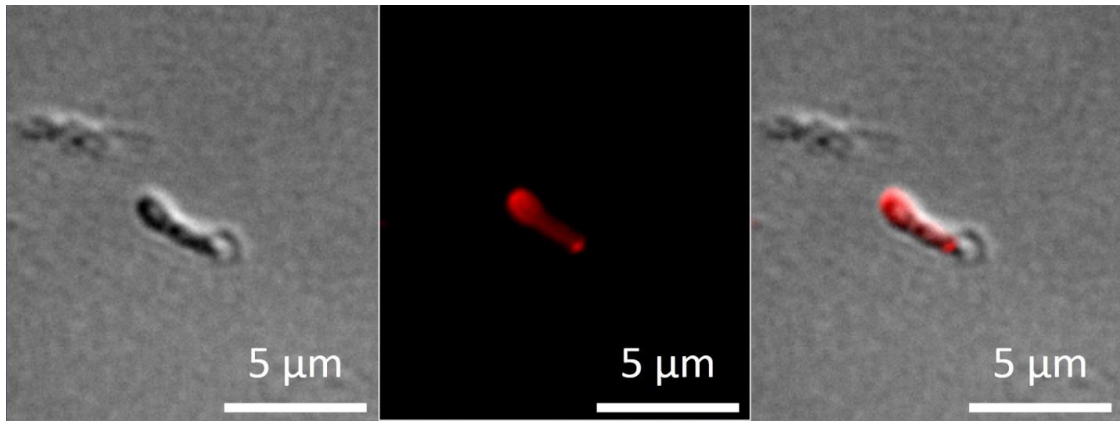


**Figure 8.15** Confocal microscopy image of *M. tuberculosis* H37Rv treated for 24 h with 50  $\mu$ M TetraRh with 100  $\mu$ g/mL meropenem. (Scale bar: 5  $\mu$ m).

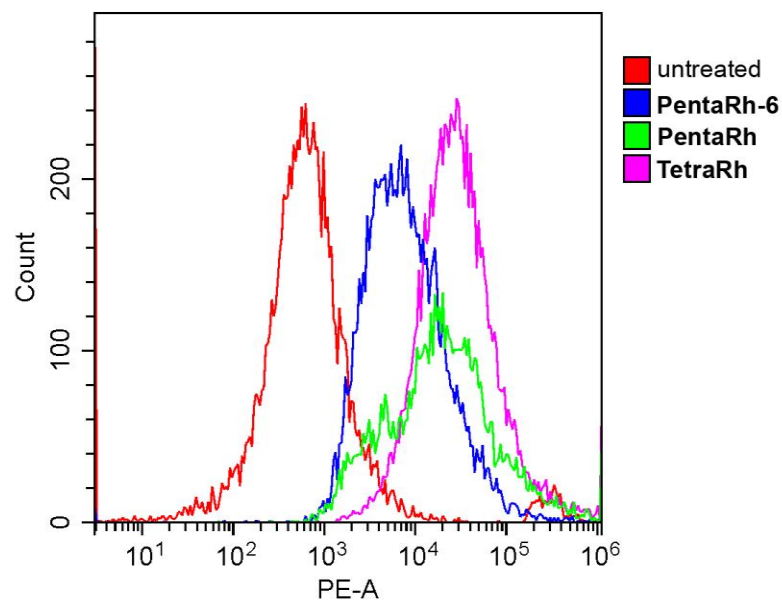


**Figure 8.16** Flow cytometry analysis of *M. tuberculosis* H37Rv treated overnight with 50  $\mu$ M of tetrapeptide or pentapeptide with variations. The Rhodamine signal is indicated on the X-axis as detected by the PE-A channel (excitation/ emission maxima  $\sim$ 546/579).

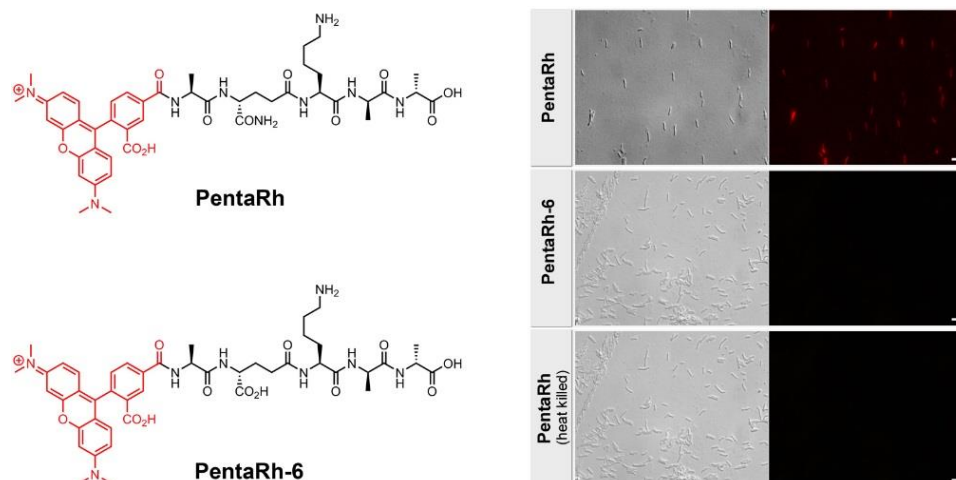


**Figure 8.17** Confocal microscopy image of *M. tuberculosis* treated for 24 h with 50  $\mu$ M **PentaRh** or **PentaRh-6**. (Scale bar: 5  $\mu$ m).

### **8.4 Conclusions**

In conclusion, we have demonstrated for the first time that synthetic tetra-peptide analogs of nascent PG can be incorporated onto PG scaffolds by Ldts in live bacterial cells. The tolerability of *N*-terminal modification on the synthetic stem peptide allowed for a fluorescent handle to quantify Ldt-based PG incorporation and track the delineation of Ldts across cell surfaces in *E. faecium*, *M. smegmatis*, and *M. tuberculosis*. With these cellular probe in hand, we showed how subtle structural modifications to the primary sequence of the stem peptide can control crosslinking efficiency, including recapitulating *in vitro* results related to iso-Glu amidation. These results are the first live cell confirmation that the enzymes responsible for the amidation of iso-Glu (MurT/GatD) may be potential drug targets. Upon evaluating how crosslinking was altered when challenged with antibiotics, an induction in labeling with the tetra- but not the penta-peptide probe was observed. Additional studies are ongoing to understand if this could represent a drug-resistance mechanism that is related to cellular stress.

## **8.5 Materials and Methods**

All peptide related reagents (resin, coupling reagent, deprotection reagent, amino acids, and cleavage reagents) were purchased from ChemImpex. All other reagents were purchased from Sigma and were used without purification. Bacterial strains *Enterococcus faecium* D344s and M9 were grown in BHI for all experiments. *Enterococcus faecium* ATCC BAA-2317 (VanA) and *Enterococcus faecium* ATCC BAA-2127 (drug sensitive) were grown in Trypticase soy broth (TSB). All *Mycobacterium smegmatis* strains were grown in lysogeny broth (LB) containing 0.05% Tween-80 unless noted otherwise.

**Flow cytometry analysis of bacteria labeling with TetraFl or PentaFl.** Brain heart infusion (BHI) broth containing 100  $\mu$ M **TetraFl** or **PentaFl** were prepared. *Enterococcus faecium* WT (D344s) or *Enterococcus faecium* drug-resistant (M9) from an overnight culture were added to the medium (1:100 dilution) and allowed to grow overnight at 37 °C with shaking at 250 rpm. The bacteria were harvested at 6,000g and washed three times with original culture volume of 1x PBS followed by fixation with 2% formaldehyde in 1x PBS for 30 min at ambient temperature. The cells were washed once more to remove formaldehyde and then analyzed using a BDFacs Canto II flow cytometer using a 488nm argon laser (L1) and a 530/30 bandpass filter (FL1). A minimum of 10, 000 events were counted for each data set. The data was analyzed using the FACSDiva version 6.1.1. For *Mycobacterium smegmatis* ATCC 14468, the previous procedure was repeated except using LB (0.05% tween) as the growth media.

**Flow cytometry analysis of *E. Faecium* labeled with tetrapeptide or pentapeptide variations.** Brain heart infusion (BHI) broth containing 100  $\mu$ M of compounds were prepared. *Enterococcus faecium* WT (D344s) or *Enterococcus faecium* drug-resistant (M9)



from an overnight culture were added to the medium (1:100 dilution) and allowed to grow overnight at 37 °C with shaking at 250 rpm. The bacteria were harvested at 6,000g and washed three times with original culture volume of 1x PBS followed by fixation with 2% formaldehyde in 1x PBS for 30 min at ambient temperature. The cells were washed once more to remove formaldehyde and then analyzed using a BDFacs Canto II flow cytometer using the previously stated parameters. For *Mycobacterium smegmatis* ATCC 14468, the previous procedure was repeated except using LB (0.05% tween) as the growth media.

**Flow cytometry analysis of antibiotic treated *E. Faecium* M9 labeled with TetraFl or PentaFl.** Brain heart infusion (BHI) broth containing 100 µM **TetraFl** or **PentaFl** were prepared. To the medium were added antibiotics ampicillin, amoxicillin, meropenem, imipenem, ceftriaxone, aztreonam, vancomycin, or erythromycin at varying sub-mic concentrations. *Enterococcus faecium* (M9) was added to the corresponding medium (1:100 dilution) and allowed to grow overnight at 37 °C with shaking at 250 rpm. The bacteria were harvested at 6,000g and washed three times with original culture volume of 1x PBS followed by fixation with 2% formaldehyde in 1x PBS for 30 min at ambient temperature. The cells were washed once more to remove formaldehyde and then analyzed using a BDFacs Canto II flow cytometer using the previously stated parameters. For *Mycobacterium smegmatis* ATCC 14468, the previous procedure was repeated except using LB (0.05% tween) as the growth media.

**Time course analysis of antibiotic treated *E. Faecium* M9 labeled with TetraFl.** Brain heart infusion (BHI) broth containing 100 µM **TetraFl** was prepared. To the medium were added antibiotics ampicillin (final concentration 16 µg/mL) or meropenem (final concentration 8 µg/mL), or DMSO (final concentration 1%). *Enterococcus faecium* (M9)

was added to the corresponding medium (1:10 dilution) and incubated at 37 °C with shaking at 250 rpm. Samples were collected at various time points, washed three times with 1x PBS, and fixed with 2% formaldehyde in 1x PBS for 30 min at ambient temperature. The cells were washed once more to remove formaldehyde and then analyzed using a BDFacs Canto II flow cytometer using the previously stated parameters.

**Confocal microscopy analysis of *E. faecium* labeled with TetraRh, PentaFl, and DADA.** Brain heart infusion (BHI) broth containing 500 µM **TetraRh**, 500 µM **PentaFl**, and 5 mM **DADA** was prepared. *Enterococcus faecium* (D344s) from an overnight growth was added to the medium (1:10 dilution) and incubated at 37 °C with shaking at 250 rpm for 5 minutes. The bacteria were immediately harvested at 6,000g and washed three times with original culture volume of 1x PBS followed by fixation with 2% formaldehyde in 1x PBS for 30 min at ambient temperature. The cells were washed once more to remove formaldehyde and then analyzed using a Nikon C2 confocal microscope. For *Mycobacterium smegmatis* ATCC 14468 (WT), the previous procedure was repeated except using LB (0.05% tween) as the growth media and a 30 minute incubation.

***In vivo* labeling of *E. Faecium* with TetraRh in live *C. elegans*.** N2 *Caenorhabditis elegans* were maintained by standard protocol using nematode growth agar with bacterial lawns of *E. coli* OP50 (source) on a 60mm x 15mm cell culture dish. *C. elegans* were grown to contain primarily L4 larval stage nematodes by incubation at ambient temperature for ~48-52 h, washed off the plates with M9 buffer, and washed three times with M9 buffer. For washing steps, the *C. elegans* were pelleted at 1000g. The *C. elegans* were resuspended in 400 µL of M9 buffer containing 10% BHI broth and transferred to a sterile 24 multiwell plate. *E. faecium* (100 µL from overnight growth) was washed and added to the 400 µL

suspension of *C. elegans*. The *C. elegans* were incubated at ambient temperature for 4 h, harvested at 1000g and washed three times with M9 buffer to remove bacteria on the outside of the *C. elegans*. The *C. elegans* were then resuspended in 500 µL of M9 buffer containing 10% BHI broth and 50 µM **TetraRh**, and incubated at ambient temperature for 2 h. The *C. elegans* were harvested at 1000g and washed three times with M9 buffer and resuspended in 10mM sodium azide in M9 buffer and analyzed by confocal microscopy.

**Bacterial growth conditions for *M. smegmatis* mc<sup>2</sup>155 and *M. tuberculosis* H37Rv.**

*Mycobacterium smegmatis* mc<sup>2</sup>155 was grown at 37 °C in Middlebrook 7H9 broth supplemented with 0.2% glucose, 0.2% glycerol, 0.085% NaCl and 0.05% Tween80. *M. tuberculosis* H37Rv was grown at 37 °C in Middlebrook 7H9 broth supplemented with 10% OADC. The 7H9 Middlebrook broth cultures were incubated 37 °C with shaking at a 100 rpm. The antibiotics used for media supplementation were at the following concentrations: Meropenem (100 µg/ml) and clavulanate (100 µg/ml) which have sub-lethal effects on mycobacteria.

**Confocal microscopy and Flow cytometry analysis of *M. smegmatis* mc<sup>2</sup>155 and *M. tuberculosis* H37Rv labeled with TetraRh, PentaRh and PentaRh6 probes.**

Five millilitres cultures of *M. smegmatis* mc<sup>2</sup>155 and *M. tuberculosis* H37Rv were grown at 37 °C to an OD<sub>600nm</sub> of 0.8 and 1, respectively, in Middlebrook 7H9 broth. The 5 ml cultures of *M. smegmatis* and *M. tuberculosis* H37Rv were pelleted by centrifugation at 4000 xg for 5 min. The supernatant was discarded and the cells were resuspended in 2.5 ml of Middlebrook 7H9 broth. Four microliters of either the **TetraRh**, **PentaRh** and **PentaRh6** (5 mM) PG probe was added to 396 µl of *M. smegmatis* mc<sup>2</sup>155 and *M. tuberculosis* H37Rv cells (making a 50 µM **TetraRh**, **PentaRh** or **PentaRh6** probe). As controls, Meropenem-

Clavulanate (100 µg/ml) treated - and heat killed - *M. smegmatis* mc<sup>2</sup>155 and *M. tuberculosis* H37Rv were also used for the labeling experiment. Heat killing was performed on a heating block set at 65 °C and inserted into a safety hood for 24 h prior to addition of the PG probes. The *M. smegmatis* and *M. tuberculosis* labelling experiment was performed for 24 h, however, sampling for analysis of probe incorporation was done after 30 min, 3 h, 6 h, 9 h and 24 h of incubation at 37°C. Thereafter, the cells were washed in 1x PBS (500 µl) three times to remove unincorporated probe and the cells were then resuspended in 100 µl of PBS followed by fixation with 2.5% glutaraldehyde for 24 h. The cells were washed three times with 1x PBS (500 µl) to remove the glutaraldehyde and then resuspended in 500 µl 1x PBS. For confocal microscopy, 5 µl of the cells was spotted on glass slides and viewed with the Zeiss Observer Z1 inverted fluorescence microscope under the DS-red channel (excitation/ emission maxima ~546/579) and the images were analyzed with the ZEN lite software (Zeiss). For flow cytometry analysis of incorporation of the different probes, 100 µl of the cells was transferred to a 96 well plate and the Cytoflex flow cytometer (Beckman Coulter) was used for analysis of probe incorporation. The PE-A channel (excitation/ emission maxima ~470/585) was used for detection of the Rhodamine signal (excitation/ emission maxima ~561/578). The gain for the PE-A channel was reduced from 370 to 120.

## **8.6 References**

- (1) Vollmer, W.; Blanot, D.; de Pedro, M. A. *FEMS Microbiol Rev* **2008**, *32*, 149.
- (2) Vollmer, W.; Bertsche, U. *Biochim Biophys Acta* **2008**, *1778*, 1714.
- (3) Typas, A.; Banzhaf, M.; Gross, C. A.; Vollmer, W. *Nat Rev Microbiol* **2011**, *10*, 123.
- (4) Alvarez, L.; Espaillet, A.; Hermoso, J. A.; de Pedro, M. A.; Cava, F. *Microb Drug Resist* **2014**, *20*, 190.
- (5) Lam, H.; Oh, D. C.; Cava, F.; Takacs, C. N.; Clardy, J.; de Pedro, M. A.; Waldor, M. K. *Science* **2009**, *325*, 1552.
- (6) Cava, F.; de Pedro, M. A.; Lam, H.; Davis, B. M.; Waldor, M. K. *EMBO J* **2011**, *30*, 3442.
- (7) Raymond, J. B.; Mahapatra, S.; Crick, D. C.; Pavelka, M. S., Jr. *J Biol Chem* **2005**, *280*, 326.
- (8) Wang, Y.; Lazor, K. M.; DeMeester, K. E.; Liang, H.; Heiss, T. K.; Grimes, C. L. *J Am Chem Soc* **2017**, *139*, 13596.
- (9) Vollmer, W. *FEMS Microbiol Rev* **2008**, *32*, 287.
- (10) Mahapatra, S.; Yagi, T.; Belisle, J. T.; Espinosa, B. J.; Hill, P. J.; McNeil, M. R.; Brennan, P. J.; Crick, D. C. *J Bacteriol* **2005**, *187*, 2747.
- (11) Davis, K. M.; Weiser, J. N. *Infect Immun* **2011**, *79*, 562.
- (12) Chang, J. D.; Foster, E. E.; Wallace, A. G.; Kim, S. J. *Sci Rep* **2017**, *7*, 46500.
- (13) Courvalin, P. *Clin Infect Dis* **2006**, *42 Suppl 1*, S25.
- (14) Mainardi, J. L.; Villet, R.; Bugg, T. D.; Mayer, C.; Arthur, M. *FEMS Microbiol Rev* **2008**, *32*, 386.
- (15) Boudreau, M. A.; Fisher, J. F.; Mobashery, S. *Biochemistry* **2012**, *51*, 2974.
- (16) Shah, I. M.; Laaberki, M. H.; Popham, D. L.; Dworkin, J. *Cell* **2008**, *135*, 486.
- (17) Rangan, K. J.; Pedicord, V. A.; Wang, Y. C.; Kim, B.; Lu, Y.; Shaham, S.; Mucida, D.; Hang, H. C. *Science* **2016**, *353*, 1434.
- (18) Girardin, S. E.; Boneca, I. G.; Viala, J.; Chamaillard, M.; Labigne, A.; Thomas, G.; Philpott, D. J.; Sansonetti, P. J. *J Biol Chem* **2003**, *278*, 8869.
- (19) Girardin, S. E.; Travassos, L. H.; Herve, M.; Blanot, D.; Boneca, I. G.; Philpott, D. J.; Sansonetti, P. J.; Mengin-Lecreulx, D. *J Biol Chem* **2003**, *278*, 41702.
- (20) Wolf, A. J.; Underhill, D. M. *Nat Rev Immunol* **2018**, *18*, 243.
- (21) Sharif, S.; Kim, S. J.; Labischinski, H.; Chen, J.; Schaefer, J. *J Bacteriol* **2013**, *195*, 1421.
- (22) Vollmer, W.; Holtje, J. V. *J Bacteriol* **2004**, *186*, 5978.
- (23) Coyette, J.; Perkins, H. R.; Polacheck, I.; Shockman, G. D.; Ghuyssen, J. M. *Eur J Biochem* **1974**, *44*, 459.
- (24) Lecoq, L.; Dubee, V.; Triboulet, S.; Bougault, C.; Hugonnet, J. E.; Arthur, M.; Simorre, J. P. *ACS Chem Biol* **2013**, *8*, 1140.

- (25) Mainardi, J. L.; Legrand, R.; Arthur, M.; Schoot, B.; van Heijenoort, J.; Gutmann, L. *J Biol Chem* **2000**, *275*, 16490.
- (26) Magnet, S.; Arbeloa, A.; Mainardi, J. L.; Hugonnet, J. E.; Fourgeaud, M.; Dubost, L.; Marie, A.; Delfosse, V.; Mayer, C.; Rice, L. B.; Arthur, M. *J Biol Chem* **2007**, *282*, 13151.
- (27) Lavollay, M.; Arthur, M.; Fourgeaud, M.; Dubost, L.; Marie, A.; Veziris, N.; Blanot, D.; Gutmann, L.; Mainardi, J. L. *J Bacteriol* **2008**, *190*, 4360.
- (28) Peltier, J.; Courtin, P.; El Meouche, I.; Lemeë, L.; Chapot-Chartier, M. P.; Pons, J. L. *J Biol Chem* **2011**, *286*, 29053.
- (29) Magnet, S.; Dubost, L.; Marie, A.; Arthur, M.; Gutmann, L. *J Bacteriol* **2008**, *190*, 4782.
- (30) Pavelka, M. S., Jr.; Mahapatra, S.; Crick, D. C. *Microbiol Spectr* **2014**, *2*, MGM2.
- (31) Squeglia, F.; Ruggiero, A.; Berisio, R. *Chemistry* **2018**, *24*, 2533.
- (32) Kieser, K. J.; Baranowski, C.; Chao, M. C.; Long, J. E.; Sassetti, C. M.; Waldor, M. K.; Sacchettini, J. C.; Ioerger, T. R.; Rubin, E. J. *Proc Natl Acad Sci U S A* **2015**, *112*, 13087.
- (33) Gupta, R.; Lavollay, M.; Mainardi, J. L.; Arthur, M.; Bishai, W. R.; Lamichhane, G. *Nat Med* **2010**, *16*, 466.
- (34) Sanders, A. N.; Wright, L. F.; Pavelka, M. S., Jr. *Microbiology* **2014**, *160*, 1795.
- (35) Sacco, E.; Hugonnet, J. E.; Josseaume, N.; Cremniter, J.; Dubost, L.; Marie, A.; Patin, D.; Blanot, D.; Rice, L. B.; Mainardi, J. L.; Arthur, M. *Mol Microbiol* **2010**, *75*, 874.
- (36) de Jonge, B. L.; Handwerger, S.; Gage, D. *Antimicrob Agents Chemother* **1996**, *40*, 863.
- (37) Arthur, M.; Depardieu, F.; Snaith, H. A.; Reynolds, P. E.; Courvalin, P. *Antimicrob Agents Chemother* **1994**, *38*, 1899.
- (38) Gutmann, L.; Billot-Klein, D.; al-Obeid, S.; Klare, I.; Francoual, S.; Collatz, E.; van Heijenoort, J. *Antimicrob Agents Chemother* **1992**, *36*, 77.
- (39) Sacco, E.; Cortes, M.; Josseaume, N.; Rice, L. B.; Mainardi, J. L.; Arthur, M. *MBio* **2014**, *5*, e01446.
- (40) Kuru, E.; Hughes, H. V.; Brown, P. J.; Hall, E.; Tekkam, S.; Cava, F.; de Pedro, M. A.; Brun, Y. V.; VanNieuwenhze, M. S. *Angew Chem Int Ed Engl* **2012**, *51*, 12519.
- (41) Kuru, E.; Tekkam, S.; Hall, E.; Brun, Y. V.; Van Nieuwenhze, M. S. *Nat Protoc* **2015**, *10*, 33.
- (42) Siegrist, M. S.; Whiteside, S.; Jewett, J. C.; Aditham, A.; Cava, F.; Bertozzi, C. R. *ACS Chem Biol* **2013**, *8*, 500.
- (43) Siegrist, M. S.; Swarts, B. M.; Fox, D. M.; Lim, S. A.; Bertozzi, C. R. *FEMS Microbiol Rev* **2015**, *39*, 184.
- (44) Lebar, M. D.; May, J. M.; Meeske, A. J.; Leiman, S. A.; Lupoli, T. J.; Tsukamoto, H.; Losick, R.; Rudner, D. Z.; Walker, S.; Kahne, D. *J Am Chem Soc* **2014**, *136*, 10874.
- (45) Lupoli, T. J.; Tsukamoto, H.; Doud, E. H.; Wang, T. S.; Walker, S.; Kahne, D. *J Am Chem Soc* **2011**, *133*, 10748.

- (46) Liechti, G. W.; Kuru, E.; Hall, E.; Kalinda, A.; Brun, Y. V.; VanNieuwenhze, M.; Maurelli, A. T. *Nature* **2014**, *506*, 507.
- (47) Monteiro, J. M.; Pereira, A. R.; Reichmann, N. T.; Saraiva, B. M.; Fernandes, P. B.; Veiga, H.; Tavares, A. C.; Santos, M.; Ferreira, M. T.; Macario, V.; VanNieuwenhze, M. S.; Filipe, S. R.; Pinho, M. G. *Nature* **2018**, *554*, 528.
- (48) Yang, X.; Lyu, Z.; Miguel, A.; McQuillen, R.; Huang, K. C.; Xiao, J. *Science* **2017**, *355*, 744.
- (49) Bisson-Filho, A. W.; Hsu, Y. P.; Squyres, G. R.; Kuru, E.; Wu, F.; Jukes, C.; Sun, Y.; Dekker, C.; Holden, S.; VanNieuwenhze, M. S.; Brun, Y. V.; Garner, E. C. *Science* **2017**, *355*, 739.
- (50) Welsh, M. A.; Taguchi, A.; Schaefer, K.; Van Tyne, D.; Lebreton, F.; Gilmore, M. S.; Kahne, D.; Walker, S. *J Am Chem Soc* **2017**, *139*, 17727.
- (51) Gautam, S.; Kim, T.; Shoda, T.; Sen, S.; Deep, D.; Luthra, R.; Ferreira, M. T.; Pinho, M. G.; Spiegel, D. A. *Angew Chem Int Ed Engl* **2015**, *54*, 10492.
- (52) Gautam, S.; Kim, T.; Spiegel, D. A. *J Am Chem Soc* **2015**, *137*, 7441.
- (53) Ngadjeua, F.; Braud, E.; Saidjalolov, S.; Iannazzo, L.; Schnappinger, D.; Ehrt, S.; Hugonnet, J. E.; Mengin-Lecreulx, D.; Patin, D.; Etheve-Quellejeu, M.; Fonvielle, M.; Arthur, M. *Chemistry* **2018**.
- (54) Mainardi, J. L.; Morel, V.; Fourgeaud, M.; Cremniter, J.; Blanot, D.; Legrand, R.; Frehel, C.; Arthur, M.; Van Heijenoort, J.; Gutmann, L. *J Biol Chem* **2002**, *277*, 35801.
- (55) Zapun, A.; Philippe, J.; Abrahams, K. A.; Signor, L.; Roper, D. I.; Breukink, E.; Vernet, T. *ACS Chem Biol* **2013**, *8*, 2688.
- (56) Liu, X.; Gallay, C.; Kjos, M.; Domenech, A.; Slager, J.; van Kessel, S. P.; Knoops, K.; Sorg, R. A.; Zhang, J. R.; Veening, J. W. *Mol Syst Biol* **2017**, *13*, 931.
- (57) Dubee, V.; Arthur, M.; Fief, H.; Triboulet, S.; Mainardi, J. L.; Gutmann, L.; Sollogoub, M.; Rice, L. B.; Etheve-Quellejeu, M.; Hugonnet, J. E. *Antimicrob Agents Chemother* **2012**, *56*, 3409.
- (58) Mainardi, J. L.; Hugonnet, J. E.; Rusconi, F.; Fourgeaud, M.; Dubost, L.; Moumi, A. N.; Delfosse, V.; Mayer, C.; Gutmann, L.; Rice, L. B.; Arthur, M. *J Biol Chem* **2007**, *282*, 30414.
- (59) Blair, J. M.; Webber, M. A.; Baylay, A. J.; Ogbolu, D. O.; Piddock, L. J. *Nat Rev Microbiol* **2015**, *13*, 42.
- (60) Miller, W. R.; Munita, J. M.; Arias, C. A. *Expert Rev Anti Infect Ther* **2014**, *12*, 1221.
- (61) Foucault, M. L.; Depardieu, F.; Courvalin, P.; Grillot-Courvalin, C. *Proc Natl Acad Sci U S A* **2010**, *107*, 16964.
- (62) Muller, C.; Massier, S.; Le Breton, Y.; Rince, A. *Mol Microbiol* **2018**, *107*, 416.
- (63) Kellogg, S. L.; Little, J. L.; Hoff, J. S.; Kristich, C. J. *Antimicrob Agents Chemother* **2017**, *61*.
- (64) Desbonnet, C.; Tait-Kamradt, A.; Garcia-Solache, M.; Dunman, P.; Coleman, J.; Arthur, M.; Rice, L. B. *MBio* **2016**, *7*, e02188.

- (65) Pilhofer, M.; Aistleitner, K.; Biboy, J.; Gray, J.; Kuru, E.; Hall, E.; Brun, Y. V.; VanNieuwenhze, M. S.; Vollmer, W.; Horn, M.; Jensen, G. J. *Nat Commun* **2013**, *4*, 2856.
- (66) Fleurie, A.; Lesterlin, C.; Manuse, S.; Zhao, C.; Cluzel, C.; Lavergne, J. P.; Franz-Wachtel, M.; Macek, B.; Combet, C.; Kuru, E.; VanNieuwenhze, M. S.; Brun, Y. V.; Sherratt, D.; Grangeasse, C. *Nature* **2014**, *516*, 259.
- (67) Faure, L. M.; Fiche, J. B.; Espinosa, L.; Ducret, A.; Anantharaman, V.; Luciano, J.; Lhospice, S.; Islam, S. T.; Treguier, J.; Sotes, M.; Kuru, E.; Van Nieuwenhze, M. S.; Brun, Y. V.; Theodoly, O.; Aravind, L.; Nollmann, M.; Mignot, T. *Nature* **2016**, *539*, 530.
- (68) Qiao, Y.; Lebar, M. D.; Schirner, K.; Schaefer, K.; Tsukamoto, H.; Kahne, D.; Walker, S. *J Am Chem Soc* **2014**, *136*, 14678.
- (69) Pires, M. M.; Pidgeon, S. E. *Angew Chem Int Ed Engl* **2017**.
- (70) Fura, J. M.; Pidgeon, S. E.; Birabaharan, M.; Pires, M. M. *ACS Infect Dis* **2016**, *2*, 302.
- (71) Sarkar, S.; Libby, E. A.; Pidgeon, S. E.; Dworkin, J.; Pires, M. M. *Angew Chem Int Ed Engl* **2016**, *55*, 8401.
- (72) Pidgeon, S. E.; Fura, J. M.; Leon, W.; Birabaharan, M.; Vezenov, D.; Pires, M. M. *Angew Chem Int Ed Engl* **2015**, *54*, 6158.
- (73) Sarkar, S.; Pires, M. M. *PLoS One* **2015**, *10*, e0117613.
- (74) Fura, J. M.; Sabulski, M. J.; Pires, M. M. *ACS Chem Biol* **2014**, *9*, 1480.
- (75) Pidgeon, S. E.; Pires, M. M. *ACS Chem Biol* **2017**.
- (76) Fura, J. M.; Kearns, D.; Pires, M. M. *J Biol Chem* **2015**, *290*, 30540.
- (77) Pidgeon, S. E.; Pires, M. M. *ACS Chem Biol* **2017**, *12*, 1913.
- (78) Pidgeon, S. E.; Pires, M. M. *Angew Chem Int Ed Engl* **2017**, *56*, 8839.
- (79) van der Aart, L. T.; Lemmens, N.; van Wamel, W. J.; van Wezel, G. P. *Antimicrob Agents Chemother* **2016**, *60*, 4930.
- (80) Wheeler, R.; Mesnage, S.; Boneca, I. G.; Hobbs, J. K.; Foster, S. J. *Mol Microbiol* **2011**, *82*, 1096.
- (81) Zapun, A.; Vernet, T.; Pinho, M. G. *FEMS Microbiol Rev* **2008**, *32*, 345.
- (82) Bartlett, T. M.; Bratton, B. P.; Duvshani, A.; Miguel, A.; Sheng, Y.; Martin, N. R.; Nguyen, J. P.; Persat, A.; Desmarais, S. M.; VanNieuwenhze, M. S.; Huang, K. C.; Zhu, J.; Shaevitz, J. W.; Gitai, Z. *Cell* **2017**, *168*, 172.
- (83) Garcia-Lara, J.; Needham, A. J.; Foster, S. J. *FEMS Immunol Med Microbiol* **2005**, *43*, 311.
- (84) Sifri, C. D.; Begun, J.; Ausubel, F. M.; Calderwood, S. B. *Infect Immun* **2003**, *71*, 2208.
- (85) Garsin, D. A.; Villanueva, J. M.; Begun, J.; Kim, D. H.; Sifri, C. D.; Calderwood, S. B.; Ruvkun, G.; Ausubel, F. M. *Science* **2003**, *300*, 1921.
- (86) Pidgeon, S. E.; Pires, M. M. *Bioconjug Chem* **2017**, *28*, 2310.



(87) Sabulski, M. J.; Pidgeon, S. E.; Pires, M. M. *Chem Sci* **2017**, *8*, 6804.

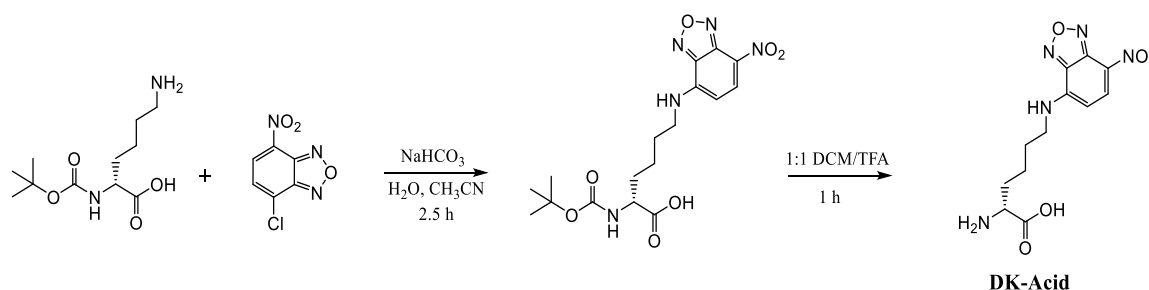
(88) Botella, H.; Yang, G.; Ouerfelli, O.; Ehrt, S.; Nathan, C. F.; Vaubourgeix, J. *MBio* **2017**, *8*.

### A.3 Appendix for Chapter 3

#### Compound Synthesis and Characterization

Nuclear magnetic resonance (NMR) spectra were recorded on a Bruker DRX500 (500MHz) NMR spectrometer.  $^1\text{H}$  NMR spectra are tabulated in the following order: multiplicity (s, singlet; d, doublet; t, triplet; m, multiplet; br, broad), number of protons.

#### Scheme S1. Synthesis of DK-Acid.

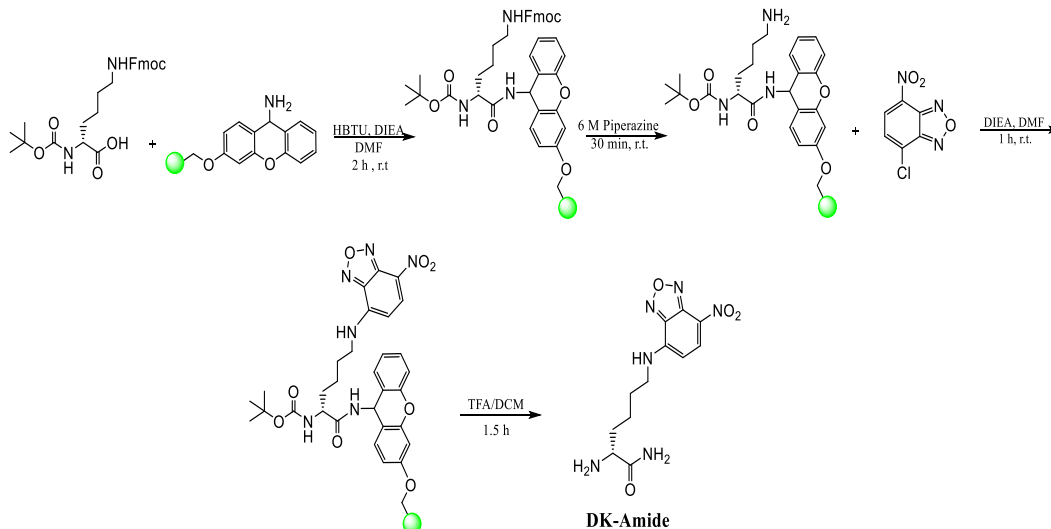


Sodium bicarbonate (2.20 g, 27 mmol), Boc-D-Lys-OH (950 mg, 3.8 mmol) followed by NBD-Cl (615 mg, 3.0 mmol) were added to 40 mL of  $\text{H}_2\text{O}/\text{CH}_3\text{CN}$  (1:3). The reaction mixture was stirred at room temperature for 2.5 h after which  $\text{CH}_3\text{CN}$  was removed *in vacuo*. The aqueous solution was acidified with 1N HCl and extracted with EtOAc (3 x 50 mL). The organic layers were combined, dried over  $\text{MgSO}_4$ , filtered, and concentrated *in vacuo*. The residue was dissolved in 40 mL of DCM/TFA (1:1) and stirred at room temperature for 1 h. The solvent was removed *in vacuo* and the residue was triturated with cold diethyl ether to yield **DK-Acid**.

$^1\text{H}$  NMR (500 MHz,  $\text{CD}_3\text{OD}$ ) :  $\delta$  8.49 (d,  $J = 8.9$ , 1H), 6.33 (d,  $J = 8.9$ , 1H), 3.97 (t, 1H), 3.56 (br. s, 2H), 1.99 (br. m, 2H), 1.83 (m, 2H), 1.61 (br. M, 2H).

$^{13}\text{C}$  NMR (500 MHz,  $\text{CD}_3\text{OD}$ ) :  $\delta$  170.42, 137.11, 131.18, 129.46, 115.76, 113.50, 98.31, 52.38, 42.89, 29.84, 27.33, 22.13. MS (ESI)  $[\text{M}+\text{H}^+]$ : 310.1 (calculated) ; 310.3 (found)

## Scheme S2. Synthesis of DK-Amide.

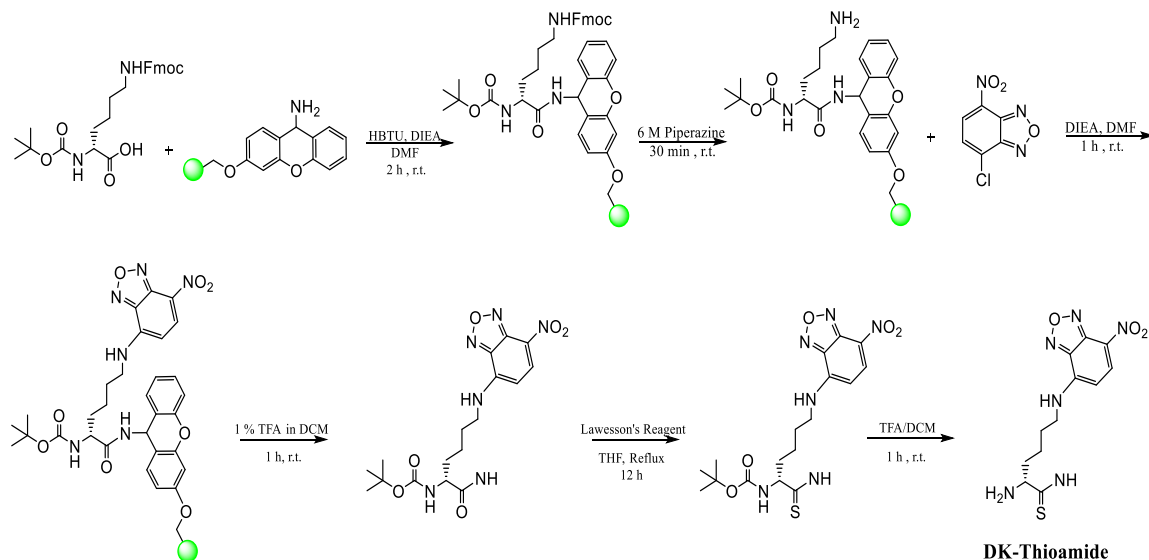


A 25 mL synthetic flask was charged with Sieber Amide Resin (1.00 g, 0.41 mmol) and washed with  $\text{CH}_2\text{Cl}_2$  (3 x 10 mL) and DMF (3 x 10 mL).  $N^{\alpha}$ -Boc- $N^{\epsilon}$ -Fmoc-D-lysine (3 eq, 575 mg, 1.23 mmol), HBTU (3 eq, 475 mg, 1.25 mmol), and DIEA (6 eq, 0.430 mL, 2.47 mmol) in DMF (15 mL) were added to the reaction flask and agitated for 2 h at room temperature. The resin was washed with DMF,  $\text{CH}_2\text{Cl}_2$ , MeOH,  $\text{CH}_2\text{Cl}_2$ , and DMF (3 x 10 mL each). The Fmoc protecting group was removed with 6 M piperazine/100 mM HOBt in DMF (15 mL) for 30 min at room temperature, then the resin was washed as before. A solution of NBD-Cl (5 eq, 400 mg, 2.05 mmol) and DIEA (10 eq, 0.700 mL, 4.02 mmol) in DMF (10 mL) was added to the resin and agitated in the dark for 1 h at room temperature, afterwards the resin was washed. A solution of TFA/DCM (1:1, 25 mL) was added to the resin and agitated for 1 h at room temperature. The resin was filtered and the resulting solution was concentrated *in vacuo*. The residue was triturated with cold diethyl ether to yield **DK-Amide**.

$^1\text{H}$  NMR (500 MHz, DMSO) :  $\delta$  8.51 (d,  $J = 8.6$ , 1H), 6.40 (d,  $J = 8.5$ , 1H), 3.73 (t, 1H), 1.74 (m, 2H), 1.68 (m, 2H), 1.40 (br. m, 2H).

$^{13}\text{C}$  NMR (500 MHz, DMSO) :  $\delta$  171.06, 150.21, 145.78, 144.94, 138.62, 121.13, 99.86, 52.67, 43.61, 30.97, 27.81, 22.12. MS (ESI) [ $\text{M}+\text{H}^+$ ]: 309.1 (calculated) ; 309.3 (found)

### Scheme S3. Synthesis of DK-Thioamide.



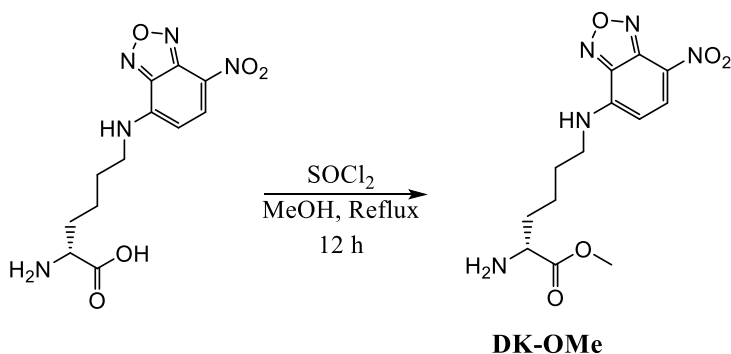
The  $\text{N}^\alpha$ -Boc- $\text{N}^\epsilon$ -Fmoc-D-lysine loading, deprotection, and NBD-Cl coupling procedure of **S2** was repeated. Boc-protected D-Lys(NBD) was cleaved from the Sieber Amide Resin with 1% TFA in DCM for 1 h at room temperature. The solution in a 250 mL RB flask was concentrated *in vacuo* and the residue was dissolved in anhydrous THF (50 mL). The flask was flushed with  $\text{N}_2$ , afterwards the addition of Lawesson's Reagent (10 eq, 1.65 g, 4.1 mmol). The mixture was refluxed for 12 h and then diluted with 0.5M NaOH (50 mL). The THF was removed *in vacuo*, EtOAc (50 mL) was added and the EtOAc/NaOH biphasic mixture was stirred for 1 h at room temperature. The aqueous layer was further extracted with EtOAc (3 x 50 mL). The organic layers were combined, dried over  $\text{MgSO}_4$ , filtered, and concentrated *in vacuo*. The boc-protected DK-Thioamide was purified via silica

column with DCM/MeOH and concentrated *in vacuo*. The residue was dissolved in 40 mL of TFA/DCM (1:1) and stirred at room temperature for 1 h. The solvent was removed *in vacuo* and the residue was triturated with cold diethyl ether to yield **DK-Thioamide**.

$^1\text{H}$  NMR (500 MHz,  $\text{CD}_3\text{OD}$ ) :  $\delta$  8.53 (d,  $J = 8.9$ , 1H), 6.36 (d,  $J = 8.7$ , 1H), 4.07 (t, 1H), 3.56 (br. m, 2H), 1.95 (m, 2H), 1.83 (m, 2H), 1.56 (m, 2H).

$^{13}\text{C}$  NMR (500 MHz,  $\text{CD}_3\text{OD}$ ) :  $\delta$  161.37, 144.52, 137.15, 132.51, 117.76, 115.45, 113.34, 57.30, 54.35, 33.71, 27.55, 22.13. MS (ESI)  $[\text{M}+\text{H}^+]$ : 325.1 (calculated) ; 325.4 (found)

#### Scheme S4. Synthesis of DK-OMe.

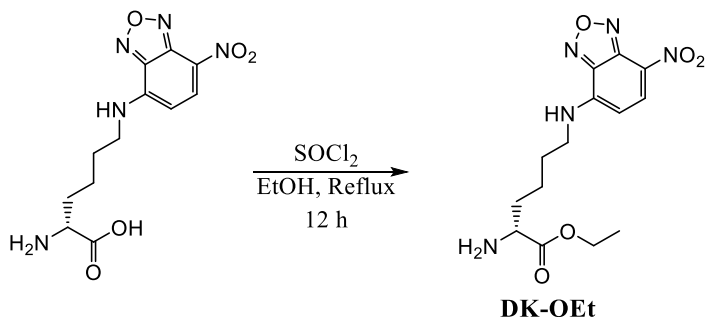


**DK-Acid** (300mg, 0.97 mmol) from **S1** was dissolved in MeOH (50 mL). The mixture was cooled to 0 °C and the RB flask was flushed with  $\text{N}_2$ . Thionyl chloride (5 eq, 0.60 mL, 5.0 mmol) was added dropwise over ice, afterwards the mixture was refluxed for 12 h. The solution was concentrated *in vacuo* and the remaining crude material was used without further purification.

$^1\text{H}$  NMR (500 MHz,  $\text{CD}_3\text{OD}$ ) :  $\delta$  8.57 (d,  $J = 7.8$ , 1H), 6.30 (d,  $J = 8.2$ , 1H), 4.12 (t, 1H), 3.83 (s, 3H), 3.55 (br. m, 2H), 2.03 (m, 2H), 1.85 (m, 2H), 1.63 (br. m, 2H).

$^{13}\text{C}$  NMR (500 MHz,  $\text{CD}_3\text{OD}$ ) :  $\delta$  169.80, 145.57, 144.52, 137.36, 135.88, 98.59, 52.54, 52.43, 48.54, 42.81, 29.80, 27.39, 22.33. MS (ESI)  $[\text{M}+\text{H}^+]$ : 324.1 (calculated) ; 324.2 (found)

#### Scheme S5. Synthesis of DK-OEt.

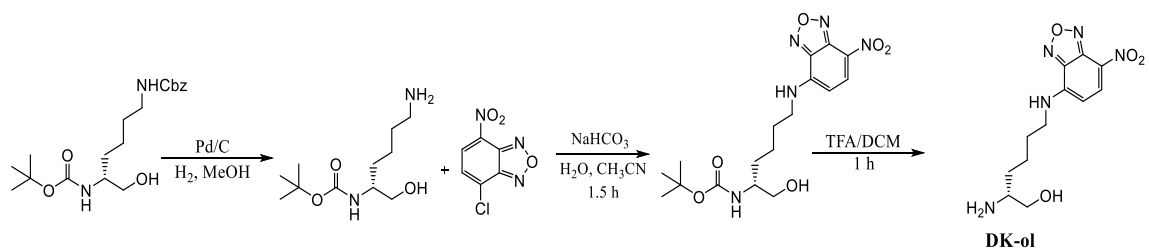


**DK-Acid** (300mg, 0.97 mmol) from **S1** was dissolved in  $\text{EtOH}$  (50 mL). The mixture was cooled to  $0\text{ }^\circ\text{C}$  and the RB flask was flushed with  $\text{N}_2$ . Thionyl chloride (5 eq, 0.60 mL, 5.0 mmol) was added dropwise over ice, afterwards the mixture was refluxed for 12 h. The solution was concentrated *in vacuo* and the remaining crude material was used without further purification.

$^1\text{H}$  NMR (500 MHz,  $\text{CD}_3\text{OD}$ ) :  $\delta$  8.46 (br. d, 1H), 6.35 (br. d, 1H), 4.28 (m, 2H), 4.05 (t, 1H), 3.60 (q, 2H), 2.00 (m, 2H), 1.86 (m, 2H), 1.62 (m, 2H), 1.16 (t, 3H).

$^{13}\text{C}$  NMR (500 MHz,  $\text{CD}_3\text{OD}$ ) :  $\delta$  169.27, 145.36, 144.26, 137.80, 129.32, 121.98, 98.81, 62.33, 56.91, 52.74, 30.44, 22.31, 16.89, 13.34. MS (ESI)  $[\text{M}+\text{H}^+]$ : 338.1 (calculated) ; 338.4 (found)

#### Scheme S6. Synthesis of DK-ol.

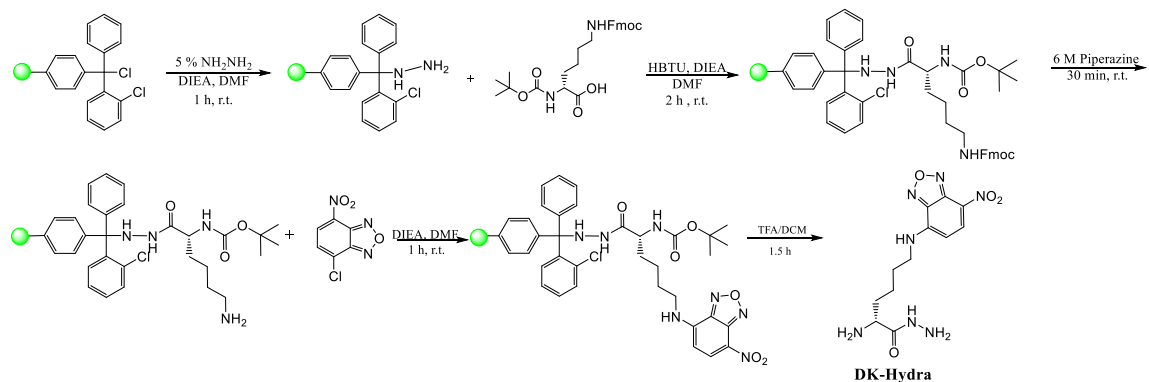


Boc-D-lysine (Cbz) (300 mg, 0.81 mmol) was dissolved in MeOH (20 mL), followed by the addition of 10% Pd/C (30 mg, 0.27 mmol). The RB flask was flushed with H<sub>2</sub> and the mixture was stirred for 12 h at room temperature. The solution was filtered and concentrated *in vacuo*. The remaining procedure was followed as in **S1**.

<sup>1</sup>H NMR (500 MHz, DMSO) : δ 8.50 (d, J = 8.5, 1H), 6.39 (d, J = 8.5, 1H), 3.52 (m, 2H), 3.05 (t, 1H), 1.67 (m, 2H), 1.53 (m, 2H), 1.42 (m, 2H).

<sup>13</sup>C NMR (500 MHz, DMSO) : δ 144.78, 144.73, 138.62, 121.35, 116.29, 99.65, 61.09, 52.88, 43.82, 29.07, 27.81, 22.75. MS (ESI) [M+H<sup>+</sup>]: 296.1 (calculated) ; 296.2 (found)

### Scheme S7. Synthesis of DK-Hydra.



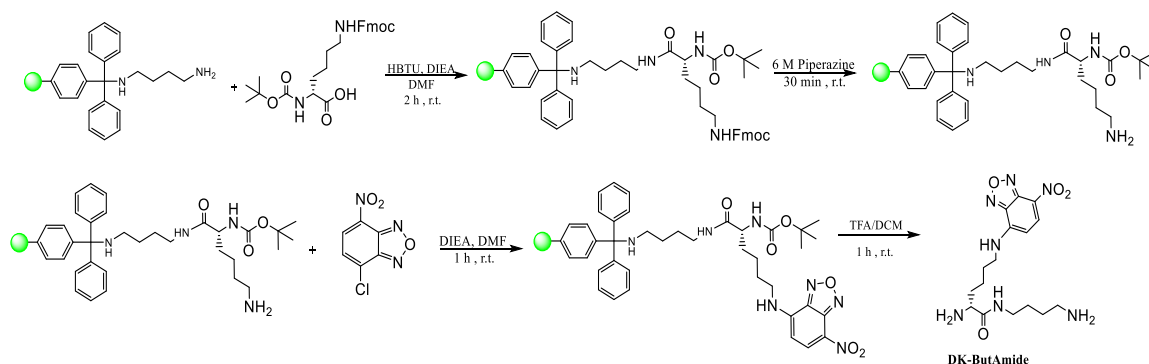
A 25 mL synthetic flask charged with 2-Chlorotrityl Resin (500 mg, 0.72 mmol) was initially washed with CH<sub>2</sub>Cl<sub>2</sub> (3 x 10 mL) and DMF (3 x 10 mL). To the resin was added NH<sub>2</sub>NH<sub>2</sub> (0.750 mL) in DMF (15 mL). The resin was agitated for 1 h at room temperature followed by washes with DMF, CH<sub>2</sub>Cl<sub>2</sub>, MeOH, CH<sub>2</sub>Cl<sub>2</sub>, and DMF (3 x 10 mL each). N<sup>α</sup>-

Boc-N<sup>ε</sup>-Fmoc-D-lysine (3 eq, 1.00 g, 2.15 mmol), HBTU (3 eq, 813 mg, 2.15 mmol), and DIEA (6 eq, 0.750 mL, 4.29 mmol) in DMF (10 mL) were added to the reaction flask and agitated for 2 h at room temperature. The resin was washed as before and the Fmoc protecting group was removed with 6 M piperazine/100 mM HOBt in DMF (15 ml) for 30 min at room temperature. The resin was washed and a solution of NBD-Cl (5 eq, 710 mg, 3.56 mmol) and DIEA (10 eq, 1.25 mL, 7.18 mmol) in DMF (10 mL) was added to the resin and agitated in the dark for 1 h at room temperature, afterwards the resin was washed. A solution of TFA/DCM (1:1, 25 mL) was added to the resin and agitated for 1 h at room temperature. The resin was filtered and the resulting solution was concentrated *in vacuo*. The residue was triturated with cold diethyl ether to yield **DK-Hydra**.

<sup>1</sup>H NMR (500 MHz, CD<sub>3</sub>OD) : δ 8.53 (d, J = 8.8, 1H), 6.36 (d, J = 8.4, 1H), 3.79 (t, 1H), 3.57 (br. m, 2H), 1.90 (m, 2H), 1.84 (m, 2H), 1.54 (m, 2H).

<sup>13</sup>C NMR (500 MHz, DMSO) : δ 171.70, 145.99, 145.15, 138.41, 121.13, 116.50, 99.86, 56.67, 52.88, 30.55, 27.81, 22.75. MS (ESI) [M+H<sup>+</sup>]: 324.1 (calculated) ; 324.2(found)

#### Scheme S8. Synthesis of DK-ButAmide.



A 25 mL synthetic flask charged with 1,4-Diaminobutane trityl resin (500 mg, 0.385 mmol) was initially washed with CH<sub>2</sub>Cl<sub>2</sub> (3 x 10 mL) and DMF (3 x 10 mL). N<sup>α</sup>-Boc-N<sup>ε</sup>-Fmoc-

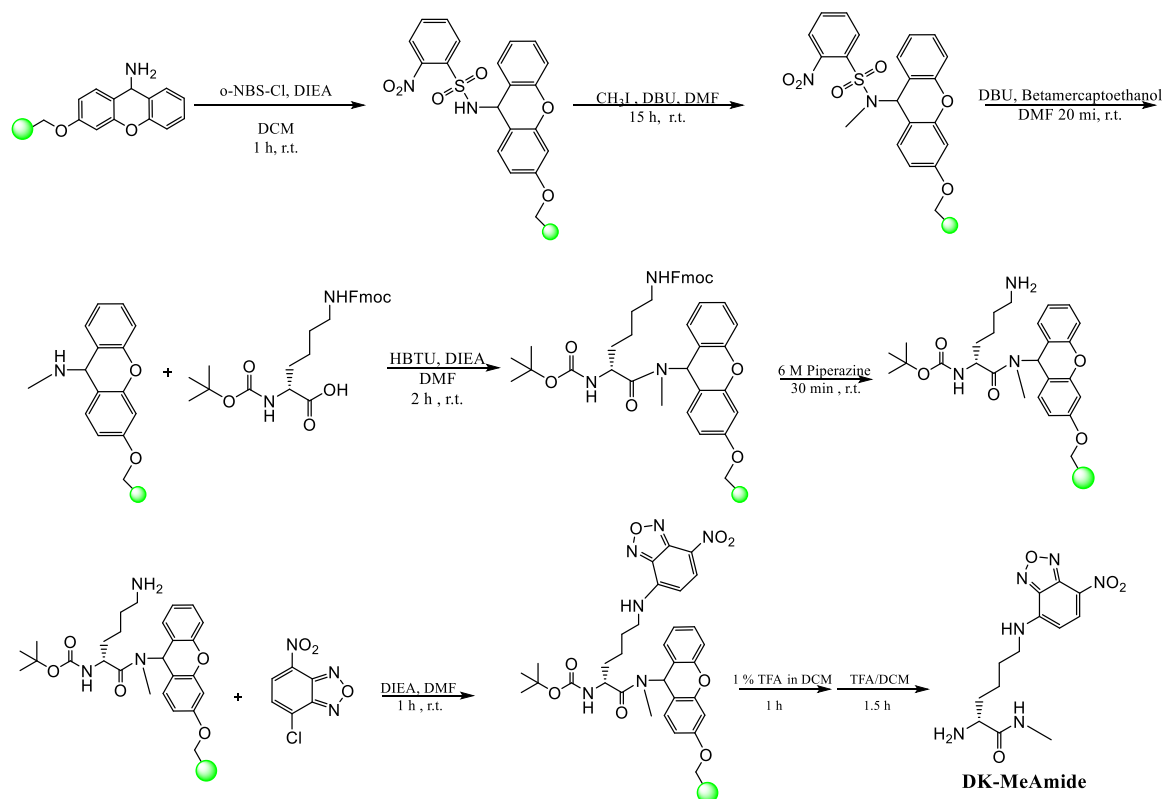


D-lysine (3 eq, 540 mg, 1.15 mmol), HBTU (3 eq, 438 mg, 1.15 mmol), and DIEA (6 eq, 0.400 mL, 2.31 mmol) in DMF (15 mL) were added to the reaction flask and agitated for 2 h at room temperature. The resin was washed with DMF, CH<sub>2</sub>Cl<sub>2</sub>, MeOH, CH<sub>2</sub>Cl<sub>2</sub>, and DMF (3 x 10 mL each). The Fmoc protecting group was removed with 6 M piperazine/100 mM HOBt in DMF (15 ml) for 30 min at room temperature, then washed as before. A solution of NBD-Cl (5 eq, 385 mg, 1.92 mmol) and DIEA (10 eq, 0.670 mL, 3.85 mmol) in DMF (10 mL) was added to the resin and agitated in the dark for 1 h at room temperature, afterwards the resin was washed. A solution of TFA/DCM (1:1, 25 mL) was added to the resin and agitated for 1 h at room temperature. The resin was filtered and the resulting solution was concentrated *in vacuo*. The residue was triturated with cold diethyl ether to yield **DK-ButAmide**.

<sup>1</sup>H NMR (500 MHz, DMSO) : δ 8.50 (d, 1H), 6.39 (d, J = 7.9, 1H), 3.69 (br. t, 1H), 3.44 (m, 2H), 3.10 (m, 2H), 1.72 (m, 2H), 1.67 (m, 2H), 1.57 (m, 2H), 1.52 (m, 2H), 1.45 (m, 2H), 1.38 (m, 2H).

<sup>13</sup>C NMR (500 MHz, DMSO) : δ 168.96, 145.78, 144.73, 138.62, 120.71, 116.08, 99.65, 65.52, 52.67, 49.09, 43.40, 31.18, 26.12, 24.86, 22.12, 16.01. MS (ESI) [M+H<sup>+</sup>]: 380.2 (calculated) ; 380.0 (found)

### Scheme S9. Synthesis of DK-MeAmide.



A 25 mL synthetic flask was charged with Sieber Amide Resin (1.00 g, 0.41 mmol) and washed with  $\text{CH}_2\text{Cl}_2$  (3 x 10 mL) and DMF (3 x 10 mL). A solution of *o*-NBS-Cl (5 eq, 450 mg, 2.03 mmol) and DIEA (10 eq, 0.720 mL, 4.10 mmol) in DCM (15 mL) was added to the resin and agitated for 1 h at room temperature in the dark. The resin was washed with DMF,  $\text{CH}_2\text{Cl}_2$ , MeOH,  $\text{CH}_2\text{Cl}_2$ , and DMF (3 x 10 mL each). A solution of  $\text{CH}_3\text{I}$  (20 eq, 1.15 g, 8.15 mmol), DBU (10 eq, 0.640 mL, 4.29 mmol) in DMF (15 mL) was added to the resin and agitated for 15 h at room temperature in the dark. The resin was washed as before followed by the addition of DBU (10 eq, 0.640 mL, 4.29 mmol) and BME (5 eq, 0.145 mL, 2.05 mmol) in DMF (15 mL). The resin was agitated for 20 min. at room temperature and washed.  $\text{N}^\alpha$ -Boc- $\text{N}^\epsilon$ -Fmoc-D-lysine (3 eq, 575 mg, 1.23 mmol), HBTU (3

eq, 475 mg, 1.25 mmol), and DIEA (6 eq, 0.430 mL, 2.47 mmol) in DMF (15 mL) were added to the reaction flask and agitated for 2 h at room temperature. The resin was washed with DMF, CH<sub>2</sub>Cl<sub>2</sub>, MeOH, CH<sub>2</sub>Cl<sub>2</sub>, and DMF (3 x 10 mL each). The Fmoc protecting group was removed with 6 M piperazine/100 mM HOBt in DMF (15 ml) for 30 min at room temperature, then washed as before. A solution of NBD-Cl (5 eq, 400 mg, 2.05 mmol) and DIEA (10 eq, 0.700 mL, 4.02 mmol) in DMF (10 mL) was added to the resin and agitated in the dark for 1 h at room temperature, afterwards the resin was washed. The boc-protected D-Lys(NBD) methyl amide was cleaved from resin with 1% TFA in DCM for 1 h at room temperature. The solution was concentrated *in vacuo* and the residue was purified via silica column with DCM/MeOH. The purified boc-protected D-Lys(NBD) methyl amide was added to a solution of a solution of TFA/DCM (1:1, 25 mL) and stirred for 1 h at room temperature. The solution was concentrated *in vacuo* and the resulting residue was triturated with cold diethyl ether to yield **DK-MeAmide**.

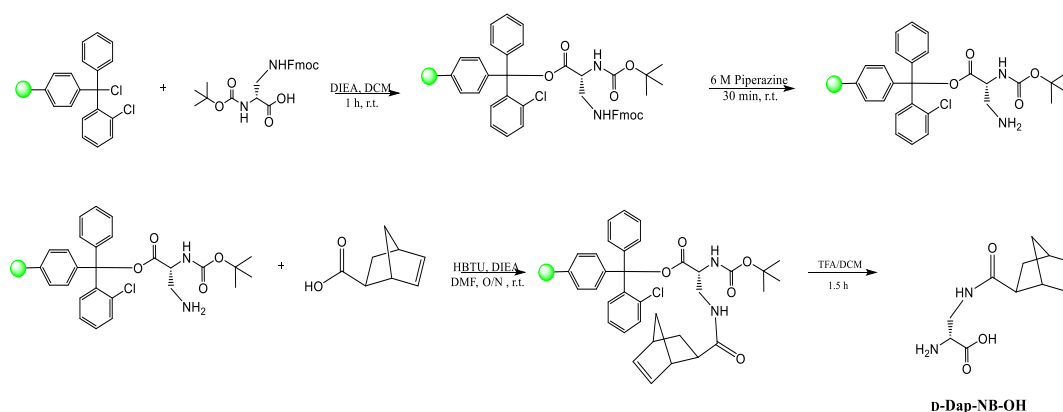
<sup>1</sup>H NMR (500 MHz, CD<sub>3</sub>OD) : δ 8.46 (d, 1H), 6.31 (d, J = 7.6, 1H), 3.83 (t, 1H), 3.54 (br. s, 2H), 2.78 (s, 3H), 1.91 (m, 2H), 1.83 (m, 2H), 1.54 (m, 2H).

<sup>13</sup>C NMR (500 MHz, CD<sub>3</sub>OD) : δ 169.38, 144.52, 144.09, 137.36, 121.98, 115.87, 98.38, 65.94, 53.30, 30.97, 25.07, 21.91, 14.11. MS (ESI) [M+H<sup>+</sup>]: 323.1 (calculated) ; 323.4 (found)

#### A.4 Appendix for Chapter 4

Compound Synthesis and Characterization Nuclear magnetic resonance (NMR) spectra were recorded on a Bruker DRX500 (500MHz) NMR spectrometer. <sup>1</sup>H NMR spectra are tabulated in the following order: multiplicity (s, singlet; d, doublet; t, triplet; m, multiplet; br, broad), number of protons.

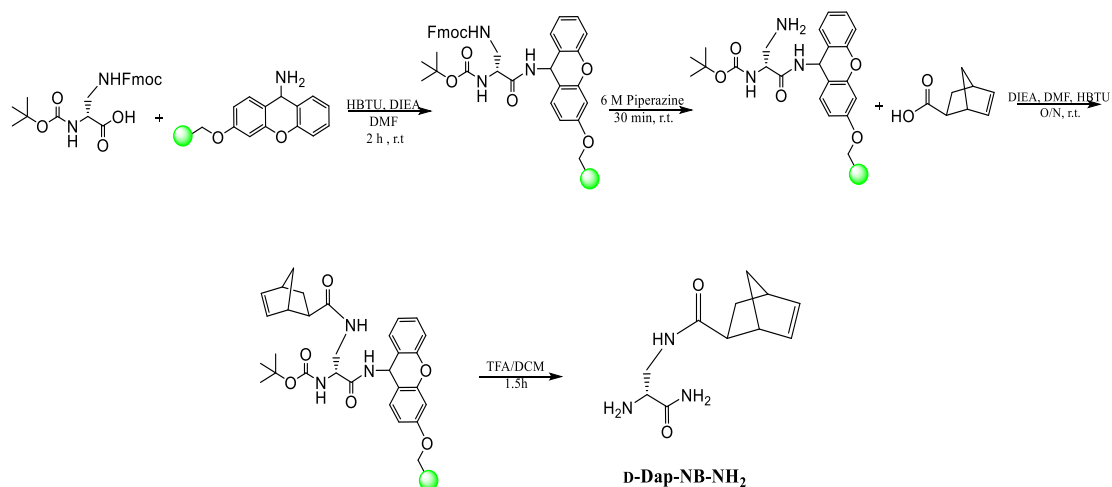
##### Scheme S1. Synthesis of D-Dap-NB-OH.



A 25 mL synthetic flask charged with 2-Chlorotrityl Resin (500 mg, 0.72 mmol) was initially washed with CH<sub>2</sub>Cl<sub>2</sub> (3 x 10 mL) and DMF (3 x 10 mL). To the resin was added N $\alpha$ -BocN $\beta$ -Fmoc-D-2,3-diaminopropionic acid (3 eq, 914 mg, 2.15 mmol), HBTU (3 eq, 813 mg, 2.15 mmol), and DIEA (6 eq, 0.750 mL, 4.29 mmol) in DMF (10 mL) and agitated for 2 h at room temperature. The resin was washed with DMF, CH<sub>2</sub>Cl<sub>2</sub>, MeOH, CH<sub>2</sub>Cl<sub>2</sub>, and DMF (3 x 10 mL each). The Fmoc protecting group was removed with 6 M piperazine/100 mM HOBT in DMF (15 ml) for 30 min at room temperature. The resin was washed and a solution of 5-norbornene-2-carboxylic acid (5 eq, 493 mg, 3.57 mmol), HBTU (5 eq, 1.36 g, 3.57 mmol) and DIEA (10 eq, 1.25 mL, 7.18 mmol) in DMF (10 mL) was added to the resin and agitated overnight at room temperature, afterwards the resin was washed as before. A solution of TFA/DCM (1:1, 25 mL) was added to the resin and agitated

for 1 h at room temperature. The resin was filtered and the resulting solution was concentrated in vacuo. The residue was triturated with cold diethyl ether to yield D-Dap-NB-OH. <sup>1</sup>H NMR (500 MHz, CD<sub>3</sub>OD) : δ 6.15 (m, 1H), 5.90 (m 1H), 4.08 (m, 1H), 3.71 (m, 1H), 3.65 (m, 1H), 3.33 (m, 1H), 3.15 (m, 1H), 2.95 (m, 1H), 2.90 (m, 1H), 1.85 (m, 1H), 1.40 (m, 1H), 1.35 (m, 1H). <sup>13</sup>C NMR (500 MHz, CD<sub>3</sub>OD) : δ 178.02, 168.96, 137.57, 131.46, 53.72, 49.72, 46.14, 44.03, 42.98, 38.97, 29.07. MS (ESI) [M+H<sup>+</sup>]: 225.2 (calculated) ; 225.4 (found)

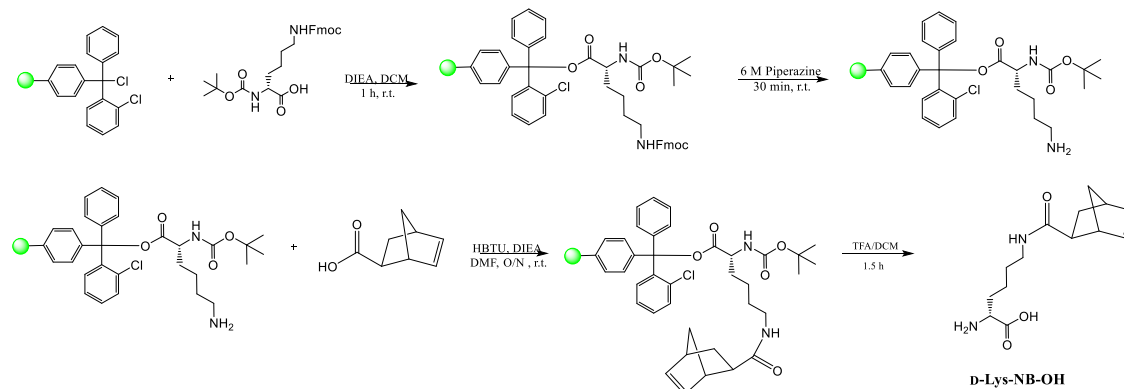
### Scheme S2. Synthesis of D-Dap-NB-NH<sub>2</sub>.



A 25 mL synthetic flask was charged with Sieber Amide Resin (1.00 g, 0.41 mmol) and washed with CH<sub>2</sub>Cl<sub>2</sub> (3 x 10 mL) and DMF (3 x 10 mL). Nα -Boc-Nβ -Fmoc-D-2,3-diaminopropionic acid (3 eq, 523 mg, 1.23 mmol), HBTU (3 eq, 466 mg, 1.23 mmol), and DIEA (6 eq, 0.430 mL, 2.47 mmol) in DMF (15 mL) were added to the reaction flask and agitated for 2 h at room temperature. The resin was washed with DMF, CH<sub>2</sub>Cl<sub>2</sub>, MeOH, CH<sub>2</sub>Cl<sub>2</sub>, and DMF (3 x 10 mL each). The Fmoc protecting group was removed with 6 M piperazine/100 mM HOBt in DMF (15 ml) for 30 min at room temperature, then the resin was washed as before. 5-norbornene-2-carboxylic acid (5 eq, 283 mg, 2.05 mmol), HBTU

(5 eq, 776 mg, 2.05 mmol) and DIEA (10 eq, 0.70 mL, 4.10 mmol) in DMF (10 mL) was added to the resin and agitated overnight at room temperature, afterwards the resin was washed as before. A solution of TFA/DCM (1:1, 25 mL) was added to the resin and agitated for 1 h at room temperature. The resin was filtered and the resulting solution was concentrated in vacuo. The residue was triturated with cold diethyl ether to yield D-Dap-NB-NH<sub>2</sub>. <sup>1</sup>H NMR (500 MHz, CD<sub>3</sub>OD) : δ 6.13 (m, 1H), 5.92 (m, 1H), 4.02 (m, 1H), 3.71 (m, 1H), 3.65 (m, 1H), 3.33 (m, 1H), 3.15 (m, 1H), 2.95 (m, 1H), 2.90 (m, 1H), 1.85 (m, 1H), 1.40 (m, 1H), 1.35 (m, 1H). <sup>13</sup>C NMR (500 MHz, CD<sub>3</sub>OD) : δ 177.70, 168.71, 137.30, 131.68, 53.72, 49.30, 46.56, 43.82, 42.77, 40.66, 28.65. MS (ESI) [M+H<sup>+</sup>]: 224.2 (calculated) ; 224.4 (found)

### Scheme S3. Synthesis of D-Lys-NB-OH.



A 25 mL synthetic flask charged with 2-Chlorotrityl Resin (500 mg, 0.72 mmol) was initially washed with CH<sub>2</sub>Cl<sub>2</sub> (3 x 10 mL) and DMF (3 x 10 mL). To the resin was added N $\alpha$ -BocN $\epsilon$ -Fmoc-D-lysine (3 eq, 1.00 g, 2.15 mmol), HBTU (3 eq, 813 mg, 2.15 mmol), and DIEA (6 eq, 0.750 mL, 4.29 mmol) in DMF (10 mL) and agitated for 2 h at room temperature. The resin was washed with DMF, CH<sub>2</sub>Cl<sub>2</sub>, MeOH, CH<sub>2</sub>Cl<sub>2</sub>, and DMF (3 x 10 mL each). The Fmoc protecting group was removed with 6 M piperazine/100 mM HOBt in DMF (15 mL) for 30 min at room temperature. The resin was washed and a solution of

5-norbornene-2-carboxylic acid (5 eq, 493 mg, 3.57 mmol), HBTU (5 eq, 1.36 g, 3.57 mmol) and DIEA (10 eq, 1.25 mL, 7.18 mmol) in DMF (10 mL) was added to the resin and agitated overnight at room temperature, afterwards the resin was washed as before. A solution of TFA/DCM (1:1, 25 mL) was added to the resin and agitated for 1 h at room temperature. The resin was filtered and the resulting solution was concentrated in vacuo. The residue was triturated with cold diethyl ether to yield D-Lys-NB-OH. <sup>1</sup>H NMR (500 MHz, CD<sub>3</sub>OD) : δ 6.18 (m, 1H), 5.89 (m 1H), 3.91 (m, 1H), 3.49 (m, 2H), 3.20 (m, 1H), 2.85 (m, 1H), 1.90 (m, 1H), 1.85 (m, 2H), 1.55 (m, 2H), 1.45 (m, 2H), 1.35 (m, 2H), 1.22 (m, 2H). <sup>13</sup>C NMR (500 MHz, CD<sub>3</sub>OD) : δ 175.91, 170.64, 137.57, 131.88, 52.67, 49.51, 46.14, 44.24, 42.56, 38.55, 29.95, 28.65, 28.35, 22.33. MS (ESI) [M+H<sup>+</sup> ]: 267.3 (calculated) ; 267.1 (found)

**Scheme S4. Synthesis of D-Dap-Tet-NH<sub>2</sub>.** D-Dap-Tet-NH<sub>2</sub> Methyl-thiocarbohydrazide Thiocarbohydrazide (4.98 g, 46.9 mmol) was dissolved in 200 mL of absolute ethanol and brought to reflux. MeI (3.2 mL, 1.1 eq) in 20 mL of absolute ethanol was added dropwise over 15 minutes and then refluxed for 1 hr with stirring. The solution was then filtered hot using a C type filter crucible and the filtrate was cooled to room temperature over 12 hr. The solution was decanted and the solid product was dried in vacuo to obtain methyl-thiocarbohydrazide. Methyl-thiomethyl-tetrazine Methyl-thiocarbohydrazide (6.10 g, 50.4 mmol) was dissolved in 150 mL absolute ethanol. Triethyl orthoacetate (10.1 mL, 1.1 eq.) was added, then after five minutes triethyl amine (7.0 mL, 1.0 eq.) was added. The reaction mixture was refluxed for 30 minutes to form an orange colored solution. NaNO<sub>2</sub> (3.43 g, 1.0 eq.) and TFA (1.87 mL, 1.0 eq) were added and the solution was refluxed for an additional 30 minutes. Hexane (150 mL) was added and the

solution was cooled to room temperature followed by the addition of water (300 mL). The mixture was extracted with diethyl ether (3 x 100 mL). The organic layer was dried with MgSO<sub>4</sub> and concentrated in vacuo to ~5-10 mL of product. The oil was purified by silica gel column with EtOAc:Hexane to obtain methyl-thiomethyl-tetrazine. Boc-D-Dap-Tet-OH Na<sup>-</sup> -Boc-D-2,3-diaminopropionic acid (1.0032 g, 4.92 mmol) and methyl-thiomethyltetrazine (980 mg, 6.88 mmol) were dissolved in 20 mL of dry methanol and refluxed for 36 hr. The solution was cooled to room temperature and concentrated in vacuo. The reaction mixture was dissolved in 50 mL EtOAc. The organic mixture was washed with 0.5 M NaOH (100 mL). The aqueous layer was then washed with EtOAc (3 x 50 mL). The aqueous layer was then acidified with 1 M HCl to pH 5. The aqueous layer was then washed with EtOAc (3 x 50 mL). The organic layers were combined, dried with MgSO<sub>4</sub>, and concentrated in vacuo. The product was purified by silica gel column with DCM:MeOH to obtain Boc-D-Dap-Tet-OH as a purple oil. D-Dap-Tet-NH<sub>2</sub> A 25 mL synthetic flask was charged with Sieber Amide Resin (1.00 g, 0.41 mmol) and washed with CH<sub>2</sub>Cl<sub>2</sub> (3 x 10 mL) and DMF (3 x 10 mL). Boc-D-Dap-Tet-OH (356 mg, 1.19 mmol), HBTU (451 mg, 1.19 mmol), and DIEA (0.42 mL, 2.41 mmol) in DMF (15 mL) were added to the reaction flask and agitated for 2 hr at room temperature. The resin was washed with DMF, CH<sub>2</sub>Cl<sub>2</sub>, MeOH, CH<sub>2</sub>Cl<sub>2</sub>, and DMF (3 x 10 mL each). A solution of TFA/DCM (1:1, 25 mL) was added to the resin and agitated for 1 h at room temperature. The resin was filtered and the resulting solution was concentrated in vacuo. The residue was triturated with cold diethyl ether to yield D-Dap-Tet-NH<sub>2</sub>. <sup>1</sup>H NMR (500 MHz, CD<sub>3</sub>OD) : δ 4.10 (m, 1H), 2.15 (s, 3H), 1.30 (m, 2H), <sup>13</sup>C NMR (500 MHz, CD<sub>3</sub>OD) : δ

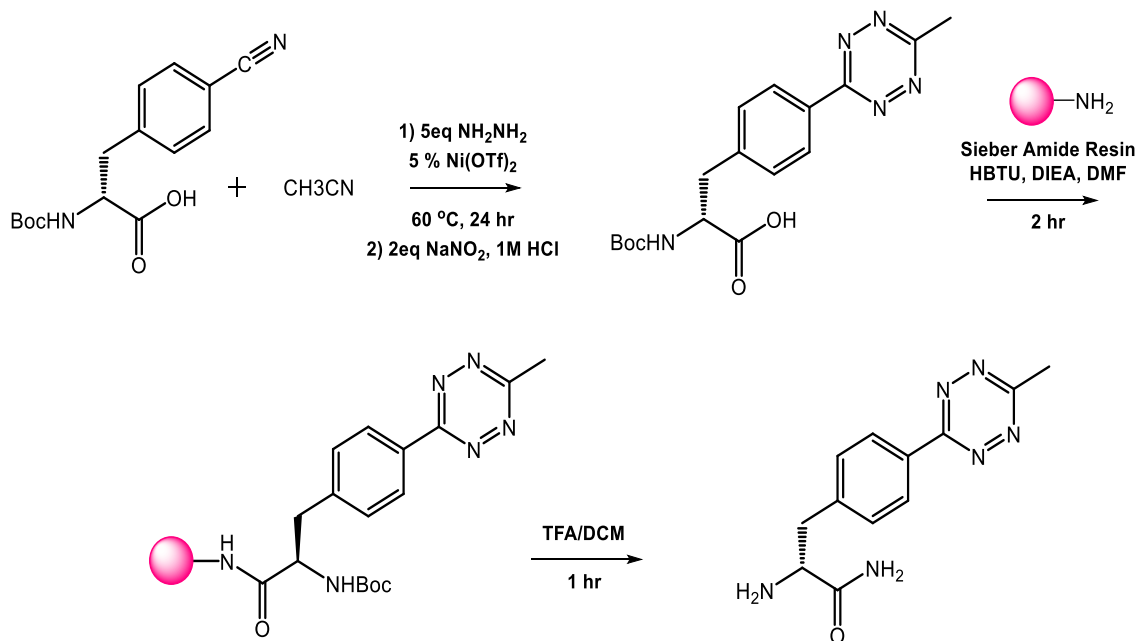


169.59, 160.16, 159.88, 57.09, 53.93, 22.96. MS (ESI) [M+H<sup>+</sup>]: 198.1 (calculated) ; 198.0  
(found)

## A.5 Appendix for Chapter 5

### Compound Synthesis and Characterization

#### Scheme S1. Synthesis of D-4-(6-methyl-tetrazin-3-yl)phenylpropanamide (D-Tet)

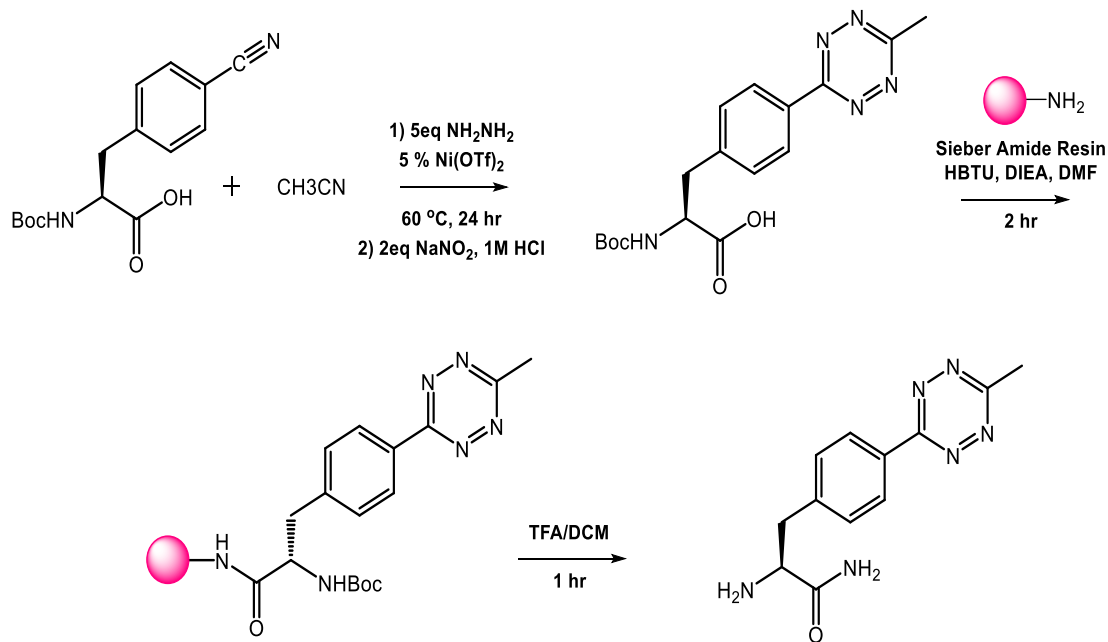


Boc-4-cyano-D-phenylalanine (1.00 g, 3.45 mmol) was added to a microwave reaction vessel with a stir bar. Nickel (II) trifluoromethanesulfonate (61.6 mg, 0.17 mmol), acetonitrile (1.80 mL, 34.5 mmol), and anhydrous hydrazine (5.50 mL, 172 mmol) were added. The vessel was sealed and the mixture stirred in an oil bath for 24 hr at 60 °C. The solution was cooled to room temperature, followed by the dropwise addition of sodium nitrite (4.76g, 69.0 mmol) in 8 mL of water. 1M HCl was added dropwise until gas evolution ceased and pH of the solution was 3. The mixture was extracted with EtOAc, organic phase dried with MgSO<sub>4</sub>. The solution was concentrated *in vacuo* and residue purified using silica column chromatography (DCM/MeOH). The purified Boc-protected

tetrazine was dissolved in DMF (20 mL), followed by the addition of HBTU (3 eq, 3.16g, 8.33 mmol) and DIEA (6 eq, 2.90 mL, 16.6 mmol). The mixture was added to a peptide vessel containing sieber amide resin (5.00g, 2.05 mmol) and the vessel was shaken for 2 hr at ambient temperature. The resin was washed with DMF, CH<sub>2</sub>Cl<sub>2</sub>, MeOH, CH<sub>2</sub>Cl<sub>2</sub>, and DMF (3 x 15 mL each). The resin was transferred to a round bottom flask and a solution of TFA/DCM (30:70, 30 mL) was added and stirred for 1 hr on ice. The resin was filtered and the resulting solution was concentrated *in vacuo*. The residue was triturated with cold diethyl ether and the precipitate was purified by reverse-phase HPLC to yield **D-Tet** as a pink solid.

<sup>1</sup>H NMR (500 MHz, CD<sub>3</sub>OD) : δ 3.05 (s, 3H, C-CH<sub>3</sub>), 3.20-3.38 (m, 2H, CH-CH<sub>2</sub>-C-), 4.20 (t, 1H, CH-CH<sub>2</sub>), 7.59 (d, 2H, -CH<sub>2</sub>-C-CH-CH-), 8.55 (d, 2H, -CH<sub>2</sub>-C-CH-CH-) <sup>13</sup>C NMR (125 MHz, CD<sub>3</sub>OD) : δ 19.72, 37.15, 53.93, 128.02, 130.13, 131.74, 139.13, 163.74, 167.51, 170.15. HRMS: [M+H] calculated: 259.1229 found: 259.1310

**Scheme S2. Synthesis of L-4-(6-methyl-tetrazin-3-yl)phenylpropanamide (L-Tet)**



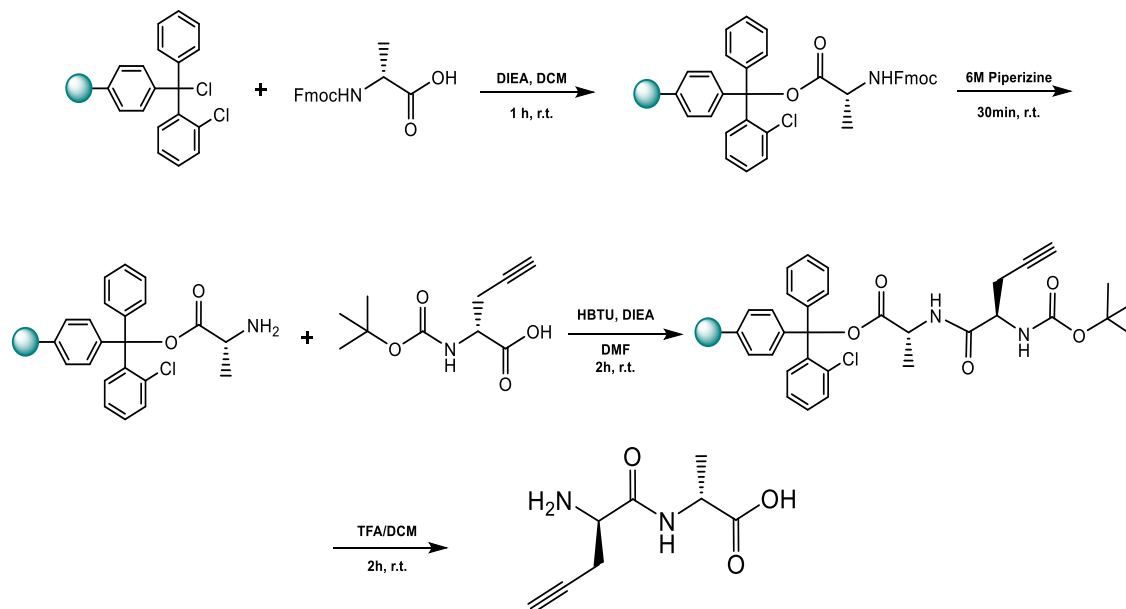
Boc-4-cyano-L-phenylalanine (1.00 g, 3.45 mmol) was synthesized following the same procedure as Scheme S1 to yield **L-Tet** as a pink solid.

$^1\text{H}$  NMR (500 MHz,  $(\text{CD}_3)_2\text{CO}$ ) :  $\delta$  3.02 (s, 3H, C- $\text{CH}_3$ ), 3.48-3.65 (m, 2H, CH- $\text{CH}_2$ -C-), 5.15 (t, 1H, CH- $\text{CH}_2$ ), 7.69 (d, 2H, - $\text{CH}_2$ -C-CH-CH-), 8.48 (d, 2H, - $\text{CH}_2$ -C-CH-CH-)  $^{13}\text{C}$  NMR (125 MHz,  $(\text{CD}_3)_2\text{CO}$ ) :  $\delta$  20.43, 37.45, 63.56, 128.02, 130.74, 131.65, 140.73, 161.61, 163.88, 167.97. HRMS:  $[\text{M}+\text{H}]$  calculated: 259.1229 found: 259.1341

## A.6 Appendix for Chapter 6

### Compound Synthesis and Characterization

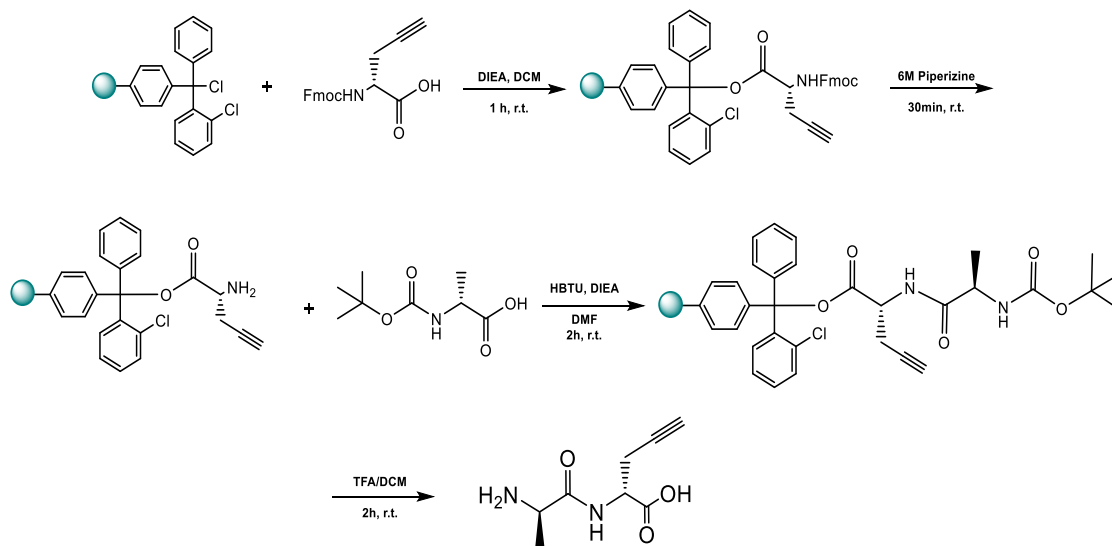
#### Scheme S1. Synthesis of D-propargylglycine-D-alanine (D-Pra-D-Ala)



A 25 mL peptide synthesis vessel was charged with 2-Chlorotrityl chloride resin (500mg, 0.55mmol) was added Fmoc-D-alanine (1.1 eq, 188 mg, 0.605 mmol) and DIEA (3 eq, 0.286 mL, 1.65 mmol) in DCM (15 mL). The resin was agitated for 1 h at ambient temperature and then washed with DMF, DCM, MeOH, CH<sub>2</sub>Cl<sub>2</sub>, and DMF (3 x 10 mL each). The Fmoc protecting group was removed with 6 M piperazine/100 mM HOBt in DMF (15 ml) for 30 min at ambient temperature, then washed as before. Boc-D-propargylglycine (3 eq, 351 mg, 1.65 mmol), HBTU (3 eq, 625 mg, 1.65 mmol), and DIEA (6 eq, 0.574 mL, 3.30 mmol) in DMF (10 mL) were added to the reaction flask and agitated for 2 h at ambient temperature. The resin was washed as before and added to a solution of TFA/DCM (1:1, 20 mL) with agitation for 2 h at ambient temperature. The resin was filtered and resulting solution concentrated *in vacuo*. The residue was triturated with cold diethyl ether to yield **D-Pra-D-Ala**.

$^1\text{H}$  NMR (500 MHz,  $\text{CD}_3\text{OD}$ ) :  $\delta$  1.44 (d, 3H,  $\text{CH}-\text{CH}_3$ ), 2.66 (t, 1H,  $\text{C}\equiv\text{CH}$ ), 2.85 (m, 2H,  $\text{CH}-\text{CH}_2-\text{C}-$ ), 4.03 (q, 1H,  $\text{CH}-\text{CH}_2$ ), 4.44 (q, 1H,  $\text{CH}-\text{CH}_3$ )  $^{13}\text{C}$  NMR (125 MHz,  $\text{CD}_3\text{OD}$ ) :  $\delta$  16.20, 21.05, 48.16, 51.48, 73.57, 75.93, 166.91, 173.80 HRMS:  $[\text{M}+\text{H}]^+$  calculated: 185.0921 found: 185.0926.

**Scheme S2. Synthesis of D-alanine-D-propargylglycine (D-Ala-D-Pra)**

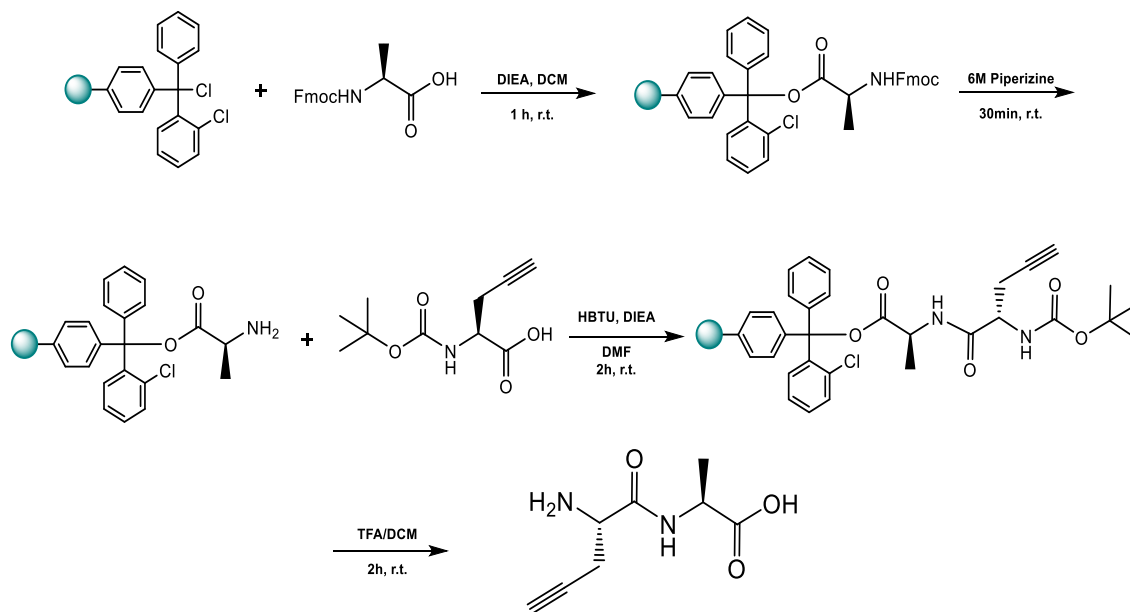


A 25 mL peptide synthesis vessel was charged with 2-Chlorotrityl chloride resin (500mg, 0.55mmol) was added Fmoc-D-propargylglycine (1.1 eq, 202 mg, 0.605 mmol) and DIEA (3 eq, 0.286 mL, 1.65 mmol) in DCM (15 mL). The resin was agitated for 1 h at ambient temperature and then washed with DMF, DCM, MeOH,  $\text{CH}_2\text{Cl}_2$ , and DMF (3 x 10 mL each). The Fmoc protecting group was removed with 6 M piperazine/100 mM HOBt in DMF (15 ml) for 30 min at ambient temperature, then washed as before. Boc-D-alanine (3 eq, 312 mg, 1.65 mmol), HBTU (3 eq, 625 mg, 1.65 mmol), and DIEA (6 eq, 0.574 mL, 3.30 mmol) in DMF (10 mL) were added to the reaction flask and agitated for 2 h at ambient temperature. The resin was washed as before and added to a solution of TFA/DCM

(1:1, 20 mL) with agitation for 2 h at ambient temperature. The resin was filtered and resulting solution concentrated *in vacuo*. The residue was triturated with cold diethyl ether to yield **D-Ala-D-Pra**.

$^1\text{H}$  NMR (500 MHz,  $\text{CD}_3\text{OD}$ ) :  $\delta$  1.53 (d, 3H,  $\text{CH-CH}_3$ ), 2.38 (t, 1H,  $\text{C}\equiv\text{CH}$ ), 2.77 (m, 2H,  $\text{CH-CH}_2\text{-C-}$ ), 4.07 (q, 1H,  $\text{CH-CH}_2$ ), 4.54 (q, 1H,  $\text{CH-CH}_3$ )  $^{13}\text{C}$  NMR (125 MHz,  $\text{CD}_3\text{OD}$ ) :  $\delta$  16.34, 20.87, 48.80, 51.54, 71.12, 78.59, 169.91, 171.61 HRMS:  $[\text{M}+\text{H}]^+$  calculated: 185.0921 found: 185.0923.

### Scheme S3. Synthesis of L-propargylglycine-L-alanine (L-Pra-L-Ala)

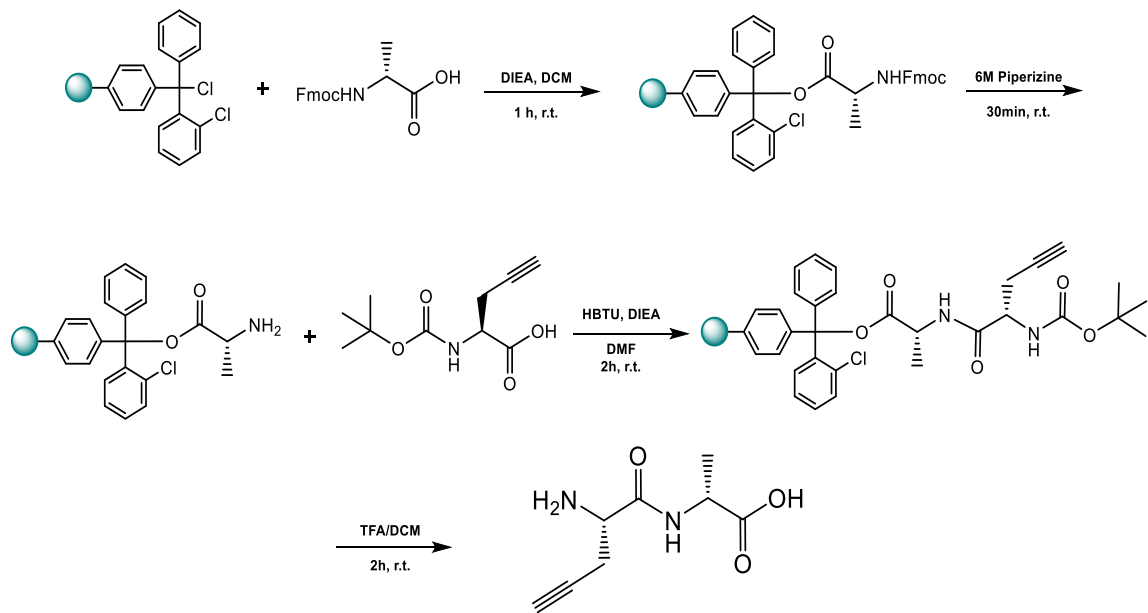


A 25 mL peptide synthesis vessel was charged with 2-Chlorotrityl chloride resin (500mg, 0.55mmol) was added Fmoc-L-alanine (1.1 eq, 188 mg, 0.605 mmol) and DIEA (3 eq, 0.286 mL, 1.65 mmol) in DCM (15 mL). The resin was agitated for 1 h at ambient temperature and then washed with DMF, DCM, MeOH,  $\text{CH}_2\text{Cl}_2$ , and DMF (3 x 10 mL each). The Fmoc protecting group was removed with 6 M piperazine/100 mM HOBt in DMF (15 ml) for 30 min at ambient temperature, then washed as before. Boc-L-

propargylglycine (3 eq, 351 mg, 1.65 mmol), HBTU (3 eq, 625 mg, 1.65 mmol), and DIEA (6 eq, 0.574 mL, 3.30 mmol) in DMF (10 mL) were added to the reaction flask and agitated for 2 h at ambient temperature. The resin was washed as before and added to a solution of TFA/DCM (1:1, 20 mL) with agitation for 2 h at ambient temperature. The resin was filtered and resulting solution concentrated *in vacuo*. The residue was triturated with cold diethyl ether to yield **L-Pra-L-Ala**.

$^1\text{H}$  NMR (500 MHz,  $\text{CD}_3\text{OD}$ ) :  $\delta$  1.44 (d, 3H,  $\text{CH-CH}_3$ ), 2.61 (t, 1H,  $\text{C}\equiv\text{CH}$ ), 2.86 (m, 2H,  $\text{CH-CH}_2\text{-C-}$ ), 4.06 (q, 1H,  $\text{CH-CH}_2$ ), 4.44 (q, 1H,  $\text{CH-CH}_3$ )  $^{13}\text{C}$  NMR (125 MHz,  $\text{CD}_3\text{OD}$ ) :  $\delta$  16.19, 21.03, 48.20, 51.40, 73.58, 75.94, 167.01, 173.91 HRMS:  $[\text{M}+\text{H}]^+$  calculated: 185.0921 found: 185.0931.

#### Scheme S4. Synthesis of L-propargylglycine-D-alanine (L-Pra-D-Ala)



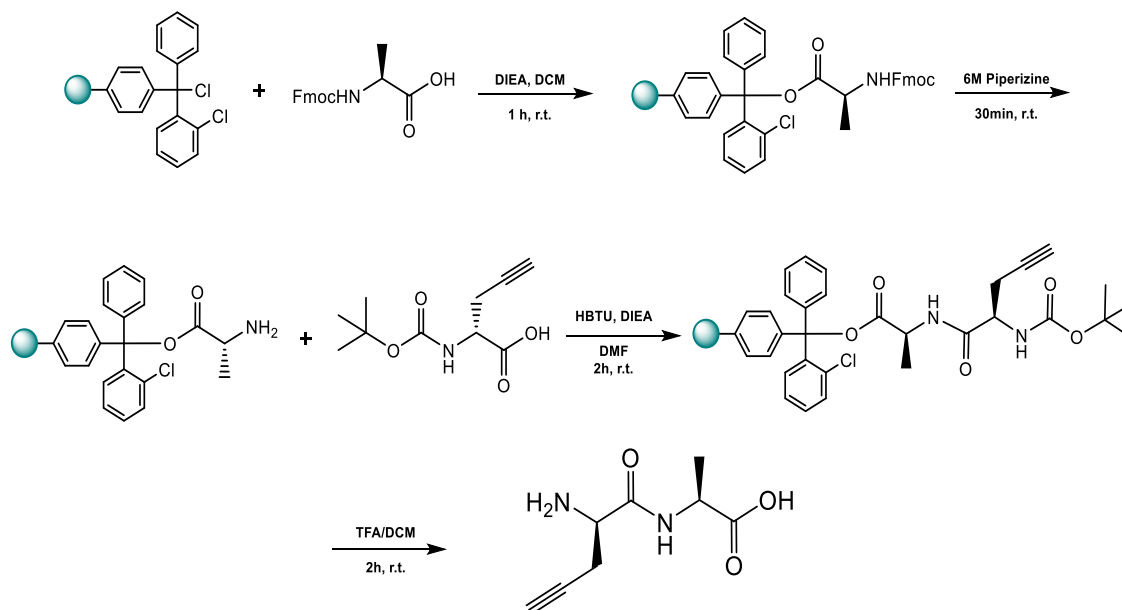
A 25 mL peptide synthesis vessel was charged with 2-Chlorotrityl chloride resin (500mg, 0.55mmol) was added Fmoc-D-alanine (1.1 eq, 188 mg, 0.605 mmol) and DIEA (3 eq, 0.286 mL, 1.65 mmol) in DCM (15 mL). The resin was agitated for 1 h at ambient



temperature and then washed with DMF, DCM, MeOH, CH<sub>2</sub>Cl<sub>2</sub>, and DMF (3 x 10 mL each). The Fmoc protecting group was removed with 6 M piperazine/100 mM HOBt in DMF (15 ml) for 30 min at ambient temperature, then washed as before. Boc-L-propargylglycine (3 eq, 351 mg, 1.65 mmol), HBTU (3 eq, 625 mg, 1.65 mmol), and DIEA (6 eq, 0.574 mL, 3.30 mmol) in DMF (10 mL) were added to the reaction flask and agitated for 2 h at ambient temperature. The resin was washed as before and added to a solution of TFA/DCM (1:1, 20 mL) with agitation for 2 h at ambient temperature. The resin was filtered and resulting solution concentrated *in vacuo*. The residue was triturated with cold diethyl ether to yield **L-Pra-D-Ala**.

<sup>1</sup>H NMR (500 MHz, CD<sub>3</sub>OD) : δ 1.46 (d, 3H, CH-CH<sub>3</sub>), 2.62 (t, 1H, C≡CH), 2.87 (m, 2H, CH-CH<sub>2</sub>-C-), 4.10 (q, 1H, CH-CH<sub>2</sub>), 4.43 (q, 1H, CH-CH<sub>3</sub>) <sup>13</sup>C NMR (125 MHz, CD<sub>3</sub>OD) : δ 16.40, 20.99, 48.49, 51.42, 73.57, 75.89, 167.11, 174.51 HRMS: [M+H]<sup>+</sup> calculated: 185.0921 found: 185.0931.

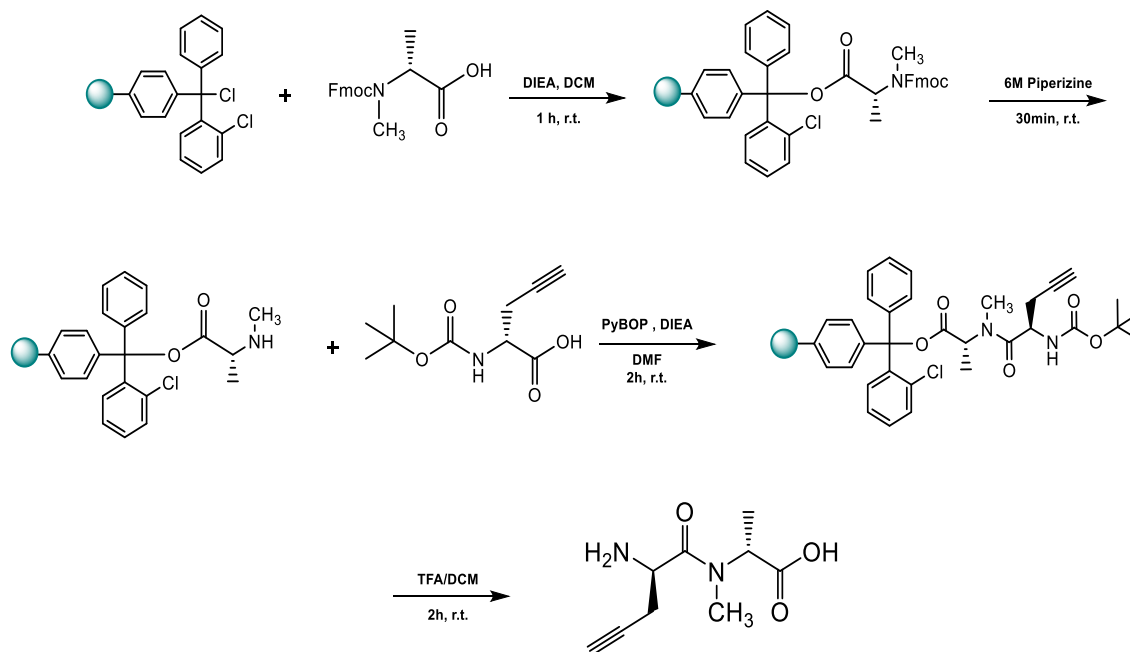
### Scheme S5. Synthesis of D-propargylglycine-L-alanine (D-Pra-L-Ala)



A 25 mL peptide synthesis vessel was charged with 2-Chlorotrityl chloride resin (500mg, 0.55mmol) was added Fmoc-L-alanine (1.1 eq, 188 mg, 0.605 mmol) and DIEA (3 eq, 0.286 mL, 1.65 mmol) in DCM (15 mL). The resin was agitated for 1 h at ambient temperature and then washed with DMF, DCM, MeOH, CH<sub>2</sub>Cl<sub>2</sub>, and DMF (3 x 10 mL each). The Fmoc protecting group was removed with 6 M piperazine/100 mM HOBt in DMF (15 ml) for 30 min at ambient temperature, then washed as before. Boc-D-propargylglycine (3 eq, 351 mg, 1.65 mmol), HBTU (3 eq, 625 mg, 1.65 mmol), and DIEA (6 eq, 0.574 mL, 3.30 mmol) in DMF (10 mL) were added to the reaction flask and agitated for 2 h at ambient temperature. The resin was washed as before and added to a solution of TFA/DCM (1:1, 20 mL) with agitation for 2 h at ambient temperature. The resin was filtered and resulting solution concentrated *in vacuo*. The residue was triturated with cold diethyl ether to yield **D-Pra-L-Ala**.

$^1\text{H}$  NMR (500 MHz,  $\text{CD}_3\text{OD}$ ) :  $\delta$  1.45 (d, 3H,  $\text{CH-CH}_3$ ), 2.64 (t, 1H,  $\text{C}\equiv\text{CH}$ ), 2.86 (m, 2H,  $\text{CH-CH}_2\text{-C-}$ ), 4.10 (q, 1H,  $\text{CH-CH}_2$ ), 4.45 (q, 1H,  $\text{CH-CH}_3$ )  $^{13}\text{C}$  NMR (125 MHz,  $\text{CD}_3\text{OD}$ ) :  $\delta$  16.10, 20.96, 48.53, 51.41, 73.53, 75.91, 167.06, 174.54 HRMS:  $[\text{M}+\text{H}]^+$  calculated: 185.0921 found: 185.0931.

**Scheme S6. Synthesis of D-propargylglycine-N-methyl-D-alanine (D-Pra-N-Me-D-Ala)**

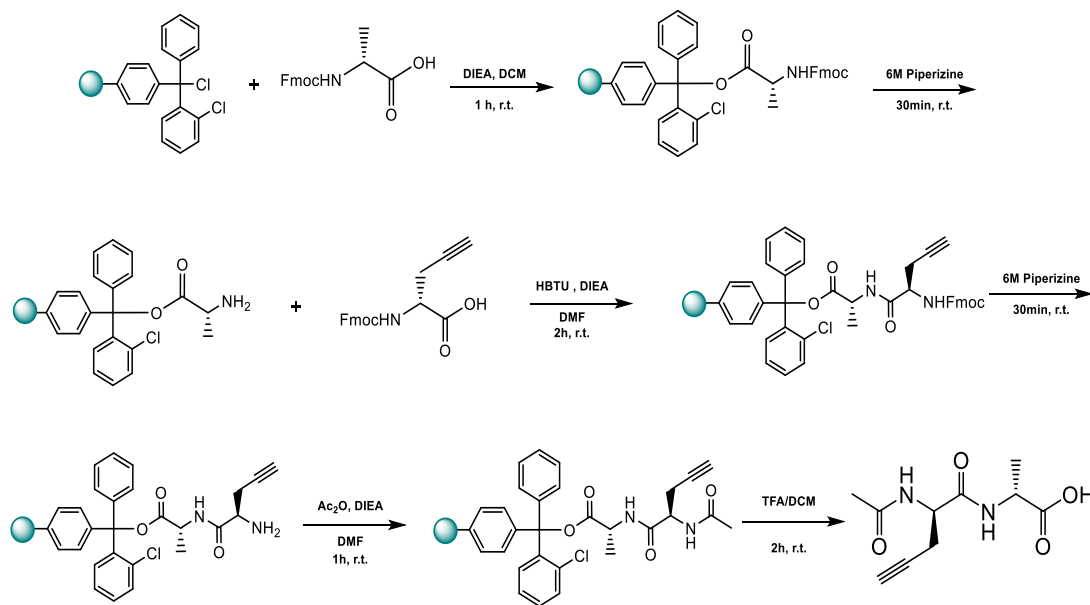


A 25 mL peptide synthesis vessel was charged with 2-Chlorotrityl chloride resin (500mg, 0.55mmol) was added Fmoc-*N*-methyl-D-alanine (1.1 eq, 196 mg, 0.605 mmol) and DIEA (3 eq, 0.286 mL, 1.65 mmol) in DCM (15 mL). The resin was agitated for 1 h at ambient temperature and then washed with DMF, DCM, MeOH,  $\text{CH}_2\text{Cl}_2$ , and DMF (3 x 10 mL each). The Fmoc protecting group was removed with 6 M piperazine/100 mM HOBt in DMF (15 ml) for 30 min at ambient temperature, then washed as before. Boc-D-propargylglycine (3 eq, 351 mg, 1.65 mmol), PyBOP (3 eq, 858 mg, 1.65 mmol), and DIEA (6 eq, 0.574 mL, 3.30 mmol) in DMF (10 mL) were added to the reaction flask and agitated

for 2 h at ambient temperature. The resin was washed as before and added to a solution of TFA/DCM (1:1, 20 mL) with agitation for 2 h at ambient temperature. The resin was filtered and resulting solution concentrated *in vacuo*. The residue was triturated with cold diethyl ether to yield **D-Pra-N-Me-D-Ala**.

$^1\text{H}$  NMR (500 MHz,  $\text{CD}_3\text{OD}$ ) :  $\delta$  1.66 (d, 3H,  $\text{CH-CH}_3$ ), 2.51 (t, 1H,  $\text{C}\equiv\text{CH}$ ), 2.74 (m, 2H,  $\text{CH-CH}_2\text{-C-}$ ), 2.99 (s, 3H,  $\text{NH-CH}_3$ ) 4.02 (q, 1H,  $\text{CH-CH}_2$ ), 4.17 (q, 1H,  $\text{CH-CH}_3$ )  $^{13}\text{C}$  NMR (125 MHz,  $\text{CD}_3\text{OD}$ ) :  $\delta$  18.94, 24.27, 31.33, 53.82, 57.32, 72.48, 78.73, 165.13, 169.09 HRMS:  $[\text{M}+\text{H}]^+$  calculated: 199.1077 found: 199.1069.

### Scheme S7. Synthesis of Acetyl-D-propargylglycine-D-alanine (Ac-D-Pra-D-Ala)

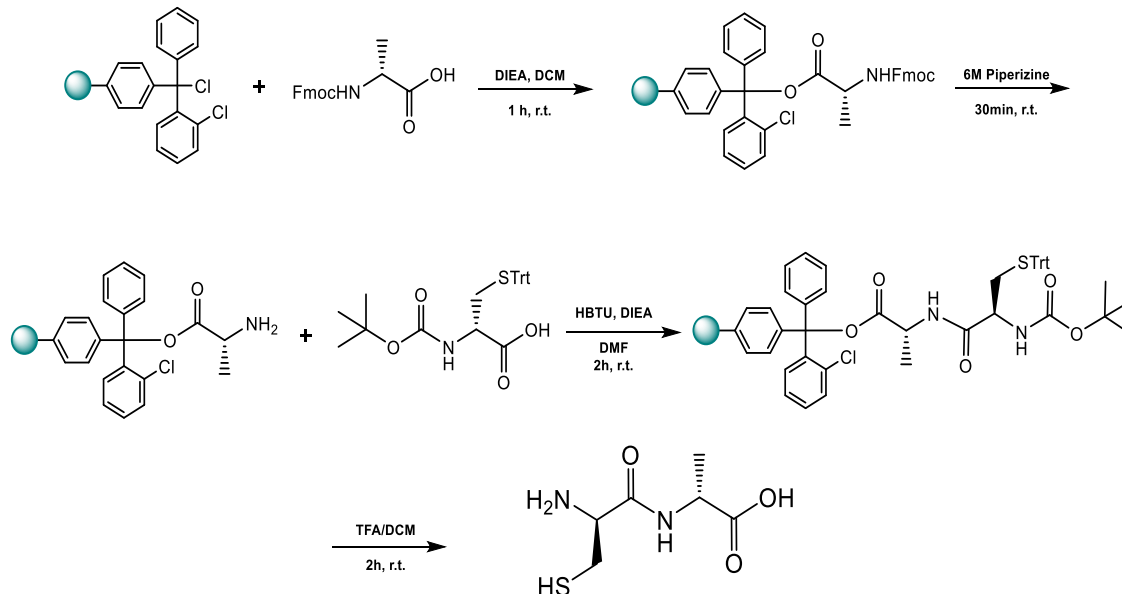


A 25 mL peptide synthesis vessel was charged with 2-Chlorotrityl chloride resin (500mg, 0.55mmol) was added Fmoc-D-alanine (1.1 eq, 188 mg, 0.605 mmol) and DIEA (3 eq, 0.286 mL, 1.65 mmol) in DCM (15 mL). The resin was agitated for 1 h at ambient temperature and then washed with DMF, DCM, MeOH,  $\text{CH}_2\text{Cl}_2$ , and DMF (3 x 10 mL each). The Fmoc protecting group was removed with 6 M piperazine/100 mM HOBt in

DMF (15 ml) for 30 min at ambient temperature, then washed as before. Fmoc-D-propargylglycine (3 eq, 552 mg, 1.65 mmol), HBTU (3 eq, 625 mg, 1.65 mmol), and DIEA (6 eq, 0.574 mL, 3.30 mmol) in DMF (10 mL) were added to the reaction flask and agitated for 2 h at ambient temperature. The resin was washed as before and the Fmoc protecting group was removed with 6 M piperazine/100 mM HOBt in DMF (15 ml) for 30 min at ambient temperature. The resin was washed and added acetic anhydride (10 eq, 0.512 mL, 5.5 mmol) and DIEA (10 eq, 0.956 mL, 5.5 mmol) in DMF (10mL) and agitated for 30 min at ambient temperature. The resin was washed and added to a solution of TFA/DCM (1:1, 20 mL) with agitation for 2 h at ambient temperature. The resin was filtered and resulting solution concentrated *in vacuo*. The residue was triturated with cold diethyl ether to yield **Ac-D-Pra-D-Ala**.

$^1\text{H}$  NMR (500 MHz,  $\text{CD}_3\text{OD}$ ) :  $\delta$  1.41 (d, 3H, CH- $\text{CH}_3$ ), 2.02 (s, 3H, OC- $\text{CH}_3$ ), 2.35 (m, 1H, C $\equiv$ C- $\text{CH}$ ), 2.64 (m, 2H, CH- $\text{CH}_2$ -C-) 4.40 (q, 1H, CH- $\text{CH}_2$ ), 4.53 (q, 1H, CH- $\text{CH}_3$ )  
 $^{13}\text{C}$  NMR (125 MHz,  $\text{CD}_3\text{OD}$ ) :  $\delta$  16.30, 20.99, 21.24, 52.16, 70.66, 78.95, 170.85, 172.00,  
174.25 HRMS: [M-H] calculated: 225.0894 found: 225.0874.

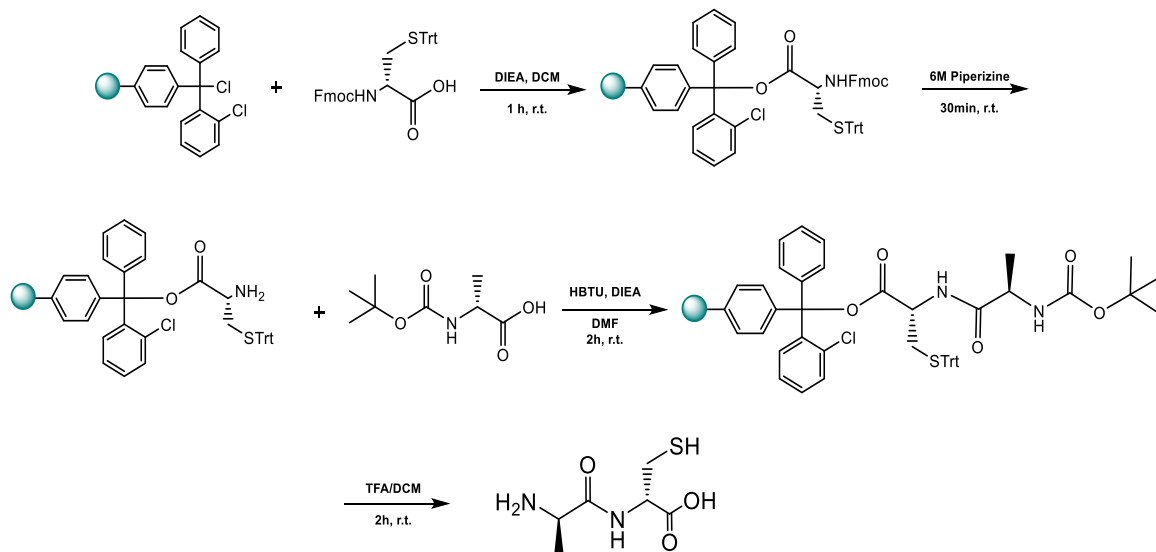
### Scheme S8. Synthesis of D-cysteine-D-alanine (D-Cys-D-Ala)



A 25 mL peptide synthesis vessel was charged with 2-Chlorotrityl chloride resin (500mg, 0.55mmol) was added Fmoc-D-alanine (1.1 eq, 188 mg, 0.605 mmol) and DIEA (3 eq, 0.286 mL, 1.65 mmol) in DCM (15 mL). The resin was agitated for 1 h at ambient temperature and then washed with DMF, DCM, MeOH, CH<sub>2</sub>Cl<sub>2</sub>, and DMF (3 x 10 mL each). The Fmoc protecting group was removed with 6 M piperazine/100 mM HOBt in DMF (15 ml) for 30 min at ambient temperature, then washed as before. Boc-S-trityl-D-cysteine (3 eq, 763 mg, 1.65 mmol), HBTU (3 eq, 625 mg, 1.65 mmol), and DIEA (6 eq, 0.574 mL, 3.30 mmol) in DMF (10 mL) were added to the reaction flask and agitated for 2 h at ambient temperature. The resin was washed as before and added to a solution of TFA/DCM (1:1, 20 mL) with agitation for 2 h at ambient temperature. The resin was filtered and resulting solution concentrated *in vacuo*. The residue was triturated with cold diethyl ether to yield **D-Cys-D-Ala**.

$^1\text{H}$  NMR (500 MHz,  $\text{CD}_3\text{OD}$ ) :  $\delta$  1.45 (d, 1H,  $\text{CH-CH}_3$ ), 3.08 (m, 2H,  $\text{CH-CH}_2\text{-SH}$ ), 4.18 (t, 1H,  $\text{CH-CH}_2$ ), 4.43 (q, 1H,  $\text{CH-CH}_3$ )  $^{13}\text{C}$  NMR (125 MHz,  $\text{CD}_3\text{OD}$ ) :  $\delta$  15.90, 25.28, 48.50, 54.25, 167.13, 174.56 HRMS:  $[\text{M}+\text{H}]^+$  calculated: 193.0641 found: 193.0649.

**Scheme S9. Synthesis of D-alanine-D-cysteine (D-Ala-D-Cys)**

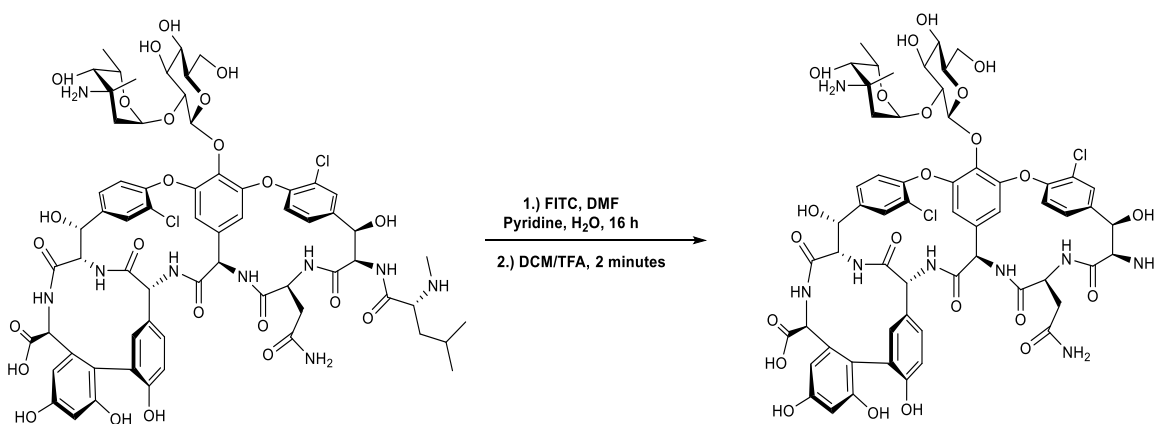


A 25 mL peptide synthesis vessel was charged with 2-Chlorotrityl chloride resin (500mg, 0.55mmol) was added Fmoc-S-trityl-D-cysteine (1.1 eq, 354 mg, 0.605 mmol) and DIEA (3 eq, 0.286 mL, 1.65 mmol) in DCM (15 mL). The resin was agitated for 1 h at ambient temperature and then washed with DMF, DCM, MeOH,  $\text{CH}_2\text{Cl}_2$ , and DMF (3 x 10 mL each). The Fmoc protecting group was removed with 6 M piperazine/100 mM HOBt in DMF (15 ml) for 30 min at ambient temperature, then washed as before. Boc-D-alanine (3 eq, 312 mg, 1.65 mmol), HBTU (3 eq, 625 mg, 1.65 mmol), and DIEA (6 eq, 0.574 mL, 3.30 mmol) in DMF (10 mL) were added to the reaction flask and agitated for 2 h at ambient temperature. The resin was washed as before and added to a solution of TFA/DCM (1:1, 20 mL) with agitation for 2 h at ambient temperature. The resin was filtered and

resulting solution concentrated *in vacuo*. The residue was triturated with cold diethyl ether to yield **D-Ala-D-Cys**.

$^1\text{H}$  NMR (500 MHz,  $\text{CD}_3\text{OD}$ ) :  $\delta$  1.55 (d, 1H, CH- $\text{CH}_3$ ), 2.97 (m, 2H, CH- $\text{CH}_2$ -SH), 4.13 (t, 1H, CH- $\text{CH}_2$ ), 4.66 (q, 1H, CH- $\text{CH}_3$ )  $^{13}\text{C}$  NMR (125 MHz,  $\text{CD}_3\text{OD}$ ) :  $\delta$  16.36, 25.29, 48.88, 54.91, 170.15, 171.61 HRMS:  $[\text{M}+\text{H}]^+$  calculated: 193.0641 found: 193.0643.

### Scheme S10. Synthesis of Desleucyl-vancomycin

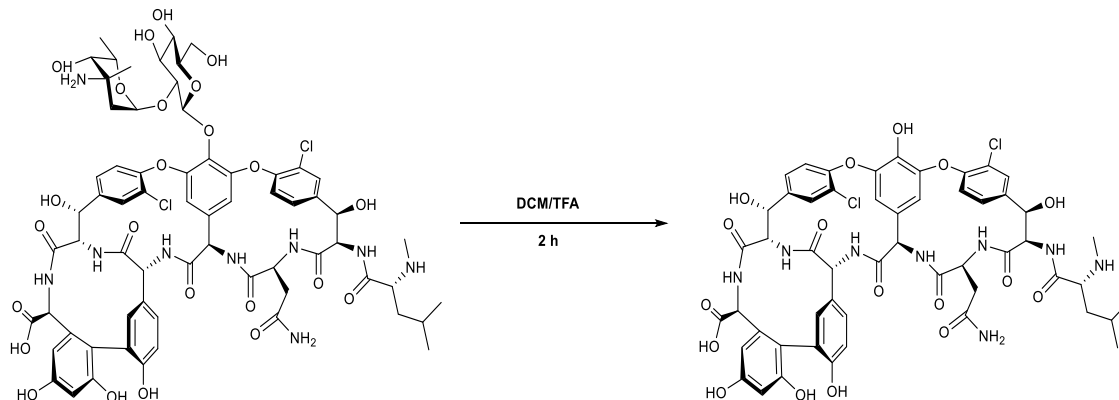


Vancomycin hydrochloride (100 mg, 0.067 mmol) was dissolved in pyridine (1.0 mL) and water (1.0 mL). Fluorescein isothiocyanate (FITC) (29 mg, 0.075 mmol) in DMF (0.5 mL) was added to the solution and stirred for 16 h. The solution was concentrated *in vacuo*, resuspended in water (3 mL), and lyophilized. The resultant powder was dissolved in dichloromethane (1 mL) and trifluoroacetic acid (1 mL). The mixture was stirred for 2 min and immediately concentrated *in vacuo*. Water (5 mL) was added to the residue and extracted with diethyl ether (2 x 5 mL). The aqueous layer was lyophilized and powder resuspended in water (3 mL) and filtered. The filtrate was purified by reverse-phase HPLC and lyophilized to yield pure desleucyl-vancomycin as a white powder.

MS (ESI)  $[\text{M}+\text{H}]^+$  calculated: 1323.3 found: 1323.3.



### Scheme S13. Synthesis of Aglycon-vancomycin



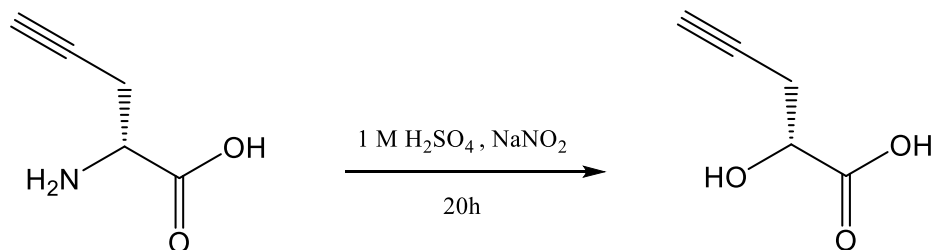
Vancomycin hydrochloride (100 mg, 0.067 mmol) was dissolved in DCM (5.0 mL) and TFA (5.0 mL) and stirred at ambient temperature for 2 h. The solution was concentrated *in vacuo* and the crude product lyophilized. The crude powder was purified by reverse-phase HPLC and lyophilized to yield pure aglycon-vancomycin as a white powder.

MS (ESI)  $[M+H]^+$  calculated: 1144.9 found: 1145.4.

## A.7 Appendix for Chapter 7

### Compound Synthesis and Characterization

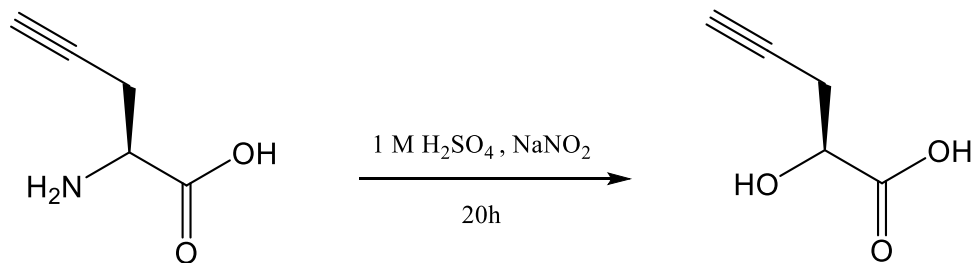
#### Scheme S1. Synthesis of D-2-Hydroxy-pent-4-ynoic acid (D-Laclick)



Adapted from literature.<sup>1</sup> D-propargylglycine (1.00 g, 8.85 mmol) was dissolved in 1 M H<sub>2</sub>SO<sub>4</sub> (50 mL) and cooled to 0 °C. A solution of sodium nitrite (40% aq, 6.5 mL) was added dropwise, maintaining the temperature at or below 0 °C. The reaction was stirred for 3 h at 0 °C, then allowed to warm to ambient temperature for 17 h. The mixture was extracted with EtOAc (3 x 75 mL), organic layers dried with MgSO<sub>4</sub>, and concentrated *in vacuo* to yield **D-Laclick** as a yellow oil which was used without further purification.

<sup>1</sup>H NMR (500 MHz, CD<sub>3</sub>OD) : δ 2.27 (m, 1H, C≡CH), 2.60 (m, 2H, CH-CH<sub>2</sub>-C-), 4.18 (q, 1H, CH-CH<sub>2</sub>)<sup>13</sup>C NMR (125 MHz, D<sub>2</sub>O) : δ 23.89, 69.51, 71.32, 80.40, 177.85 HRMS: [M-H]<sup>-</sup> calculated: 113.0244 found: 113.0216

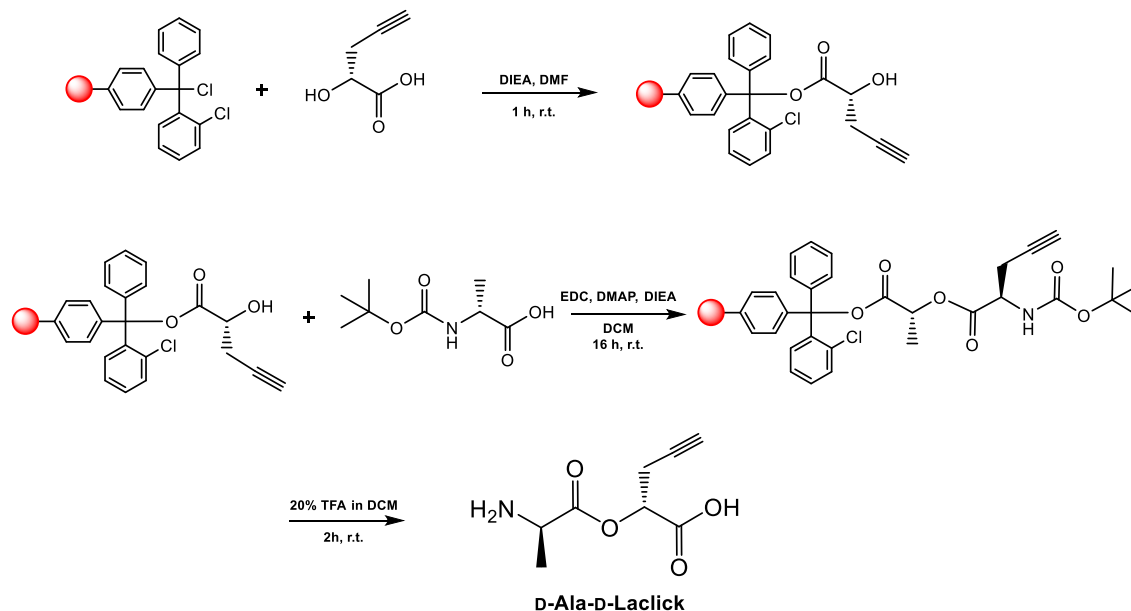
#### Scheme S2. Synthesis of L-2-Hydroxy-pent-4-ynoic acid (L-Laclick)



L-propargylglycine (1.00 g, 8.85 mmol) was dissolved in 1 M H<sub>2</sub>SO<sub>4</sub> (50 mL) and cooled to 0 °C. A solution of sodium nitrite (40% aq, 6.5 mL) was added dropwise, maintaining the temperature at or below 0 °C. The reaction was stirred for 3 h at 0 °C, then allowed to warm to ambient temperature for 17 h. The mixture was extracted with EtOAc (3 x 75 mL), organic layers dried with MgSO<sub>4</sub>, and concentrated *in vacuo* to yield **L-Laclick** as a yellow oil which was used without further purification.

<sup>1</sup>H NMR (500 MHz, CD<sub>3</sub>OD) : δ 2.27 (m, 1H, C≡CH), 2.63 (m, 2H, CH-CH<sub>2</sub>-C-), 4.27 (q, 1H, CH-CH<sub>2</sub>), 5.43 (br, 1H, CH-OH) <sup>13</sup>C NMR (125 MHz, CD<sub>3</sub>OD) : δ 24.01, 68.87, 70.56, 79.12, 174.61 HRMS: [M-H]<sup>-</sup> calculated: 113.0244 found: 113.0253

### Scheme S3. Synthesis of D-Ala-D-Laclick.

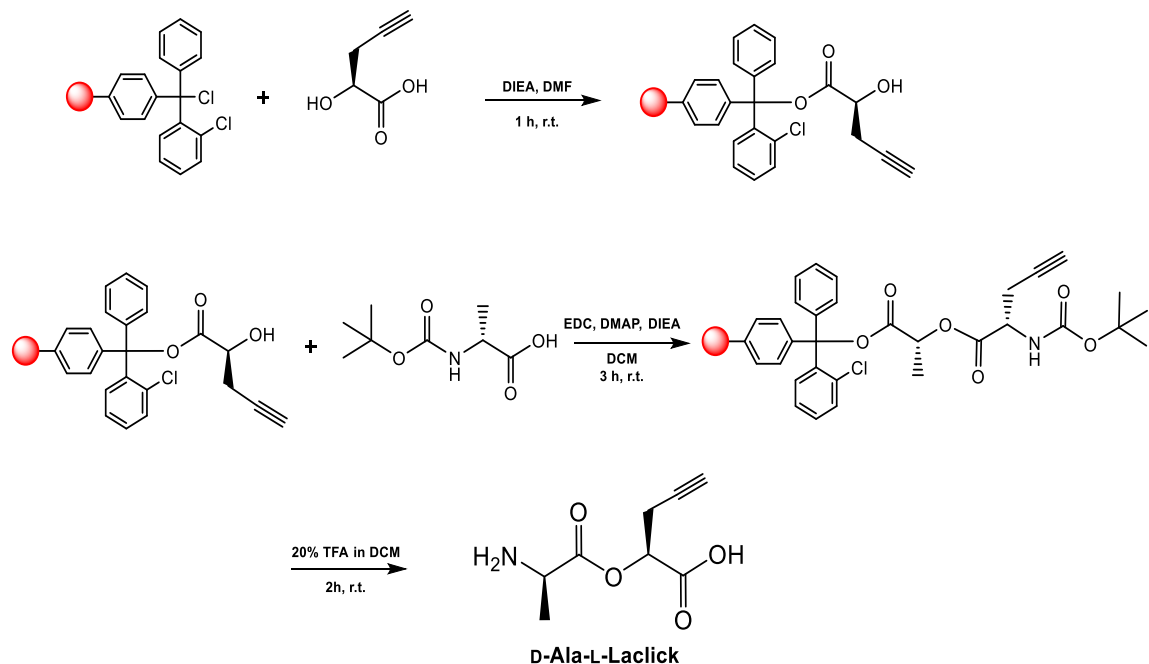


A 25 mL peptide synthesis vessel was charged with 2-Chlorotrityl chloride resin (500mg, 0.55mmol) was added D-Laclick (1.1 eq, 68.9 mg, 0.605 mmol) and DIEA (3 eq, 0.286 mL, 1.65 mmol) in dry DMF (15 mL). The resin was agitated for 1 h at ambient temperature and then washed with DMF, DCM, MeOH, CH<sub>2</sub>Cl<sub>2</sub>, and DMF (3 x 10 mL each). Boc-D-alanine (3 eq, 312 mg, 1.65 mmol), EDC (3 eq, 255 mg, 1.65 mmol), DMAP (3 eq, 201

mg, 1.65 mmol) and DIEA (6 eq, 0.574 mL, 3.30 mmol) in DCM (10 mL) were added to the reaction flask and agitated 16 h at ambient temperature. The resin was washed as before and added to a solution of TFA (20%) in DCM (20 mL) with agitation for 2 h at ambient temperature. The resin was filtered and resulting solution concentrated *in vacuo*. The residue was triturated with cold diethyl ether and purified by reverse-phase HPLC using H<sub>2</sub>O-MeOH to yield **D-Ala-D-Laclick**.

<sup>1</sup>H NMR (400 MHz, CD<sub>3</sub>OD) : δ 1.61 (d, 3H, -CH<sub>3</sub>), 2.42 (m, 1H, C≡CH), 2.84 (m, 2H, CH-CH<sub>2</sub>-C-), 4.20 (q, 1H, CH-CH<sub>3</sub>), 5.27 (t, 1H, CH-CH<sub>2</sub>) <sup>13</sup>C NMR (100 MHz, CD<sub>3</sub>OD) : δ 14.94, 20.71, 48.26, 71.16, 71.68, 77.50, 169.08, 169.30 HRMS: [M+H]<sup>+</sup> calculated: 186.0761 found: 186.0774

#### Scheme S4. Synthesis of D-Ala-L-Laclick.

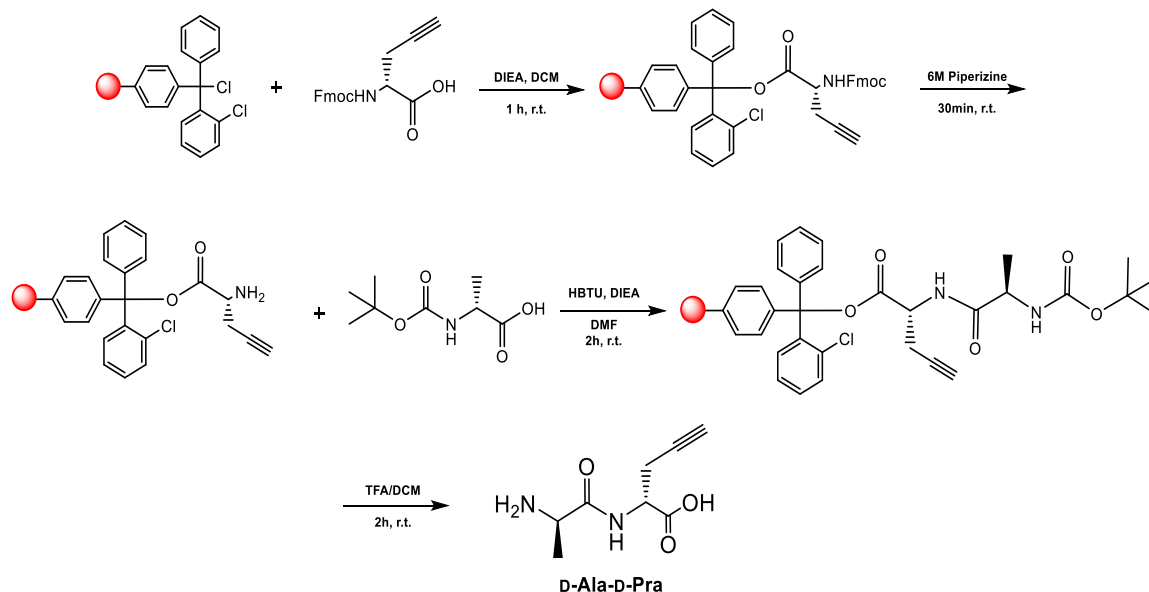


A 25 mL peptide synthesis vessel was charged with 2-Chlorotrityl chloride resin (500mg, 0.55mmol) was added L-Laclick (1.1 eq, 68.9 mg, 0.605 mmol) and DIEA (3 eq, 0.286 mL, 1.65 mmol) in dry DMF (15 mL). The resin was agitated for 1 h at ambient temperature

and then washed with DMF, DCM, MeOH, CH<sub>2</sub>Cl<sub>2</sub>, and DMF (3 x 10 mL each). Boc-D-alanine (3 eq, 312 mg, 1.65 mmol), EDC (3 eq, 255 mg, 1.65 mmol), DMAP (3 eq, 201 mg, 1.65 mmol) and DIEA (6 eq, 0.574 mL, 3.30 mmol) in DCM (10 mL) were added to the reaction flask and agitated overnight at ambient temperature. The resin was washed as before and added to a solution of TFA (20%) in DCM (20 mL) with agitation for 2 h at ambient temperature. The resin was filtered and resulting solution concentrated *in vacuo*. The residue was triturated with cold diethyl ether and purified by reverse-phase HPLC using H<sub>2</sub>O-MeOH to yield **D-Ala-L-Lalck**.

<sup>1</sup>H NMR (400 MHz, CD<sub>3</sub>OD) : δ 1.62 (d, 3H, -CH<sub>3</sub>), 2.43 (m, 1H, C≡CH), 2.85 (m, 2H, CH-CH<sub>2</sub>-C-), 4.21 (q, 1H, CH-CH<sub>3</sub>), 5.26 (t, 1H, CH-CH<sub>2</sub>) <sup>13</sup>C NMR (100 MHz, CD<sub>3</sub>OD) : δ 14.94, 20.69, 48.29, 71.13, 71.68, 77.48, 169.09, 169.29 HRMS: [M+H]<sup>+</sup> calculated: 186.0761 found: 186.0782

#### Scheme S5. Synthesis of D-Ala-D-Pra.

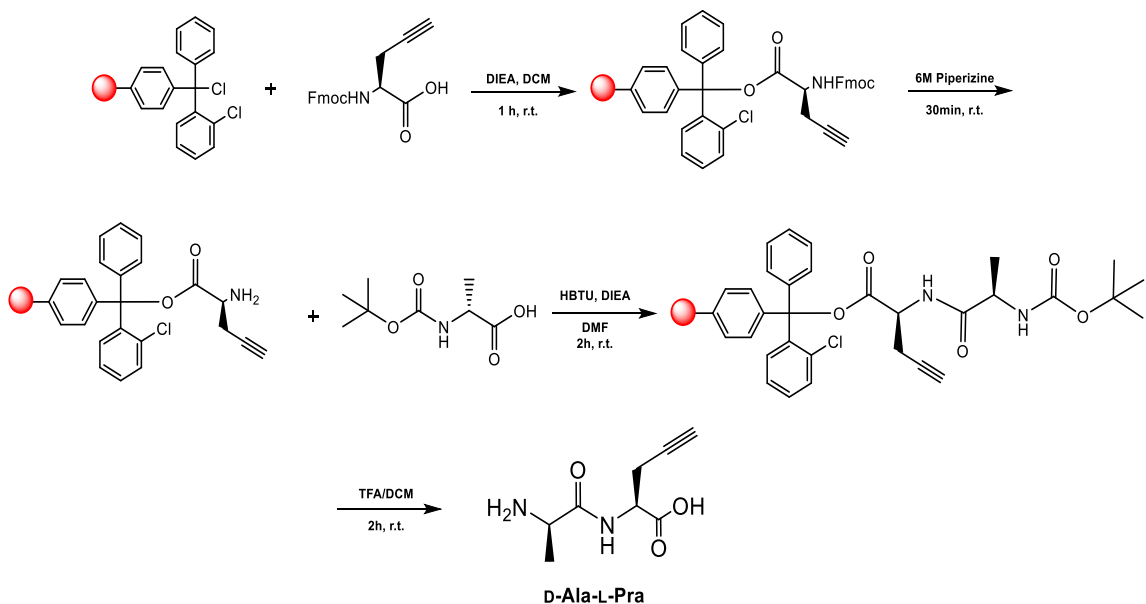


A 25 mL peptide synthesis vessel was charged with 2-Chlorotrityl chloride resin (500mg, 0.55mmol) was added Fmoc-D-propargylglycine (1.1 eq, 202 mg, 0.605 mmol) and DIEA

(3 eq, 0.286 mL, 1.65 mmol) in DCM (15 mL). The resin was agitated for 1 h at ambient temperature and then washed with DMF, DCM, MeOH, CH<sub>2</sub>Cl<sub>2</sub>, and DMF (3 x 10 mL each). The Fmoc protecting group was removed with 6 M piperazine/100 mM HOBt in DMF (15 ml) for 30 min at ambient temperature, then washed as before. Boc-D-alanine (3 eq, 312 mg, 1.65 mmol), HBTU (3 eq, 625 mg, 1.65 mmol), and DIEA (6 eq, 0.574 mL, 3.30 mmol) in DMF (10 mL) were added to the reaction flask and agitated for 2 h at ambient temperature. The resin was washed as before and added to a solution of TFA/DCM (1:1, 20 mL) with agitation for 2 h at ambient temperature. The resin was filtered and resulting solution concentrated *in vacuo*. The residue was triturated with cold diethyl ether to yield **D-Ala-D-Pra**.

<sup>1</sup>H NMR (500 MHz, CD<sub>3</sub>OD) : δ 1.55 (d, 3H, -CH<sub>3</sub>), 2.39 (m, 1H, C≡CH), 2.78 (m, 2H, CH-CH<sub>2</sub>-C-), 4.09 (q, 1H, CH-CH<sub>3</sub>), 4.59 (t, 1H, CH-CH<sub>2</sub>) <sup>13</sup>C NMR (125 MHz, CD<sub>3</sub>OD) : δ 16.34, 20.87, 48.80, 51.54, 71.12, 78.59, 169.91, 171.61 HRMS: [M+H]<sup>+</sup> calculated: 185.0921 found: 185.0923

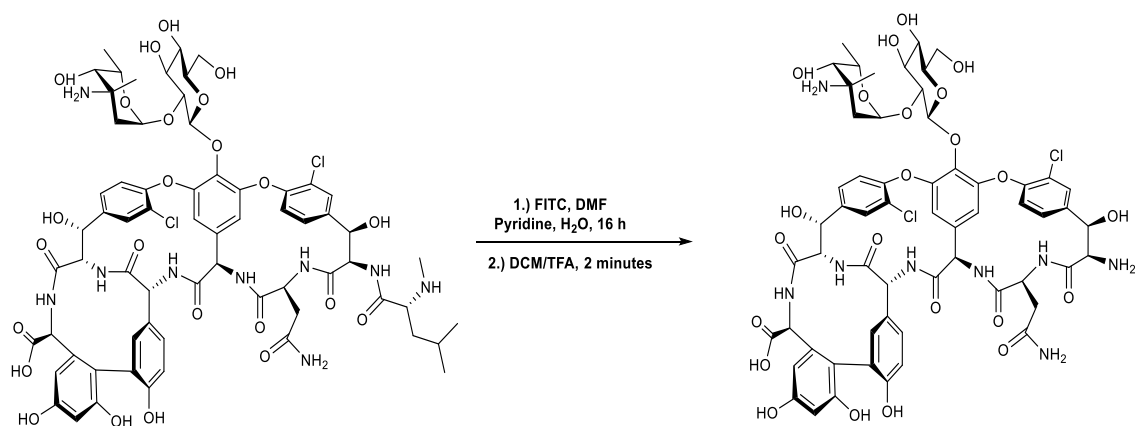
### Scheme S6. Synthesis of D-Ala-L-Pra.



A 25 mL peptide synthesis vessel was charged with 2-Chlorotrityl chloride resin (500mg, 0.55mmol) was added Fmoc-L-propargylglycine (1.1 eq, 202 mg, 0.605 mmol) and DIEA (3 eq, 0.286 mL, 1.65 mmol) in DCM (15 mL). The resin was agitated for 1 h at ambient temperature and then washed with DMF, DCM, MeOH, CH<sub>2</sub>Cl<sub>2</sub>, and DMF (3 x 10 mL each). The Fmoc protecting group was removed with 6 M piperazine/100 mM HOBt in DMF (15 ml) for 30 min at ambient temperature, then washed as before. Boc-D-alanine (3 eq, 312 mg, 1.65 mmol), HBTU (3 eq, 625 mg, 1.65 mmol), and DIEA (6 eq, 0.574 mL, 3.30 mmol) in DMF (10 mL) were added to the reaction flask and agitated for 2 h at ambient temperature. The resin was washed as before and added to a solution of TFA/DCM (1:1, 20 mL) with agitation for 2 h at ambient temperature. The resin was filtered and resulting solution concentrated *in vacuo*. The residue was triturated with cold diethyl ether to yield **D-Ala-L-Pra**.

<sup>1</sup>H NMR (400 MHz, D<sub>2</sub>O) : δ 1.39 (d, 3H, -CH<sub>3</sub>), 2.26 (m, 1H, C≡CH), 2.62 (m, 2H, CH-CH<sub>2</sub>-C-), 3.97 (q, 1H, CH-CH<sub>3</sub>), 4.48 (t, 1H, CH-CH<sub>2</sub>) <sup>13</sup>C NMR (100 MHz, D<sub>2</sub>O) : δ 16.98, 20.96, 49.03, 51.46, 72.07, 79.18, 170.83, 173.60 HRMS: [M+H]<sup>+</sup> calculated: 185.0921 found: 185.0948.

### Scheme S7. Synthesis of Deslucyl-vancomycin

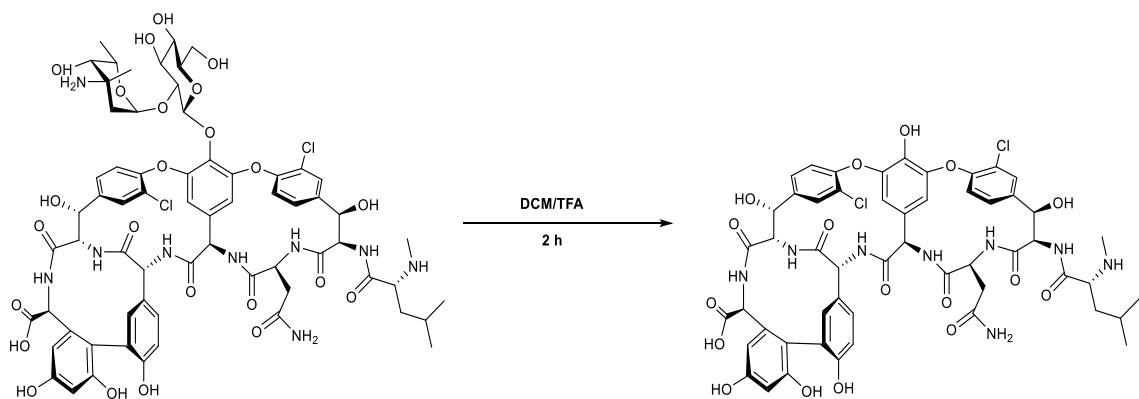


Vancomycin hydrochloride (100 mg, 0.067 mmol) was dissolved in pyridine (1.0 mL) and water (1.0 mL). Fluorescein isothiocyanate (FITC) (29 mg, 0.075 mmol) in DMF (0.5 mL) was added to the solution and stirred for 16 h. The solution was concentrated *in vacuo*, resuspended in water (3 mL), and lyophilized. The resultant powder was dissolved in dichloromethane (1 mL) and trifluoroacetic acid (1 mL). The mixture was stirred for 2 min and immediately concentrated *in vacuo*. Water (5 mL) was added to the residue and extracted with diethyl ether (2 x 5 mL). The aqueous layer was lyophilized and powder resuspended in water (3 mL) and filtered. The filtrate was purified by reverse-phase HPLC and lyophilized to yield pure deslucyl-vancomycin as a white powder.

MS (ESI) [M+H]<sup>+</sup> calculated: 1323.3 found: 1323.3



### Scheme S8. Synthesis of Aglycon-vancomycin

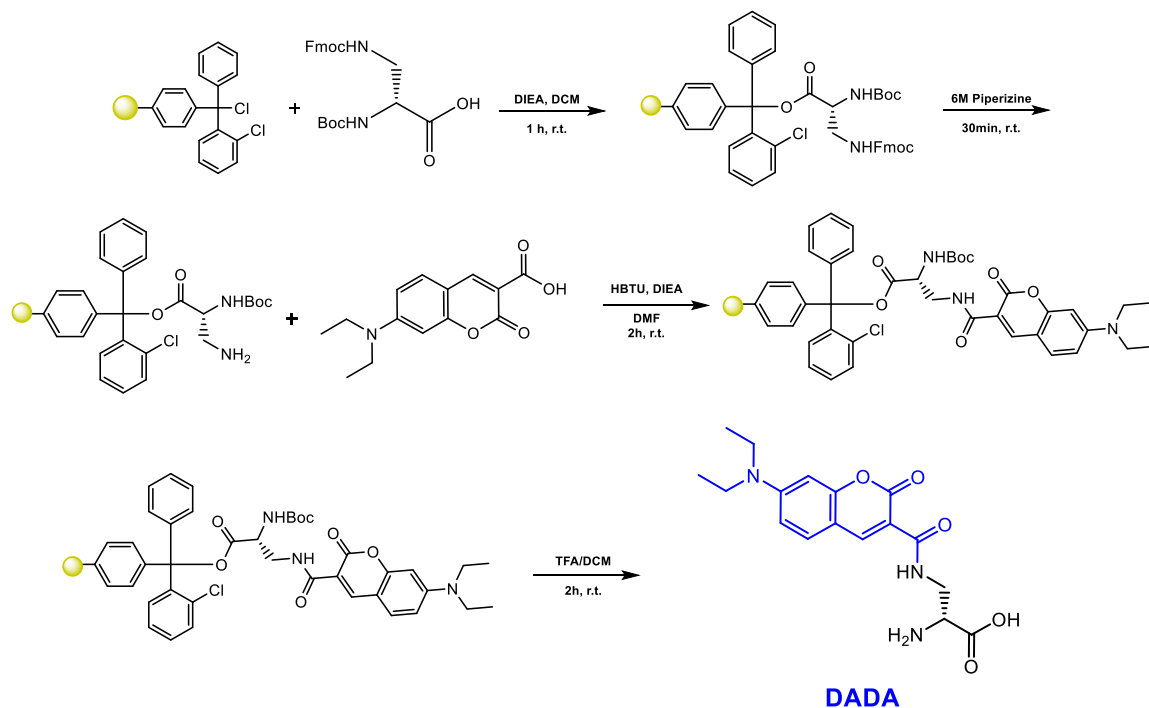


Vancomycin hydrochloride (100 mg, 0.067 mmol) was dissolved in DCM (5.0 mL) and TFA (5.0 mL) and stirred at ambient temperature for 2 h. The solution was concentrated *in vacuo* and the crude product lyophilized. The crude powder was purified by reverse-phase HPLC and lyophilized to yield pure aglycon-vancomycin as a white powder.

MS (ESI)  $[M+H]^+$  calculated: 1144.9 found: 1145.4

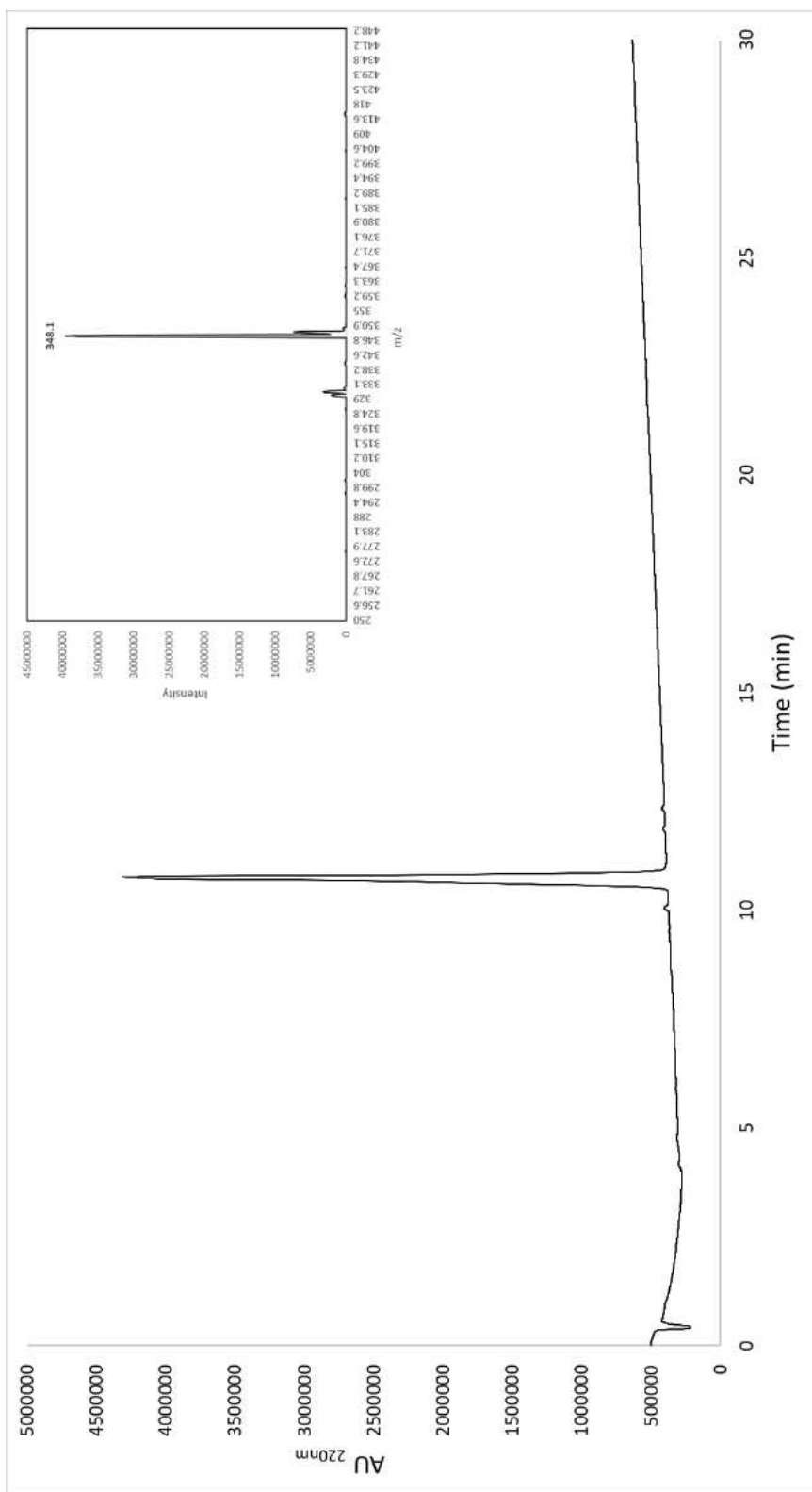
## A.8 Appendix for Chapter 8

### Scheme S1. Synthesis of (Diethylamino)coumarin-carbonyl-amino-D-alanine (**DADA**)



A 25 mL peptide synthesis vessel charged with 2-Chlorotrityl chloride resin (500mg, 0.55mmol) was added  $N^{\alpha}$ -Boc- $N^{\beta}$ -Fmoc-D-2,3-diaminopropionic acid (1.1 eq, 258 mg, 0.605 mmol) and DIEA (3 eq, 0.286 mL, 1.65 mmol) in dry DCM (15 mL). The resin was shaken for 1 h at ambient temperature and washed with MeOH and DCM (3 x 15 mL each). The Fmoc protecting group was removed with 6 M piperazine/100 mM HOBt in DMF (15 ml) for 30 min then washed as before. 7-(Diethylamino)coumarin-3-carboxylic acid (3 eq, 430 mg, 1.65 mmol), HBTU (3 eq, 625 mg, 1.65 mmol), and DIEA (6 eq, 0.574 mL, 3.30 mmol) in DMF (15 mL) were added to the reaction flask and agitated for 2 h at ambient temperature. The resin was washed as before and added to a solution of TFA/DCM (2:1, 20 mL) with agitation for 2 h at ambient temperature. The resin was filtered and resulting solution concentrated *in vacuo*. The residue was triturated with cold diethyl ether and purified using reverse phase HPLC using H<sub>2</sub>O/MeOH to yield **DADA**. The sample was analyzed for purity using a Shimadzu LC 2020 with a Phenomenex Luna 5 $\mu$  C18(2) 100 $\text{\AA}$  (30 x 2.00 mm) column; gradient elution with H<sub>2</sub>O/CH<sub>3</sub>CN.

$^1\text{H}$  NMR (400 MHz, DMSO) :  $\delta$  1.15 (t, 6H,  $\text{CH}_2\text{-CH}_3$ ), 3.80 (m, 2H,  $\text{-CH-CH}_2\text{-NH}$ ), 4.15 (t, 1H,  $\text{-CH-CH}_2\text{-NH-}$ ), 6.65 (s, 1H,  $\text{-C-CH-C-}$ ), 6.85 (d, 1H,  $\text{-C-CH-CH-}$ ), 7.70 (d, 1H,  $\text{-CH-CH-C-}$ ), 8.70 (s, 1H,  $\text{-C-CH-C-}$ )  $^{13}\text{C}$  NMR (DMSO) :  $\delta$  12.76, 44.82, 52.43, 96.28, 108.00, 109.28, 110.70, 132.22, 148.41, 153.09, 157.79, 162.01, 163.84, 169.92 ESI-MS:  $[\text{M}+\text{H}]^+$  calculated: 348.1 found: 348.1





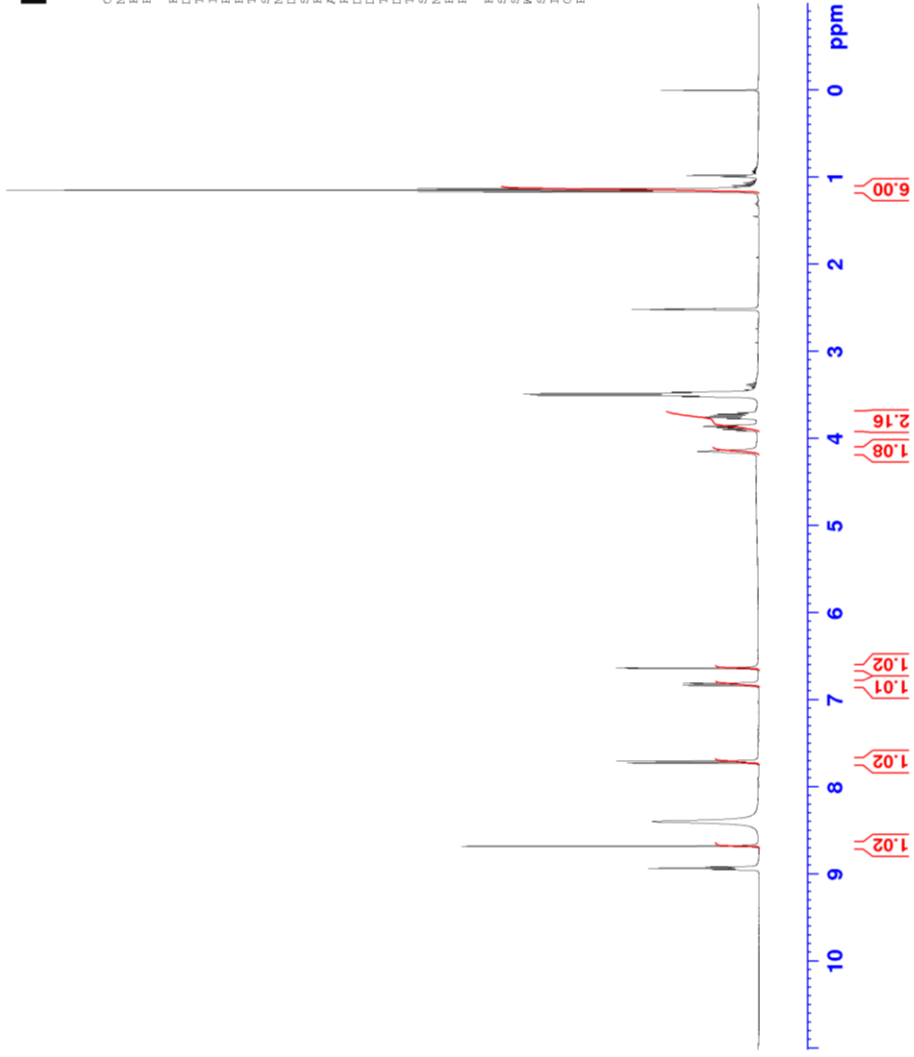
Current Data Parameters  
NAME D-Dsp-DiethylaminoCoumarin  
EXPNO 1  
PROCNO 1

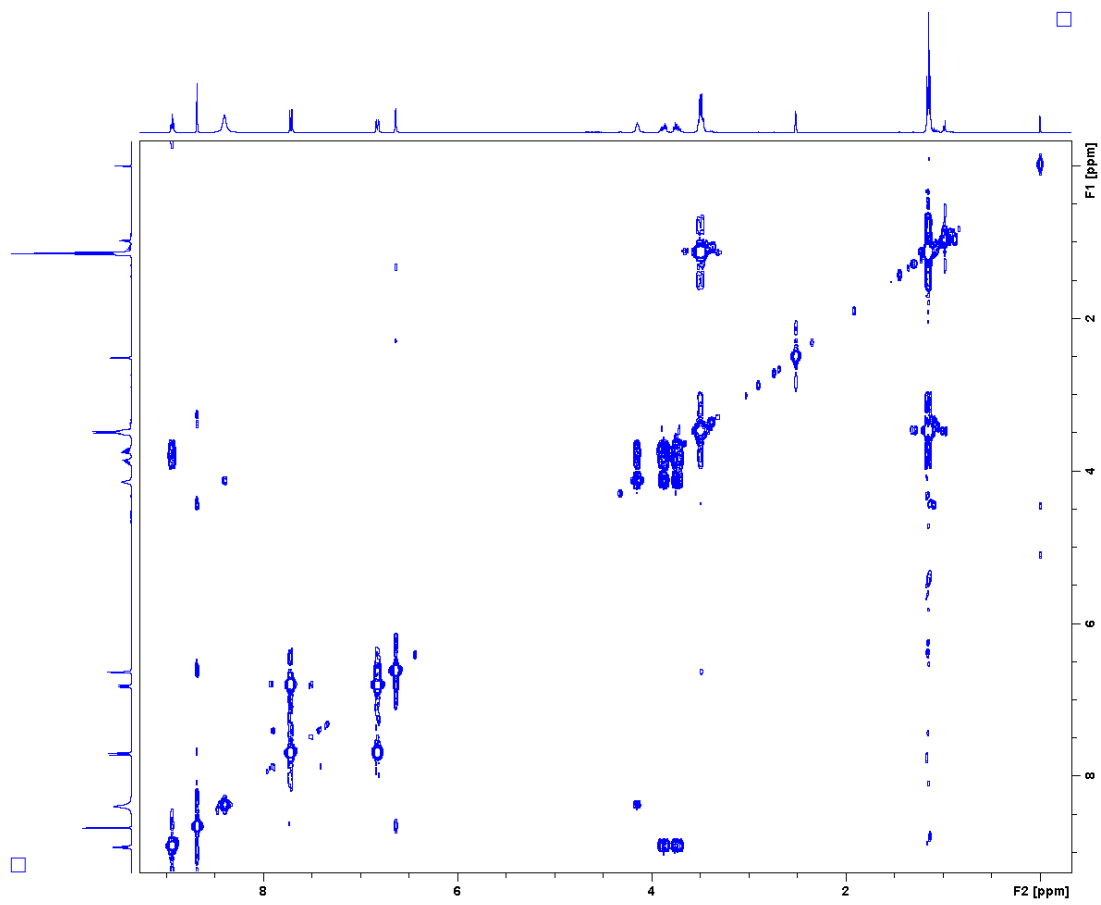
F2 - Acquisition Parameters

Date\_ 20100227  
Time 20:27 h  
INSTRUM spect  
PROBHD Z116098\_0480 ( zq30  
TD 49152  
SOLVENT DMSO  
NS 16  
DS 0  
SWH 4807.692 Hz  
FIDRES 0.195625 Hz  
AQ 5.1118078 sec  
RG 327.500  
DM 104.000 usec  
DE 6.50 usec  
TE 290.6 K  
D1 1.00000000 sec  
DELTA 0.00000000 sec  
SFO1 400.1320017 MHz  
NUC1 1H  
P1 8.77 usec  
PLW1 17.00000000 W

F2 - Processing parameters

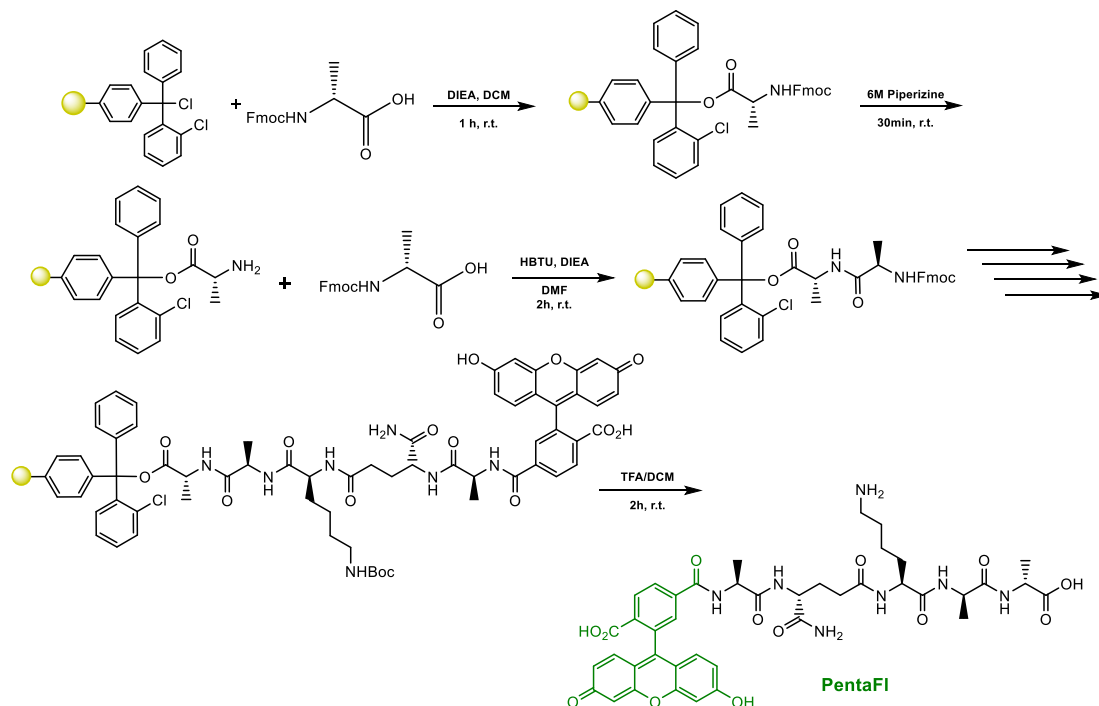
SI 65536  
SF 400.1299968 MHz  
WDW EM  
SSB 0  
LB 0  
GB 0  
PC 1.00







## Scheme S2. Synthesis of PentaFl

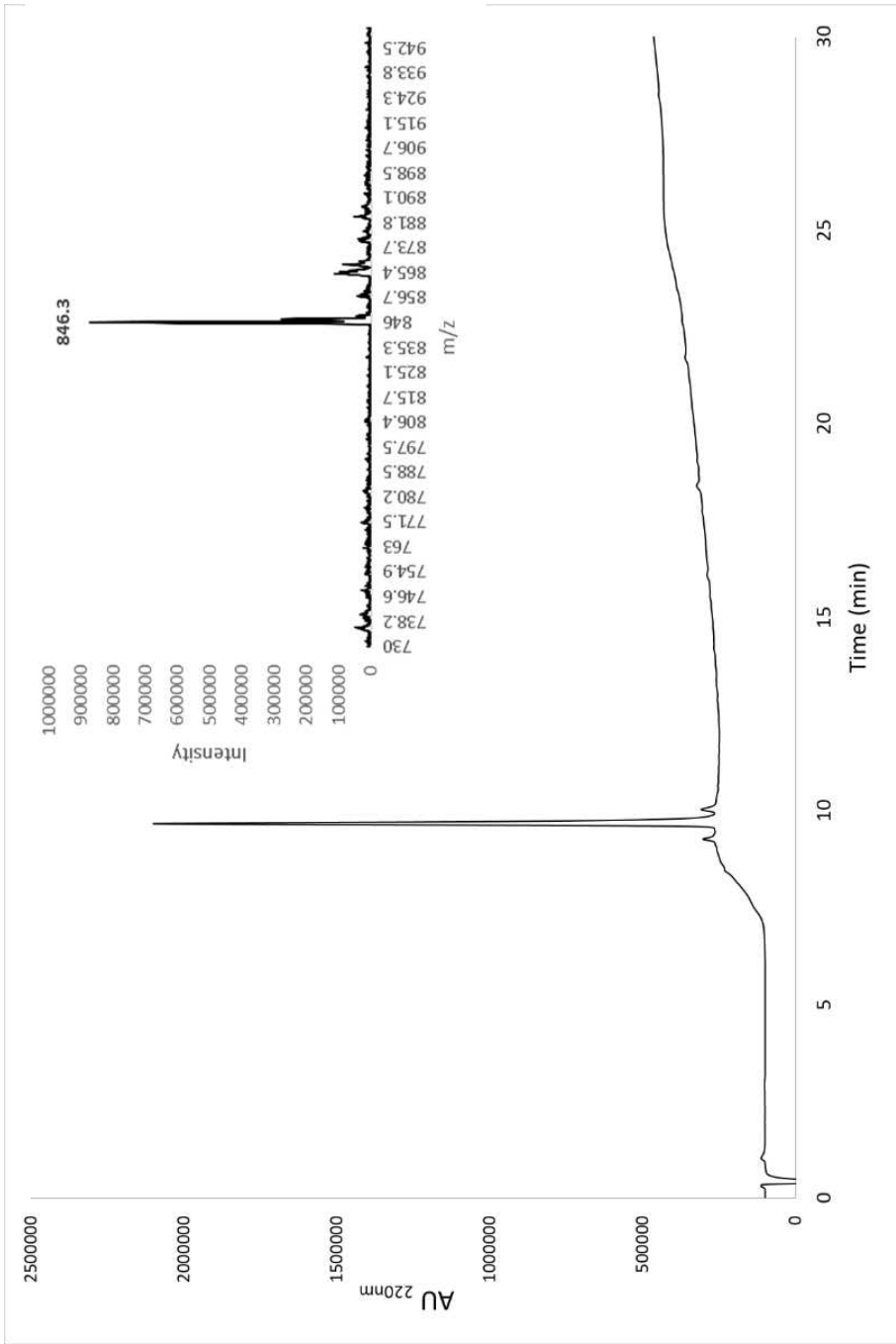


A 25 mL peptide synthesis vessel charged with 2-Chlorotrityl chloride resin (500mg, 0.55mmol) was added Fmoc-D-alanine (1.1 eq, 188 mg, 0.605 mmol) and DIEA (3 eq, 0.286 mL, 1.65 mmol) in dry DCM (15 mL). The resin was agitated for 1 h at ambient temperature and washed with MeOH and DCM (3 x 15 mL each). The Fmoc protecting group was removed with 6 M piperazine/100 mM HOBt in DMF (15 ml) for 30 min at ambient temperature, then washed as before. Fmoc-D-alanine (3 eq, 513 mg, 1.65 mmol), HBTU (3 eq, 625 mg, 1.65 mmol), and DIEA (6 eq, 0.574 mL, 3.30 mmol) in DMF (15 mL) were added to the reaction flask and agitated for 2 h at ambient temperature. The Fmoc deprotection and coupling procedure was repeated as before using the same equivalencies with Fmoc-L-Lys(Boc)-OH, Fmoc-D-glutamic acid  $\alpha$ -amide, and Fmoc-L-alanine. The Fmoc group of L-alanine was deprotected and resin coupled with 5(6)-carboxyfluorescein (2 eq, 413 mg, 1.1 mmol), HBTU (2 eq, 416 mg, 1.1 mmol) and DIEA (6 eq, 0.574 mL, 3.30 mmol) in DMF (15 mL) shaking overnight. The resin was washed as before and added to a solution of TFA/DCM (2:1, 20 mL) with agitation for 2 h at ambient temperature. The resin was filtered and resulting solution concentrated *in vacuo*. The residue was triturated with cold diethyl ether and

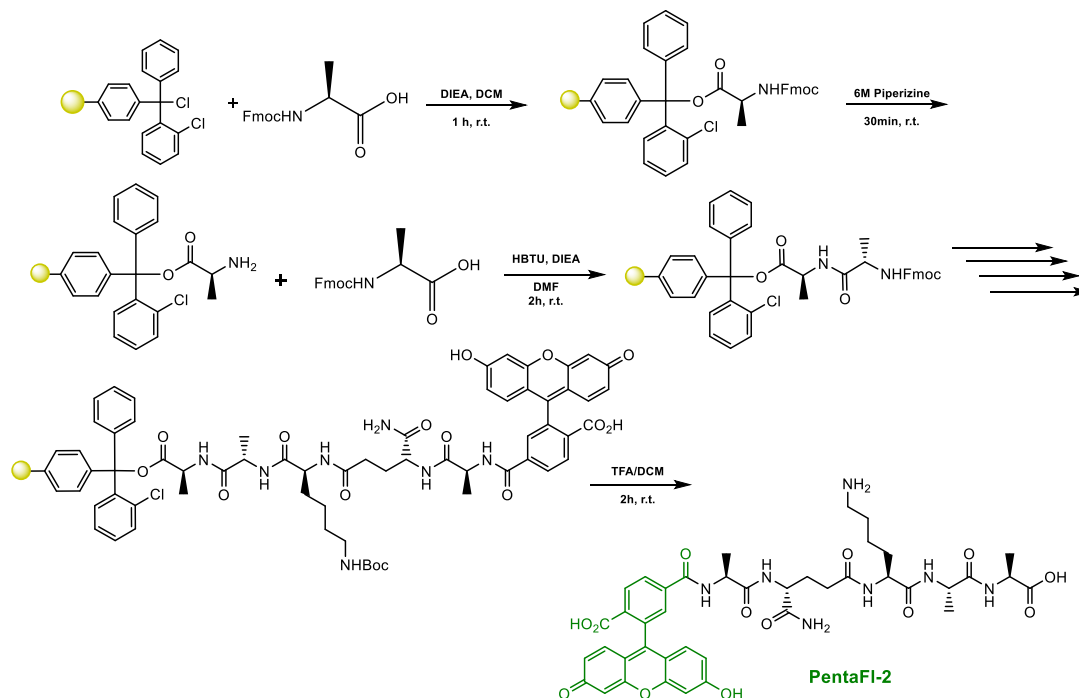


purified using reverse phase HPLC using H<sub>2</sub>O/MeOH to yield **PentaFl**. The sample was analyzed for purity using a Shimadzu LC 2020 with a Phenomenex Luna 5 $\mu$  C18(2) 100Å (30 x 2.00 mm) column; gradient elution with H<sub>2</sub>O/CH<sub>3</sub>CN.

ESI-MS: [M+H]<sup>+</sup> calculated: 846.3 found: 846.3



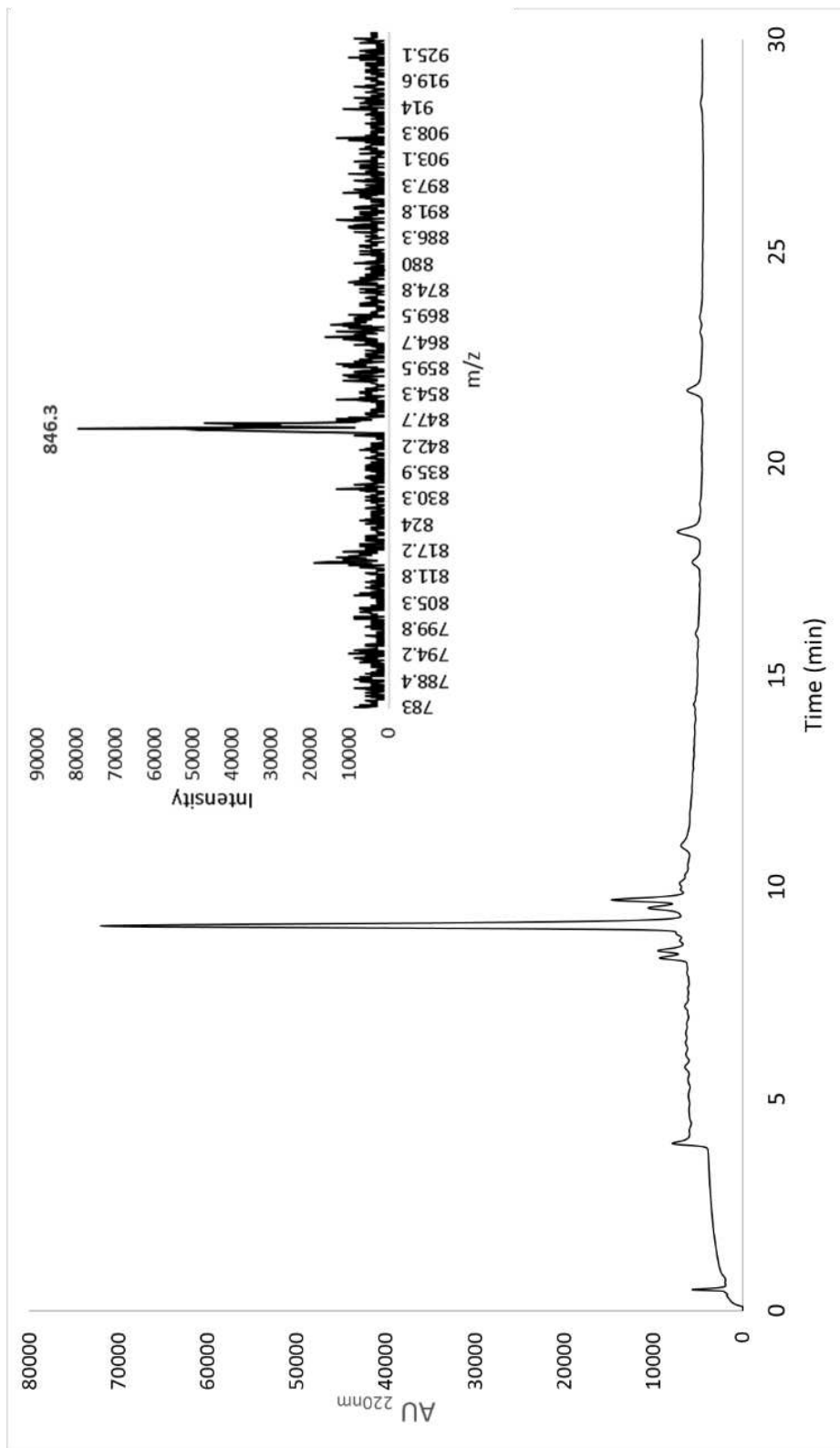
### Scheme S3. Synthesis of PentaFl-2



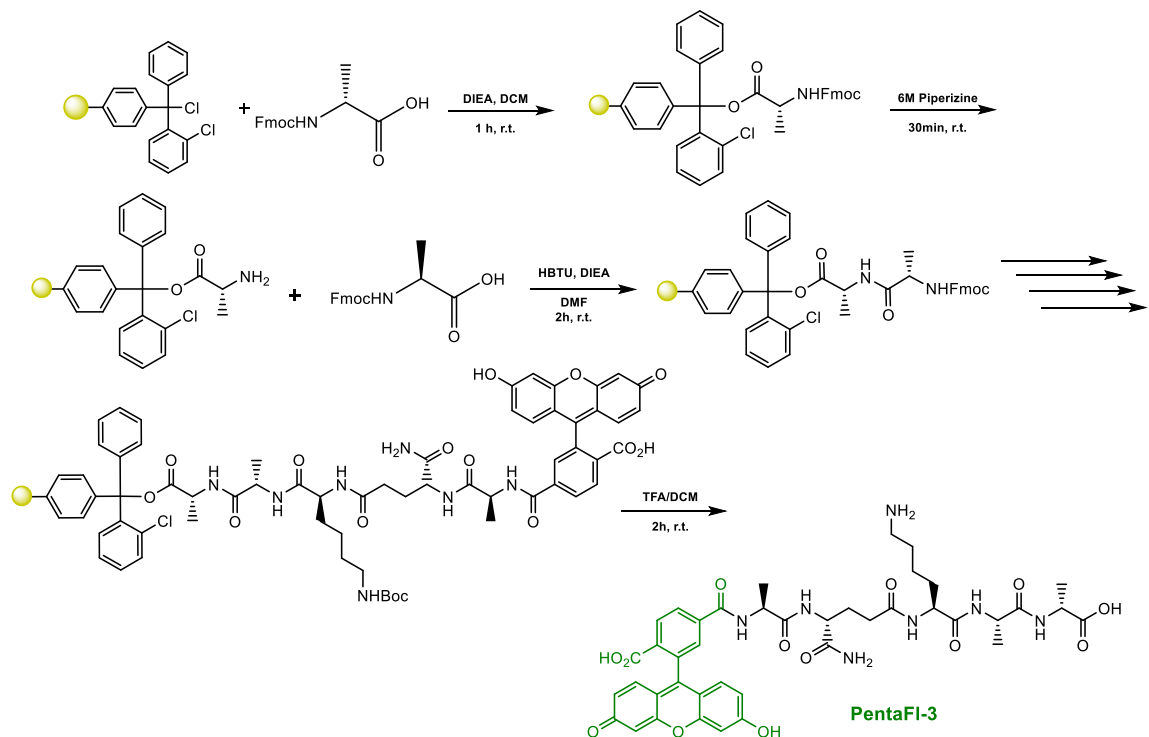
To a 25 mL peptide synthesis vessel charged with 2-Chlorotrityl chloride resin (500mg, 0.55mmol) was added Fmoc-L-alanine (1.1 eq, 188 mg, 0.605 mmol) and DIEA (3 eq, 0.286 mL, 1.65 mmol) in dry DCM (15 mL). The resin was agitated for 1 h at ambient temperature and washed with MeOH and DCM (3 x 15 mL each). The Fmoc protecting group was removed with 6 M piperazine/100 mM HOBt in DMF (15 ml) for 30 min at ambient temperature, then washed as before. Fmoc-L-alanine (3 eq, 513 mg, 1.65 mmol), HBTU (3 eq, 625 mg, 1.65 mmol), and DIEA (6 eq, 0.574 mL, 3.30 mmol) in DMF (15 mL) were added to the reaction flask and agitated for 2 h at ambient temperature. The Fmoc deprotection and coupling procedure was repeated as before using the same equivalencies with Fmoc-L-Lys(Boc)-OH, Fmoc-D-glutamic acid  $\alpha$ -amide, and Fmoc-L-alanine. The Fmoc group of L-alanine was deprotected and resin coupled with 5(6)-carboxyfluorescein (2 eq, 413 mg, 1.1 mmol), HBTU (2 eq, 416 mg, 1.1 mmol) and DIEA (6 eq, 0.574 mL, 3.30 mmol) in DMF (15 mL) shaking overnight. The resin was washed as before and added to a solution of TFA/DCM (2:1, 20 mL) with agitation for 2 h at ambient temperature. The resin was filtered and

resulting solution concentrated *in vacuo*. The residue was triturated with cold diethyl ether and purified using reverse phase HPLC using H<sub>2</sub>O/MeOH to yield **PentaFl-2**. The sample was analyzed for purity using a Shimadzu LC 2020 with a Phenomenex Luna 5 $\mu$  C18(2) 100Å (30 x 2.00 mm) column; gradient elution with H<sub>2</sub>O/CH<sub>3</sub>CN.

ESI-MS: [M+H]<sup>+</sup> calculated: 846.3 found: 846.3



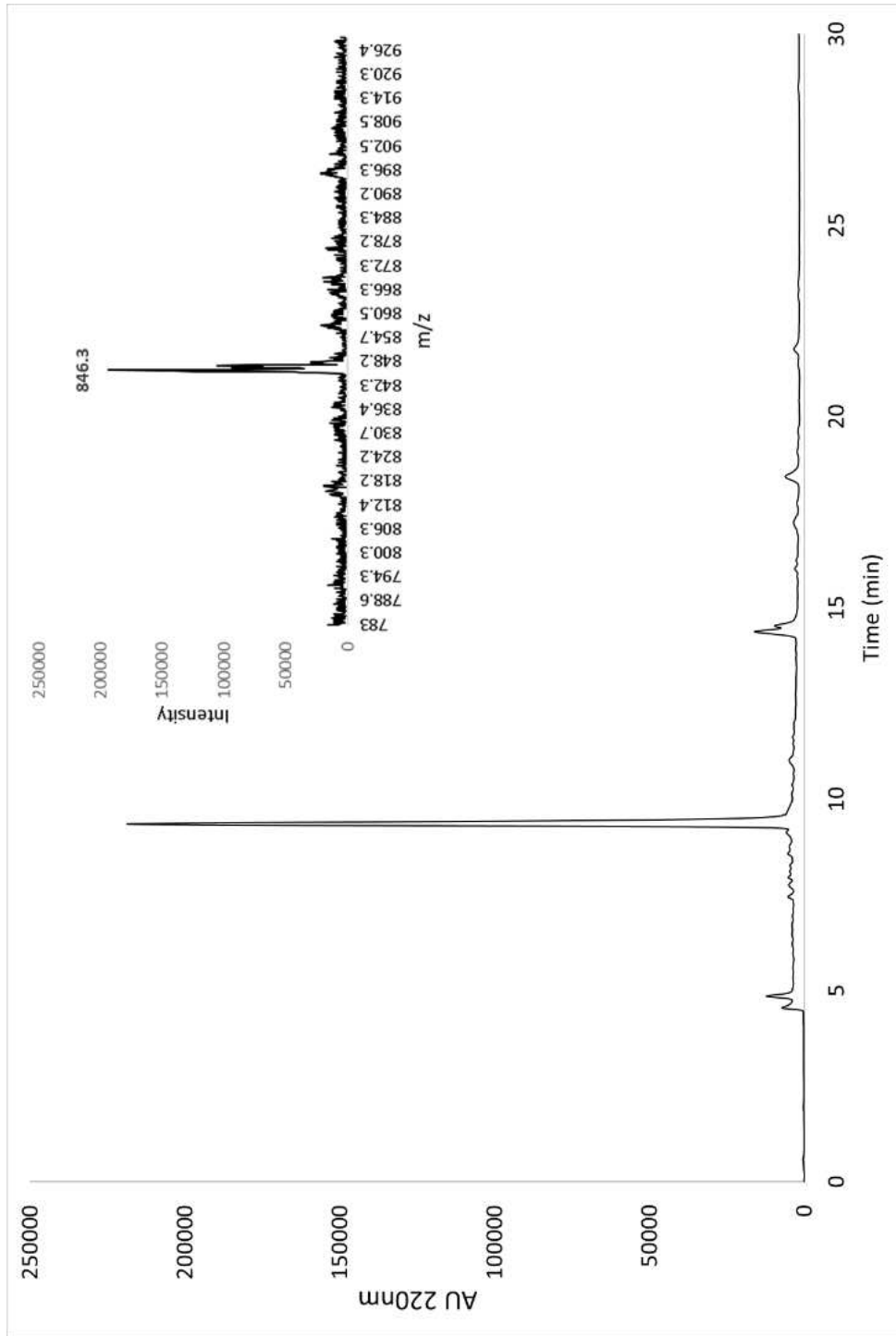
### Scheme S4. Synthesis of PentaFl-3



To a 25 mL peptide synthesis vessel charged with 2-Chlorotrityl chloride resin (500mg, 0.55mmol) was added Fmoc-D-alanine (1.1 eq, 188 mg, 0.605 mmol) and DIEA (3 eq, 0.286 mL, 1.65 mmol) in dry DCM (15 mL). The resin was agitated for 1 h at ambient temperature and washed with MeOH and DCM (3 x 15 mL each). The Fmoc protecting group was removed with 6 M piperazine/100 mM HOBt in DMF (15 ml) for 30 min at ambient temperature, then washed as before. Fmoc-L-alanine (3 eq, 513 mg, 1.65 mmol), HBTU (3 eq, 625 mg, 1.65 mmol), and DIEA (6 eq, 0.574 mL, 3.30 mmol) in DMF (15 mL) were added to the reaction flask and agitated for 2 h at ambient temperature. The Fmoc deprotection and coupling procedure was repeated as before using the same equivalencies with Fmoc-L-Lys(Boc)-OH, Fmoc-D-glutamic acid  $\alpha$ -amide, and Fmoc-L-alanine. The Fmoc group of L-alanine was deprotected and resin coupled with 5(6)-carboxyfluorescein (2 eq, 413 mg, 1.1 mmol), HBTU (2 eq, 416 mg, 1.1 mmol) and DIEA (6 eq, 0.574 mL, 3.30 mmol) in DMF (15 mL) shaking overnight. The resin was washed as before and added to a solution of TFA/DCM (2:1, 20 mL) with agitation for 2 h at ambient temperature. The resin was filtered and

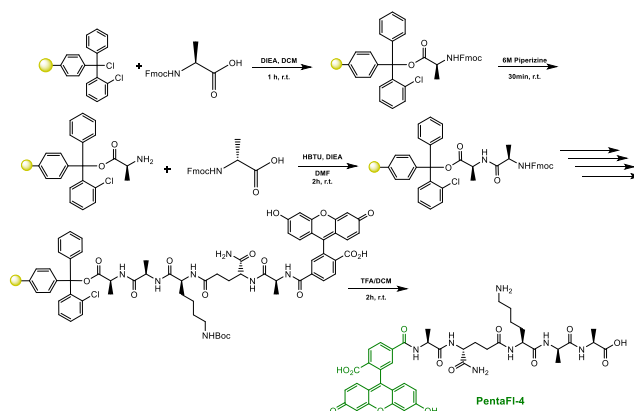
resulting solution concentrated *in vacuo*. The residue was triturated with cold diethyl ether and purified using reverse phase HPLC using H<sub>2</sub>O/MeOH to yield **PentaFl-3**. The sample was analyzed for purity using a Shimadzu LC 2020 with a Phenomenex Luna 5 $\mu$  C18(2) 100Å (30 x 2.00 mm) column; gradient elution with H<sub>2</sub>O/CH<sub>3</sub>CN.

ESI-MS: [M+H]<sup>+</sup> calculated: 846.3 found: 846.3



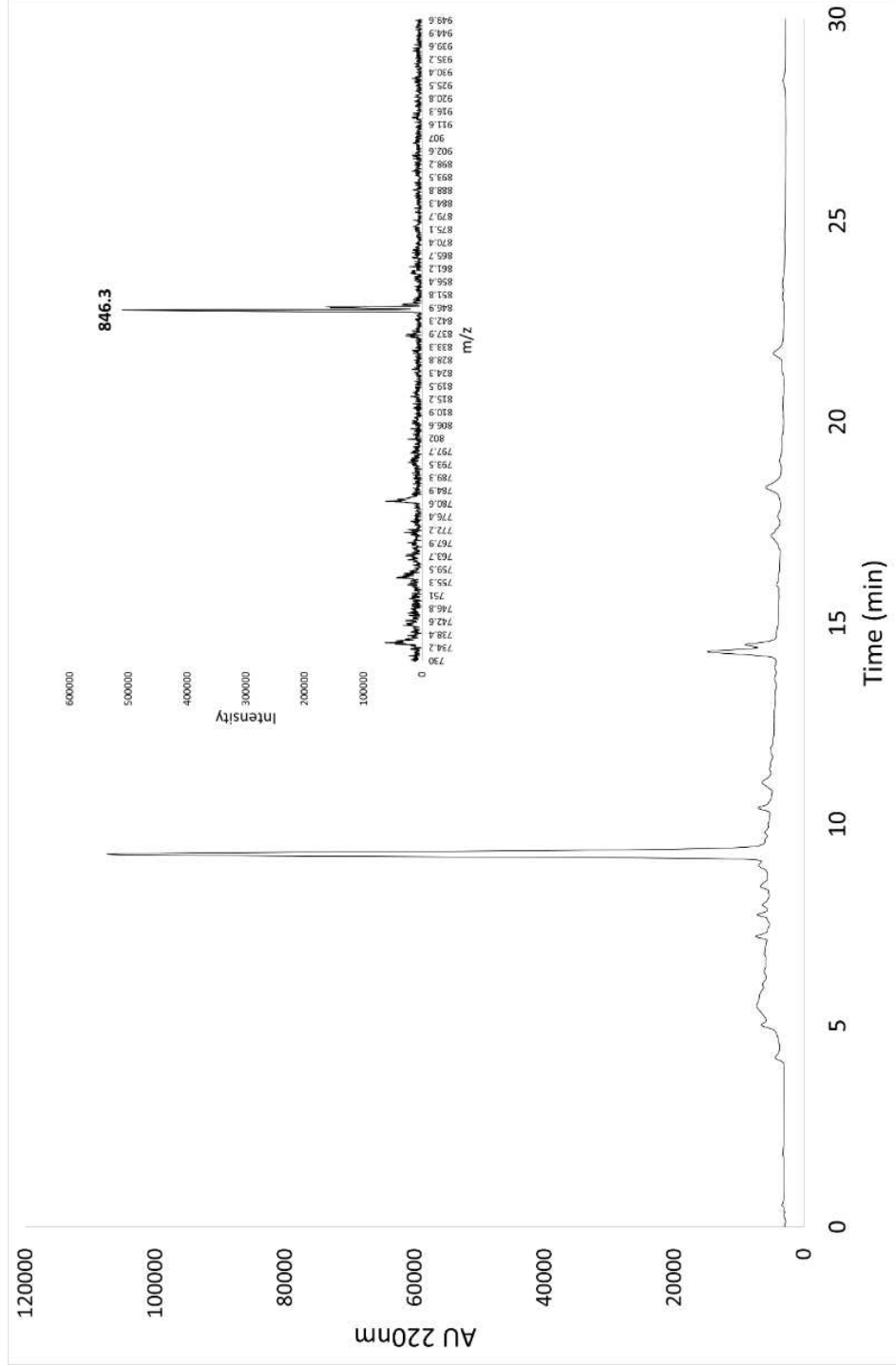


### Scheme S5. Synthesis of **PentaFl-4**

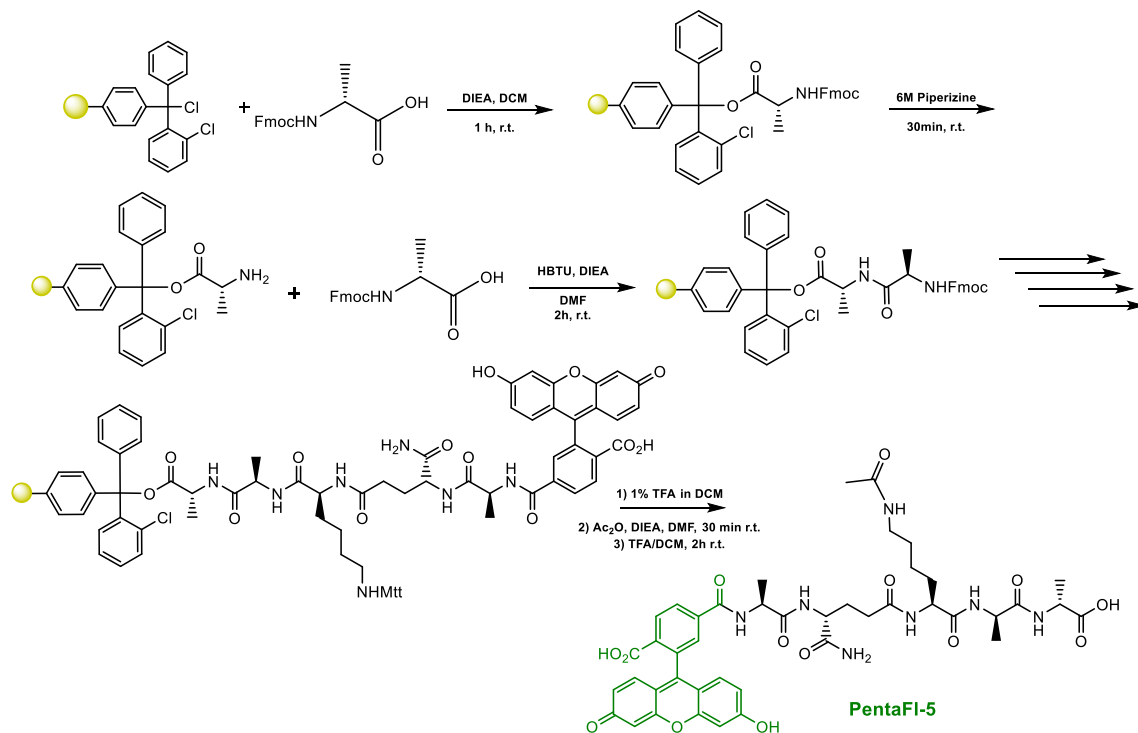


To a 25 mL peptide synthesis vessel charged with 2-Chlorotrityl chloride resin (500mg, 0.55mmol) was added Fmoc-L-alanine (1.1 eq, 188 mg, 0.605 mmol) and DIEA (3 eq, 0.286 mL, 1.65 mmol) in dry DCM (15 mL). The resin was agitated for 1 h at ambient temperature and washed with MeOH and DCM (3 x 15 mL each). The Fmoc protecting group was removed with 6 M piperazine/100 mM HOBt in DMF (15 ml) for 30 min at ambient temperature, then washed as before. Fmoc-D-alanine (3 eq, 513 mg, 1.65 mmol), HBTU (3 eq, 625 mg, 1.65 mmol), and DIEA (6 eq, 0.574 mL, 3.30 mmol) in DMF (15 mL) were added to the reaction flask and agitated for 2 h at ambient temperature. The Fmoc deprotection and coupling procedure was repeated as before using the same equivalencies with Fmoc-L-Lys(Boc)-OH, Fmoc-D-glutamic acid  $\alpha$ -amide, and Fmoc-L-alanine. The Fmoc group of L-alanine was deprotected and resin coupled with 5(6)-carboxyfluorescein (2 eq, 413 mg, 1.1 mmol), HBTU (2 eq, 416 mg, 1.1 mmol) and DIEA (6 eq, 0.574 mL, 3.30 mmol) in DMF (15 mL) shaking overnight. The resin was washed as before and added to a solution of TFA/DCM (2:1, 20 mL) with agitation for 2 h at ambient temperature. The resin was filtered and resulting solution concentrated *in vacuo*. The residue was triturated with cold diethyl ether and purified using reverse phase HPLC using H<sub>2</sub>O/MeOH to yield **PentaFl-4**. The sample was analyzed using a Shimadzu LC 2020 with a Phenomenex Luna 5 $\mu$  C18(2) 100 $\text{\AA}$  (30 x 2.00 mm) column; gradient elution with H<sub>2</sub>O/CH<sub>3</sub>CN.

ESI-MS: [M+H]<sup>+</sup> calculated: 846.3 found: 846.3



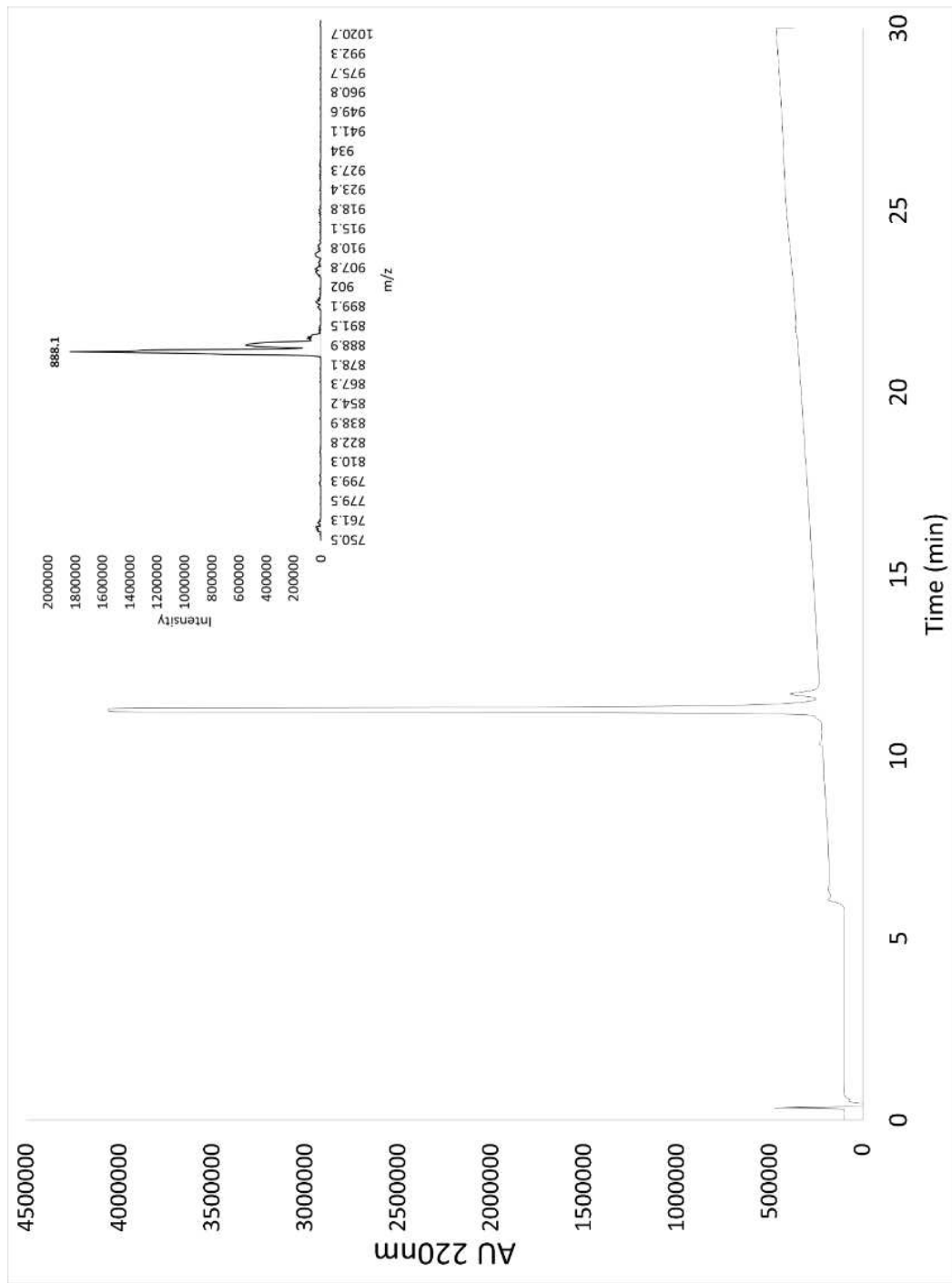
## Scheme S6. Synthesis of PentaFI-5



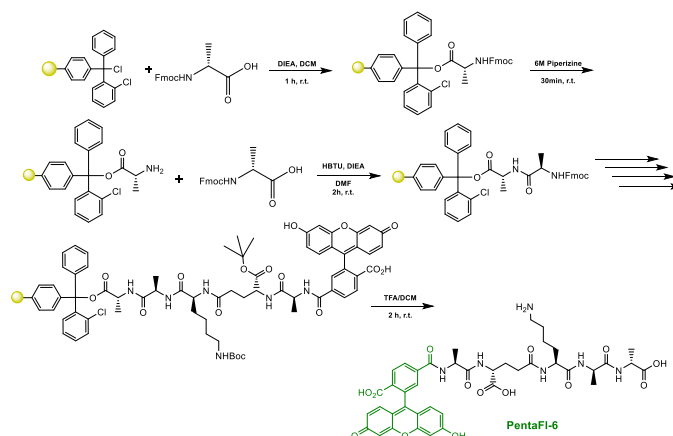
To a 25 mL peptide synthesis vessel charged with Fmoc-D-Alanine Wang resin (950 mg, 0.55 mmol). The Fmoc protecting group was removed with 6 M piperazine/100 mM HOBt in DMF (15 ml) for 30 min at ambient temperature, then washed with MeOH and DCM (3 x 15 mL each). Fmoc-D-alanine (3 eq, 513 mg, 1.65 mmol), HBTU (3 eq, 625 mg, 1.65 mmol), and DIEA (6 eq, 0.574 mL, 3.30 mmol) in DMF (15 mL) was added to the reaction flask and agitated for 2 h at ambient temperature. The Fmoc deprotection and coupling procedure was repeated as before using the same equivalencies with Fmoc-L-Lys(Mtt)-OH, Fmoc-D-glutamic acid  $\alpha$ -amide and Fmoc-L-alanine. The Fmoc group of L-alanine was deprotected and resin coupled with 5(6)-carboxyfluorescein (2 eq, 413 mg, 1.1 mmol), HBTU (2 eq, 416 mg, 1.1 mmol) and DIEA (6 eq, 0.574 mL, 3.30 mmol) in DMF (15 mL) shaking overnight. The resin was washed as before and added to a solution of 1% TFA / 5% TIPS in DCM and shaken for 10 min and washed. The step was repeated five times for removal of the Mtt group. Acetic anhydride (5 eq, 0.260 mL) and DIEA (10 eq, 0.956 mL) in DMF was added and resin shaken for 30 min at ambient temperature. The

resin was washed and added to a solution of TFA/DCM (2:1, 20 mL) with agitation for 2 h at ambient temperature. The resin was filtered and resulting solution concentrated *in vacuo*. The residue was triturated with cold diethyl ether and purified using reverse phase HPLC using H<sub>2</sub>O/MeOH to yield **TetraFl-3**. The sample was analyzed for purity using a Shimadzu LC 2020 with a Phenomenex Luna 5 $\mu$  C18(2) 100Å (30 x 2.00 mm) column; gradient elution with H<sub>2</sub>O/CH<sub>3</sub>CN.

ESI-MS: [M+H]<sup>+</sup> calculated: 888.3 found: 888.1

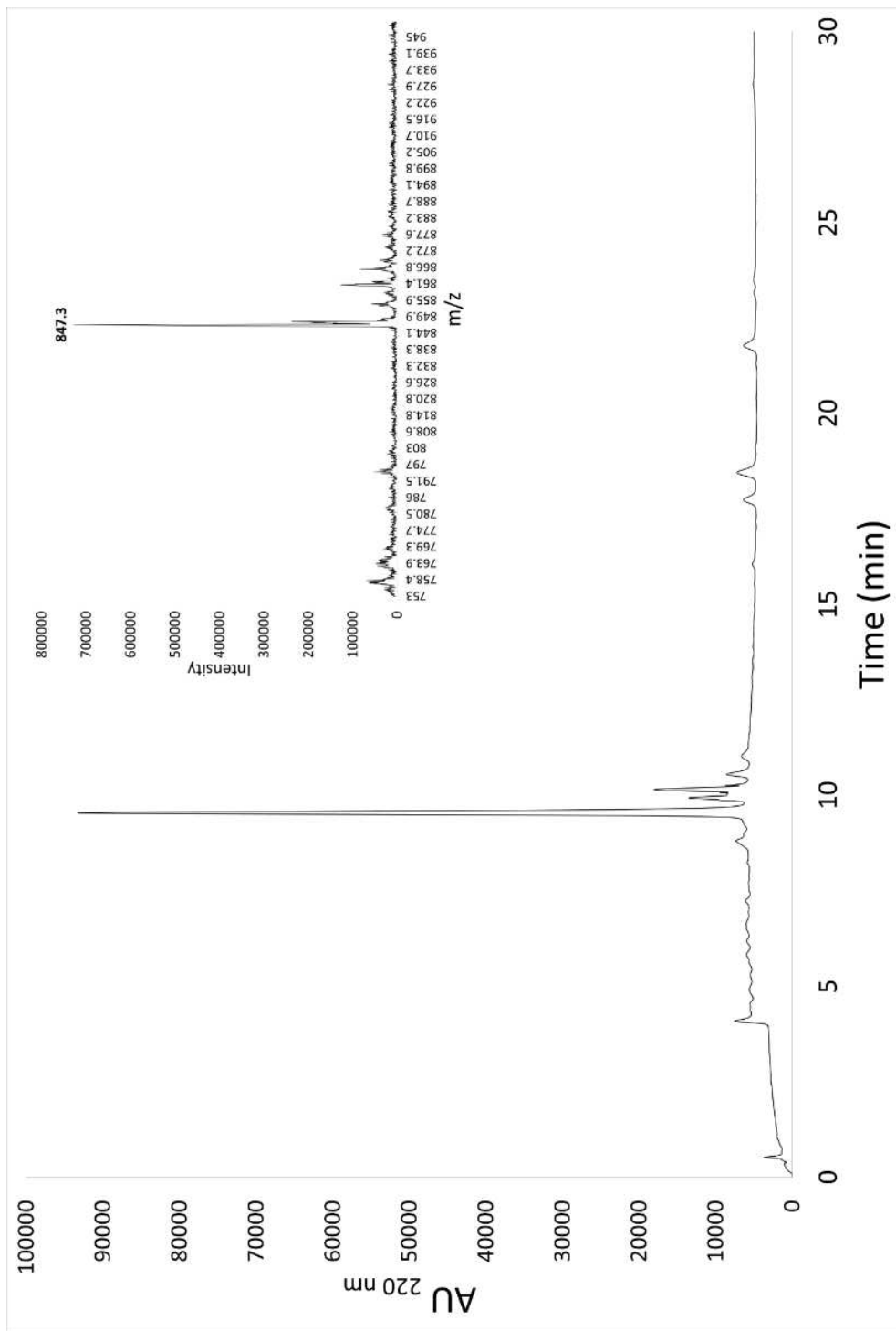


## Scheme S7. Synthesis of PentaFl-6

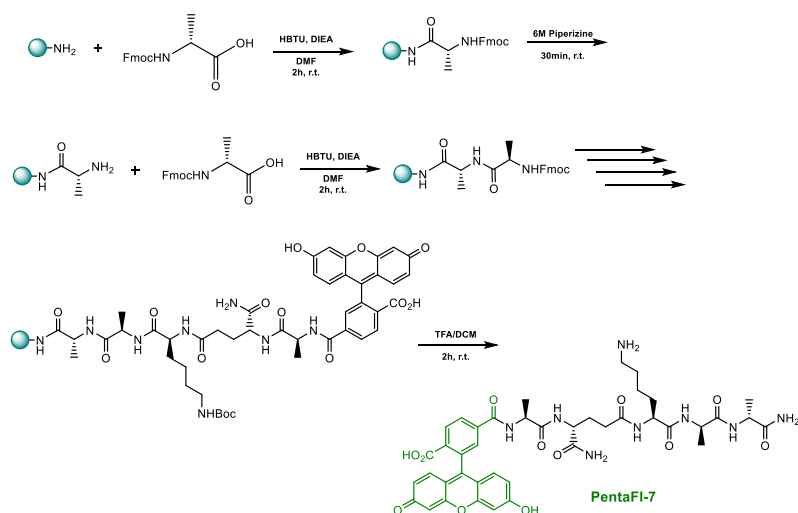


To a 25 mL peptide synthesis vessel charged with 2-Chlorotrityl chloride resin (500mg, 0.55mmol) was added Fmoc-D-alanine (1.1 eq, 188 mg, 0.605 mmol) and DIEA (3 eq, 0.286 mL, 1.65 mmol) in dry DCM (15 mL). The resin was agitated for 1 h at ambient temperature and washed with MeOH and DCM (3 x 15 mL each). The Fmoc protecting group was removed with 6 M piperazine/100 mM HOBt in DMF (15 ml) for 30 min at ambient temperature, then washed as before. Fmoc-D-alanine (3 eq, 513 mg, 1.65 mmol), HBTU (3 eq, 625 mg, 1.65 mmol), and DIEA (6 eq, 0.574 mL, 3.30 mmol) in DMF (15 mL) were added to the reaction flask and agitated for 2 h at ambient temperature. The Fmoc deprotection and coupling procedure was repeated as before using the same equivalencies with Fmoc-L-Lys(Boc)-OH, Fmoc-D-Glu(OtBu)-OH, and Fmoc-L-alanine. The Fmoc group of L-alanine was deprotected and resin coupled with 5(6)-carboxyfluorescein (2 eq, 413 mg, 1.1 mmol), HBTU (2 eq, 416 mg, 1.1 mmol) and DIEA (6 eq, 0.574 mL, 3.30 mmol) in DMF (15 mL) shaking overnight. The resin was washed as before and added to a solution of TFA/DCM (2:1, 20 mL) with agitation for 2 h at ambient temperature. The resin was filtered and resulting solution concentrated *in vacuo*. The residue was triturated with cold diethyl ether and purified using reverse phase HPLC using H<sub>2</sub>O/MeOH to yield **PentaFl-6**. The sample was analyzed for purity using a Shimadzu LC 2020 with a Phenomenex Luna 5 $\mu$  C18(2) 100Å (30 x 2.00 mm) column; gradient elution with H<sub>2</sub>O/CH<sub>3</sub>CN.

ESI-MS: [M+H]<sup>+</sup> calculated: 847.3 found: 847.3



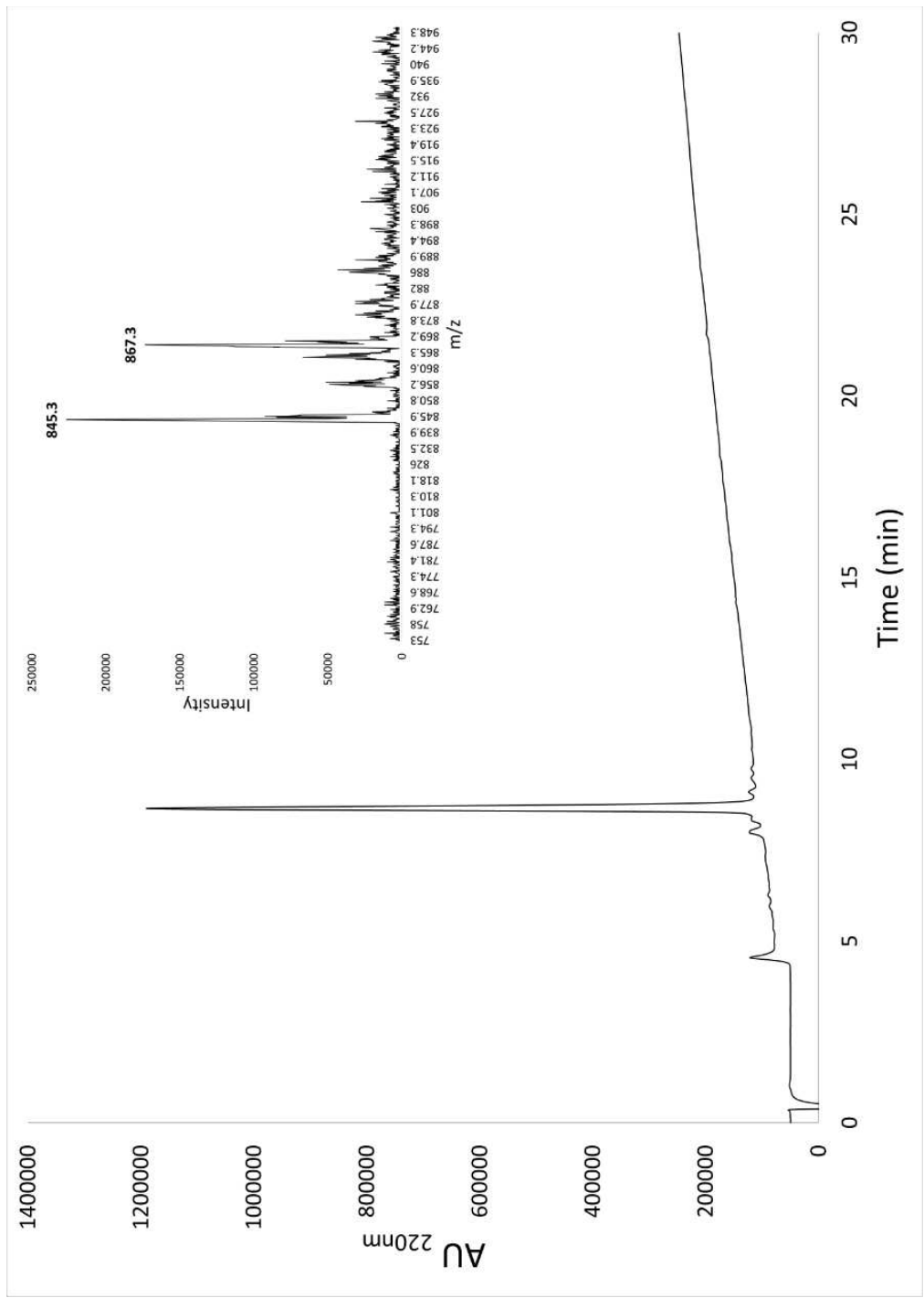
## Scheme S8. Synthesis of PentaFl-7



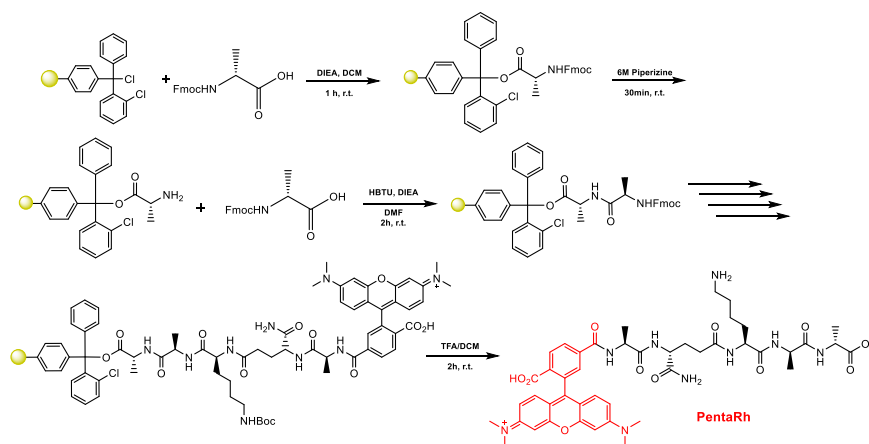
To a 25 mL peptide synthesis vessel charged with Rink Amide Resin (500mg, 0.30mmol). The Fmoc protecting group was removed with 6 M piperazine/100 mM HOBt in DMF (15 ml) for 30 min at ambient temperature, then washed with MeOH and DCM (3 x 15 mL each). Fmoc-D-alanine (3 eq, 280 mg, 0.90 mmol), HBTU (3 eq, 341 mg, 0.90 mmol), and DIEA (6 eq, 0.314 mL, 1.80 mmol) in DMF (15 mL) were added to the reaction flask and agitated for 2 h at ambient temperature. The Fmoc deprotection and coupling procedure was repeated as before using the same equivalencies with Fmoc-D-alanine, Fmoc-L-Lys(Boc)-OH, Fmoc-D-glutamic acid  $\alpha$ -amide, and Fmoc-L-alanine. The Fmoc group of L-alanine was deprotected and resin coupled with 5(6)-carboxyfluorescein (2 eq, 226 mg, 0.60 mmol), HBTU (2 eq, 228 mg, 0.60 mmol) and DIEA (6 eq, 0.314 mL, 1.80 mmol) in DMF (15 mL) shaking overnight. The resin was washed as before and added to a solution of TFA/DCM (2:1, 20 mL) with agitation for 2 h at ambient temperature. The resin was filtered and resulting solution concentrated *in vacuo*. The residue was triturated with cold diethyl ether and purified using reverse phase HPLC using H<sub>2</sub>O/MeOH to yield **PentaFl-7**. The sample was analyzed for purity using a Shimadzu LC 2020 with a Phenomenex Luna 5 $\mu$  C18(2) 100Å (30 x 2.00 mm) column; gradient elution with H<sub>2</sub>O/CH<sub>3</sub>CN.

ESI-MS: [M+H]<sup>+</sup> calculated: 845.3 found: 845.3



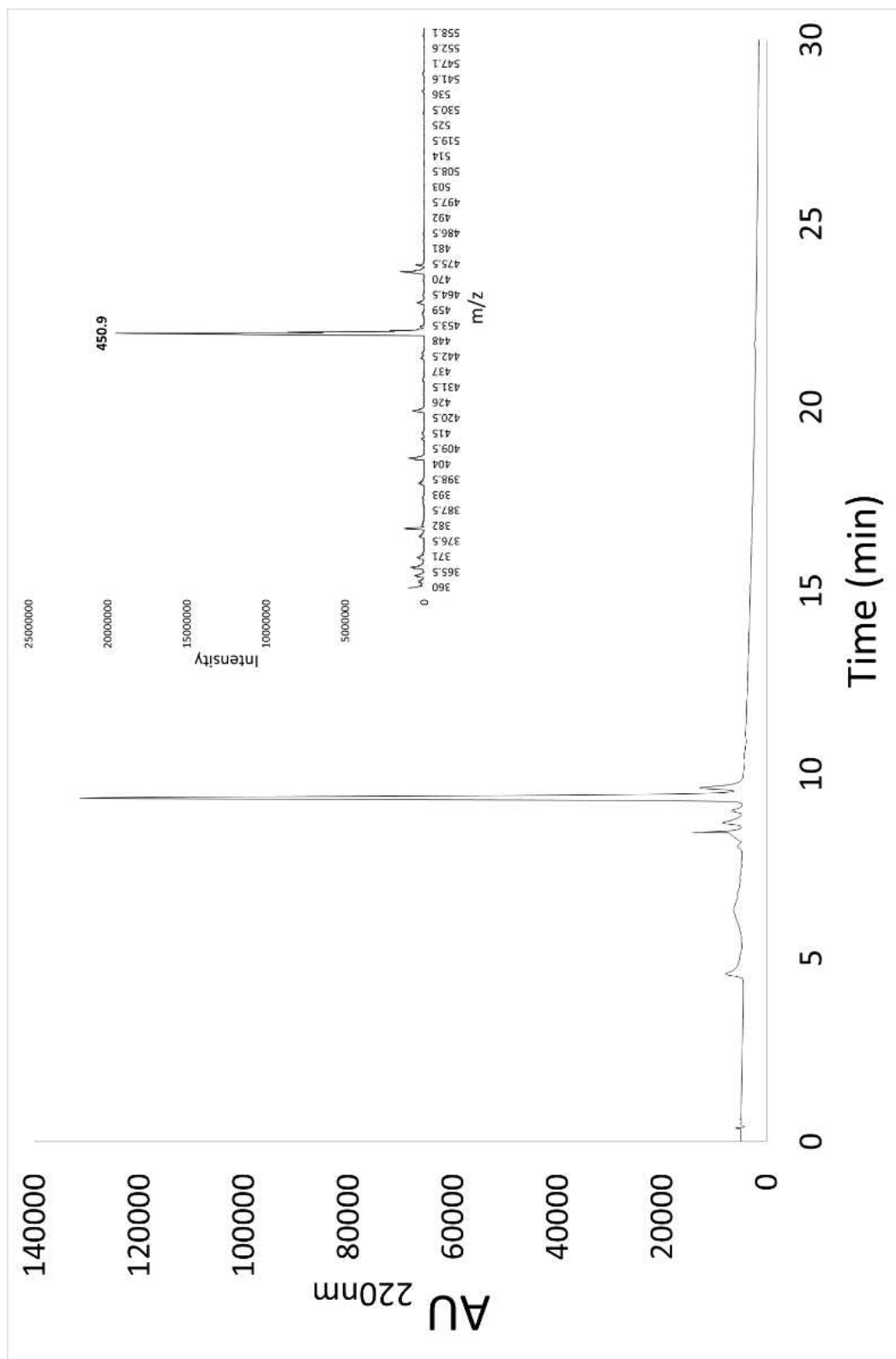


## Scheme S9. Synthesis of PentaRh

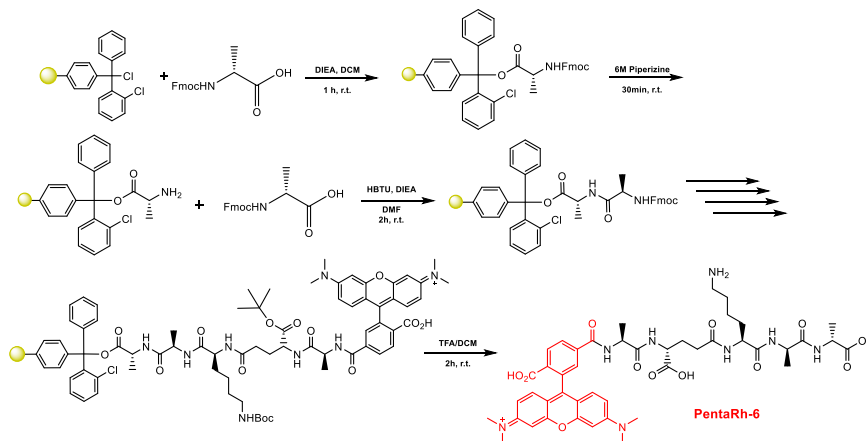


To a 25 mL peptide synthesis vessel charged with 2-Chlorotrityl chloride resin (500mg, 0.55mmol) was added Fmoc-D-alanine (1.1 eq, 188 mg, 0.605 mmol) and DIEA (3 eq, 0.286 mL, 1.65 mmol) in dry DCM (15 mL). The resin was agitated for 1 h at ambient temperature and washed with MeOH and DCM (3 x 15 mL each). The Fmoc protecting group was removed with 6 M piperazine/100 mM HOBt in DMF (15 ml) for 30 min at ambient temperature, then washed as before. Fmoc-D-alanine (3 eq, 513 mg, 1.65 mmol), HBTU (3 eq, 625 mg, 1.65 mmol), and DIEA (6 eq, 0.574 mL, 3.30 mmol) in DMF (15 mL) were added to the reaction flask and agitated for 2 h at ambient temperature. The Fmoc deprotection and coupling procedure was repeated as before using the same equivalencies with Fmoc-L-Lys(Boc)-OH, Fmoc-D-glutamic acid  $\alpha$ -amide, and Fmoc-L-alanine. The Fmoc group of L-alanine was deprotected and resin coupled with 5(6)-carboxy-tetramethylrhodamine (2 eq, 474 mg, 1.1 mmol), HBTU (2 eq, 416 mg, 1.1 mmol) and DIEA (6 eq, 0.574 mL, 3.30 mmol) in DMF (15 mL) shaking overnight. The resin was washed as before and added to a solution of TFA/DCM (2:1, 20 mL) with agitation for 2 h at ambient temperature. The resin was filtered and resulting solution concentrated *in vacuo*. The residue was triturated with cold diethyl ether and purified using reverse phase HPLC using H<sub>2</sub>O/MeOH to yield **PentaRh-6**. The sample was analyzed for purity using a Shimadzu LC 2020 with a Phenomenex Luna 5 $\mu$  C18(2) 100Å (30 x 2.00 mm) column; gradient elution with H<sub>2</sub>O/CH<sub>3</sub>CN.

ESI-MS: [M+2H]<sup>2+</sup> calculated: 451.2 found: 450.9

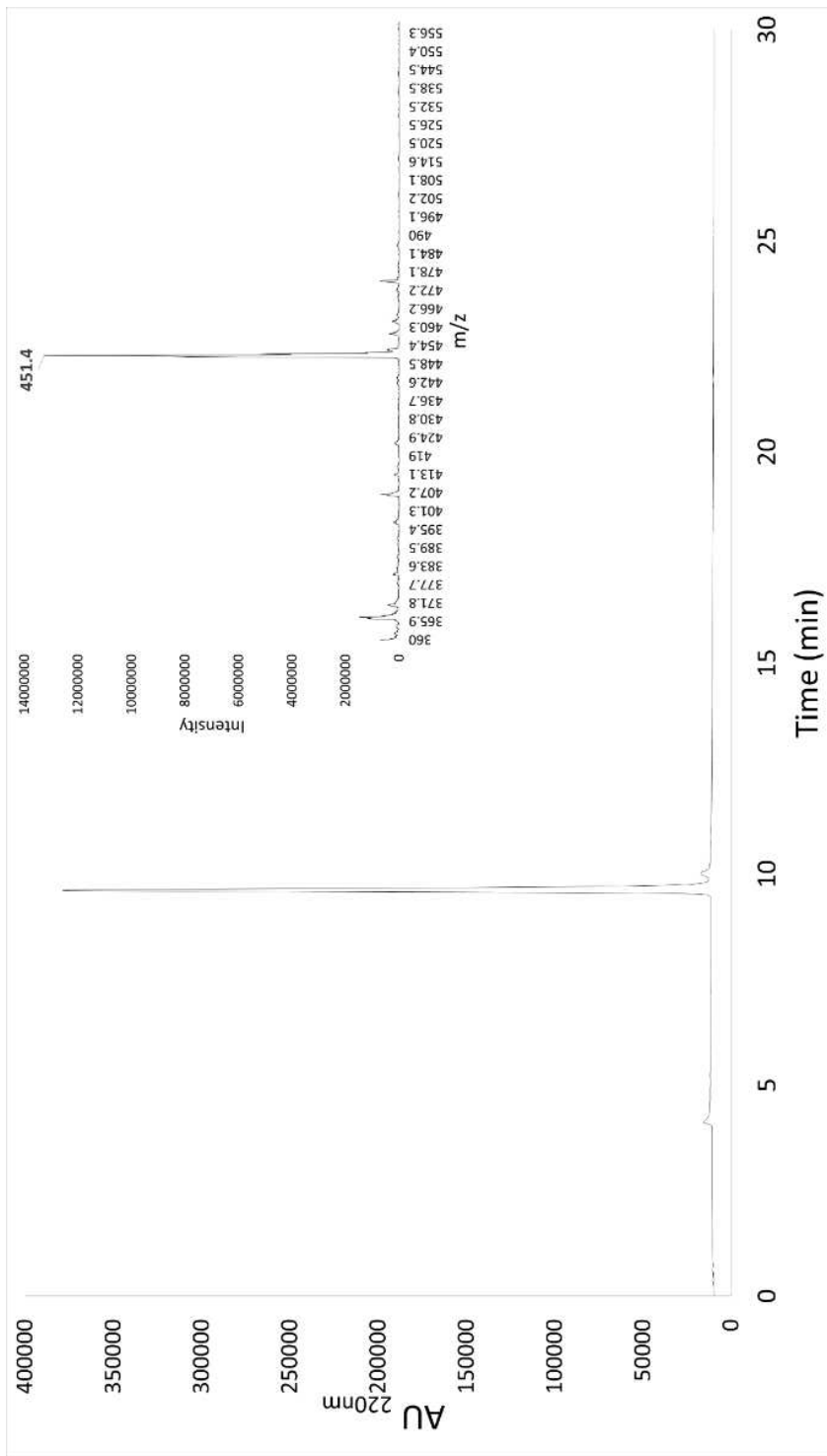


## Scheme S10. Synthesis of **PentaRh-6**

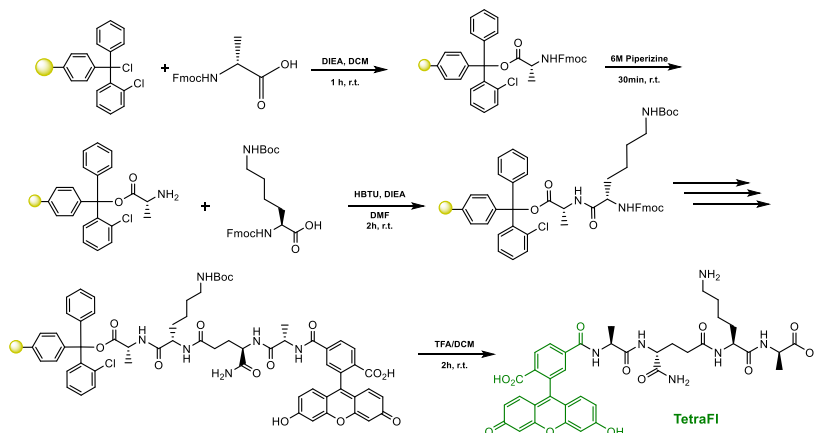


To a 25 mL peptide synthesis vessel charged with 2-Chlorotrityl chloride resin (500mg, 0.55mmol) was added Fmoc-D-alanine (1.1 eq, 188 mg, 0.605 mmol) and DIEA (3 eq, 0.286 mL, 1.65 mmol) in dry DCM (15 mL). The resin was agitated for 1 h at ambient temperature and washed with MeOH and DCM (3 x 15 mL each). The Fmoc protecting group was removed with 6 M piperazine/100 mM HOBt in DMF (15 ml) for 30 min at ambient temperature, then washed as before. Fmoc-D-alanine (3 eq, 513 mg, 1.65 mmol), HBTU (3 eq, 625 mg, 1.65 mmol), and DIEA (6 eq, 0.574 mL, 3.30 mmol) in DMF (15 mL) were added to the reaction flask and agitated for 2 h at ambient temperature. The Fmoc deprotection and coupling procedure was repeated as before using the same equivalencies with Fmoc-L-Lys(Boc)-OH, Fmoc-D-Glu(OtBu)-OH, and Fmoc-L-alanine. The Fmoc group of L-alanine was deprotected and resin coupled with 5(6)-carboxy-tetramethylrhodamine (2 eq, 474 mg, 1.1 mmol), HBTU (2 eq, 416 mg, 1.1 mmol) and DIEA (6 eq, 0.574 mL, 3.30 mmol) in DMF (15 mL) shaking overnight. The resin was washed as before and added to a solution of TFA/DCM (2:1, 20 mL) with agitation for 2 h at ambient temperature. The resin was filtered and resulting solution concentrated *in vacuo*. The residue was triturated with cold diethyl ether and purified using reverse phase HPLC using H<sub>2</sub>O/MeOH to yield **PentaRh-6**. The sample was analyzed for purity using a Shimadzu LC 2020 with a Phenomenex Luna 5µ C18(2) 100Å (30 x 2.00 mm) column; gradient elution with H<sub>2</sub>O/CH<sub>3</sub>CN.

ESI-MS: [M+2H]<sup>2+</sup> calculated: 451.7 found: 451.4

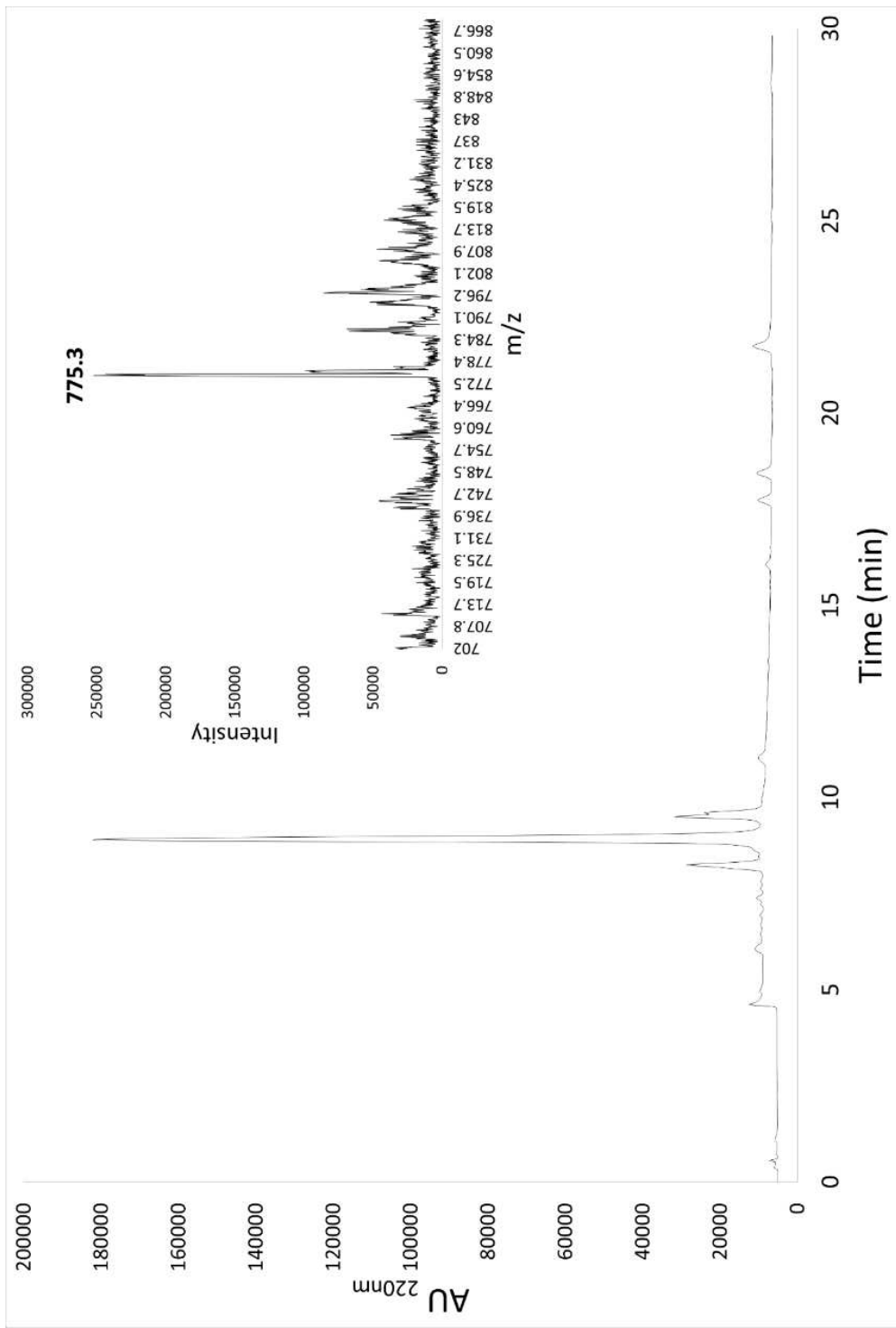


### Scheme S11. Synthesis of TetraFl

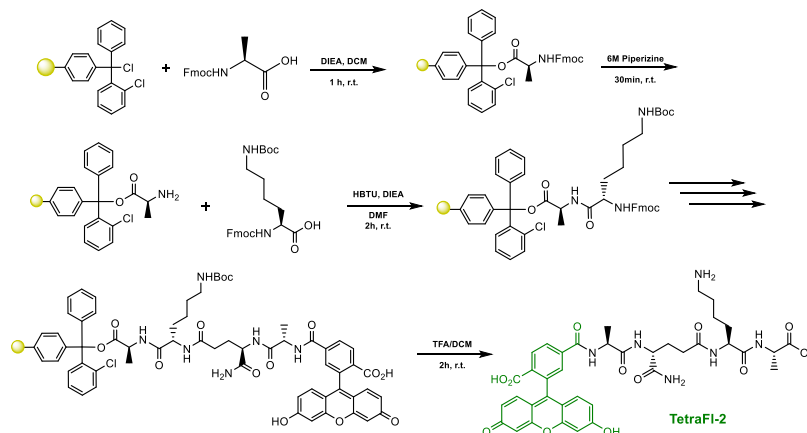


To a 25 mL peptide synthesis vessel charged with 2-Chlorotrityl chloride resin (500mg, 0.55mmol) was added Fmoc-D-alanine (1.1 eq, 188 mg, 0.605 mmol) and DIEA (3 eq, 0.286 mL, 1.65 mmol) in dry DCM (15 mL). The resin was agitated for 1 h at ambient temperature and washed with MeOH and DCM (3 x 15 mL each). The Fmoc protecting group was removed with 6 M piperazine/100 mM HOBt in DMF (15 ml) for 30 min at ambient temperature, then washed as before. Fmoc-L-Lys(Boc)-OH (3 eq, 773 mg, 1.65 mmol), HBTU (3 eq, 625 mg, 1.65 mmol), and DIEA (6 eq, 0.574 mL, 3.30 mmol) in DMF (15 mL) were added to the reaction flask and agitated for 2 h at ambient temperature. The Fmoc deprotection and coupling procedure was repeated as before using the same equivalencies with Fmoc-D-glutamic acid  $\alpha$ -amide and Fmoc-L-alanine. The Fmoc group of L-alanine was deprotected and resin coupled with 5(6)-carboxyfluorescein (2 eq, 413 mg, 1.1 mmol), HBTU (2 eq, 416 mg, 1.1 mmol) and DIEA (6 eq, 0.574 mL, 3.30 mmol) in DMF (15 mL) shaking overnight. The resin was washed as before and added to a solution of TFA/DCM (2:1, 20 mL) with agitation for 2 h at ambient temperature. The resin was filtered and resulting solution concentrated *in vacuo*. The residue was triturated with cold diethyl ether and purified using reverse phase HPLC using H<sub>2</sub>O/MeOH to yield **TetraFl**. The sample was analyzed for purity using a Shimadzu LC 2020 with a Phenomenex Luna 5 $\mu$  C18(2) 100Å (30 x 2.00 mm) column; gradient elution with H<sub>2</sub>O/CH<sub>3</sub>CN.

ESI-MS: [M+H]<sup>+</sup> calculated: 775.3 found: 775.3



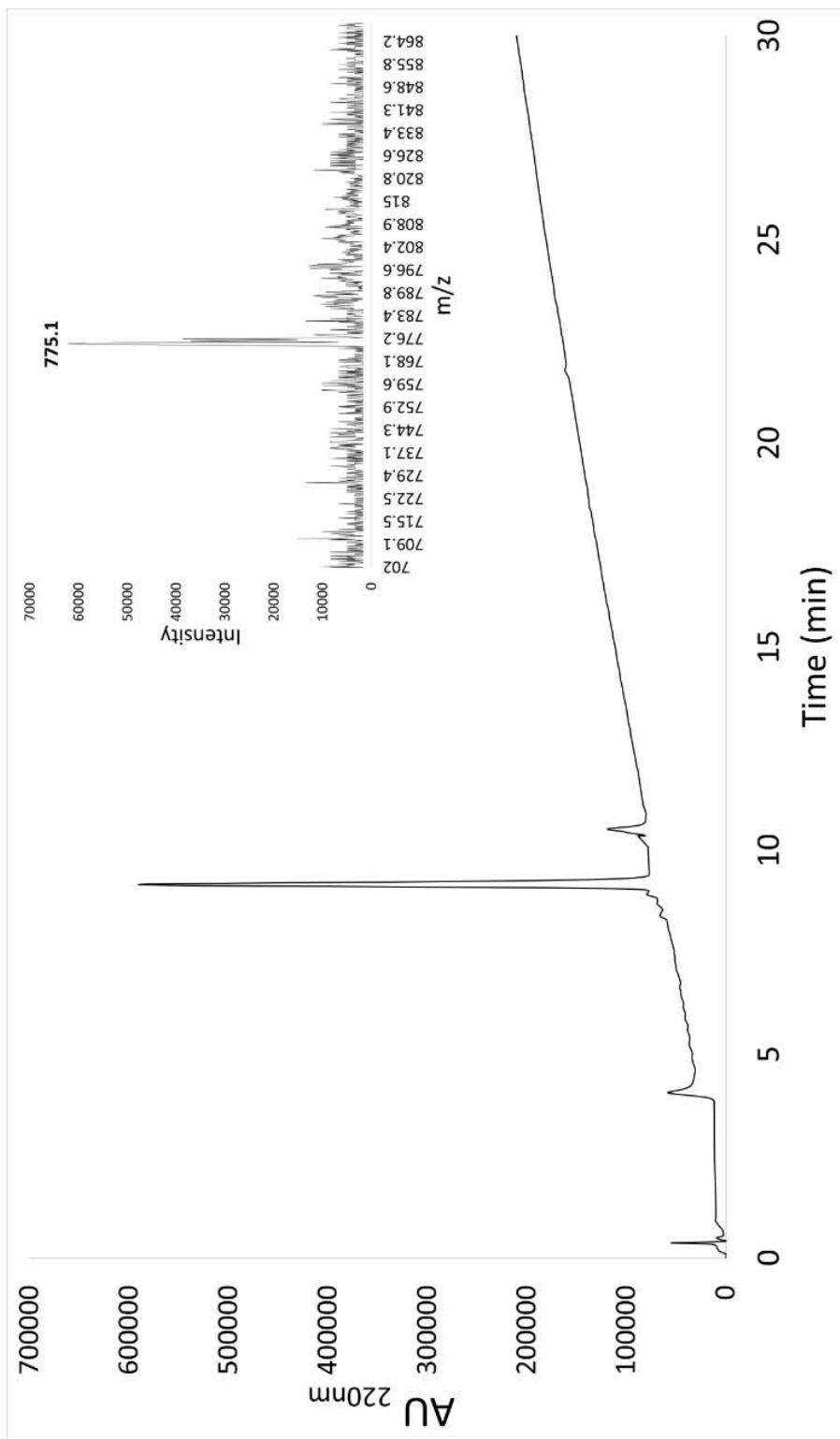
## Scheme S12. Synthesis of TetraFl-2



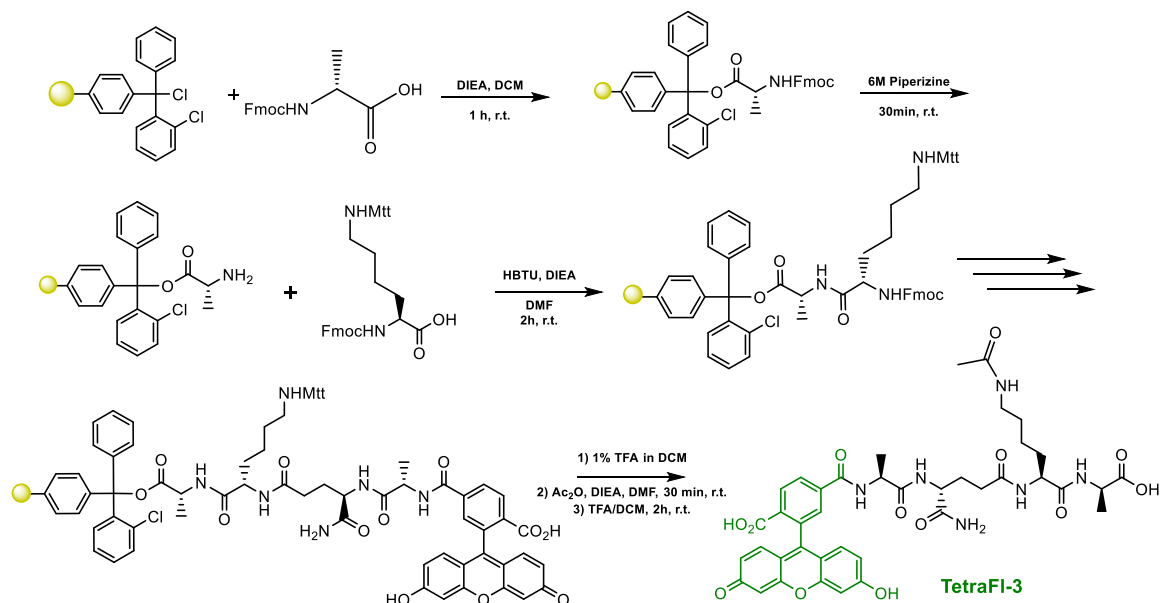
To a 25 mL peptide synthesis vessel charged with 2-Chlorotrityl chloride resin (500mg, 0.55mmol) was added Fmoc-L-alanine (1.1 eq, 188 mg, 0.605 mmol) and DIEA (3 eq, 0.286 mL, 1.65 mmol) in dry DCM (15 mL). The resin was agitated for 1 h at ambient temperature and washed with MeOH and DCM (3 x 15 mL each). The Fmoc protecting group was removed with 6 M piperazine/100 mM HOBt in DMF (15 ml) for 30 min at ambient temperature, then washed as before. Fmoc-L-Lys(Boc)-OH (3 eq, 773 mg, 1.65 mmol), HBTU (3 eq, 625 mg, 1.65 mmol), and DIEA (6 eq, 0.574 mL, 3.30 mmol) in DMF (15 mL) were added to the reaction flask and agitated for 2 h at ambient temperature. The Fmoc deprotection and coupling procedure was repeated as before using the same equivalencies with Fmoc-D-glutamic acid  $\alpha$ -amide and Fmoc-L-alanine. The Fmoc group of L-alanine was deprotected and resin coupled with 5(6)-carboxyfluorescein (2 eq, 413 mg, 1.1 mmol), HBTU (2 eq, 416 mg, 1.1 mmol) and DIEA (6 eq, 0.574 mL, 3.30 mmol) in DMF (15 mL) shaking overnight. The resin was washed as before and added to a solution of TFA/DCM (2:1, 20 mL) with agitation for 2 h at ambient temperature. The resin was filtered and resulting solution concentrated *in vacuo*. The residue was triturated with cold diethyl ether and purified using reverse phase HPLC using H<sub>2</sub>O/MeOH to yield **TetraFl-2**. The sample was analyzed for purity using a Shimadzu LC 2020 with a Phenomenex Luna 5 $\mu$  C18(2) 100Å (30 x 2.00 mm) column; gradient elution with H<sub>2</sub>O/CH<sub>3</sub>CN.

ESI-MS: [M+H]<sup>+</sup> calculated: 775.3 found: 775.1





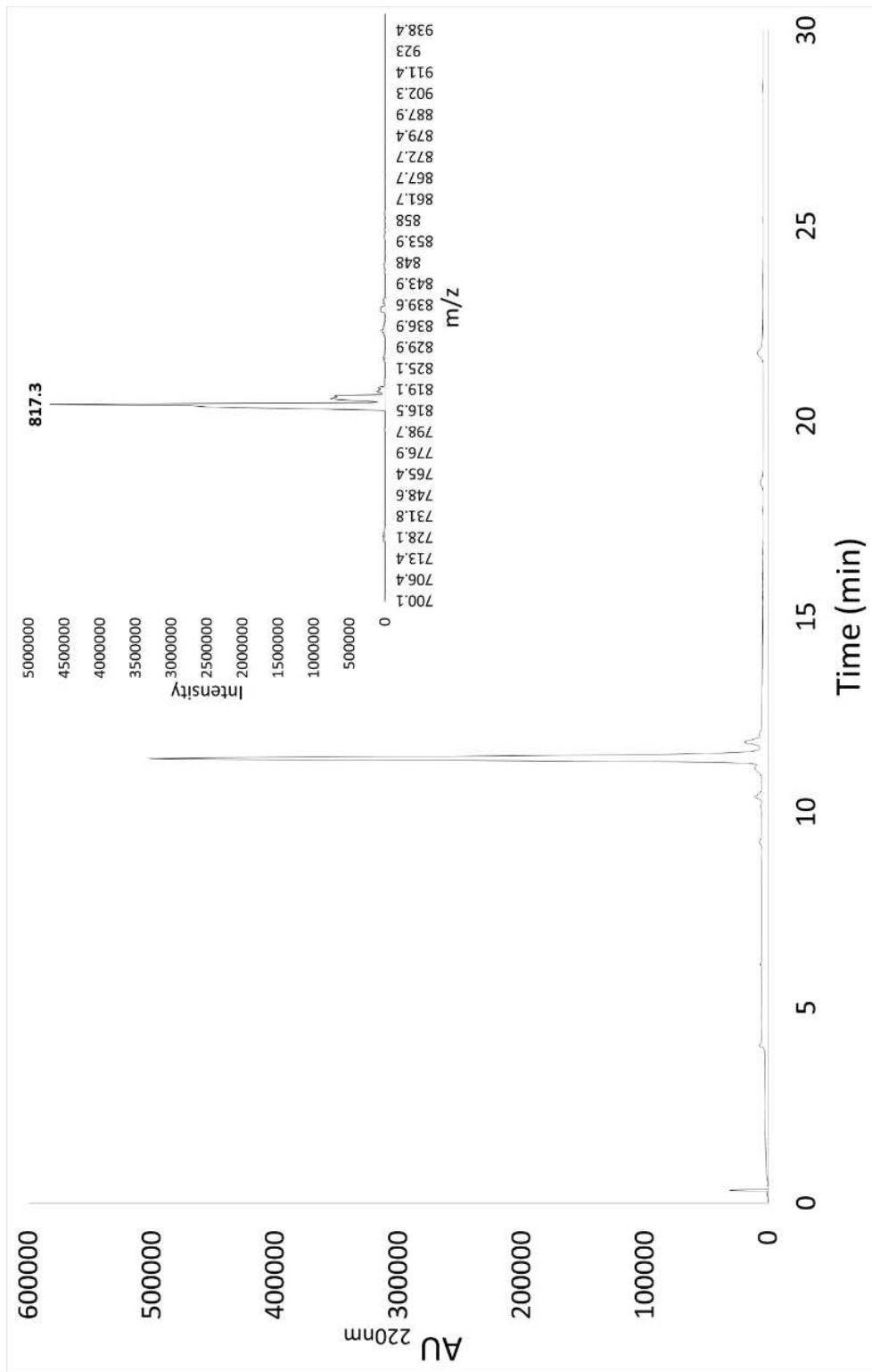
**Scheme S13. Synthesis of TetraFl-3**



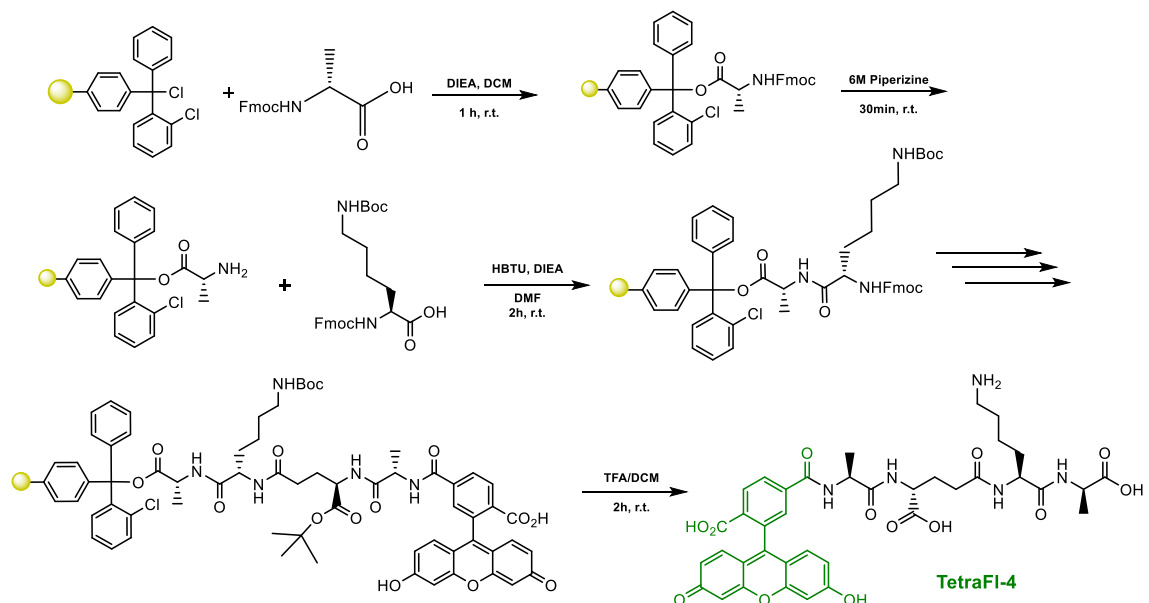
To a 25 mL peptide synthesis vessel charged with Fmoc-D-Alanine Wang resin (950 mg, 0.55 mmol). The Fmoc protecting group was removed with 6 M piperazine/100 mM HOBt in DMF (15 ml) for 30 min at ambient temperature, then washed with MeOH and DCM (3 x 15 mL each). Fmoc-L-Lys(Mtt)-OH (3 eq, 1.02 g, 1.65 mmol), HBTU (3 eq, 625 mg, 1.65 mmol), and DIEA (6 eq, 0.574 mL, 3.30 mmol) in DMF (15 mL) was added to the reaction flask and agitated for 2 h at ambient temperature. The Fmoc deprotection and coupling procedure was repeated as before using the same equivalencies with Fmoc-D-glutamic acid  $\alpha$ -amide and Fmoc-L-alanine. The Fmoc group of L-alanine was deprotected and resin coupled with 5(6)-carboxyfluorescein (2 eq, 413 mg, 1.1 mmol), HBTU (2 eq, 416 mg, 1.1 mmol) and DIEA (6 eq, 0.574 mL, 3.30 mmol) in DMF (15 mL) shaking overnight. The resin was washed as before and added to a solution of 1% TFA / 5% TIPS in DCM and shaken for 10 min and washed. The step was repeated five times for removal of the Mtt group. Acetic anhydride (5 eq, 0.260 mL) and DIEA (10 eq, 0.956 mL) in DMF was added and resin shaken for 30 min at ambient temperature. The resin was washed and added to a solution of TFA/DCM (2:1, 20 mL) with agitation for 2 h at ambient temperature. The resin was filtered and

resulting solution concentrated *in vacuo*. The residue was triturated with cold diethyl ether and purified using reverse phase HPLC using H<sub>2</sub>O/MeOH to yield **TetraFl-3**. The sample was analyzed for purity using a Shimadzu LC 2020 with a Phenomenex Luna 5 $\mu$  C18(2) 100Å (30 x 2.00 mm) column; gradient elution with H<sub>2</sub>O/CH<sub>3</sub>CN.

ESI-MS: [M+H]<sup>+</sup> calculated: 817.3 found: 817.3



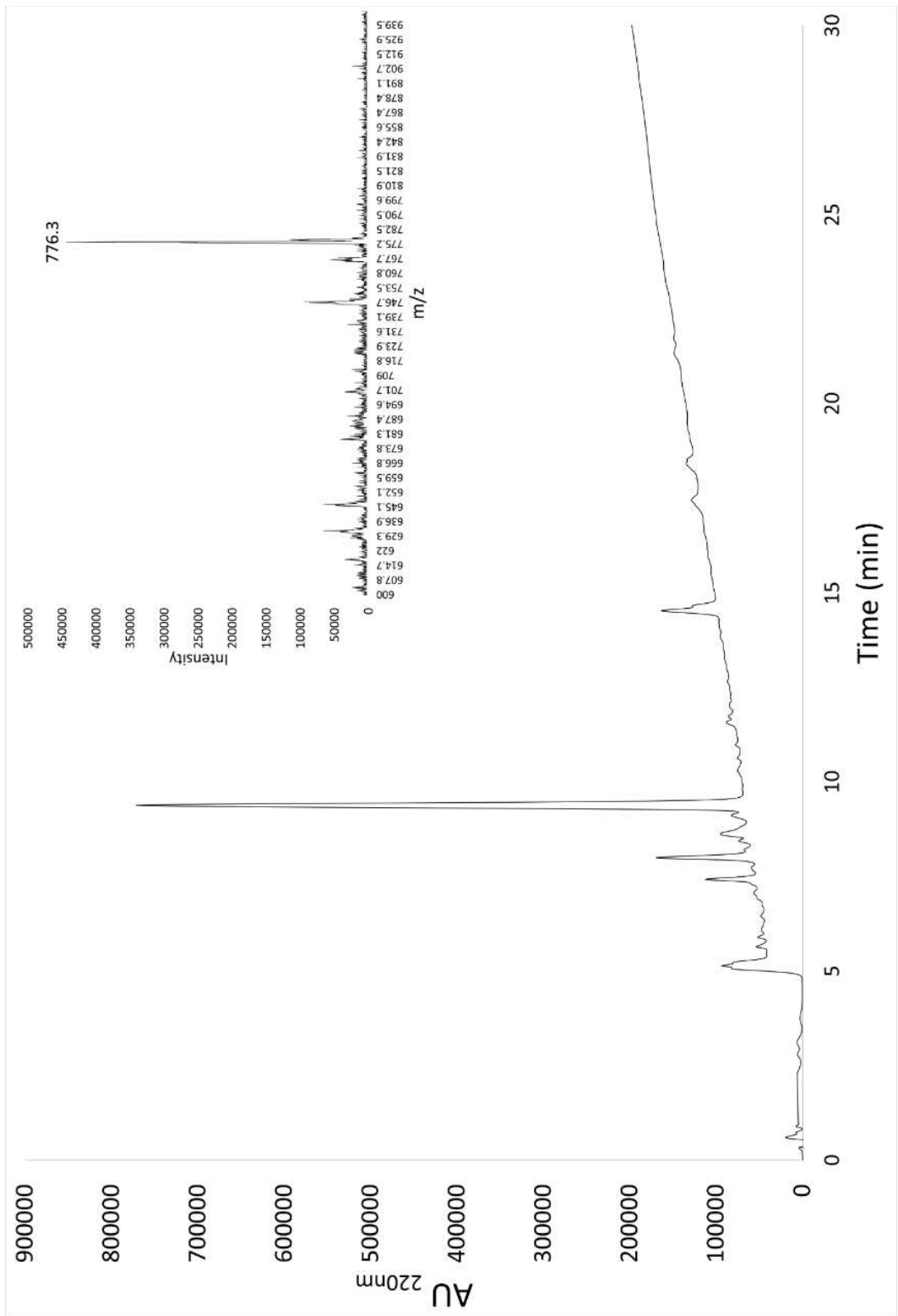
### Scheme S14. Synthesis of TetraFl-4



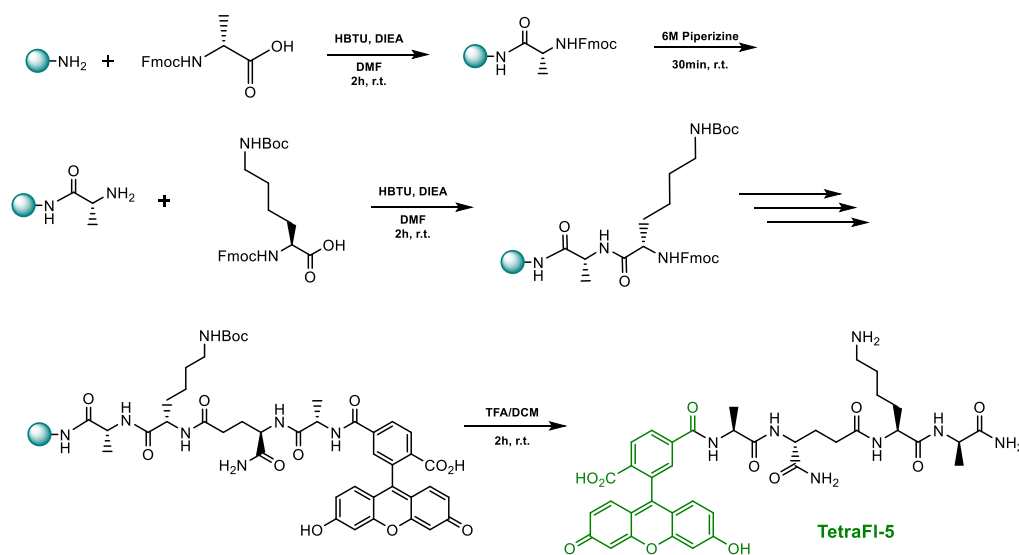
To a 25 mL peptide synthesis vessel charged with 2-Chlorotrityl chloride resin (500mg, 0.55mmol) was added Fmoc-D-alanine (1.1 eq, 188 mg, 0.605 mmol) and DIEA (3 eq, 0.286 mL, 1.65 mmol) in dry DCM (15 mL). The resin was agitated for 1 h at ambient temperature and washed with MeOH and DCM (3 x 15 mL each). The Fmoc protecting group was removed with 6 M piperazine/100 mM HOBt in DMF (15 ml) for 30 min at ambient temperature, then washed as before. Fmoc-L-Lys(Boc)-OH (3 eq, 773 mg, 1.65 mmol), HBTU (3 eq, 625 mg, 1.65 mmol), and DIEA (6 eq, 0.574 mL, 3.30 mmol) in DMF (15 mL) were added to the reaction flask and agitated for 2 h at ambient temperature. The Fmoc deprotection and coupling procedure was repeated as before using the same equivalencies with Fmoc-D-Glu(OtBu)-OH and Fmoc-L-alanine. The Fmoc group of L-alanine was deprotected and resin coupled with 5(6)-carboxyfluorescein (2 eq, 413 mg, 1.1 mmol), HBTU (2 eq, 416 mg, 1.1 mmol) and DIEA (6 eq, 0.574 mL, 3.30 mmol) in DMF (15 mL) shaking overnight. The resin was washed as before and added to a solution of TFA/DCM (2:1, 20 mL) with agitation for 2 h at ambient temperature. The resin was filtered and resulting solution concentrated

*in vacuo*. The residue was triturated with cold diethyl ether and purified using reverse phase HPLC using H<sub>2</sub>O/MeOH to yield **TetraFl-4**. The sample was analyzed for purity using a Shimadzu LC 2020 with a Phenomenex Luna 5 $\mu$  C18(2) 100Å (30 x 2.00 mm) column; gradient elution with H<sub>2</sub>O/CH<sub>3</sub>CN.

ESI-MS: [M+H]<sup>+</sup> calculated: 776.2 found: 776.3



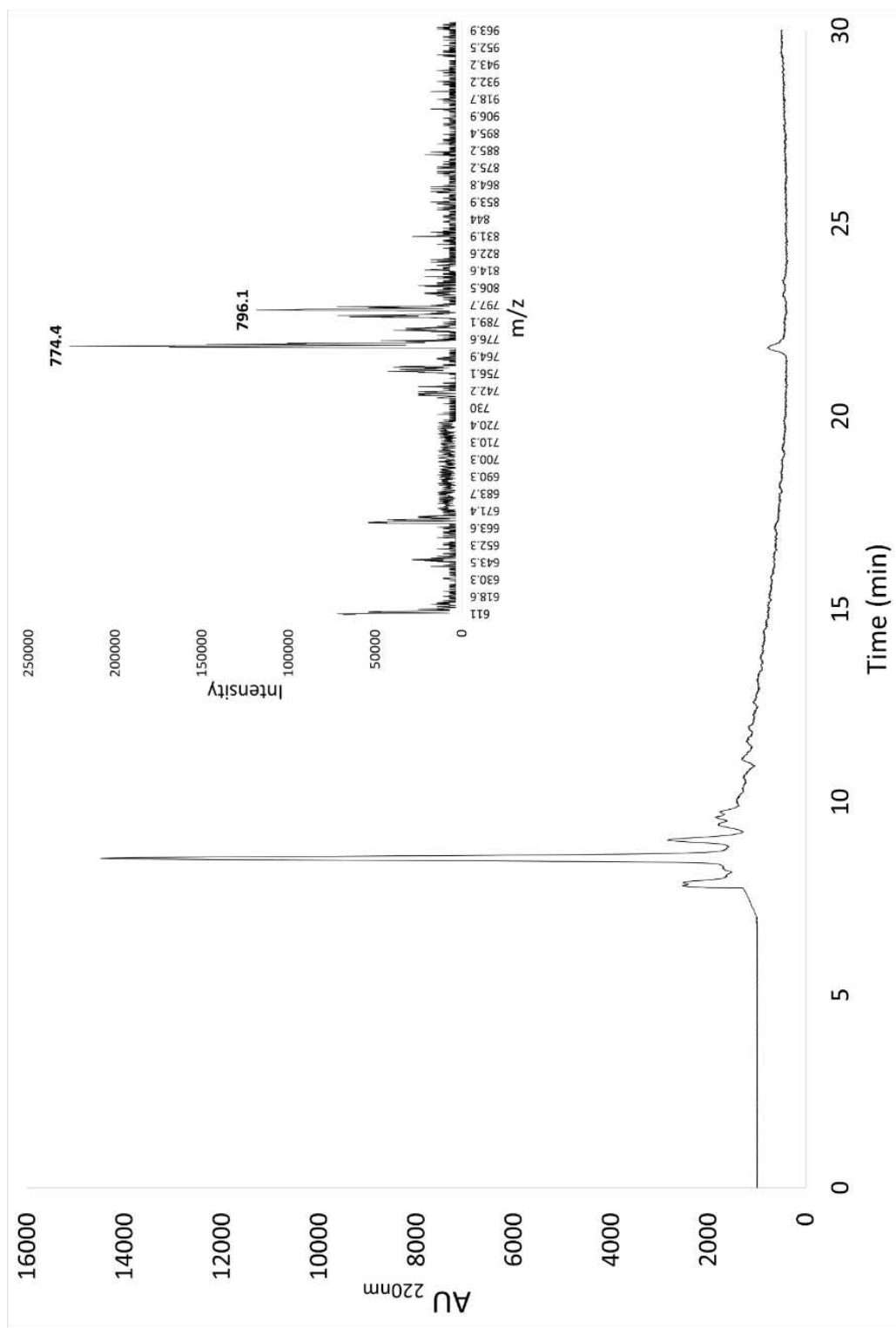
### Scheme S15. Synthesis of **TetraFl-5**



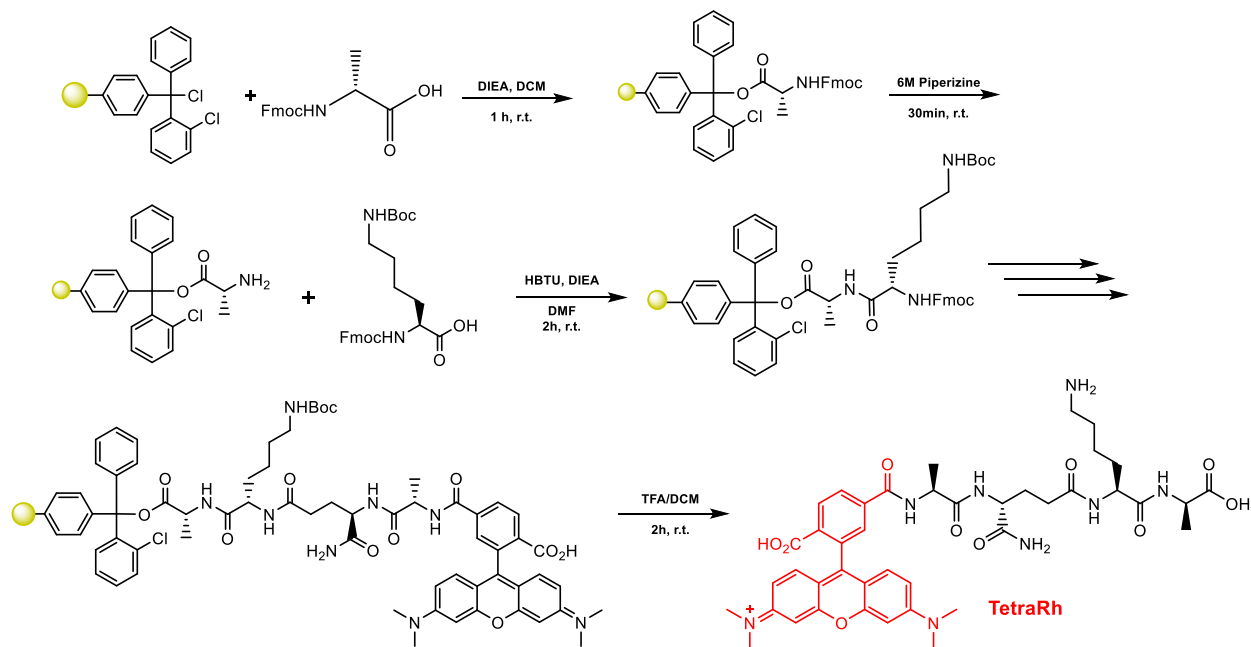
To a 25 mL peptide synthesis vessel charged with Rink Amide Resin (500mg, 0.30mmol). The Fmoc protecting group was removed with 6 M piperazine/100 mM HOBt in DMF (15 ml) for 30 min at ambient temperature, then washed with MeOH and DCM (3 x 15 mL each). Fmoc-D-alanine (3 eq, 280 mg, 0.90 mmol), HBTU (3 eq, 341 mg, 0.90 mmol), and DIEA (6 eq, 0.314 mL, 1.80 mmol) in DMF (15 mL) were added to the reaction flask and agitated for 2 h at ambient temperature. The Fmoc deprotection and coupling procedure was repeated as before using the same equivalencies with Fmoc-L-Lys(Boc)-OH, Fmoc-D-glutamic acid  $\alpha$ -amide, and Fmoc-L-alanine. The Fmoc group of L-alanine was deprotected and resin coupled with 5(6)-carboxyfluorescein (2 eq, 226 mg, 0.60 mmol), HBTU (2 eq, 228 mg, 0.60 mmol) and DIEA (6 eq, 0.314 mL, 1.80 mmol) in DMF (15 mL) shaking overnight. The resin was washed as before and added to a solution of TFA/DCM (2:1, 20 mL) with agitation for 2 h at ambient temperature. The resin was filtered and resulting solution concentrated *in vacuo*. The residue was triturated with cold diethyl ether and purified using reverse phase HPLC using H<sub>2</sub>O/MeOH to yield **TetraFl-5**. The sample was analyzed for purity using a Shimadzu LC 2020 with a Phenomenex Luna 5 $\mu$  C18(2) 100Å (30 x 2.00 mm) column; gradient elution with H<sub>2</sub>O/CH<sub>3</sub>CN.

ESI-MS: [M+H]<sup>+</sup> calculated: 774.3 found: 774.4





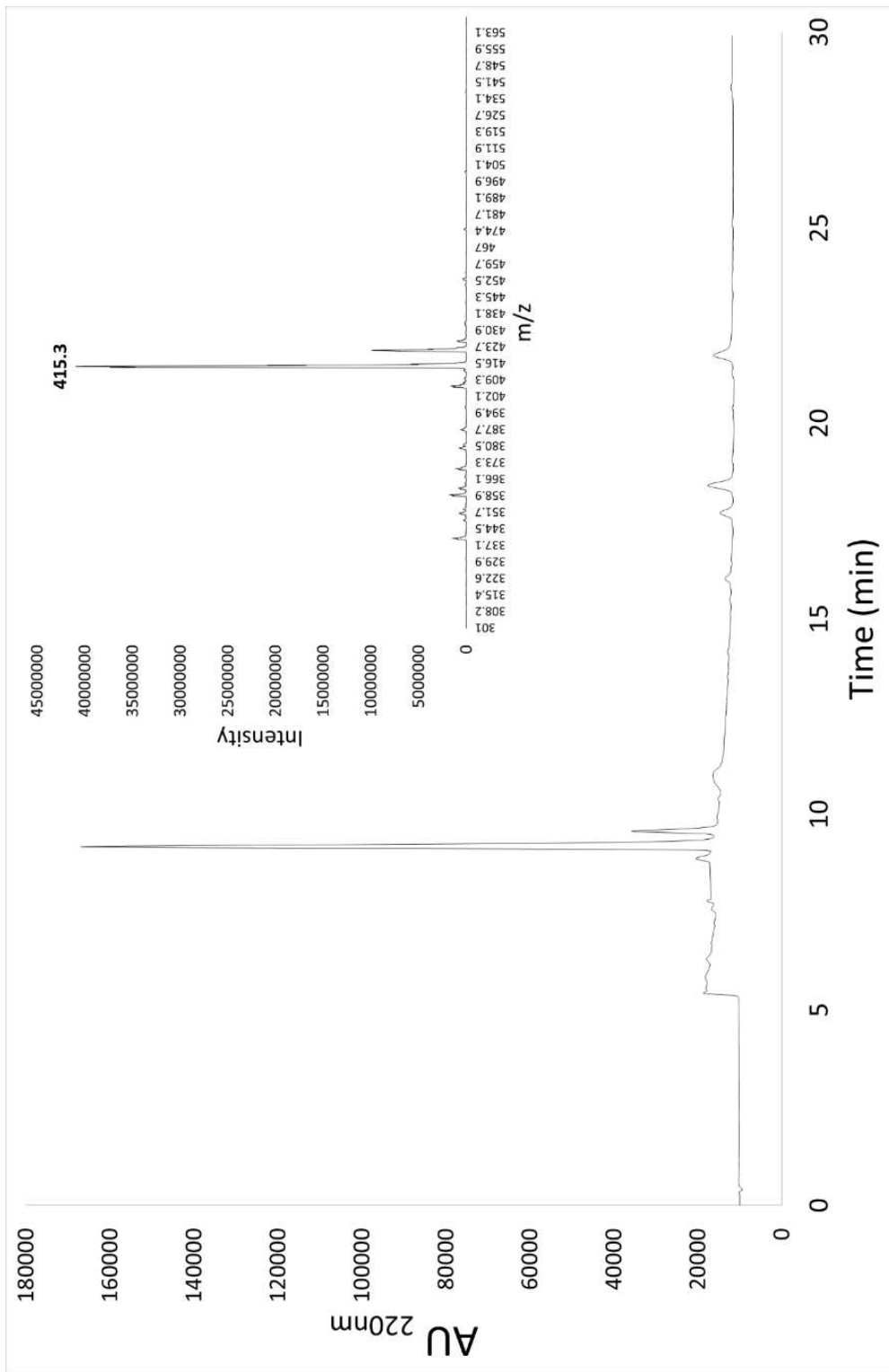
**Scheme S16. Synthesis of TetraRh**



To a 25 mL peptide synthesis vessel charged with 2-Chlorotrityl chloride resin (500mg, 0.55mmol) was added Fmoc-D-alanine (1.1 eq, 188 mg, 0.605 mmol) and DIEA (3 eq, 0.286 mL, 1.65 mmol) in dry DCM (15 mL). The resin was agitated for 1 h at ambient temperature and washed with MeOH and DCM (3 x 15 mL each). The Fmoc protecting group was removed with 6 M piperazine/100 mM HOBt in DMF (15 ml) for 30 min at ambient temperature, then washed as before. Fmoc-L-Lys(Boc)-OH (3 eq, 773 mg, 1.65 mmol), HBTU (3 eq, 625 mg, 1.65 mmol), and DIEA (6 eq, 0.574 mL, 3.30 mmol) in DMF (15 mL) were added to the reaction flask and agitated for 2 h at ambient temperature. The Fmoc deprotection and coupling procedure was repeated as before using the same equivalencies with Fmoc-D-glutamic acid  $\alpha$ -amide and Fmoc-L-alanine. The Fmoc group of L-alanine was deprotected and resin coupled with 5(6)-carboxy-tetramethylrhodamine (2 eq, 474 mg, 1.1 mmol), HBTU (2 eq, 416 mg, 1.1 mmol) and DIEA (6 eq, 0.574 mL, 3.30 mmol) in DMF (15 mL) shaking overnight. The resin was washed as before and added to a solution of TFA/DCM (2:1, 20 mL) with agitation for 2 h at ambient temperature. The resin was filtered and resulting solution concentrated *in vacuo*. The residue was triturated with cold diethyl ether and purified using

reverse phase HPLC using H<sub>2</sub>O/MeOH to yield **TetraRh**. The sample was analyzed for purity using a Shimadzu LC 2020 with a Phenomenex Luna 5 $\mu$  C18(2) 100Å (30 x 2.00 mm) column; gradient elution with H<sub>2</sub>O/CH<sub>3</sub>CN.

ESI-MS: [M+2H]<sup>2+</sup> calculated: 415.7 found: 415.3



# Sean E. Pidgeon

## EDUCATION

---

*Ph.D. Biochemistry, Department of Chemistry, Lehigh University* 2013-2018

Principal Investigator: Professor Marcos M. Pires

*Bachelor of Science in Biochemistry, Department of Chemistry, Wilkes University* 2009-2013

Research Advisor: Professor Amy L. Bradley

*Cum Laude*

## RESEARCH EXPERIENCE

---

### *Lehigh University Department of Chemistry*

- Synthesis and evaluation of modified D-amino acids to elucidate mechanisms of peptidoglycan synthesis and cell wall biosynthetic machinery
- Development of new immunotherapy methodologies to combat pathogenic bacteria
- Designed and developed diagnostic assays for detection of proteins associated with antibiotic resistance

### *Wilkes University Department of Chemistry*

- Synthesis and characterization of allosteric antagonists for glutamate receptors
- Development of microwave-assisted chemical reactions for undergraduate organic chemistry lab

## PROFESSIONAL EXPERIENCE

---

Lehigh University General Chemistry Teaching Assistant (Fall 2017)

- Assisted undergraduate students in Organic Chemistry I and II laboratory

Lehigh University Organic Chemistry Teaching Assistant (Fall 2013-Spring 2016)

- Assisted undergraduate students in Organic Chemistry I and II laboratory
- Prepared and assisted Organic Chemistry I/II recitation sessions

Lehigh University Research Assistant (Spring 2014-Present)

- Trained undergraduate/graduate students in the research setting on basic laboratory techniques
- Guided and supervised undergraduate/graduate research projects
- Managed daily laboratory operations (i.e. instruments/equipment, supplies, troubleshooting procedures)

Wilkes University Teaching Assistant (Spring 2010-Spring 2013)

- Assisted undergraduate students in Organic Chemistry I/II and General Chemistry I/II laboratory

## PUBLICATIONS

---

1. **Pidgeon, S.E.**, et al., *Metabolic Profiling of Bacteria by Unnatural C-terminated D-Amino Acids*. *Angewandte Chemie*, 2015. **54**(21): p. 6158-62.
2. **Pidgeon, S.E.** and M.M. Pires, *Metabolic remodeling of bacterial surfaces via tetrazine ligations*. *Chemical communications*, 2015. **51**(51): p. 10330-3.
3. **Pidgeon, S.E.\***, J.M. Fura\*, et al., *Dipeptide-Based Metabolic Labeling of Bacterial Cells for Endogenous Antibody Recruitment*. *ACS infectious diseases*, 2016. **2**(4): p. 302-309.  
\*Contributed equally

4. Sarkar, S., E.A. Libby, **S.E. Pidgeon**, et al., *In Vivo Probe of Lipid II-Interacting Proteins*. *Angewandte Chemie*, 2016. **55**(29): p. 8401-4.
5. **Pidgeon, S.E.** and M.M. Pires, *Vancomycin-Dependent Response in Live Drug-Resistant Bacteria by Metabolic Labeling*. *Angewandte Chemie*, 2017. **56**(30): p. 8839-8843.
6. **Pidgeon, S.E.** and M.M. Pires, *Cell Wall Remodeling by a Synthetic Analog Reveals Metabolic Adaptation in Vancomycin Resistant Enterococci*. *ACS chemical biology*, 2017. **12**(7): p. 1913-1918.
7. **Pidgeon, S.E.** and M.M. Pires, *Cell Wall Remodeling of Staphylococcus aureus in Live Caenorhabditis elegans*. *Bioconjugate chemistry*, 2017. **28**(9): p. 2310-2315.
8. Sabulski, M.J., **S.E. Pidgeon**, and M.M. Pires, *Immuno-targeting of Staphylococcus aureus via surface remodeling complexes*. *Chemical science*, 2017. **8**(10): p. 6804-6809.
9. Fura, J.M., S. Sarkar, **S.E. Pidgeon**, et al., *Combating Bacterial Pathogens with Immunomodulation and Infection Tolerance Strategies*. *Current topics in medicinal chemistry*, 2017. **17**(3): p. 290-304.
10. Feigman, M.S., Kim S., **S.E. Pidgeon**, et al., *Synthetic Immunotherapeutics against Gram-negative Pathogens*. *Cell chemical biology*, 2018. 25: p. 1-10.
11. **Pidgeon, S.E.**, et al., L,D-transpeptidase Crosslinking of Peptidoglycan is Spatially Segregated from D,D-transpeptidases, *Under Revision*. *Nature Communications*.
12. **Pidgeon, S.E.** and M.M. Pires, Peptidoglycan Transpeptidases Have Unique Structural Requirements for the Acyl Donor and Acyl Acceptor Substrates, *Manuscript in Preparation*, 2019.
13. **Pidgeon, S.E.** and M.M. Pires, Metabolic Labeling of Bacterial Cell Surfaces, *Manuscript in Preparation Current Opinion in Chemical Biology*, 2019.

## SKILLS

---

Standard Microbiology Aseptic Techniques	Bacterial Culture (BSL-2)
Protein Expression and Purification	Confocal Microscopy
Bioanalytical Protein Characterization	Synthetic Organic Chemistry
SDS-PAGE	Flow Cytometry
Immunoassays	Infectious Disease Models
Peptide Synthesis	GC-MS/LC-MS/MALDI
Liquid Chromatography (RP, Normal Phase)	UV-Vis

## HONORS AND AWARDS

---

- CAS Graduate Student Research Grant Recipient (2017)
- Lehigh University Department of Chemistry Fellowship Recipient (2016-2017)
- American Chemical Society Outstanding Senior Chemistry Major (2013)
  - Susquehanna Valley Section of the American Chemical Society
- Wilkes University Dean's List
- Wilkes University Deans' Scholarship (2009-2013)

## PRESENTATIONS

---

*Cell Wall Piracy by Synthetic Analogs Reveals Metabolic Adaption in Vancomycin Resistant Enterococci*

Sean E. Pidgeon and Marcos M. Pires

Poster Presentation at Gordon Conference, Chemistry and Biology of Peptides, Ventura California (2017)

*Cell Wall Piracy by Synthetic Analogs Reveals Metabolic Adaption in Vancomycin Resistant Enterococci*

Sean E. Pidgeon and Marcos M. Pires

Poster Presentation at The 25th American Peptide Symposium, Whistler Canada (2017)

*Cell Wall Piracy by Synthetic Analogs Reveals Metabolic Adaption in Vancomycin Resistant Enterococci*

Sean E. Pidgeon and Marcos M. Pires

Poster Presentation at Emerging Paradigms in Drug Discovery & Chemical Biology, New York Academy of Sciences (2016)

*Metabolic remodeling of bacterial surfaces via tetrazine ligations*

Sean E. Pidgeon and Marcos M. Pires

Poster Presentation at 9th Frontiers in Chemistry and Biology Interface Symposium, Johns Hopkins University (2016)

*En route synthesis of MTEP/MPEP analogs selective for mGluR5*

Sean E. Pidgeon and Amy L. Bradley, Ph.D.

Poster Presentation at 245th ACS National Meeting & Exposition, New Orleans, LA (2013)

*Microwave-assisted ketal protection and Grignard synthesis of diacetone alcohol*

Sean E. Pidgeon, Alison Duda, and Amy L. Bradley, Ph.D.

Poster Presentation at 244th ACS National Meeting & Exposition, Philadelphia, PA (2012)